University of Alberta

Systematics and palaeobiology of the crested hadrosaurine, *Saurolophus*, from Canada and Mongolia

by

Philip Robert Bell

A thesis submitted to the Faculty of Graduate Studies and Research
in partial fulfilment of the requirements for the degree of

Doctor of Philosophy
in
Systematics and Evolution

Department of Biological Sciences

Fall 2011
Edmonton, Alberta

Dedicated to my incredible family.

Can I come home now?

ABSTRACT

Reappraisal of *Saurolophus* confirms *Saurolophus osborni* and *Saurolophus angustirostris* as distinct species. Synapomorphies of *Saurolophus* include a spike-like pseudonarial crest formed by the nasals, frontals, and prefrontals; tripartite frontals with anteroventral and posterodorsal extensions that buttress the underside of the nasals; posterodorsal process on the prefrontal that buttresses the posterolateral edge of the nasal crest; and the presence of at least one supraorbital element. Phylogenetic analysis supports the close relationship between *Saurolophus, Prosaurolophus,* and *Kerberosaurus.* Material from the Maastrichtian Moreno Formation, California, previously assigned to *Saurolophus* is poorly preserved and lacks important diagnostic elements. This taxon shares traits of both *Saurolophus* and *Edmontosaurus*; however, as no unambiguous synapomorphies could be identified, this material is conservatively reassigned to Hadrosaurinae indet. The integument of *Saurolophus* varies significantly along the length of the body in both species. For the first time in the Dinosauria, soft tissue anatomy can be used to differentiate between species of single genus. A new standardised scheme for scale descriptions is also proposed. A *Saurolophus* bonebed from Mongolia represents the only dinosaur bonebed that preserves skin impressions. Ontogenetic evidence from this site suggests *Barsboldia sicinskii,* the only other hadrosaurid from the Nemegt Formation, is a junior synonym of *Saurolophus angustirostris*. An *Edmontosaurus* bonebed from the Horseshoe Canyon Formation (Alberta) contains nine animals including at least one *Albertosaurus*. The assemblage was subject to exposure, trampling, and rampant scavenging over a relatively short period (<1 year?). Future directions for hadrosaurid research are discussed.

ACKNOWLEDGEMENTS

To my supervisor, colleague, and mate, P. Currie – Thankyou! You took a leap of faith when you accepted me. I hope you like what you see. To the indefatigable E. Koppelhus – this would be nothing but a few scraps of paper without you. You are an inspiration and force unparalleled by NASA. I thank my examining committee, P. Currie, M. Caldwell, D. Brinkman, and M. Gingras, who have provided invaluable guidance along the way. Additional examiners for my Candidacy (A. Murray, F. Sperling, and chairperson M. Wilson) and defense (P. Lemelin, J. Horner) all suitably inspired and scared me. The entire UALVP graduate team, especially V. Arbour, M. Burns, M. James, D. Larson, M. Reichel, L. Shychoski, and E. Snively, has been a fountain of knowledge, help, inspiration, and most importantly, comic relief. Many thanks to C. Coy, N. Howard (UALVP), M. Ryan (CMNH), D. Brinkman, D. Eberth, B. Strilisky, D. Tanke, D. Lloyd (TMP), D. Evans, K. Seymour, I. Morrison (ROM), K. Shepherd, M. Feuerstack (CMN), C. Mehling (AMNH), M. Borsuk-Biatynickia (ZPAL), C. Tsogbaatar, D. Badamgarov, R. Barsbold (MPC), V. Alifanov, T. Tumanova (PIN), A. Paulina Carabajal (CF), L. Chiappe (LACM), and P. May (Research Casting International) who graciously provided access to specimens, stimulated discussion, and assisted me in so many ways. Members of the 2008 Korean International Dinosaur (KID) Project and Nomadic Expeditions (2009, 2010) are gratefully acknowledged for their enthusiastic assistance and companionship in the field, especially our leaders, Y.-N. Lee, P. Currie, M. Ryan, and D. Evans. Published and in press versions of some chapters benefited from reviews by T. Gates, P. Godefroit, H.-D. Sues, R. Cuthbertson, R. Cifelli, and three anonymous reviewers. Funding from the Dinosaur Research Institute and the KID Project are gratefully acknowledged. I must also thank my

Macquarie Uni (Syd.) palaeo crew (2001-2004), especially J. Talent, G. Brock, and R. Mawson for getting me to where I am today. I am forever grateful to the many friends I have made while in Canada – I could not have done this without you. Also to my mates back home who have kept me sane just knowing you are there. More than anyone, I thank my amazing mum and dad who have encouraged me in every aspect of life and provided so much unwavering support (financial and otherwise) through my many mad decisions, not least getting into palaeontology and moving to Canada. To my brother and sister and her family, you have helped me more than you will ever know – I hope some of this makes sense because this is for you too. Lastly, to my wonderful wife, Marcia, for your understanding, patience, and love. Like a Gillette razor: the best a man can get!

TABLE OF CONTENTS

LIST OF TABLES

LIST OF FIGURES

ABBREVIATIONS

AMNH, American Museum of Natural History, New York, USA.

CMN, Canadian Museum of Nature, Ottawa, Ontario, Canada.

KID, Korean International Dinosaur Project, Hwaseong Paleontological Laboratory, Hwaseong City, South Korea.

LACM/CIT, Natural History Museum of Los Angeles County (formerly at California Institute of Technology), Los Angeles, California, USA.

MOR, Museum of the Rockies, Bozeman, Montana, USA.

MPC, Mongolian Paleontological Center, Ulaan Baatar, Mongolia.

PIN, Palaeontologiceski Institut, Academii Nauk, Moscow, Russia.

TMP, Royal Tyrrell Museum of Palaeontology, Drumheller, Alberta, Canada.

UALVP, University of Alberta Laboratory for Vertebrate Paleontology, Edmonton, Alberta, Canada.

ZPAL, Institute of Palaeobiology of the Polish Academy of Sciences, Warsaw, Poland.

CHAPTER 1

GENERAL INTRODUCTION

Hadrosaurids were among the most common and diverse groups of Late Cretaceous dinosaurs in Asia, Europe, and North America (Ryan and Evans 2005), although sparse records also exist in South America (Hill et al. 2002, Novas 2009) and Antarctica (Case et al. 2000). Among dinosaurs, the hadrosaurid fossil record is one of the most comprehensive, represented by complete skeletons (Brown 1913, 1916), bonebeds (Varricchio and Horner 1993, Gangloff and Fiorillo 2010), skin impressions and soft tissue (Osborn 1912, Brown 1916, Manning et al. 2009), eggs with neonatal skeletons (Horner 1999), hatchlings (Horner and Makela 1979, Horner and Currie 1994), trackways (Currie et al. 1991), coprolites (Chin 2007), and probable gut contents (Tweet et al. 2008).

The Hadrosauridae are a monophyletic group of derived ornithischians that can be defined as the most recent common ancestor of *Saurolophus osborni* and *Lambeosaurus lambe* and all its descendants (Prieto-Marquez 2010). The type genus and species (*Hadrosaurus foulkii*) of the family was erected based on incomplete postcranial remains and teeth discovered in 1858 from the Woodbury Formation of New Jersey; however, these remains have since been regarded as non-diagnostic and the genus is considered a *nomen dubium* (Prieto-Marquez et al. 2006). Hadrosauridae is traditionally divided into two subfamilies: Lambeosaurinae, comprising at least twelve genera characterised by hollow cranial crests formed by the elaboration of the nasal and premaxillary bones; and Hadrosaurinae, which comprises at least eleven genera of flat-headed or solid-crested forms. In a recent review of the Hadrosauridae, Prieto-Marquez (2010) recovered the holotype specimen of Hadrosauridae ('*Hadrosaurus foulkii*') outside of the traditional family grouping and proposed the new name, Saurolophidae, to encompass the two subfamilies. Furthermore, he proposed the name

Saurolophinae to replace Hadrosaurinae. Despite these results, the names Hadrosauridae and Hadrosaurinae are retained here in order to avoid confusion and because the names are historically entrenched in the literature. Moreover, the type specimen of *Hadrosaurus* is considered undiagnostic (Prieto-Marquez et al. 2006) in which case the ICZN does not demand the changing of higher level taxonomic names.

Derived hadrosaurids evolved from *Iguanodon*-grade ornithischians sometime prior to the appearance of *Aralosaurus* from the ?Turonian–early Santonian of Kazakhstan (Godefroit et al. 2004a). However, the non-hadrosaurid hadrosauroid record extends back to the Barremian of China (Wang and Xu 2001, Van Itterbeeck et al. 2004). Hadrosauridae reached its acme in terms of both diversity and abundance during the Campanian–Maastrichtian before their extinction at the K-T boundary. Broadly Laurasian in distribution, mounting evidence strongly suggests an Asian origin for both subfamilies (Godefroit et al. 1998, 2004a, b, 2008) with major dispersal events occurring throughout the Late Cretaceous in a predominantly west-to-east direction via the Beringian Isthmus into North America (Jerzykiewicz and Russell 1991, Russell 1993).

Interchange across Beringia resulted in a similar taxonomic composition (at least at the family level) between Campanian–Maastrichtian terrestrial faunas of Mongolia and western North America (Jerzykiewicz and Russell 1991). Although it was historically vogue to name new Asian dinosaurs based on their similar North American relatives (see Hurum and Sabath 2003 for a review of Asian tyrannosaurid nomenclature), only a single genus, (*Saurolophus*) is currently accepted as co-occurring in Asia and North America. *Saurolophus* is a large (up to 12 m long) hadrosaurine hadrosaurid characterised by a solid, spike-

like crest that extends posterodorsally from the top of the skull. The type species, *Saurolophus osborni*, was discovered by Barnum Brown in 1911 in rocks of the Horseshoe Canyon Formation near Tolman Ferry, Alberta. In terms of the number of specimens recovered, *Saurolophus osborni* is one of the rarest Maastrichtian hadrosaurids. Brown described the skull (Brown 1912) and skeleton (Brown 1913), which was virtually complete. However, he assigned an isolated, 'booted' ischium (AMNH 5225) as the plesiotype to replace the broken element in the holotype. A partial 'booted' ischium from the Amur region of far Eastern Russia, was designated the type of *Saurolophus kryschtovici* by Riabinin (1930) based on comparison with the plesiotype of *Saurolophus osborni*. AMNH 5225 was provisionally re-identified as *Hypacrosaurus* by Russell and Chamney (1967) and *Saurolophus kryschtovici* is now unanimously regarded as a *nomen dubium* (Young 1958, Maryańska and Osmólska 1981, Weishampel and Horner 1990, Norman and Sues 2000, Horner et al. 2004). Additional fragmentary material from the Maastrichtian-aged Almond and Moreno formations of Wyoming and California, respectively, have also been referred to *Saurolophus* sp. (Morris 1973, Gates and Farke 2009); however, these identifications are equivocal.

The only other named species in the genus, *Saurolophus angustirostris,* was discovered in 1948 in the upper Campanian-?Maastrichtian Nemegt Formation of Mongolia (Rozhdestvensky 1952). *Saurolophus angustirostris* is one of the most common dinosaurs from that formation comprising approximately 20% of the vertebrate fossils collected from the Nemegt (Currie 2009). In addition to isolated skeletons, the Russian-Mongolian expeditions discovered a vast *Saurolophus* bonebed, which they named the Dragon's Tomb (Efremov 1958). They collected at least three skeletons, including skin impressions, from animals of various

ontogenetic stages, which would allow Rozhdestvensky (1957, 1965) to comment on the ontogeny of that species and remark on the likeness of juvenile *Saurolophus angustirostris* to adults of *Saurolophus osborni*. Later expeditions to the Gobi by the Polish-Mongolian Palaeontological Expeditions (1965–1971) recovered additional material of *Saurolophus angustirostris* (Kielan-Jaworowska and Barsbold 1972) stimulating further descriptive works (Maryańska and Osmólska 1979, 1981, 1984). Despite the apparent interest, in none of these papers were the species of *Saurolophus* adequately compared and descriptions were cursory by modern standards. The panel mount of the holotype of *Saurolophus osborni* complicated matters further in preventing subsequent workers from observing details of the anatomy, particularly in the skull, that would permit meaningful comparisons between the two species. Because of this, opinions differed on the cranial anatomy of *Saurolophus osborni* (Ostrom 1961, Horner 1992, Horner et al. 2004) and the validity of its Mongolian relative has been questioned (Norman and Sues 2000).

The purpose of this study is to re-evaluate the genus *Saurolophus* and provide new information on its ontogeny (developmental history), biology, biogeography, distribution, and phylogenetic position. Cranial allometry (changes in the relative proportions of parts of the skull as a result of growth) was not included but will be described elsewhere. The main body of this thesis is divided into eight chapters beginning with redescriptions of *Saurolophus osborni* (Chapter 2), *Saurolophus angustirostris* (Chapter 3), and the Californian material referred to that genus (Chapter 4). Chapter 5 describes and compares skin impressions belonging to *Saurolophus osborni* and *Saurolophus angustirostris.* Chapters 6 and 7 look at the excavation history, geology, and implications of two

hadrosaur bonebeds; the Dragon's Tomb from the Nemegt Formation of Mongolia (Chapter 6) and an *Edmontosaurus* bonebed from the Horseshoe Canyon Formation in Alberta (Chapter 7). The thesis concludes with a final chapter (Chapter 8) that discusses and synthesises the findings of the preceding eight chapters.

Saurolophus osborni was erected on the basis of a superb skull and skeleton collected from the Maastrichtian beds of the upper Horseshoe Canyon Formation, Alberta. Initial descriptions by Brown (1912, 1913) were brief and left several important anatomical features – particularly those related to the cranial crest – open to interpretation. Subsequent mounting of the holotype (AMNH 5220) has further denied attempts to clarify these features. Additional specimens from the Horseshoe Canyon Formation (including the virtually undescribed paratype) shed new light on the anatomy and relationships of this rare taxon. In Chapter 2, *Saurolophus osborni* is redescribed and rediagnosed based on all known specimens of this species. The phylogenetic context of this species is also reviewed based on this new information.

Saurolophus angustirostris, from the Nemegt Formation of south-central Mongolia, bears a close resemblance to *Saurolophus osborni*. Despite a number of descriptive works (Rozhdestvensky 1952, 1957, Maryańska and Osmólska 1979, 1981, 1984), a complete comparison with the Canadian species has never been undertaken. Other comparisons, based on juvenile material of *Saurolophus angustirostris,* further confused matters leading Norman and Sues (2000) to suggest that these two forms might, in fact be conspecific. Following new information presented in Chapter 2, the status of *Saurolophus angustirostris* is reviewed. A comprehensive redescription of *Saurolophus angustirostris* is based

on a well-preserved series of skulls that provide insight into the cranial development (ontogeny) of this taxon. Descriptions are paired with bone-by-bone comparisons of *Saurolophus osborni* along with comments on the ontogenetic development of the individual bones where possible. Phylogenetic re-evaluation resolves the close taxonomic relationship of these two species, yet *Saurolophus angustirostris* is formally distinguished from *Saurolophus osborni*, and a new diagnosis of the genus is presented.

Two partial hadrosaurid skeletons collected in 1939 and 1940 from the late Maastrichtian Moreno Formation in central California are among the most complete dinosaur remains from that state. The poorly-preserved remains were assigned to cf. *Saurolophus* by Morris (1973) on account of the proportions of the skull rather than any anatomical features. Because these specimens putatively represent a major geographical range extension for this genus, the best of these two skulls (LACM-CIT 2852) is evaluated. Similarities between LACM-CIT 2852, *Saurolophus* and *Edmontosaurus* are acknowledged, but the poor preservation and plastic deformation of the bones confound attempts to refine taxonomy of this specimen below Hadrosaurinae. LACM-CIT 2852 is conservatively assigned to Hadrosaurinae indet.

Hadrosaurid skin impressions are relatively common, yet few attempts have been made to assess the taxonomic utility of scale morphology and patterning. Remarkable preservation at the Dragon's Tomb bonebed in south-central Mongolia permits reconstruction of the integumentary covering of *Saurolophus angustirostris* for the first time. This chapter proposes a new standardised system for scale description to reduce ambiguities and facilitate better comparisons between taxa. Integumentary impressions are described for

major anatomical regions in *Saurolophus angustirostris* based on multiple individuals from the Dragon's Tomb and elsewhere in the Nemegt Formation. Descriptions are compared where possible to those of *Saurolophus osborni* thereby affording the first glimpse of integumentary variation between species of a single hadrosaurid genus. A preliminary synthesis of hadrosaurid skin impressions is presented in Chapter 5 in an attempt to identify inter- and intra-specific similarities and variation within this major group of ornithischians.

Discovered in 1948 by the Russian-Mongolian Expeditions to the Gobi Desert, the Dragon's Tomb is the single largest accumulation of *Saurolophus angustirostris* in the world. In addition to well-preserved and complete skeletons, the Dragon's Tomb yields extensive impressions of the integument of this taxon. Although referred to in passing in the English literature, the only notable account of this remarkable locality is that of Efremov (1955) in Russian. Chapter 6 explores the discovery and history of the Dragon's Tomb and documents illegal poaching activity that has subsequently spoilt much of the exposure. The provenance of many of the best specimens of *Saurolophus angustirostris* is also traced back to this locality. Evaluation of some of the largest individuals collected from the Dragon's Tomb raises questions about the validity of the only other possible hadrosaurid from the Nemegt Formation, *Barsboldia sicinskii.*

The taphonomic history of a monodominant hadrosaurine bonebed is examined in Chapter 7. The bonebed is from the lower Horseshoe Canyon Formation excavated near Edmonton, Alberta. Although hadrosaurid-dominated bonebeds are a relatively common taphonomic feature within the lower Horseshoe Canyon Formation, they have never been systematically described. Following the methods of Behrensmeyer (1991) and Eberth et al. (2007), a

detailed analysis of all available taphonomic data is presented based on systematic excavations undertaken at the Danek Bonebed over a period of five years. Initially identified as *Saurolophus* (Bell 2007), all diagnostic material can now be assigned to *Edmontosaurus*. The taphonomic history of the Danek Bonebed is compared with other mudstone-hosted hadrosaurid bonebeds from North America. The Danek Bonebed, however, is unique among all other described hadrosaurid bonebeds in the unusually high proportion of bite-marked bones, suggesting scavenging played a major role in the reworking of the assemblage.

References

Bell, P.R. 2007. The Danek Bonebed: an unusual dinosaur assemblage from the Horseshoe Canyon Formation, Edmonton, Alberta. Journal of Vertebrate Paleontology 27: 46A.

Behrensmeyer, A.K., 1991. Terrestrial vertebrate accumulations. In: A. Allison, D.E.G. Briggs (eds.), Taphonomy: Releasing the Data Locked in the Fossil Record., Plenum Press, New York, NY, pp. 291-335.

Brinkman, D. B., Eberth, D.A, and Currie, P. J. 2007. From bonebeds to paleobiology: applications of bonebed data. In R. R. Rogers, D.A. Eberth, and A. R. Fiorillo (eds.), Bonebeds; Genesis, Analysis, and Paleobiological Significance. University of Chicago Press, Chicago, pp. 221–264.

Brown, B. 1912. A crested dinosaur from the Edmonton Cretaceous. Bulletin of the American Museum of Natural History 31: 131–136.

Brown, B. 1913. The skeleton of *Saurolophus*, a crested duck-billed dinosaur from the Edmonton Cretaceous. Bulletin of the American Museum of Natural History 32: 387–393.

Brown, B. 1916. *Corythosaurus casuarius*: skeleton, musculature and epidermis. Bulletin of the American Museum of Natural History 35:709–723.

Case, J.A., Martin, J.E., Chaney, D.S., Reguero, M., Marenssi, S.A., Santillana, S.M., and Woodburne, M.O. 2000. The first duck-billed dinosaur (Family Hadrosauridae) from Antarctica. Journal of Vertebrate Paleontology 20: 612–614.

Chin, K. 2007. The paleobiological implications of herbivorous dinosaur coprolites from the Upper Cretaceous Two Medicine Formation of Montana; why eat wood? Palaios 22: 554-566.

Currie, P. J. 2009. Faunal distribution in the Nemegt Formation (Upper Cretaceous), Mongolia. In: Y.-N. Lee (ed.), Annual Report 2008, Korea-Mongolia International Dinosaur Project. Korean Institute Geology and Mineralogy, Seoul, Korea, pp. 143–156.

Currie, P.J., Nadon, G.C., and Lockley, M.G. 1991. Dinosaur footprints with skin impressions from the Cretaceous of Alberta and Colorado. Canadian Journal of Earth Sciences 28: 102-115.

Eberth, D.A., Rogers, R.R., and Fiorillo, A.R., 2007. A practical approach to the study of bonebeds. In: R.R. Rogers, D.A. Eberth, A R. Fiorillo (eds.) Bonebeds: Genesis, Analysis, and Paleobiological Significance. University of Chicago Press, Chicago, pp. 265-331.

Efremov, I. A. 1955. Burial of dinosaurs in Nemegt (South Gobi, MPR). In: Voprosy Geologii Azii. Izdatel'stvo Akademii Nauk SSSR, Moscow: 789–809 (in Russian).

Efremov, I.A. 1958. Road of Winds [in Russian]. The All-Union Uchebno-pedagogical publishing house, Moscow, 360 pp.

Gates, T.A. and Farke, A.A. 2009. Biostratigraphic and biogeographic implications of a hadrosaurid (Ornithopoda: Dinosauria) from the Upper Cretaceous Almond Formation of Wyoming, USA. Cretaceous Research 30: 1157–1163.

Gangloff, R.A. and Fiorillo, A.R. 2010. Taphonomy and paleoecology of a bonebed from the Prince Creek Formation, North Slope, Alaska. Palaios 25: 299-317.

Godefroit, P., Dong, J.D., Orth, C.J., Pillmore, C.L., and Tschudy, R.H. 1998. *Bactrosaurus* (Dinosauria: Hadrosauroidea) material from Iren Dabasu (Inner Mongolia, P. R. China). Bulletin de l'Institut royal des Sciences naturelles de Belgique, Sciences de la Terre 68 (Supplement): 3–70.

Godefroit, P., Alifanov, V., and Bolotsky, Y. 2004a. A reappraisal of *Aralosaurus tuberiferus* (Dinosauria, Hadrosauridae) from the Late Cretaceous of Kazakhstan. Bulletin de l'Institut royal des Sciences naturelles de Belgique, Sciences de la Terre 74 (Supplement): 139–154.

Godefroit, P., Bolotsky, Y.L., and Van Itterbeeck, J. 2004b. The lambeosaurine dinosaur *Amurosaurus riabinini*, from the Maastrichtian of Far Eastern Russia. Acta Palaeontologica Polonica 49: 585–618.

Godefroit, P., Hai, S., Yu, T., and Lauters, P. 2008. New hadrosaurid dinosaurs from the uppermost Cretaceous of northeastern China. Acta Palaeontologica Polonica 53: 47–74.

Hill, R.V., Pol, D., Rougier, G.W., Muzzopappa, P., Puerta, P. 2002. New dinosaur fossils from the Late Cretaceous La Colonia Formation, Chubut Province, Argentina. Journal of Vertebrate Paleontology 22: 65A.

Horner, J.R. 1992. Cranial morphology of *Prosaurolophus* (Ornithischia: Hadrosauridae) with descriptions of two new hadrosaurid species and an evaluation of hadrosaurid phylogenetic relationships. Museum of the Rockies Occasional Paper No. 2, 119 pp.

Horner, J.R. 1999. Egg clutches and embryos of two hadrosaurian dinosaurs. Journal of Vertebrate Paleontology 19: 607-611.

Horner, J.R., Currie, P.J., 1994. Embryonic and neonatal morphology and ontogeny of a new species of *Hypacrosaurus* (Ornithischia, Lambeosauridae) from Montana and Alberta. In: K. Carpenter, K.F. Hirsch, J.R. Horner (eds.), Dinosaur Eggs and Babies. Cambridge University Press, Cambridge, U.K., pp. 312–336.

Horner, J.R. and Makela, R. 1979. Nest of juveniles provides evidence of family structure among dinosaurs. Nature 282: 296-298.

Horner, J.R., Weishampel, D.B., and Forster, C.A. 2004. Hadrosauridae. In D.B. Weishampel, P. Dodson, and H. Osmólska (eds.), The Dinosauria, second edition. University of California Press, Berkeley, California, pp. 438-463.

Hurum, J. and Sabath, K. 2003. Giant theropod skulls from Asia and North America: skulls of *Tarbosaurus bataar* and *Tyrannosaurus rex* compared. Acta Palaeontologica Polonica 48: 161–190.

Van Itterbeeck, J., Markevich, V.S., and Horne, D.J. 2004. The age of the dinosaur-bearing Cretaceous sediments at Dashuiguo, Inner Mongolia, P.R. China, based on charophytes, ostracods and palynomorphs. Cretaceous Research 25: 391–409.

Jerzykiewicz, T. and Russell, D.A. 1991. Late Mesozoic stratigraphy and vertebrates of the Gobi Basin. Cretaceous Research 12: 345–377.

Kielan-Jaworowska and Barsbold 1972. Narrative of the Polish-Mongolian palaeontological expeditions 1967–1971. Palaeontologica Polonica 72: 5–13

Manning, P.L., Morris, P.M., McMahon, A., Jones, E., Gize, A., Macquaker, J.H.S., Wolff, G., Thompson, A., Marshall, J., Taylor, K.G., Lyson, T., Gaskell, S.,

Reamtong, O., Sellers, W.I., van Dongen, B.E., Buckley, M., and Wogelius, R.A. 2009. Mineralized soft-tissue structure and chemistry in a mummified hadrosaur from the Hell Creek Formation, North Dakota (USA). Proceedings of the Royal Society B 276: 3429–3437.

Maryańska, T. and Osmólska, H. 1979. Aspects of hadrosaurian cranial anatomy. Lethaia 12: 265–273.

Maryańska, T. and Osmólska, H. 1981. Cranial anatomy of *Saurolophus angustirostris* with comments on the Asian Hadrosauridae (Dinosauria). Palaeontologia Polonica 42: 5–24.

Maryańska, T. and Osmólska, H. 1984. Post-cranial anatomy of *Saurolophus angustirostris* with comments on other hadrosaurs. Palaeontologia Polonica 46: 119–141.

Morris, W.J. 1973. A review of Pacific coast hadrosaurs. Journal of Paleontology 47: 551–561.

Novas, F.E. 2009. The Age of Dinosaurs in South America. Indiana University Press, Indianapolis, 480 p.

Norman, D. and Sues, H.-D. 2000. Ornithopods from Kazakhstan, Mongolia and Siberia. In M.J. Benton, M.A. Shishkin, D.M. Unwin, and E.N. Korochin (eds.), The Age of Dinosaurs in Russia and Mongolia. Cambridge University press, Cambridge, UK, pp. 462-479.

Osborn, H. F. 1912. Integument of the iguanodont dinosaur *Trachodon.* American Museum of Natural History Memoir, Part II:33–54.

Ostrom, J.H. 1961. Cranial morphology of the hadrosaurian dinosaurs of North America. Bulletin of the American Museum of Natural History 122: 33-186.

Prieto-Marquez, A. 2010. Global phylogeny of Hadrosauridae (Dinosauria: Ornithopoda) using parsimony and Bayesian methods. Zoological Journal of the Linnean Society 159: 435–502.

Prieto-Marquez, A., Weishampel, D.B., and Horner, J.R. 2006. The dinosaur *Hadrosaurus foulkii,* from the Campanian of the East Coast of North America, with a reevaluation of the genus. Acta Palaeontologica Polonica 51: 77–98.

Riabinin, A.N. 1930. Towards a problem of the fauna and age of dinosaur beds on the Amur River [in Russian with English summary]. Russkoe Paleontologicheskoe Obshchestva, Monografy 11: 41–51.

Rozhdestvenskii, A.K. 1952. A new representative of duckbilled dinosaurs from the Upper Cretaceous deposits of Mongolia (in Russian). Doklody Akademic SSSR 86, 405-408.

Rozhdestvensky, A.K. 1957. The Duck-billed dinosaur *Saurolophus* from the Upper Cretaceous of Mongolia [in Russian]. Vertebrata Palasiatica 1: 129–149.

Rozhdestvensky, A.K. 1965. Growth changes in Asian dinosaurs and some problems of their taxonomy [in Russian]. Paleontologicheskii Zhurnal 3: 95–109.

Russell, D.A. 1993. The role of central Asia in dinosaurian biogeography. Canadian Journal of Earth Sciences 30: 2002–2012.

Russell, D.A. and Chamney, T.P. 1967. Notes on the biostratigraphy of dinosaurian and microfossil faunas in the Edmonton Formation (Cretaceous), Alberta. National Museum of Canada Natural History Papers 35, 22 p.

Ryan, M.J. and Evans, D.A. 2005. Ornithischian dinosaurs. In: Currie, P.J., and Koppelhus, E.B. (eds.) Dinosaur Provincial Park; a spectacular ancient ecosystem revealed. Indiana University Press, Indianapolis, p. 312–348.

Tweet, J.S., Chin, K., Braman, D.R., Murphy, N.L. 2008. Probable gut contents within a specimen of *Brachylophosaurus canadensis* (Dinosauria, Hadrosauridae) from the Upper Cretaceous Judith River Formation of Montana. Palaios 23: 624-635.

Varricchio, D. J. and Horner, J.R. 1993. Hadrosaurid and lambeosaurid bone beds from the Upper Cretaceous Two Medicine Formation of Montana: taphonomic and biologic implications. Canadian Journal of Earth Science 30: 997–1006.

Wang, X. and Xu, X. 2001. A new iguanodontid (*Jinzhousaurus yangi* gen. et sp. nov.) from the Yixian Formation of western Liaoning, China. Chinese Science Bulletin 46: 419–423.

Weishampel, D.B. and Horner, J.R. 1990. Hadrosauridae. In D. Weishampel, P. Dodson, and H. Osmólska (eds.) The Dinosauria. University of California Press, Berkeley, pp. 534-561.

Young, C.C. 1958. The dinosaurian remains of Laiyang, Shantung. Palaeontologia Sinica 16: 53–138.

CHAPTER 2

REDESCRIPTION OF THE SKULL OF *SAUROLOPHUS OSBORNI* BROWN 1912 (ORNITHISCHIA: HADROSAURIDAE).

A version of this chapter was published as P.R. Bell (2010) Redescription of the skull of *Saurolophus osborni* Brown 1912 (Ornithischia: Hadrosauridae) Cretaceous Research Doi:10,1016/j.cretres.2010.10.002

Introduction

The Hadrosauridae is divisible into two subfamilies; the crested Lambeosaurinae and the flat-headed Hadrosaurinae. Although typically non-crested, several hadrosaurines have incipient and/or solid crests formed by outgrowths of the nasals and in some forms, the frontals. *Saurolophus osborni* is a large (up to 11m), solid-crested hadrosaurine from the upper Horseshoe Canyon Formation of Alberta, Canada. The type specimen (AMNH 5220), a virtually complete skull and skeleton discovered in 1911, was described by Brown (1912, 1913). The specimen was prepared as a panel mount and mounted behind glass with its right side (the side on which the animal was found lying) exposed. A second skeleton (paratype, AMNH 5221), found the same year, was largely eroded and left in situ; however, the well-preserved and disarticulated skull was collected, the braincase of which was figured by Brown (1912) but remains largely undescribed. A third skull (CMN 8796) was found in 1925 by C.M. Sternberg in the same formation and figured in Russell and Chamney (1967). This skull, despite good preservation, was heavily reconstructed during restoration so that it is difficult to make critical anatomical observations. The identification of two specimens (LACM/CIT-2760 and LACM/CIT-2852) from the Moreno Formation in California (Morris 1973) as cf. *Saurolophus* is dubious. The specimens are being described by D. Evans and the author and will not be discussed here.

Saurolophus is palaeobiogeographically important as it is the only Late Cretaceous dinosaur genus to co-occur in North America and Asia. The only other species in the genus, *S. angustirostris* Rozhdestvenskii 1952, is recovered from the Maastrichtian Nemegt Formation of Mongolia. The genus is typified by a slender 'pseudo-narial' crest (Ostrom 1961) that projects caudodorsally above the orbits, extending over the caudal margin of the skull in adults. More recent osteological descriptions of *S. angustirostris* (Maryańska and Osmólska 1981, 1984) were limited in their comparisons of the two species of *Saurolophus* and relied entirely on Brown's cursory descriptions of the type species. Because the holotype of *S. osborni* was mounted behind glass in such a way that prevented further study, considerable confusion has arisen regarding the exact nature of the crest and the relationship between the two species (Ostrom 1961, Horner 1992, Norman & Sues 2000, Lund & Gates 2006).

The aim of this study is to 1) provide a comprehensive osteological description of the skull of *S. osborni*; 2) clarify important aspects of the cranial architecture, in particular the pseudonarial crest; 3) emend the diagnosis of the type species to provide the basis for comparisons with *S. angustirostris*, and 4) reassess the phylogenetic position of this species.

Materials and methods

The redescription is based on the three known specimens of *Saurolophus osborni* from Alberta. Because the holotype was mounted behind an immovable glass panel, the paratype (AMNH 5221) and referred specimen CMN 8796 were central to this study, which was supplemented by the holotype. Measurements of the holotype were taken using the original values obtained by Brown (1912, 1913). Digital photos of the specimen images were imported into Image J software and additional measurements were extrapolated using Brown's (1912, 1913) measurements to calibrate the ruler tool. All observations of the holotype are from the right side except where noted.

Systematic palaeontology

Ornithopoda Marsh, 1881

Iguanodontia Dollo, 1888

Hadrosauridae Cope, 1869

Euhadrosauria Weishampel, Norman, et Grigorescu, 1993

Hadrosaurinae Lambe, 1918

Saurolophus Brown, 1912

Saurolophus osborni Brown, 1912, pl. 1, 2, figs. 1–4.

Holotype. AMNH 5220, almost complete skull and skeleton lacking the most distal caudal vertebrae and the distal ends of both ischia.

Paratype. AMNH 5221, nearly complete, disarticulated skull comprising left and right premaxillae, maxillae, jugals, quadrates, right quadratojugal, most of the palate, left and right dentaries, and a nearly complete braincase.

Referred Specimen. CMN 8796, partial skull.

Horizon and Locality. Only the type and paratype localities of *S. osborni* have been so far relocated. Both were collected from the Tolman Bridge area along the banks of the Red Deer River in southern Alberta, Canada (Fig. 2.1). Both specimens come from unit 4 (sensu Eberth 2004) of the Horseshoe Canyon Formation. Eberth and Deino (2005) recently provided $^{40}Ar/^{39}Ar$ dates for a bentonite layer that directly overlies coal seam #10 in Unit 2. Their date of 70.44 ± 0.17 Ma is correlated with the Campanian-Maastrichtian boundary (Eberth and Deino 2005). Therefore, *S. osborni* is of early Maastrichtian age (magnetochron 31r–31n, Eberth 2004). Eberth (2004) describes Unit 4 as a non-coaly facies made up of subequal proportions of paleochannel sandstones and overbank mudstones that represent the driest phase during deposition of the Horseshoe Canyon Formation.

Emended Diagnosis. Large hadrosaurine (up to 11 m long) with the following combination of characteristics: a solid, caudodorsally-directed cranial

crest composed of the nasals, prefrontals, and frontals that extends caudal to the squamosals in adults; frontals tripartite, each contributing a finger-like caudodorsal ramus that buttresses the underside of the nasal crest; caudodorsal ramus of the frontal is approximately one fifth of the length of the entire crest in adults; frontals are excluded from the orbital rim by the postorbital-prefrontal complex; prefrontal and supraorbital I present and remain unfused even in late ontogeny; anterior process of the jugal asymmetrical in lateral view; dorsal margin of the premaxilla straight or nearly so.

Description

Cranium

*Premaxilla***.** The paired premaxillae are elongate U-shaped elements that are in union for their entire length along the midline to form a strongly vaulted muzzle. The premaxilla is composed of a curved body that forms the typical hadrosaur 'bill' and by a dorsal and a lateral process that form the margins of the external naris (Fig. 2.2). The dorsal margin of this element is straight for its entire length in the paratype. It is slightly upturned rostral to the naris in the type, although it does not approach the exaggerated condition in *S. angustirostris*. The oral margin is upturned to form a 'lip' extending from the rostral tip of the

premaxilla to approximately the posterior margin of the naris. This is similar to the condition of *Prosaurolophus* but is not as developed as in *Edmontosaurus.* In AMNH 5221, this 'lip' is diagenetically exaggerated; in life, these edges were probably not inclined far beyond horizontal. The circumnarial fossa is clearly defined rostral and ventral to the naris but becomes indistinct caudally. The rostral margin of the fossa is subparallel to the anterior margin of the premaxilla. A finger-like extension of that fossa extends rostrally through approximately 30% of the premaxillary body length, but is visible only in disarticulated specimens (AMNH 5221). This fossa presumably received the rostrodorsal ramus of the nasal in a tongue-in-groove arrangement. The dorsal process is rhomboidal in cross-section at its midpoint and tapers to a slightly expanded, spatulate end that is triangular in cross-section. In AMNH 5220 and CMN 8796, the dorsal processes are united, becoming obscured by the nasals at about the caudal margin of the naris. In cross-section, the lateral process twists posteriorly to become virtually horizontal where it overlies a lateral extension of the nasals before terminating close to the dorsal tip of the lacrimal.

Maxilla. The maxilla (Fig. 2.3A–B) is symmetrically triangular in lateral view as in other Hadrosaurinae. Dorsally, the anterior one third of the length of the anterior process is smooth and contacts the premaxilla; the remaining two thirds is deeply grooved to receive the lacrimal in a tongue-in-groove

arrangement. The rostral tip of the maxilla is bifurcated into a ventral and dorsal rostral process (median rostral process of Weishampel 1984); however, only the triangular ventral rostral process is intact in AMNH 5221. The preserved base of the dorsal rostral process suggests that this structure was thin and delicate. It is not visible through the naris as it is in *Edmontosaurus*, *Maiasaura* and *Brachylophosaurus*, but this may simply be due to incomplete preparation of the type specimen. The oral margin is smoothly concave and supported approximately 46 tooth families in AMNH 5221. The lateral face of the maxilla is dominated by a broad, arcuate contact for the jugal. This contact is laterally offset from the tooth row and is inclined dorsomedially where it terminates as the triangular dorsal process, which lies at the midpoint of the element. Ventrally, the jugal contact is bounded by a prominent lateral shelf that overhangs one or two large foramina. This shelf extends parallel to the tooth row along the dorsal half of the posterior process where it eventually forms the caudal margin of the maxilla. Up to five foramina may be present on the lateral surface of the maxilla, and the orientation and sizes of these are variable even between the left and right sides. In AMNH 5221, the tabular posterior process contributes 42% of the length of the maxilla. The dorsal process is lateromedially narrow and the caudal edge is nearly vertical. The dorsal process contacts the palatine caudally and lacrimal rostrodorsally. The base of the dorso-caudal process is preserved in AMNH 5221 rostral to the posterodorsal corner of the caudal process. The dorsocaudal

process appears to have been short and triangular, and did not extend past the caudal margin of the maxilla where it presumably contacted the ectopterygoid. Medially, the maxilla is penetrated by a series of small foramina within a longitudinal groove that forms a convex-up arc (Fig. 2.3B). This arc terminates anteriorly just caudal to the cleft between the bifurcated anterior processes. A shorter, shallower and almost straight groove also persists between the alveolar margin and these foramina.

Nasal. In none of the specimens are the nasals complete. However, the nasal is still the longest bone in the skull, forming the greatest extent of the facial angle. They are typically hadrosaurine, not being invaded by the nasal diverticula and are nearly straight in lateral aspect. Left and right nasals are in union for most of their length but are separated rostrally by the dorsal rami of the premaxillae for the entire length of the external naris. The supranarial process forms the complete dorsal margin of the naris and terminates abruptly within a recess on the premaxilla that is a forward extension of the circumnarial fossa. Caudal to the nares, the nasals become strongly vaulted and broad between the orbits where they are bounded by the premaxilla laterally, the prefrontals caudolaterally, and by the frontals caudally. From this contact, the nasals continue posterodorsally over the skull roof to form a broad crest that, in AMNH 5220, extends above the squamosals where the crest is broken. The crest curves

slightly dorsally relative to the facial angle and is triangular in cross-section. Based on the curvature in AMNH 5220, the crest may have been almost vertical at its terminus. In AMNH 5220, which preserves more of the crest than any other specimen, the bone surface has a series of longitudinal canals that probably housed blood vessels in life. Their presence cannot be confirmed on the left side OF AMNH 5220 or in any other specimen. Although not as dense as in mammalian or ceratopsian horn cores, blood vessel grooves on the crest of *S. osborni* suggest the possible presence of a keratinous sheath. As the tip of the crest in not preserved, the presence of a bony 'cap' at its termination as in *S. angustirostris*, cannot be confirmed. In cross section, each nasal has an inverted U-shaped groove, which extends for an unknown length along the underside of the crest. The proximal portion of these grooves is occupied by a dorsocaudal process from each frontal (Fig. 2.4). The grooves are twice the width of the frontal processes and consequently only the lateral half of each groove is occupied. The nasal crest is similarly buttressed laterocaudally by elongate processes of the prefrontals.

Lacrimal. The lacrimals are preserved in articulation in AMNH 5220 and CMN 8796. The lacrimal forms scalene triangle, the shortest edge forming a portion of the orbital rim. The rostral apex lies between the premaxilla and maxilla at about the caudal border of the naris. The premaxilla overlies the entire

length of the rostrodorsal edge of the lacrimal thereby separating it from contact with the nasal at least externally. At its dorsal limit, a short spur from the prefrontal overlaps the lacrimal in AMNH 5220. Based on the disarticulated maxillae (AMNH 5221), the lacrimal and maxilla meet ventrally in a tongue-in-groove arrangement. When the jugal is attached, the caudal half of this contact is obscured; the jugal also meets the lacrimal caudoventrally and laterally.

Prefrontal. The prefrontals of *Saurolophus osborni* are radically different from all other hadrosaurs. In AMNH 5220 and CMN 8796, the prefrontals are preserved in contact with the lacrimal rostrally, nasal rostromedially, frontal caudomedially and postorbital caudally. In lateral view, the prefrontal forms the rostrodorsal sector of the orbital rim but rather than having a flattened lateral edge as in *Edmontosaurus, Prosaurolophus,* and *Kerberosaurus*, the prefrontals are upturned above the orbit so that they partially obscure the nasals in lateral aspect. Caudally, the prefrontal meets the postorbital to exclude the frontal from the orbital rim (contra Brown 1912) and rostrally, the element tapers to a thin spur of bone that extends over part of the lateral surface of the lacrimal. A suture visible on the underside of this element within the orbit divides this bone into rostral and caudal halves. Originally (and erroneously) labelled the frontal and prefrontal by Brown (1912), these correspond to prefrontal and supraorbital 1, respectively, as described for *S. angustirostris* (Maryańska and Osmólska 1981),

but unlike that taxon, the suture is perpendicular to the orbital margin rather than oblique to it. Brown (1912, p.135) describes an elongate process of the prefrontal that forms the flank of the crest, and which apparently fuses with the nasal distally. This process, not present in other hadrosaurines except *S. angustirostris*, is difficult to see in the type specimen; however, the base of this process is clearly visible on CMN 8796 (Fig. 2.4). It appears as an almost cylindrical process that is somewhat offset medially from the remainder of that element. It is surrounded in part at its base by the frontal caudally and medially by the nasal. Although incomplete, it was at least as broad as the caudodorsal process of the frontal and would have buttressed the underside of the nasal crest, as suggested by Brown (1912), for an indeterminate length.

Jugal. The jugal is roughly W-shaped in lateral view forming the ventral borders of the orbit and infratemporal fenestra (Fig. 2.5A–B). The ventral margin is almost symmetrical. The anterior process is taller than it is long and asymmetrical as in *Gryposaurus*, *Edmontosaurus*, *Kerberosaurus*, and *Prosaurolophus*. Rostrally it tapers into a narrow spur that is 'pinched' between the maxilla and the lacrimal. The medial surface of the rostral process contacts the maxillary-lacrimal suture, and is delineated caudally by a prominent dorsoventral ridge. The sutural surface is irregular and undulatory (Fig. 2.5B), which is mirrored by the maxilla in the extensive contact between the two

elements. Contact with the palatine would have been along the dorsal part of the dorsoventral ridge. The postorbital process is long and narrow, and inclined at 75° to the ventral edge of the element. The proximal half is mediolaterally compressed; distally it is rostrocaudally compressed where it meets the rostral surface of the jugal process of the postorbital for the posterior 30% of its length. The tabular caudal process broadly contacts the lateral surface of the quadratojugal. The dorsal corner of the caudal process is drawn out to contact the quadrate, thereby excluding the quadratojugal from the margin of the infratemporal fenestra. It lacks the strong jugal flange seen in *Edmontosaurus, Gryposaurus,* and *Brachylophosaurus* but is smooth and rounded as in *Prosaurolophus*. Medially, the caudal process is slightly depressed and smooth where it contacts the quadratojugal. The caudal edge is almost vertical when in contact with the rest of the skull; the rostral edge is inclined caudally.

Quadratojugal. The quadratojugal is a flat, plate-like element that incompletely separates the jugal and quadrate (Fig. 2.6A–B), but is excluded from the infratemporal fenestra by these two bones. The caudal edge is C-shaped in lateral view and is relatively robust. In planar cross-section the quadratojugal is lenticular. It is met rostrally by the caudal process of the jugal, which overlaps the rather featureless rostrolateral surface of the quadratojugal. The quadrate is received caudomedially within a sinuous depression of the quadrate that covers

the caudal quarter. The caudoventral corner extends to a point.

Postorbital. The postorbital is a Y-shaped element that defines the dorsal and caudodorsal extent of the orbit, the lateral limit of the supratemporal fenestra, and the rostrodorsal quarter of the infratemporal fenestra. Posteriorly, the cylindrical squamosal process strongly interdigitates with the squamosal. The entire medial and ventral surfaces of the squamosal process are occupied by an overlapping extension of the squamosal. The jugal process is the longest of the three processes, tapering ventrally and curving slightly rostrally from about the mid-length of the postorbital. The distal half of this process is coarsely striated, eventually becoming rostrocaudally compressed, providing the contact surface rostrally for the postorbital process of the jugal. The rostral process is deflected dorsally, forming an angle of 117° with the squamosal process, and meets with the postorbital rostrally, frontal medially and parietal caudomedially. Viewed dorsally, the rostral process is mediolaterally widest where it forms the rostral margin of the supratemporal fenestra and tapers to a point just caudal to the lateral extent of the pseudonarial crest.

Squamosal. The squamosal is a complex element that forms the caudolateral corner of the skull. Rostrally, the postorbital process has three triangular extensions that interdigitate with the postorbital. The largest of these

extends along the medial surface of the postorbital to the base of the jugal process of the postorbital. Between the pre- and postquadratic processes lies the deep squamosal cotylus, which is hemispherical and houses the dorsal head of the quadrate. The finger-like prequadratic process extends ventrally from the base of the postorbital process to form a portion of the caudodorsal margin of the infratemporal fenestra. It is flattened and striated caudally where it contacts the quadrate. The postquadratic process is mediolaterally compressed and extends caudoventrally along the dorsal margin of the paroccipital process of the exoccipital-opisthotic. Proximally, the paroccipital process rests within a concavity on the postquadratic process, which becomes shallower distally. The medially projecting parietal process is missing in both the paratype and CMN 8796, and cannot be seen in AMNH 5220. Therefore it cannot be determined if the squamosals meet at the midline or are separated from each other by the parietals.

Quadrate. Although rather rod-like in lateral view, the quadrate is variable in the degree of curvature and the shape of the pterygoid flange; AMNH 5220 (Fig. 2.7A–B) is visibly more recurved than the paratype. The mediolaterally compressed dorsal end inserts into a deep cotyle in the squamosal and is supported by the prequadratic process of the squamosal, which extends ventrally along the leading edge of the quadrate. Close to the dorsal terminus on the medial surface originates a ridge that diverts rostromedially to form the

prominent pterygoid ramus, which gives the entire element a 'v' or tick-shaped outline in planar cross-section. This ramus is roughly triangular and occupies approximately 55% of the entire height of the quadrate in AMNH 5221. It curves rostromedially from a vertical sulcus along the medial body of the quadrate, and tapers to a thin edge. In AMNH 5220, its dorsal edge is nearly straight whereas in AMNH 5221 it is smoothly concave. Its ventral margin is deeply concave in AMNH 5220 but forms an obtuse angle in the paratype with the caudal margin of the quadrate. Much of the medial surface is ornamented by a series of fine radially-oriented ridges that presumably strengthened the contact with the quadrate ramus of the pterygoid. Ventrally, the quadrate terminates in a rostrocaudally expanded lateral condyle that is roughly triangular in cross-section and forms most of the jaw joint. The medial condyle is indistinct from the lateral condyle. The rostral margin of the quadrate is dominated by the quadratojugal contact, which forms a broad arc almost 45% of the height of the quadrate. The contact surface is bevelled, widest at its dorsal and ventral extremities, and slightly crenulated at its midpoint.

Neurocranium

Parietals. The fused parietals form the caudal roof of the braincase. In lateral view, the median element is saddle-shaped and longer than high. In

dorsal view, it is transversely constricted and has a 'length/minimal width' ration of >2 as is typical of hadrosaurines (Fig. 2.8A–C). The parietals are keeled dorsally as in *Edmontosaurus* but unlike *Corythosaurus*, and slope rostroventrally to form an obtuse angle with the frontals as in *Brachylophosaurus* and also *Parasaurolophus*. In each of AMNH 5221 and CMN 8796, the rostral margin is damaged but appears straight and is dominated by the contact for the frontals in dorsal view. There is no indication that the parietals intervene between the frontals by way of a rostromedial process; however this could be an artefact of preservation. The postorbitals contact the parietals rostrolaterally, although in lateral view the laterosphenoid partially obscures this suture (Fig. 2.8B). A triangular depression tapers caudally to disappear near the dorsal keel on the dorsal surface of the parietal. Posteriorly, the parietals expand where they meet the squamosals. They were probably excluded from the caudal margin of the skull by the squamosal; however this area is damaged in both specimens. Along its ventral margin, the parietal contacts the laterosphenoid anteriorly and the prootic and opisthotic-exoccipital posteriorly. At the juncture between these four elements, the ventral margin of each side of the parietals forms angles of 110° and 130° respectively on the right and left sides in AMNH 5221. The lateral surfaces of the element are smooth and strongly concave.

Frontal. Each frontal consists of a body, which forms the skull roof, and a rostroventral and a rostrodorsal process. Together, the frontals form that part of the skull roof that encloses the cerebral and olfactory portions of the brain bound caudally by the parietal and caudolaterally by the laterosphenoid (Fig. 2.8A–D). Because of imperfect preservation in this region, it cannot be determined whether the frontoparietal suture, which is in line with the rostral borders of the supratemporal fenestrae, is straight or forms an angle between the frontals. The rostroventral process forms an angle of 105° with the longitudinal axis of the frontal body, forming a broad platform over which the nasals and prefrontals lie (Fig. 2.8D). This feature was apparently missed by Brown (1912, fig. 3) who, in his figure of the braincase (AMNH 5221), mislabelled the frontals as prefrontals and vice versa. The two rostroventral processes apparently did not fuse but abutted one another rather bluntly. Medially, each rostroventral process is thickened to form a longitudinal ridge that presumably helped strengthen the contact with the nasals ventrally and prefrontals dorsally. In lateral view, the frontals taper rostroventrally but are uniformly broad in rostral view. As the frontal platform is broken ventrally, its dorsoventral height is unknown; however, it was at least as tall as the dorsal component of the frontal. The frontal platform continues caudodorsally by way of a single finger-like ramus on each frontal that buttresses the underside of the nasal crest where it overhangs the skull roof. These are best seen on CMN 8796, which shows the buttress of the

right frontal nested within a longitudinal groove on the underside of the right nasal (Fig. 2.4). Although damaged, each buttress tapers caudodorsally to a point and is at least as high as the frontals are long. Left and right buttresses do not contact one another; the frontals meet at the base of these processes by way of a low, short median septum. The interfrontal suture and the frontal bodies are flat. Laterally, the frontals wrap partly around the base of the dorsocaudal process of the prefrontals. Brown (1912) claims that the frontal extends laterally to form a significant portion of the dorsal circumference of the orbit. However, all three specimens clearly show a suture with the postorbital that extends from the rostral border of the supratemporal fenestrae to the base of the postorbital buttress thereby excluding the frontal from the orbital rim. Ventrally, the orbital depression is separated from the cerebral cavity (and presumably the olfactory depression) by the presphenoid rostrolaterally and by the orbitosphenoid and laterosphenoid caudolaterally.

Presphenoid. With its counterpart, the presphenoid forms most of the interorbital septum, bounded dorsally, caudally, and caudoventrally by the frontal, orbitosphenoid, and basisphenoid, respectively (Fig. 2.8A–B). It is higher than it is long and roughly rectangular in lateral aspect. When viewed anteriorly, the presphenoids are Y-shaped, diverging dorsally to transmit the olfactory nerve. Just ventral to the midpoint on its caudal margin, a semi-circular

invagination forms the rostral half of the foramen for cranial nerve II. The ventral edge lies parallel to and directly above the presphenoid process of the basisphenoid, although two do not meet except at the caudoventral edge of the presphenoid.

Orbitosphenoid. The roughly semi-circular orbitosphenoid is surrounded by the laterophenoid caudally, frontal dorsally and presphenoid rostrally (Fig. 2.8A–B). The laterosphenoid-orbitosphenoid union is straight. Anteroventrally, along with the presphenoid, the orbitosphenoid partially encloses cranial nerve II. The suture along the ventral margin with the basisphenoid is poorly defined, although it seems clear that the orbitosphenoid also contributed either partly or entirely to the openings for cranial nerves III and IV (Fig. 2.8). From the dorsal margin of cranial nerve IV, a narrow groove sweeps rostrodorsally in an arc, fading out dorsal to the foramen for cranial nerve III.

*Laterosphenoid***.** Situated between the orbitosphenoid and the prootic is the dorsoventrally elongate laterosphenoid (Fig. 2.8A–B). It extents dorsally to laterally enclose the fronto-parietal suture contacting these elements dorsomedially. A median ridge is present along the lateral surface of the laterosphenoid. The middle third of its posterior edge is in union with the prootic ventral to which it becomes constricted by the large foramen for the trigeminal

nerve (Fig. 2.9). The relationship between the basisphenoid, prootic, and laterosphenoid below this point is ambiguous; however, it seems that the three converge somewhere ventral to the foramen for cranial nerve V. Similarly, it is unclear to what extent the laterosphenoid participates in the formation of the foramina for cranial nerves IV.

*Prootic***.** The large foramen for cranial nerve V divides the anterior portion of the prootic (Figs. 2.8–9). The dorsal tab-shaped process broadly contacts the laterosphenoid; the ventral process is less well defined and merges indistinguishably with the laterosphenoid and basisphenoid. As in *Kerberosaurus* but unlike *S. angustirostris* (Bolotsky and Godefroit 2004), there is no vertical groove extending from the dorsal limit of the opening for cranial nerve V. A smooth ridge extends caudally from the opening for cranial nerve V and is parallel to the dorsal margin of this element where it contacts the parietal. A weaker ridge, ventral to and posteriorly convergent with the more dorsal ridge, probably defines the junction between the prootic and exoccipital-opisthotic. Between these two ridges, immediately posterior to cranial nerve V, the prootic is perforated by a small opening for the seventh cranial nerve (Fig. 2.9).

*Basisphenoid***.** When viewed ventrally, the unpaired basisphenoid-parasphenoid complex is a triangular bone that forms the base of the braincase.

Each corner is drawn out to form a long process; the caudolateral pterygoid processes and a single, rostrally-directed parasphenoid (cultriform) process. Each pterygoid process extends ventrally and caudolaterally and terminates bluntly in the depression between the quadrate- and basisphenoid processes of the pterygoid. The ventrolateral margins of the basisphenoid are thickened to form ridges that converge rostrally and are continuous with the parasphenoid process, which lies parallel to the ventral edge of the presphenoid and curves slightly ventrally. Only the base of the parasphenoid process is in contact with the presphenoid. In lateral aspect, the parasphenoid process forms an S-shaped curve with the pterygoid processes (Fig. 2.8A). Caudal to the base of the pterygoid processes, the basisphenoid expands to form the rostral part of the basal tubera. The openings for the carotid arteries, which should be close to the base of the pterygoid processes (Ostrom 1961) are not visible in any specimen. Dorsally, no clear divisions can be discerned between the exoccipitals, prootic, laterosphenoid, or orbitosphenoid with the basisphenoid. Consequently, the extent of the basisphenoid in the formation of the openings for the second and sixth cranial nerves is unknown (Fig. 2.9). A small break perforates the basisphenoid at approximately the point where cranial nerve VI should exit, thereby preventing its identification.

*Basioccipital***.** Forming the caudoventral quarter of the brain cavity is the basioccipital (Fig. 2.8A–B). It is divided into subequal halves by a transverse constriction on its ventral surface into the occipital condyle caudally and basal tubera rostrally. The occipital condyle is formed chiefly by the basioccipital and has a slightly dimpled surface texture. In caudal view, its ventral outline is rounded; dorsally, a shallow depression forms the base of the foramen magnum. The dorsolateral edges are inclined medially where they meet the exoccipitals. Together, the basal tubera are roughly the same size as the occipital condyle although approximately one third of their total volume is formed by the basisphenoid. The surface of the suture between the two is rough.

Exoccipital-opisthotic complex. The exoccipitals and opisthotics fuse very early in both hadrosaurine and lambeosaurine ontogeny as demonstrated by neonate and embryonic remains (Horner 1992, Horner and Currie 1994). Together these elements converge medially and form the caudodorsal margin of the occiput. From the midline, each exoccipital-opisthotic rises dorsolaterally to meet the squamosal at the posterolateral corner of the skull where it rests within a sulcus on the caudal edge of the squamosal (Fig. 2.8C). From this juncture, the paraoccipital process extends ventrolaterally, tapering only slightly before terminating bluntly at about the level of the dorsal limit of the foramen magnum. The squamosal maintains contact along most of the length of rostral face of the

paraoccipital process, terminating just dorsal to the ventral limit of that process. The exoccipital-opisthotics diverge ventrally from their midline suture sending off elongate basioccipital processes (exoccipital condyloid) that fuse firmly with the dorsolateral edges of the basioccipital. The sutures between these elements are inclined medially. Where it contacts the basioccipital, the basioccipital process is slightly expanded laterally. Together, the exoccipitals contribute approximately 90% of the circumference of the laterally compressed foramen magnum (Fig. 2.8C). In lateral view, a strong ridge of bone extends rostroventrally along the lateral wall of the basioccipital process of the exoccipital. Ventral and parallel to this ridge, a row of three foramina increase in size posteriorly, the anterior most corresponding to cranial nerves IX, X, and XI, the posterior two openings providing passage for the twelfth cranial nerve (Fig. 2.9). That same ridge terminates anteriorly at about the boundary between the exoccipital-opisthotic and basioccipital. Fenestra ovalis opens immediately dorsal to this ridge and likely indicates the anterior extent of the exoccipital with the prootic.

*Supraoccipital***.** Although presumably present in both AMNH 5220 and 5221, the supraoccipital is visible, albeit damaged, only in the latter. It occupies the usual hadrosaur position between the parietals anterodorsally and exoccipital-opisthotics ventrally and caudolaterally. The caudal margin is

entirely missing; however, it is clearly occluded from the foramen magnum by the exoccipital-opisthotics. Based on the inclination of the exoccipital-opisthotics, the ventral surface of the supraoccipital would have been inclined caudally at approximately 45º as is typical for Hadrosauridae. All other features and contacts are obscured because of its incomplete preservation.

Palate

Pterygoid. The pterygoids are imperfectly preserved in both AMNH 5221 and CMN 8796. However, each consists of four triangular processes that radiate from a central plate (Fig. 2.10). The two largest processes, the palatine and dorsal quadrate processes, diverge at 139° along their dorsal edges. The former bifurcates into two rounded nubbins for contacts with the vomer and palatine. The palatine process can be seen in articulation through the orbit in CMN 8796 where it rises up to meet the palatine extensively along the leading edge of the pterygoid. The smooth lateral faces of the dorsal and ventral quadrate processes broadly contact the medial surface of the pterygoid process of the quadrate. However, the shorter ventral quadrate process is broken on both specimens. The stout ectopterygoid process projects anteroventrally and medially, and is flattened along its ventral edge where it meets the reciprocal process from the ectopterygoid. From about the midpoint of the element, three strong ridges

radiate to buttress the medial surfaces of the palatine, ectopterygoid, and ventral quadrate process. The dorsal quadrate process is not buttressed.

*Palatine***.** Although no complete palatines are known, enough can be observed through the orbits of CMN 8796 to gain an appreciation of the morphology of this bone. The right palatine is a near-vertical, subtriangular plate. Rostrally, it is expanded transversely where it contacts the jugal and lacrimal. The ventral margin is a gentle S-shaped sinuosity where it presumably came into contact with the dorsal edge of the maxilla. The dorsal extension is preserved only on the left side (contra Heaton 1972). As preserved, this triangular process is vertical; however, it is possible that this fragment has shifted and its true orientation may have differed in life. The near-vertical caudal edge of this extension is thickened along its length for its contact with the palatine process of the pterygoid.

Vomers. The laterally-compressed vomers are triangular in lateral view and are in union with each other along their entire medial surfaces. The ventral edge of the triangle is weakly concave in lateral view. The rostral half of the vomer is of uniform medio-lateral width and tapers to an acute point, the ventral edge of which is flattened towards the tip (Fig. 2.11). The relationship between the vomers, premaxillae and maxillae could not be confirmed but it is assumed

the three met along the rostral-most portion of the vomers as in other hadrosaurines (Horner 1992). The caudal process is more tabular and has one or two parallel longitudinal ridges on both medial and lateral surfaces. Ventrally, this process is narrow and blade like, but becomes more robust dorsally. The dorsal apex is the most robust part of the paired vomers, expanding transversely to meet the palatines laterally and the palatine processes of the pterygoids caudally.

Mandible

Predentary. As in all hadrosaurs, the single, horseshoe-shaped predentary encloses the edentulous portions of the dentaries to form a distinct beak. The anterior margin is smoothly squared off (not rounded as suggested by Horner et al. 2004) as it is in all other hadrosaurs. The oral margin of the predentary in AMNH 5220 preserves six low, rounded rugosities, the most lateral of which are the smallest. The caudolateral extensions of the predentary overlie the dorsal surfaces of the dentaries for approximately half the length of the edentulous portion of each of those elements. These processes are smooth and flattened along their dorsal edges, and are dorsoventrally expanded caudally. Because of the curvature of the premaxillae, the predentary does not occlude with the upper jaw except along the flattened dorsal surfaces of these caudolateral extensions.

The anterior gap was likely filled by a keratinous sheath over one or both of these elements (Sternberg 1935). On either side of the caudal midline, a short, rounded process extends caudally to support the underside of each dentary. As the predentary is preserved only in articulated specimens, information about the dorsomedial surface was not available. It is assumed that there is a medial process caudally that intervenes at the dentary symphysis as in other hadrosaurs.

Dentary. The largest bone in the mandible is the dentary and is the sole tooth-bearing element in the lower jaw. Unlike most lambeosaurines, the ventral margin is straight in lateral view, and medial inflection at the symphysis is only weakly developed. The anterior edentulous portion of the dentary is about as long as the tooth row and tapers anteriorly toward the symphysis where it meets its mate. Several small foramina exit anterolaterally in this region. The tooth row is parallel to the ventral margin of the dentary. The prominent coronoid process is offset laterally from the tooth row, arising from the caudolateral border of the dentary where it projects rostrodorsally into the space between the jugal and maxilla. Dorsally, the coronoid process expands rostrocaudally for the insertion of several of the major jaw muscles (Rybczynski et al. 2008). Caudally, the coronoid process is excavated by the Meckelian fossa, which receives the coronoid process of the surangular on its lateral margin. The Meckelian fossa continues rostrally as a deep cleft on the medial surface of the dentary ventral to

the dental battery. The angular extensively contacts the dentary ventral to this cleft. The tooth battery is the most conspicuous feature on the medial aspect of the dentary and is covered for the most part by a thin plate of bone. The medial surface of the supradentary plate is grooved for the tooth families. There are approximately forty vertical tooth families in the adult dentary (Brown 1912); however, the total number cannot be determined on any specimen of *S. osborni*. At the base of each tooth family, a special dental foramen perforates the supradentary plate. These foramina are aligned in a gently concave line in medial view. The caudal end of the tooth row is drawn out into a conical splenial process, which medially contacts the splenial.

Surangular. The largest of the postdentary elements is the surangular. Rostrally, the surangular has a tall, thin coronoid process that extends along the medial side of the coronoid process of the dentary. Behind this process, the surangular expands mediolaterally to form a broad surface for articulation with the ventral condyle on the quadrate. The surangular is covered medially by the splenial and ventrally by the angular. The caudal process is mediolaterally flattened and curves caudodorsally to form the margin of a V-shaped cleft that separates it from the angular (and possibly the splenial). The articular rests in this cleft. A ridge that originates from the lateral margin of the quadrate cotyle

extends along the length of the lateral surface of the caudal process.

Articular. The small, laterally-compressed articular resides between the surangular laterally and the splenial and angular medially. In AMNH 5220 and CMN 8796, each articular projects dorsally from the neighbouring bones to give the posterior terminus of the mandible an almost hook-like appearance. A short ridge on its lateral surface extends anteroventrally from the dorsal tip to meet a similar ridge on the caudal process of the surangular.

Angular. The strap-like angular is bowed to accommodate the curvature of the post-dentary bones. Rostrally, it extends along the ventromedial edge of the dentary below the Meckelian groove and curves dorsomedially along its caudal length where it meets with the splenial dorsally and surangular medially. At its caudal end, the surangular and angular form a V-shaped cleft for the articular.

Splenial. The splenial is preserved only in the type where it cannot be observed. It likely occupied the typical hadrosaurid position on the medial surface of the surangular just dorsal to the angular. The triangular splenial process on the dentary marks the medial extent of the splenial.

Teeth. Brown (1912) originally described sixty tooth families in the maxilla and forty-four families in the dentary of AMNH 5221. However, plaster reconstruction on these elements has all but obscured the teeth. Where they are visible on the dentaries, the teeth form asymmetrical diamonds; the long-axes are oriented perpendicular to the tooth row, and are arranged into families of three or possibly four vertically stacked teeth, up to three of which may be active at any one time. The point where the two edges of the diamond meet on the posterior edge is slightly dorsal relative to the equivalent anterior point. This results in the tooth rows being inclined at shallow angles towards the posterior of the jaw. Below the occlusal plane, each tooth contacts six neighbouring teeth. As in other hadrosaurines, each tooth has a single, straight, non-denticulate median carina that extends the length of the enamelled face. Unlike lambeosaurines, the periphery of each tooth is devoid of denticles. In occlusal view, the lateral outlines of the teeth are roughly U-shaped, whereas the median carina gives the medial outline a broadly W-shape.

*Hyoid***.** The hyoids of AMNH 5220 are disarticulated from the rest of the skull, and one lies posterior to the quadrates whereas the second is resting in the right orbit below the eye. They presumably articulated in a similar fashion to those described by Dodson (1961) for *Corythosaurus*. As preserved, left and right hyoids cannot be distinguished and are observable only in medial or lateral view.

In these aspects, the mediolaterally compressed anterior end is asymmetrical between left and right sides, one being rounded and the other flattened. Both gradually taper posteriorly, and although the ends are missing, they appear to deflect posterodorsally. There is a low, rounded ridge posterior to the anterior end, just ventral to midheight.

Phylogenetic analysis

Forty four cranial and dental characters (with modifications where noted in Appendix 2.1), compiled from Weishampel et al. (1993), Godefroit (1998, 2008), Bolotsky and Godefroit (2004), Horner et al. (2004), and Prieto-Marquez (2005), were used to determine the phylogenetic position of *Saurolophus* within the Hadrosauridae. Because the post-cranium of *S. osborni* could not be adequately reassessed, post-cranial characters were excluded. Nine ingroup taxa (*Hypacrosaurus, Lambeosaurus, Gryposaurus, Brachylophosaurus, Maiasaura, Prosaurolophus, Edmontosaurus, Kerberosaurus,* and *Saurolophus*) and two outgroups, *Iguanodon* and *Bactrosaurus*, were selected by specimen completeness, by the existence of adequate published descriptions, and/or by the availability of specimens to the author. Where genera represent multispecific groupings, the type species was taken as the representative of that genus (Godefroit et al. 2008). *Kerberosaurus* from the Amur region of eastern Russia was included in the

present analysis, as it has been recently suggested to be the sister taxon to a monophyletic clade formed by *Prosaurolophus* and *Saurolophus* (Bolotsky and Godefroit 2004). *Saurolophus angustirostris* is excluded here pending a thorough redescription (currently in preparation by the author) and comparison with the North American species. All characters were treated as unordered and assigned equal weight. Using the character matrix (Appendix 2), an exhaustive search was performed using PAUP 4.0b10 (Swofford 2002), resulting in three most parsimonious trees with a length of 69 steps. The strict consensus tree had a retention index of 0.81, a consistency index of 0.84, and a rescaled consistency index of 0.68 (Fig. 2.12). Because of the number of undetermined character states for *Kerberosaurus*, a second analysis was performed that omitted that taxon resulting in a single most parsimonious tree that retained *Saurolophus* and *Prosaurolophus* as sister taxa with no change in the length or support values. Bootstrap values achieved using the branch-and-bound option show excellent support for a Hadrosaurinae-Lambeosaurinae split; relationships within the Hadrosaurinae are generally not well supported. The only moderately well-supported clade here (*Brachylophosaurus-Maiasaura*, bootstrap = 74) has been demonstrated elsewhere (Prieto-Marquez 2005, Prieto-Marquez et al. 2006, Godefroit et al. 2008). Moderate support exists for the *Edmontosaurus-Kerberosaurus-Prosaurolophus-Saurolophus* clade, although relationships within this group are ambiguous.

The phylogenetic position of *Saurolophus* has shifted considerably in recent analyses of the Hadrosaurinae. Norman (2002) and Horner et al. (2004) suggest *Saurolophus* occupies a basal position within the basal Hadrosaurinae. Several more recent analyses place *Saurolophus* as the sister taxon to *Prosaurolophus* in a more derived position, but with variable relationships amongst other hadrosaurines (Bolotsky and Godefroit 2004, Prieto-Marquez 2005, Prieto-Marquez et al. 2006, Gates and Sampson 2007, Godefroit et al. 2008). Although postcranial characters were not used in the present analysis, the results agree well with topologies proposed by Bolotsky and Godefroit (2004) and Godefroit et al. (2008); *Brachylophosaurus* and *Maiasaura* form a well-supported clade that is the sister group to all other hadrosaurines and *Edmontosaurus* is the sister taxon to the clade that includes *Kerberosaurus, Prosaurolophus*, and *Saurolophus.* Although the strict consensus tree shows a polytomy between *Kerberosaurus*, *Prosaurolophus*, and *Saurolophus*, one of the three most parsimonious trees in this study (*Kerberosaurus* (*Prosaurolophus* + *Saurolophus*)) does match that of Godefroit et al. (2008) thereby adding some support to that phylogeny. However, resolution of these taxa in the analysis by Godefroit et al. (2008) hinged on a single character at each node (*Kerberosaurus* + *Prosaurolophus* + *Saurolophus* united by frontals that are excluded from the orbital rim by the postorbital-prefrontal complex [character 5(1), bootstrap = 58]; *Prosaurolophus* + *Saurolophus* united by a solid supracranial crest present and excavated laterally by the circumnarial fossa

[character 20(2), bootstrap = 54]) and was thus weakly supported.

Discussion and conclusions

The holotype of *Saurolophus osborni* (AMNH 5220) remains the best specimen of this curious species. Unfortunately, the fact that it is on display behind glass has prevented scrutiny since the original descriptions (Brown 1912, 1913). Brown's comments, while relevant, provide little more than a brief synopsis of the anatomy rather than a comprehensive osteological description. Considerable confusion has since arisen regarding the nature of the pseudo-narial crest in *S. osborni*. Brown (1912) posited that the nasals, frontals, and prefrontals all contributed to the formation of the crest. The nasals, he suggested, were buttressed laterally and caudally by the prefrontals and frontals and paradoxically, Brown (1912, fig. 1a) does not show the frontals in his posterior rendering of the skull. Because of these inconsistencies and because examination of the holotype has been compromised, this view has been challenged by several authors who do not regard the frontals as part of the crest (Ostrom 1961, Horner 1992, Horner et al. 2004). Observations of the crest in CMN 8796 clearly show portions of the frontal still in contact with the nasals; each frontal contributes a single caudodorsal process that is received in its own recess on the underside of the nasal crest. This condition is virtually identical to that of *S. angustirostris*

(Maryańska and Osmólska 1981, MPC 100/179). However, the posterodorsal processes of the frontals in *S. osborni* are less developed. Assuming similar proportions in crest length between the two species, the posterodorsal process would have been only one fifth the length of the crest in *S. osborni* as opposed to approximately half the length in *S. angustirostris* (Maryańska and Osmólska 1981, MPC 100/179). The broken crest in CMN 8796 shows the nasal diverticula did not invade the nasals as suggested by Ostrom (1961) on more speculative grounds.

The frontals of *Saurolophus osborni* appear unique among hadrosaurs in their configuration. Amongst other crested hadrosaurines (*Brachylophosaurus, Maiasaura, Prosaurolophus*), the frontals contribute only in *Maiasaura* to the formation of the crest, rising to form the caudal and dorsal extent of that structure (Horner 1983). In *Brachylophosaurus*, the external surfaces of the frontals as viewed from above are foreshortened and do not contribute to the formation of the crest (Prieto-Marquez 2005, fig. 8). In species of *Prosaurolophus*, the crest is derived from a short protuberance on the nasals; the frontals flatly abut the posterior margins of the nasals (Horner 1992). In the architecture of the caudodorsal process, *S. osborni* most closely resembles the lambeosaurines *Parasaurolophus* and *Charonosaurus*, in both of which there is elongation of the frontal platforms to form 'dorsal promontoria' (Godefroit et al. 2001, Evans et al. 2007). In *Charonosaurus*, this promontorium is the broadest part of the frontal

(Godefroit et al. 2001) whereas in *Parasaurolophus* the finger-like process is more narrow and reminiscent of that in *S. osborni*. A finger-like caudodorsal process was illustrated for *S. angustirostris* by Maryańska and Osmólska (1981, fig. 2); however, in MPC 100/179 this process is delicate and thin, but is broader than in *S. osborni*. Similarly, the rostroventral process, which supports the nasals and prefrontals in front of the crest, is unique to *Saurolophus*. In other crested hadrosaurines the frontal-nasal union converges on the lambeosaurine condition in which the frontal has an extended, caudally-inclined sutural surface (reversed in *Maiasaura*). The rostroventral process in *S. osborni* is elongate and rather smooth externally and does not have the deep grooves and ridges seen in lambeosaurines. Rather than forming a strong interdigitating suture between these two elements, the nasals appear to simply overlie this ramp in a comparatively weak union. This feature is shared by *S. angustirostris* (e.g. ZPAL MgD-1/159, MPC 100/179) in which the frontals can be observed through the orbits extending rostrally underneath the nasals.

The prefrontal contribution to the crest was similarly poorly described by Brown (1912). Although Brown (1912, p. 135) remarked on a prefrontal process that laterally buttressed the crest, this arrangement was never figured. Subsequent workers (Ostrom 1961, Horner 1992, Horner et al. 2004) failed to recognise the role of the prefrontals in the crest of *Saurolophus*, instead maintaining the view that the nasals were entirely responsible for crest

formation. The prefrontals in CMN 8796, although broken, preserve the base of what would have been a caudodorsal extension that would have flanked the nasals as described by Brown (1912). In *S. angustirostris*, these processes are thin and intervene at the nasofrontal suture on the skull roof. If the identification of the prefrontal on AMNH 5221 is correct, then that condition was also present in *S. osborni*.

Brown (1912) also indicated that the frontals extend laterally to form the dorsal margin of the orbit; however in all three specimens, a suture is apparent between the frontals and postorbitals, which excludes the frontals from the orbital margin, a conclusion reached first by Horner (1992). The prefrontal, which forms the dorsal orbital rim in front of the postorbital is associated with a supraorbital element as suspected by Coombs (pers. comm. in Maryańska and Osmólska 1979). These elements were mislabelled by Brown (1912) as the frontal and prefrontal, respectively. Although it is only visible in AMNH 5220, it is apparent that the suture between these two elements did not close until late in life and perhaps did not close at all. This condition is peculiar to *S. osborni* amongst hadrosaurs. Although supraorbitals have been observed in juvenile hadrosaurines (including *S. angustirostris* Maryańska and Osmólska 1979, ZPAL MgD-1/159), the suture between them tends to close relatively early in ontogeny such that it is obscured in subadult and adult individuals. A closed suture has

also been suspected in an adult specimen of *Kerberosaurus* (Bolotsky and Godefroit 2004).

By combining information from both palatines in NMC 8796, a dorsal extension of the palatine is demonstrated for the first time (contra Heaton 1972). This extension clearly shows the elongate contact with the pterygoid typical in all hadrosaurids.

Although it is not the intension of the current study to speculate on the dispersal of this group, the relationship between *Kerberosaurus, Prosaurolophus,* and *Saurolophus* indicates a complex evolutionary history. The solid cranial crest appears to have evolved at least twice in hadrosaurine phylogeny; once in the group that led to *Brachylophosaurus* and *Maiasaura* and again in the *Kerberosaurus-Prosaurolophus-Saurolophus* clade. Depending on the phylogenetic position of the flat-headed hadrosaurine *Kerberosaurus*, then the non-crested condition was either secondarily developed or was the primitive condition for *Prosaurolophus* and *Saurolophus*. Crest elongation in crested hadrosaurines (exemplified by *Saurolophus*) appears to have resulted in the convergence of several characters with some lambeosaurines, in particular with the 'parasaurolophs' (*Parasaurolophus* and *Charonosaurus*), whose crests most closely resemble that of *Saurolophus*. Crest elongation was accompanied by elongation of the frontals into a form of dorsal promontorium and by down-warping of the frontal-parietal suture to form an obtuse angle between these two elements in lateral view. In

taxa most closely related to *Saurolophus* (*Kerberosaurus* and *Prosaurolophus*) where the crest is either absent or incipient, these character states are absent. This is the case in all other hadrosaurines except *Brachylophosaurus*, in which crest elongation has indeed occurred and is accompanied by down-warping of the frontal-parietal suture.

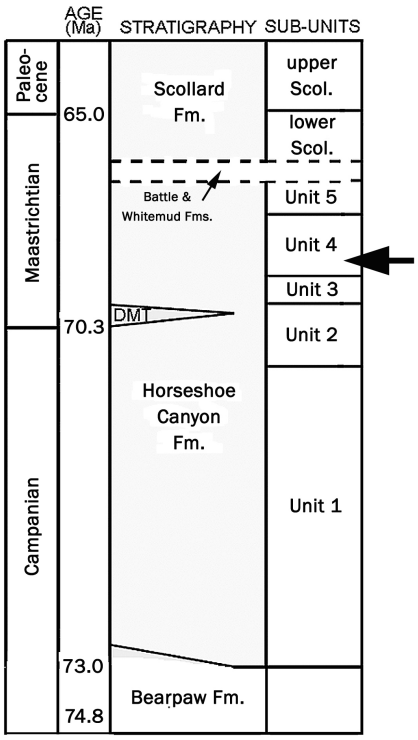

Figure 2.1. Stratigraphic column of latest Cretaceous deposits in the Central Plains of Alberta (adapted from Eberth 2004). Large arrow indicates the approximate stratigraphic position of *Saurolophus osborni*. DMT, Drumheller marine tongue.

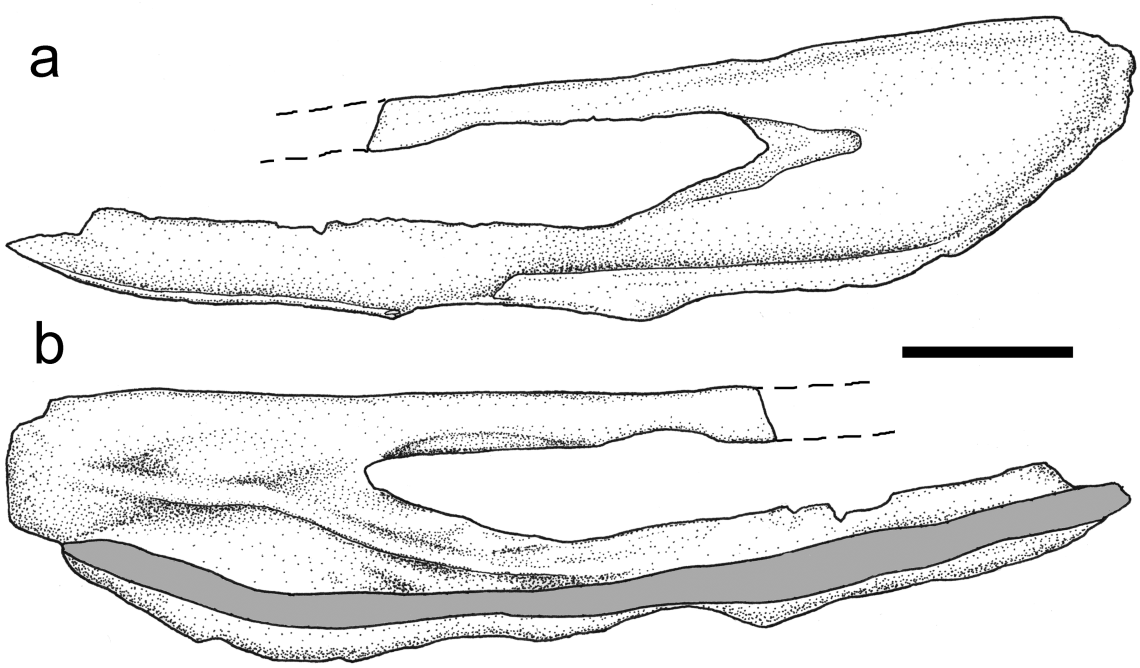

Figure 2.2. Right premaxilla of AMNH 5221 in A. lateral and, B. medial views. Scale = 10cm. Dashed lines denote approximate outline of missing areas. Shading identifies area obscured by plaster in the original specimen.

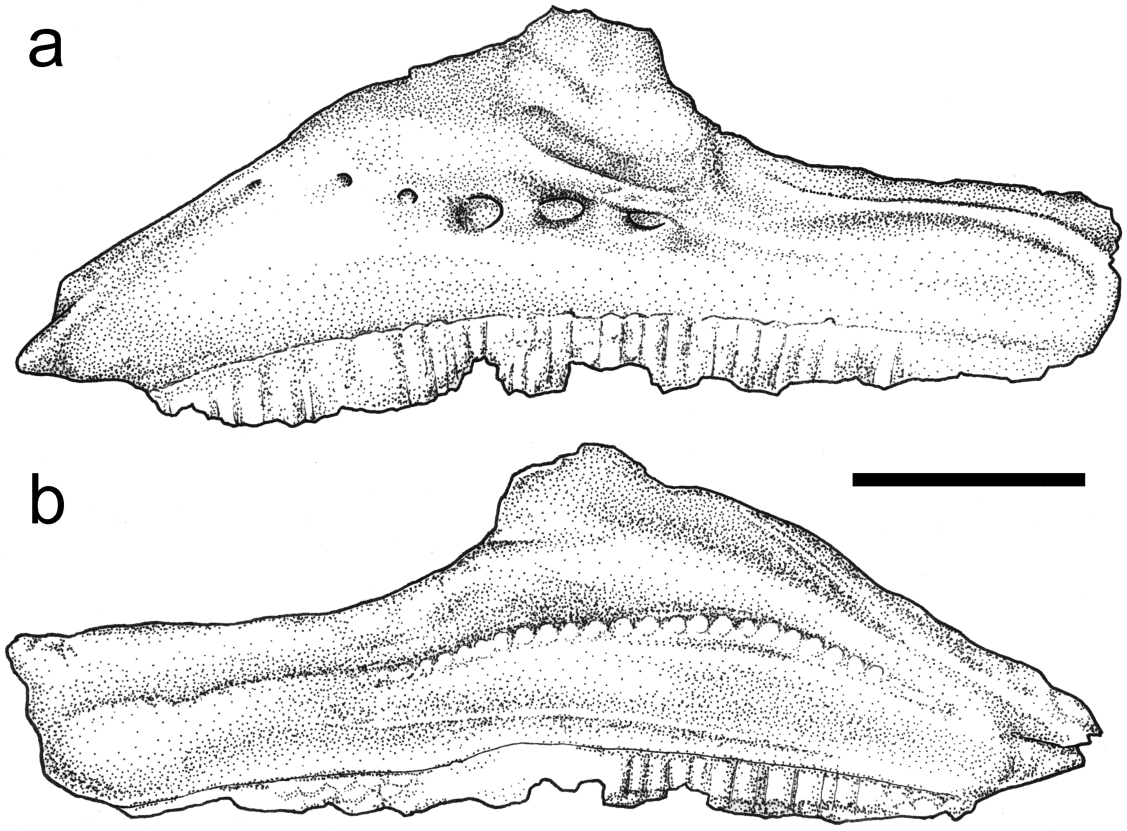

Figure 2.3. Left maxilla of AMNH 5221 in A. lateral and, B. medial views. Scale = 10cm.

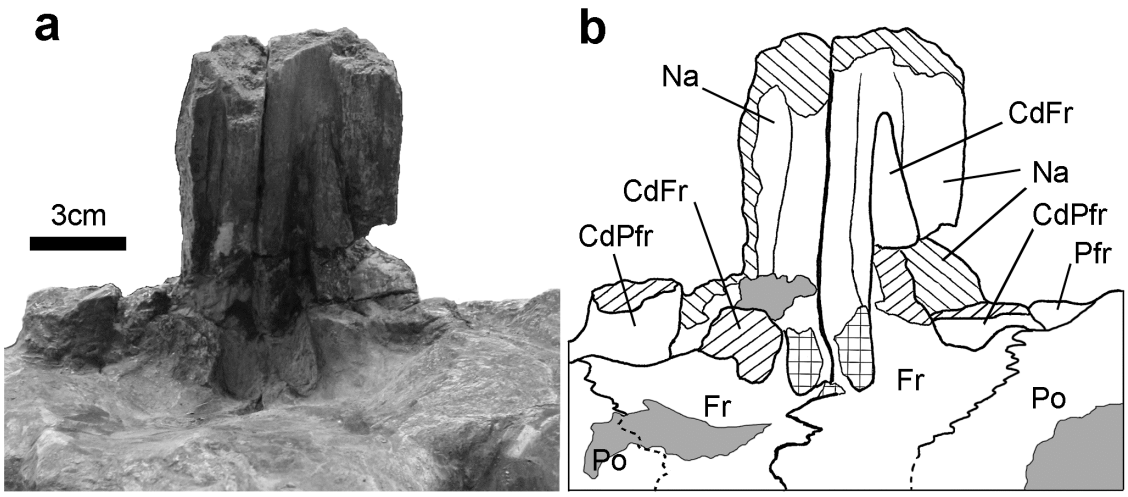

Figure 2.4. Naso-Frontal contact in *Saurolophus* (CMN 8796). A, photograph of the underside of the crest looking anteriorly. B. Interpretive drawing. Dashed lines denote approximate outline of missing areas. Shading identifies area obscured by plaster in the original specimen. Parallel lines represent broken surfaces. Cross-hatching represents matrix. CdFr, caudodorsal process of frontal; CdPfr, caudodorsal process of prefrontal; Fr, frontal; Na, nasal; Pfr, prefrontal; Po, postorbital.

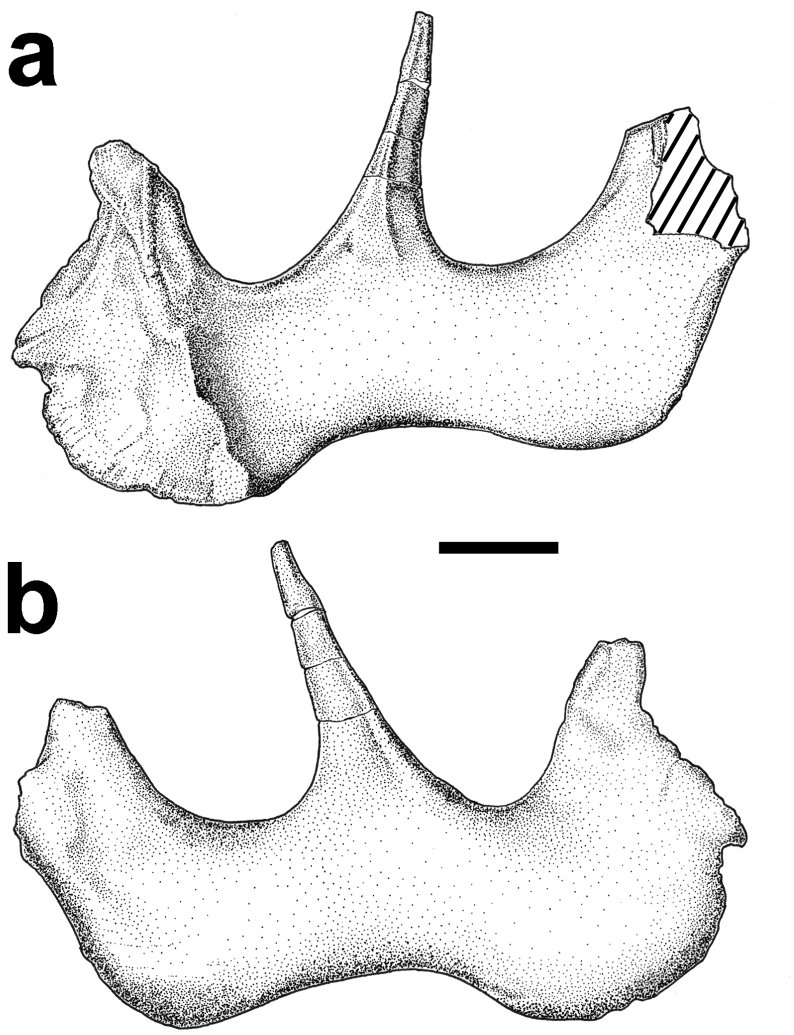

Figure 2.5. Right jugal of AMNH 5221 in A. lateral and, B. medial views. Scale = 5cm. Parallel lines denote broken surface.

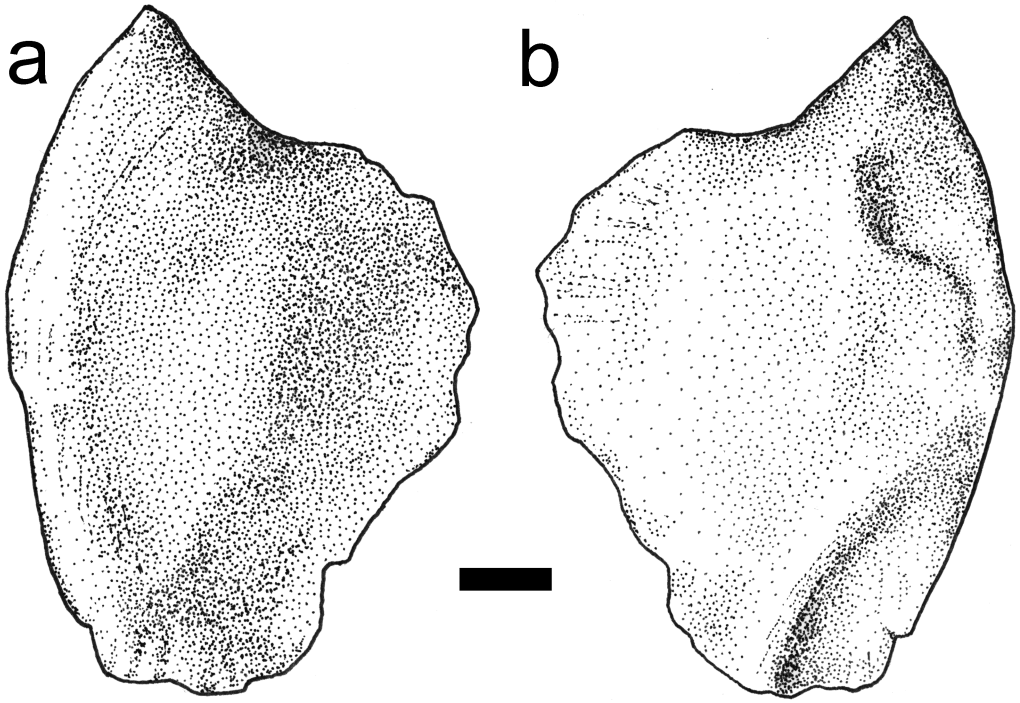

Figure 2.6. Left quadratojugal of AMNH 5221 in A. lateral and, B. medial views. Scale = 2cm.

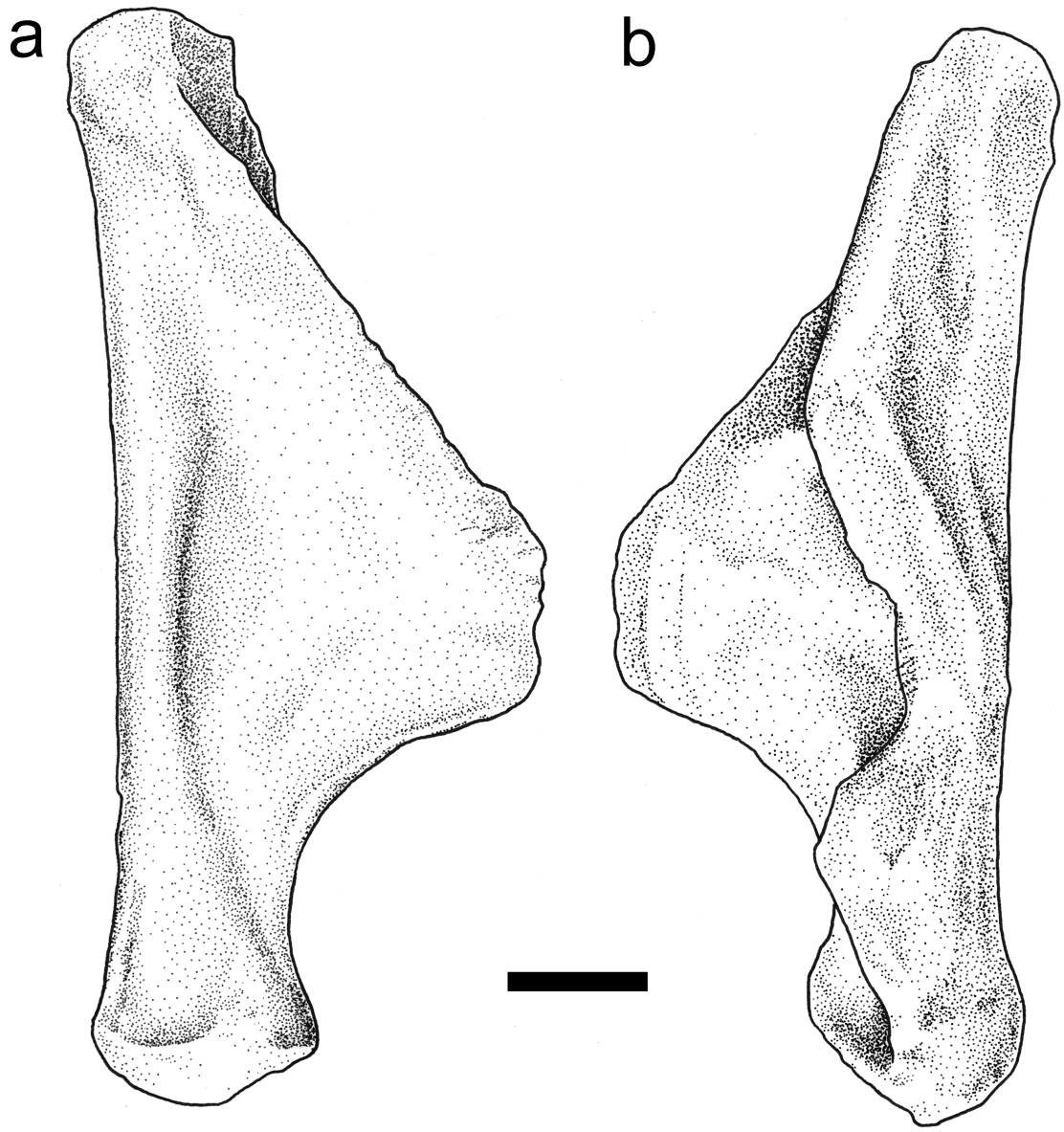

Figure 2.7. Left quadrate of holotype 5220 in A. lateral and, B. medial views.

Scale = 5cm.

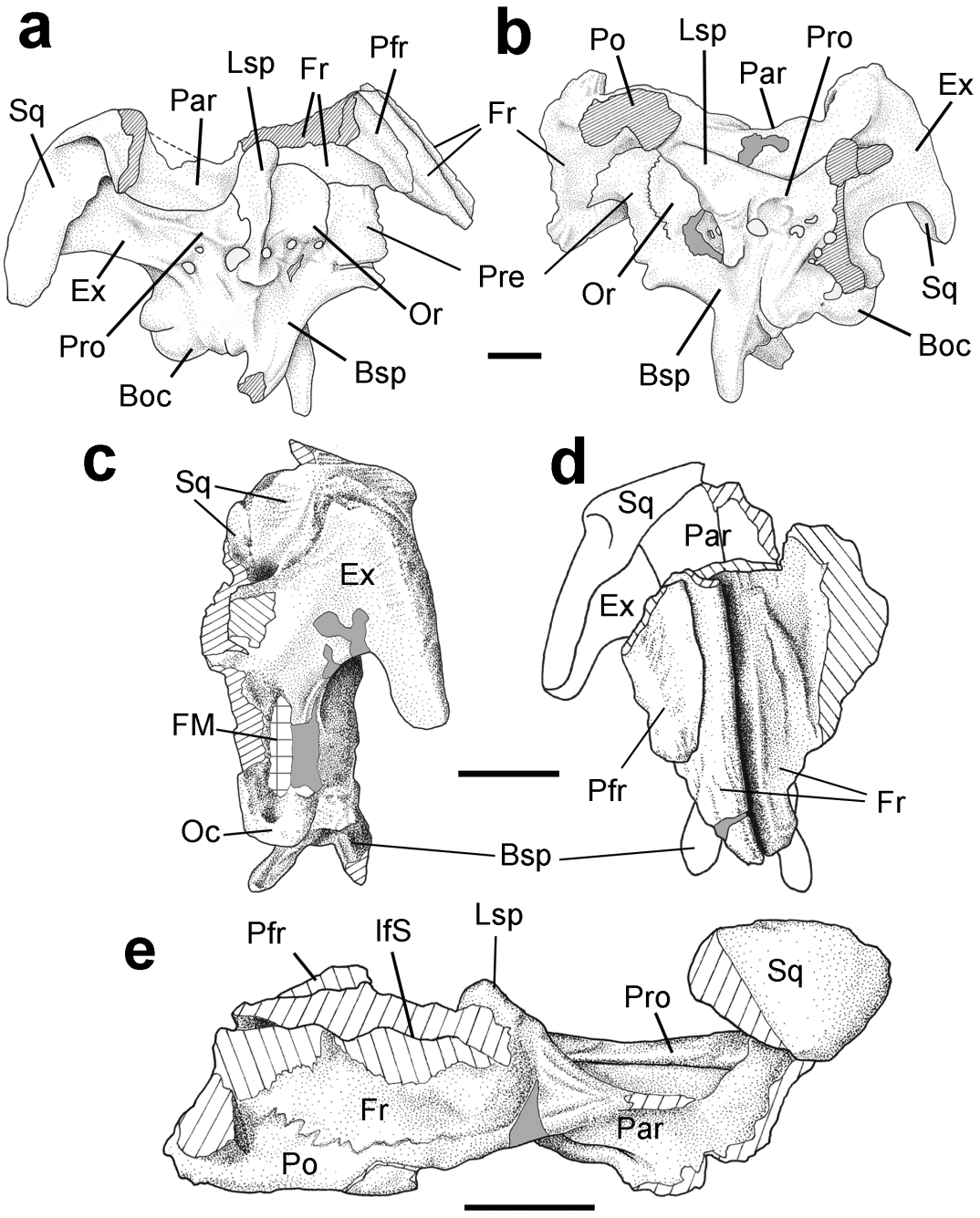

Figure 2.8. Braincase of AMNH 5221 in A. right lateral, B. left lateral, C. caudal, D. rostral, and E. dorsal views. Scale = 5cm. Shading identifies area obscured by plaster in the original specimen. Parallel lines represent broken surfaces. Cross-hatching represents matrix. Boc, basioccipital; Bsp, basisphenoid; Ex, exoccipital-

opisthotic complex; FM, foramen magnum; Fr, frontal; Ifs, interfrontal suture; Lsp, laterosphenoid; Orb, orbitosphenoid; Par, parietal; Pre, presphenoid; Pfr, prefrontal; Po, postorbital; Pro, prootic; Sq, squamosal.

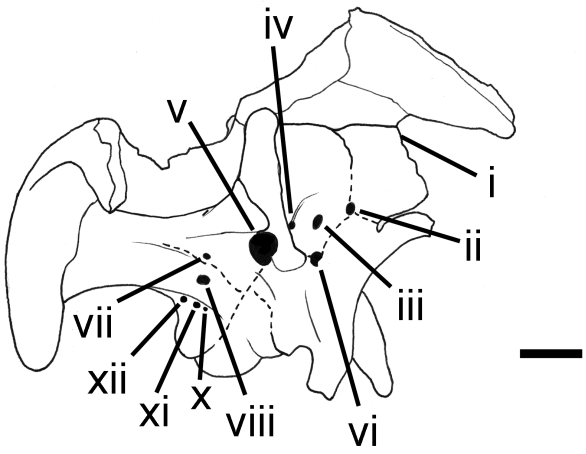

Figure 2.9. Schematic drawing of the braincase based on AMNH 5221 in right lateral aspect showing foramina for cranial nerves (I–XII) and approximate boundaries (dashed lines) between elements. Scale = 5cm.

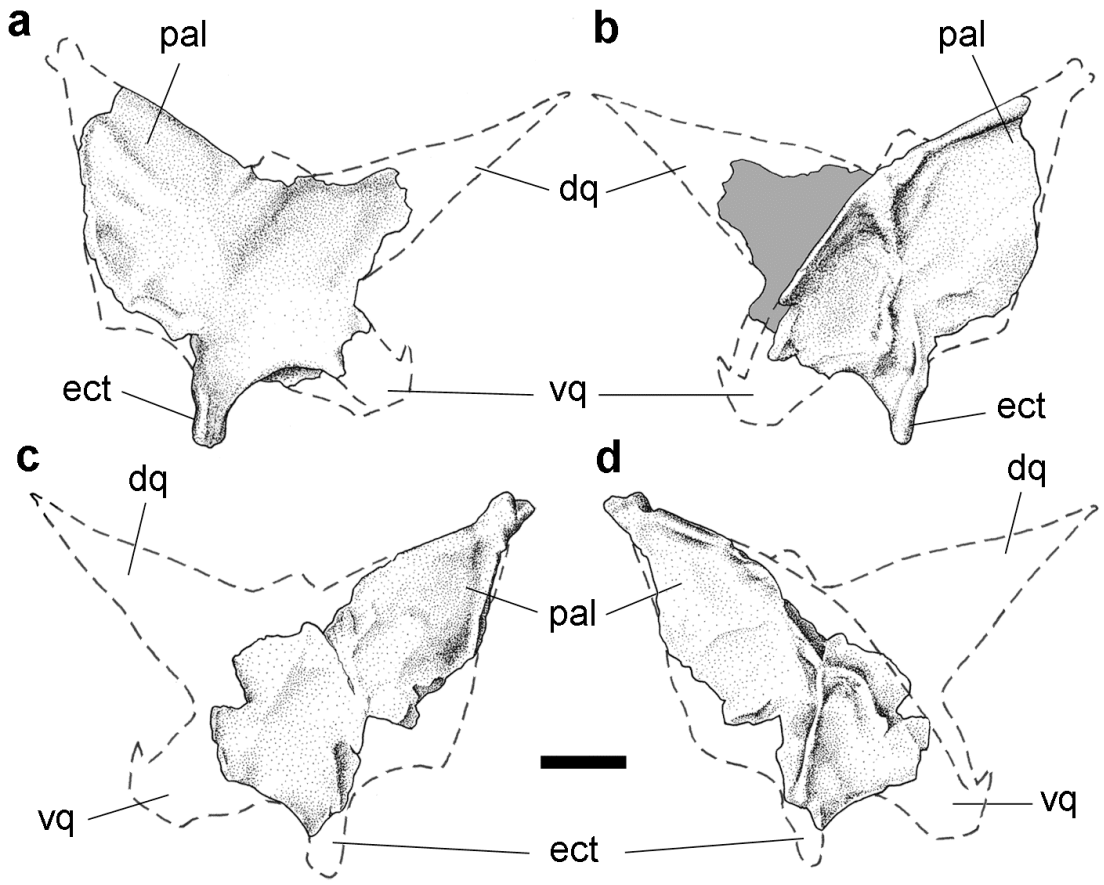

Figure 2.10. Pterygoids of AMNH 5221. A–B, left pterygoid in A. lateral and B. medial views. C–D, right pterygoid in C. lateral and B. medial views. Scale = 5cm. dq, dorsal quadrate process; ect, ectopteygoid process; pal, palatine process; vq, ventral quadrate process. Dashed line indicates the approximate outline of the missing regions; shading indicates area obscured by plaster.

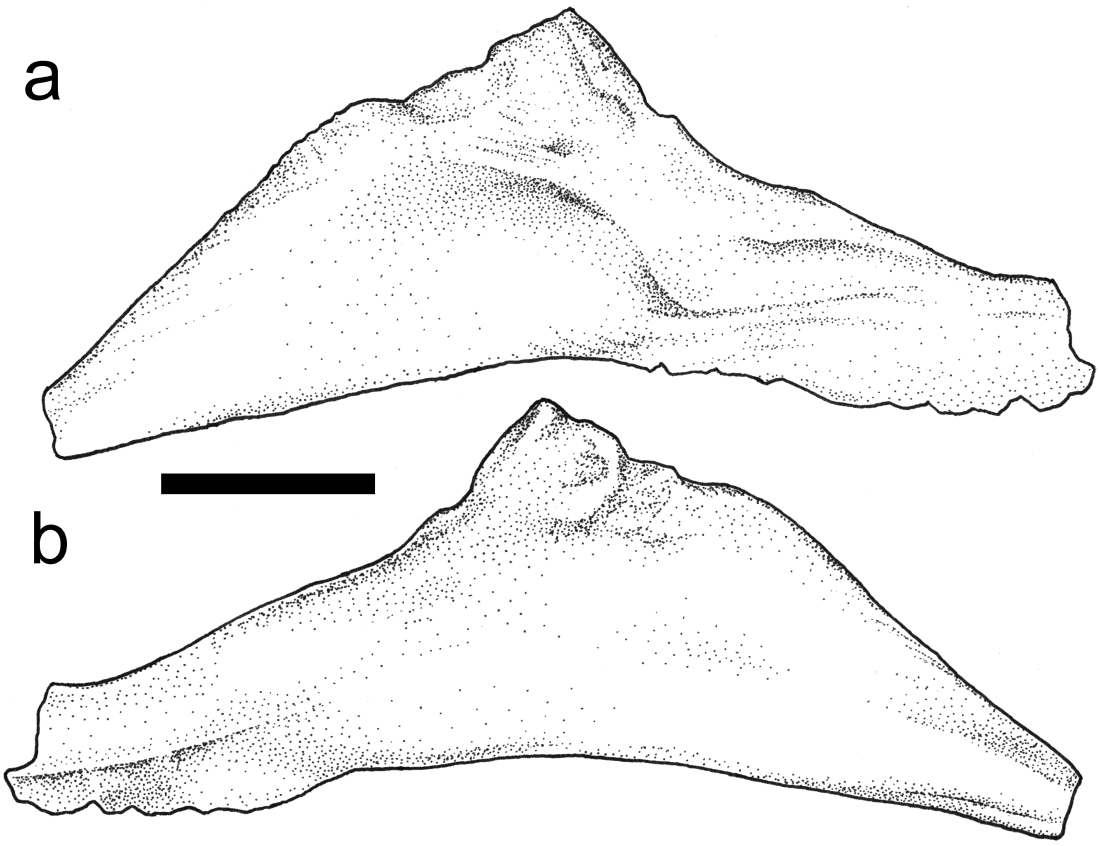

Figure 2.11. Left vomer of AMNH 5221 in A. lateral and B. medial views. Scale = 5cm.

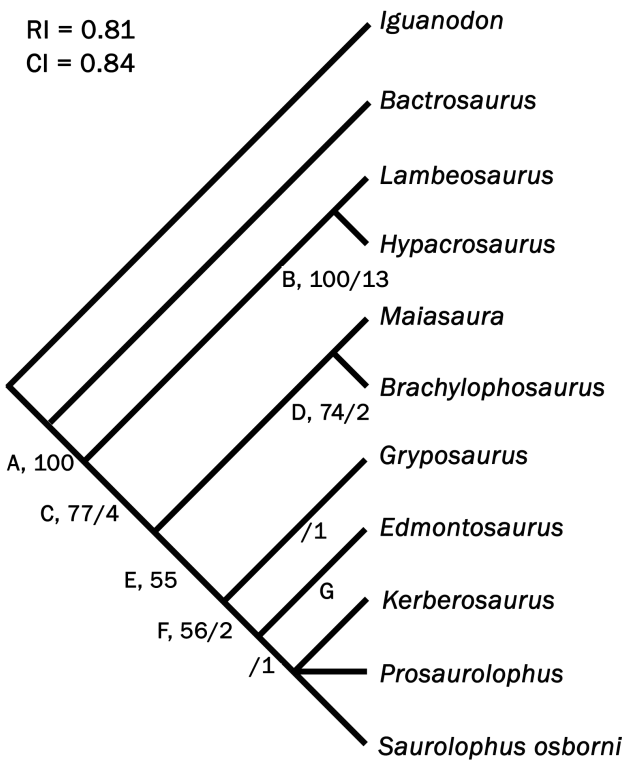

Figure 2.12. Strict consensus of three most parsimonious trees resulting from a maximum parsimony analysis using the exhaustive search option of nine ingroup and two outgroup taxa. Numbers are bootstrap values/decay indices. A, Hadrosauridae, 8(1), 19(1), 23(1), 25(1), 27(1), 29(1), 30(1), 33(1), 34(1), 35(1), 36(1), 37(1), 38(2), 39(1); B, Lambeosaurinae, 1(1), 3(1), 4(1), 5(1), 6(1), 7(1), 10(1), 12(1), 13(1), 15(2), 17(1), 20(1), 21(1), 31(1), 32(1), 40(1); C, Hadrosaurinae, 2(1), 11(1), 16(1), 28(1); D, unnamed taxon, 22(1), 27(2), 37(2); E, unnamed taxon, 24(1); F, unnamed taxon, 15(1), 16(2); G, *Edmontosaurus*, 9(3), 32(1), 38(3).

References

Bolotsky, Y.L., Godefroit, P., 2004. A new hadrosaurine dinosaur from the Late Cretaceous of far eastern Russia. Journal of Vertebrate Paleontology 24, 351–365.

Brown, B., 1912. A crested dinosaur from the Edmonton Cretaceous. Bulletin of the American Museum of Natural History 31, 131–136.

Brown, B., 1913. The skeleton of *Saurolophus*, a crested duck-billed dinosaur from the Edmonton Cretaceous. Bulletin of the American Museum of Natural History 32, 387–393.

Eberth, D.A., 2004. A revised stratigraphy for the Edmonton Group (Upper Cretaceous) and its potential sandstone reservoirs. CSPG-CHOA-CWLS Joint Conference, Calgary, Alberta, May 31-June 4, 2004; Pre-Conference Field Trip #7, 44 p.

Eberth, D.A., Deino, A., 2005. New $^{40}Ar/^{39}Ar$ ages from three bentonites in the Bearpaw, Horseshoe Canyon and Scollard formations (Upper Cretaceous-Paleocene) of southern Alberta, Canada. In: D.R. Braman, F. Therrien, E.B. Koppelhus, W. Taylor (Eds.), Dinosaur Park Symposium, Short Papers, Abstracts, and Program, Royal Tyrrell Museum, Drumheller, Alberta, September 24-25, 2005, Special Publication of the Royal Tyrrell Museum, pp. 23–24.

Evans, D.C., Reisz, R.R., Dupuis, K., 2007. A juvenile *Parasaurolophus* (Ornithischia: Hadrosauridae) braincase from Dinosaur Provincial Park, Alberta, with comments on crest ontogeny in the genus. Journal of Vertebrate Paleontology 27, 642–650.

Gates, T.A., Sampson, S.D., 2007. A new species of *Gryposaurus* (Dinosauria: Hadrosauridae) from the late Campanian Kaiparowits Formation, southern Utah, USA. Zoological Journal of the Linnean Society 151, 351–376.

Godefroit, P., Dong, J.D., Orth, C.J., Pillmore, C.L., Tschudy, R.H., 1998. *Bactrosaurus* (Dinosauria: Hadrosauroidea) material from Iren Dabasu (Inner Mongolia, P. R. China). Bulletin de l'Institut royal des Sciences naturelles de Belgique, Sciences de la Terre 68 (Supplement), 3–70.

Godefroit, P., Zan, S., Jin, L., 2001. The Maastrichtian (Late Cretaceous) lambeosaurine dinosaur *Charonosaurus jiayinensis* from north-eastern China. Bulletin de l'Institut royal des Sciences naturelles de Belgique, Sciences de la Terre 71, 119–168.

Godefroit, P., Hai, S., Yu, T., Lauters, P., 2008. New hadrosaurid dinosaurs from the uppermost Cretaceous of northeastern China. Acta Palaeontologica Polonica 53, 47–74.

Heaton, M.J., 1972. The palatal structure of some Canadian Hadrosauridae (Reptilia: Ornithischia). Canadian Journal of Earth Sciences 9, 185–205.

Hopson, J.A., 1975. The evolution of cranial display structures in hadrosaurian dinosaurs. Paleobiology 1, 21–43.

Horner, J., 1983. Cranial osteology and morphology of the type specimen of *Maiasaura peeblesorum* (Ornithischia: Hadrosauridae), with discussion of its phylogenetic position. Journal of Vertebrate Paleontology 3, 29–38.

Horner, J., 1992. Cranial morphology of *Prosaurolophus* (Ornithischia: Hadrosauridae) with descriptions of two new hadrosaurid species and an

evaluation of hadrosaurid phylogenetic relationships. Museum of the Rockies Occasional Paper No. 2, 119 pp.

Horner, J.R., Currie, P.J., 1994. Embryonic and neonatal morphology and ontogeny of a new species of *Hypacrosaurus* (Ornithischia, Lambeosauridae) from Montana and Alberta. In: K. Carpenter, K.F. Hirsch, J.R. Horner (Eds.), Dinosaur Eggs and Babies. Cambridge University Press, Cambridge, U.K., pp. 312–336.

Horner, J.R., Weishampel, D.B., Forster, C.A., 2004. Hadrosauridae. In: D.B. Weishampel, P. Dodson, H. Osmólska (Eds.), The Dinosauria, (Second Edition). University of California Press, Berkeley, California, pp. 438-463.

Lull, R.S., Wright, N.E., 1942. Hadrosaurian dinosaurs of North America. Geological Society of America, Special Paper 40, 242 pp.

Lund, E., Gates, T., 2006. A historical and biogeographical examination of hadrosaurid dinosaurs. Bulletin of the New Mexico Museum of Natural History 35, 263-276.

Maryańska, T., Osmólska, H., 1979. Aspects of hadrosaurian cranial anatomy. Lethaia 12, 265-273.

Maryańska, T., Osmólska, H., 1981. Cranial anatomy of *Saurolophus angustirostris* with comments on the Asian Hadrosauridae (Dinosauria). Palaeontologia Polonica 42, 5-24.

Maryańska, T., Osmólska, H., 1984. Post-cranial anatomy of *Saurolophus angustirostris* with comments on other hadrosaurs. Palaeontologia Polonica 46, 119-141.

Morris, W.J., 1973. A review of Pacific coast hadrosaurs. Journal of Paleontology 47, 551–561.

Norman, D., Sues, H.-D., 2000. Ornithopods from Kazakhstan, Mongolia and Siberia. In: M.J. Benton, M.A. Shishkin, D.M. Unwin, E.N. Korochin (Eds.), The Age of Dinosaurs in Russia and Mongolia. Cambridge University press, Cambridge, UK, pp. 462-479.

Ostrom, J.H., 1961. Cranial morphology of the hadrosaurian dinosaurs of North America. Bulletin of the American Museum of Natural History 122, 33-186.

Prieto-Marquez, A., 2005. New information of the cranium of *Brachylophosaurus Canadensis* (Dinosauria, Hadrosauridae), with a revision of its phylogenetic position. Journal of Vertebrate Paleontology 25, 144–156.

Prieto-Marquez, A., Gaete, R., Rivas, G., Galobart, A., Boada, M., 2006. Hadrosauroid dinosaurs from the Late Cretaceous of Spain: *Pararhabdodon isonensis* revisited and *Koutalisaurus kohlerorum* gen. et sp. nov. Journal of Vertebrate Paleontology 26, 929–943.

Rozhdestvenskii, A.K., 1952. A new representative of duckbilled dinosaurs from the Upper Cretaceous deposits of Mongolia (in Russian). Doklody Akademic SSSR 86, 405-408.

Russell, D.A., Chamney, T.P., 1967. Notes on the biostratigraphy of dinosaurian and microfossil faunas in the Edmonton Formation (Cretaceous), Alberta. National Museum of Canada Natural History Papers 35, 22 p.

Rybczynski, N., Tirabasso, A., Cuthbertson, R., Holliday, C., 2008. A three dimensional animation of *Edmontosaurus* for testing chewing hypotheses. Paleontologica Electronica 11, issue 2; 9A, 1-14, http://palaeo-electronica.org/2008_2/132/index.html. Accessed 10/10/08.

Srivastava, S., 1968. Assorted angiosperm pollen from the Edmonton Formation (Maestrichtian), Alberta, Canada. Canadian Journal of Botany 47, 975-989.

Srivastava, S., 1970. Pollen biostratigraphy and palaeoecology of the Edmonton Formation (Maestrichtian), Alberta, Canada. Palaeogeography, Palaeoclimatology, Palaeoecology 7, 221-276.

Sternberg, C.M., 1935. Hooded hadrosaurs of the Belly River series of the Upper Cretaceous: a comparison with description of new species. Bulletin of the American Museum of Natural History 77, 1-37.

Swofford, D.L., 2002. Phylogenetic analysis using parsimony (and other methods). Version 4.0b10. Sinauer Associates, Sunderland, Massaschusetts, 40pp.

Weishampel, D.B., Horner, J.R., 1990. Hadrosauridae. In D. Weishampel, P. Dodson, H. Osmólska (Eds.) The Dinosauria. University of California Press, Berkeley, pp. 534-561.

Weishampel, D.B., Norman, D.B., Grigorescu, D., 1993. *Telmatosaurus transsylvanicus* from the Late Cretaceous of Romania: the most basal hadrosaurid dinosaur. Palaeontology 36, 361–385.

Appendix 2.1: Character matrix and character desciptions

Character matrix and character descriptions used in this study as compiled and modified from Weishampel et al. (1993), Godefroit (1998, 2008), Bolotsky and Godefroit (2004), Horner et al. (2004), and Prieto-Marquez (2005).

	1-5	6-10	11-15	16-20	21-25	26-30	31-35	36-40	41-44
Iguanodon	00000	00000	00000	00000	00000	00000	00000	00000	0000
Bactrosaurus	00000	00000	00000	00000	00000	00000	00000	00000	0000
Lambeosaurus	01011	11110	10110	20110	11101	00011	10111	21111	1211
Hypacrosaurus	01011	11110	10110	20120	11101	00011	10111	21111	1211
Maiasaura	00100	00011	01000	01002	10011	00012	21110	01111	2210
Brachylophosaurus	00100	00011	01001	01201	10011	00012	21110	11121	2210
Gryposaurus	00100	00012	01001	01000	10001	10013	11110	01111	1210
Kerberosaurus	001?1	000??	?????	?2??0	10001	1?013	11110	?11??	??2?0
Prosaurolophus	00101	00012	01001	12001	10001	10013	11110	01121	1210
Edmontosaurus	00100	00013	01001	12000	10001	11013	11110	21131	1310
Saurolophus osborni	10111	02212	01001	12202	1210?	?0013	11110	01121	?210

Character Descriptions

1. Parietal: participates in occipital aspect of skull (0); completely excluded from the occiput (1).
2. Parietal: "length/minimal width" >2 (0); <2 (1).
3. Parietal: sagittal crest short, <2/3 the length of parietal (0); long, >2/3 the length of the parietal (1).
4. Parietal: midline ridge straight to slightly downwarped along length (0); strongly downwarped to below the level of the postorbital-prefrontal joint (1).
5. Frontal: participates in the orbital rim (0); excluded by postorbital-prefrontal joint (1)
6. Hollow supracranial crest: absent (0); present (1).
7. Frontal: long, "caudal length/maximal width" ratio >0.74 (0); very shortened, "caudal length/maximal width" ratio <0.6 (1); secondary elongation resulting in the backwards extension of the frontal platform (2).
8. Frontal platform: absent (0); occupying the rostral part of the frontal in adult (1); extends above rostral portion of the supratemporal fenestra (2).
9. Premaxilla: narrow, expanded laterally less than two times width at post-oral constriction, margin oriented nearly vertically (0); expanded transversely to more than two time post-oral constriction, margin flared laterally into a more horizontal orientation (1).
10. Premaxilla: reflected rim absent (0); deflected at anterolateral corner and posteriorly reflected (1); reflected along entire rim and narrow (2); reflected along entire rim, but thickened at anteroventral corner (3).
11. Premaxillary foramen present (0); absent (1).
12. Premaxilla: auxillary narial fossa absent (0); present (1).

13. Posterior premaxillary process: short, not meeting the lateral premaxillary process posterior to external naris (0); long, meets the lateral premaxillary process behind external naris to exclude the nasal, nasal passage enclosed ventrally by folded, divided premaxillae.
14. Lateral premaxillary process stops at level of lacrimal (0); continues further backward above skull roof (1).
15. External naris/basal skull length ratio <0.2 (0); >0.2 (1).
16. external naris: posterior apex formed entirely by nasal (0); formed by nasal (dorsally) and premaxilla (ventrally) (1); formed entirely by premaxilla (2).
17. Circumnarial depression absent (0); light depression incised into nasal and premaxilla (1); marked by a well-developed ridge and sometime invaginated (2).
18. Nasal: restricted to area rostral to braincase, *cavum nasi* small (0), retracted caudally to lie over braincase in adults resulting in convoluted, complex narial passageway, *cavum nasi* enlarged (1); retracted caudally to lie over braincase, narial passageway simple (2). Extra character state added to match condition in *S. osborni* and *B. canadensis*.
19. Nasal: does not participate in hollow crest (0); participates in small part of the hollow crest and is excluded from the caudodorsal margin of the crest (1); participates in half of the crest or more and forms the caudodorsal aspect of the crest (2).
20. Solid supracranial crest: absent (0); formed by nasals only (1); formed by nasals and frontals with or without contribution from prefrontals (2).
21. Supraorbital free in adults (0); fused to prefrontal (1).
22. Prefrontal: caudal portion oriented horizontally (0); participates in the lateroventral portion of the hollow crest (1); participates in the lateroventral portion of the solid crest (2). State added to match condition in *S. osborni.*
23. Squamosal: medial ramus lower than paroccipital process (0); higher than paroccipital process (1).
24. Squamosal: prequadratic process strikingly longer than rostrocaudal length of quadrate cotylus (0); only slightly longer than rostrocaudal length of quadrate cotylus (1).
25. Supraoccipital: posterior surface nearly vertical (0); steeply inclined forwardly at an angle of about 45° (1).
26. Supraoccipital/exoccipital shelf limited (0); very extended (1) above foramen magnum.
27. Postorbital pouch absent (0); well developed (1).
28. Postorbital: dorsal surface flat (0); thickened to form a dorsal promontorium (1).
29. Jugal: rostral process tapering in lateral view to fit between maxilla and lacrimal (0); dorsoventral expanded (1).
30. Jugal: rostral process angular and slightly asymmetrical in lateral view (0); rounded and symmetrically very expanded (1); isosceles-triangle shaped (2); asymmetrically strongly upturned (3).
31. Jugal flange: slightly developed, dorsoventral depth of jugal from ventral border of infratemporal fenestra to ventral edge of flange approximately equal to minimum dorsoventral depth of rostral segment of jugal between rostral and postorbital process (0); dorsoventral depth of jugal from ventral border of infratemporal fenestra to ventral edge of flange less than twice

minimum depth of rostral segment of jugal between rostral and postorbital process (1); strongly projected ventrally into semicircular boss, dorsoventral depth of jugal from ventral border of infratemporal fenestra to ventral edge of flange twice or nearly twice minimum dorsoventral depth of rostral segment of jugal between rostral and postorbital process (2).

32. Maxilla: apex caudal to centre (short caudal portion of maxilla) (0); at or rostral to centre (long and robust caudal portion of maxilla) (1).
33. Maxillary foramen: situated rostrolaterally (0); on dorsal maxilla and on premaxilla-maxilla suture (1).
34. Maxilla: ectopterygoid ridge faintly developed and inclined caudally (0); strongly developed and nearly horizontal (1).
35. Maxilla: rostromedial process present (0); wide sloping maxillary shelf (1).
36. Lacrimal-maxilla contact: present (0); extremely reduced, only anterior sharp tip of lacrimal contacting maxilla (1); lost or covered as result of jugal-premaxilla contact (2).
37. Paraquadratic foramen: present (0); absent (1).
38. Quadrate: distal head transversely expanded (0); dominated by a large hemispherical lateral condyle (1).
39. Dentary: diastema between first dentary tooth and predentary short, no more than width of 4 or 5 teeth (0); moderate, equal to approximately 1/5 to ¼ of tooth row (1); long, more than 1/3 of tooth row but less than 1/2 (2); extremely long, more than 1/2 of tooth row (3).
40. Dentary: coronoid process sub-vertical (0); inclined rostrally (1).
41. Predentary: rostral mediolateral width less than or equal to rostrocaudal length of lateral process (0); greater than or equal to rostrocaudal length of lateral process (1); greater than twice rostrocaudal length of lateral process (2).
42. Dentary: number of tooth positions in adult specimen, ≤30 (0); 34–40 (1); 42–45 (2); ≥47 (3).
43. Dentary: tooth crowns broad with dominant ridge and secondary ridges (0); miniaturised with or without faint secondary ridges (1).
44. Dentary: median carina of teeth straight (0); sinuous (1).

CHAPTER 3

CRANIAL OSTEOLOGY AND ONTOGENY OF *SAUROLOPHUS ANGUSTIROSTRIS* FROM THE LATE CRETACEOUS OF MONGOLIA WITH COMMENTS ON *SAUROLOPHUS OSBORNI* FROM CANADA

A version of this chapter has been accepted for publication: Bell, P. R. *In press.* Cranial osteology and ontogeny of *Saurolophus angustirostris* from the Late Cretaceous of Mongolia with comments on *Saurolophus osborni* from Canada. *Acta Palaeontologica Polonica.*

Introduction

The Upper Cretaceous beds of southern Mongolia are famous for their well-preserved and diverse dinosaur fauna. The ?late Campanian/early Maastrichtian Nemegt Formation alone has yielded tyrannosaurids, ornithomimids, oviraptorids, therizinosaurs, alvarezsaurids, troodontids, dromaeosaurids, avimimids, elmisaurids, ankylosaurids, hadrosaurids, and pachycephalosaurids (Weishampel et al. 2004). This diversity is palaeobiogeographically important as it is replicated in coeval beds from western North America, at least at the family level (Jerzykiewicz and Russell 1991). The only genus to occur in both regions is the hadrosaurid *Saurolophus,* represented by *S. angustirostris* from Mongolia and *S. osborni* from western Canada.

Saurolophus osborni was erected based on a virtually complete skull and skeleton from the early Maastrichtian upper Horseshoe Canyon Formation in southern Alberta, Canada (Brown 1912). The genus is notable for its solid rod-like cranial crest, which is comprised of the nasals, prefrontals, and frontals (Brown 1912; Bell 2010).

Between 1946 and 1949, the Soviet Palaeontological Expeditions to central Mongolia collected multiple skeletons of a new hadrosaurid from the localities of Nemegt and Altan Uul. Rozhdestvensky (1952) named the new animal *Saurolophus angustirostris,* stressing the gross similarity between immature specimens of that species to adults of its North American relative (Rozhdestvensky 1952, 1957, 1965). In the Nemegt Formation, *Saurolophus angustirostris* comprises approximately twenty percent of all vertebrate fossils (Currie 2009) found whereas only three unequivocal specimens of *S. osborni* have

so far been recovered from the Horseshoe Canyon Formation. Two incomplete specimens from the Moreno Formation, California, were designated as cf. *Saurolophus* by Morris (1973); however, the best-preserved specimen has recently been reassigned to Hadrosaurinae indet. (Bell and Evans 2010). A partial 'booted' ischium from the Amur region of far Eastern Russia was designated the type of *Saurolophus kryschtovici* by Riabinin (1930) based on comparison with the equally dubious plesiotype (AMNH 5225) of *S. osborni*. The plesiotype, an isolated but complete ischium from the same area as the holotype, was provisionally re-identified by Russell and Chamney (1967) as *Hypacrosaurus* and *S. kryschtovici* is unanimously regarded as a *nomen dubium* (Young 1958; Maryańska and Osmólska 1981; Weishampel and Horner 1990; Norman and Sues 2000; Horner et al. 2004).

The close similarity between the Mongolian and the Canadian species has led some authors to question the validity of *S. angustirostris.* In a supplementary description of that species, Maryańska and Osmólska (1984) listed eight cranial characters that apparently distinguished *S. angustirostris* from other hadrosaurids; however, Norman and Sues (2000) argued that the diagnostic characters listed by Maryańska and Osmólska (1984) for *S. angustirostris* may fall into the realm of individual variation. Horner (1992) later attempted to distinguish the two species by the presence of a 'frontal buttress' (posterodorsal process sensu Bell 2010) in only *S. angustirostris*. This feature has since been identified as a synapomorphy of the genus (Bell 201).

Saurolophus angustirostris is represented by multiple well-preserved skulls, the largest of which (PIN 551/357) is approximately 300% longer than the smallest (ZPAL MgD-1/159) specimen (Table 1). These specimens provide the

opportunity to separate phylogenetically important characters from individual and ontogenetic variation. The purpose of this study is to redescribe the skull of *S. angustirostris* with a focus on ontogenetic and individual variation (particularly the braincase and cranial crest) and to provide an updated diagnosis of the genus. Where possible, bones of *S. angustirostris* are compared with the corresponding element in *S. osborni* described in detail by Bell (2010) in order to reassess the interrelationships of these two species.

Methods and materials

Descriptions of *Saurolophus angustirostris* are based on an ontogenetic series represented by KID 476 (partial adult skull), ZPAL MgD-1/159 (juvenile skull and partial skeleton), ZPAL MgD-1/162 (partial subadult skull), ZPAL MgD-1/173 (partial subadult skull), MPC 100/706 (adult skull and skeleton), MPC 100/764 (adult skull), PIN 551/8 (holotype; subadult skull and skeleton), PIN 551/357 (partial adult skull), PIN 551/358 (adult skull), PIN 551/359 (juvenile skull), PIN 551/407 (adult mandible), UALVP49067 (subadult skull). All specimens come from the late Campanian-?Maastrichtian Nemegt Formation from the areas of Nemegt and Altan Uul, Mongolia except UALVP49067 and MPC 100/764, which are of unknown provenance.

All definitive specimens of *S. osborni* were included in the comparisons: AMNH 5220 (holotype; adult skull and skeleton), AMNH 5221 (paratype; adult skull and partial postcrania), CMN 8796 (adult skull).

Age class designations follow Evans' (2010) adaptation of Horner et al. (2000) where 'juvenile' corresponds to a skull length of less than 50% of the

maximum observed skull length. 'Subadults' are defined as individuals with a skull length of 50–85% and 'adults' are greater than 85% of the maximum observed skull length.

Systematic palaeontology

Dinosauria Owen, 1842

Ornithischia Seeley, 1887

Ornithopoda Marsh, 1881

Hadrosauridae Cope, 1869

Hadrosaurinae Lambe, 1918

Genus *Saurolophus* Brown, 1912

Amended diagnosis.— Large hadrosaurine hadrosaurid (up to 12 m long) with the following apomorphies: solid, caudodorsally-directed cranial crest composed of the nasals, prefrontals, and frontals that extends posterior to the squamosals in adults; posterodorsal process of prefrontal and frontal united to form dorsal promontorium that buttresses the underside of the nasal crest; frontals tripartite. Differs from other hadrosaurines with the additional characteristics: frontals excluded from the orbital rim by the postorbital-prefrontal complex; two supraorbital elements; parietal excluded by the squamosals from posterodorsal margin of occiput.

Saurolophus angustirostris Rozhdestvensky, 1952

Holotype: PIN 551/8

Type locality: Nemegt, Mongolia.

Type Horizon: Nemegt Formation (?upper Campanian/lower Maastrichtian)

Amended diagnosis.—Differs from *S. osborni* in having a skull that is at least 20% longer among the largest adults; premaxilla with strongly reflected oral margin and upturned premaxillary body in lateral aspect; broadly arcing anterior margin of the prenarial fossa; an elongate, anteriorly directed spur on the anterior process of the jugal that separates the lacrimal and maxilla, more so than in *S. osborni*; shallow quadratojugal notch on the quadrate; and more strongly bowed quadrate in lateral view.

Comparative description of the skull of *S. angustirostris*

Skull

The skull is typically hadrosaurine in general morphology (see descriptions) and forms a right triangle in lateral view at its ventral and posterior edges (Fig. 3.1). The largest specimens are significantly longer than the largest skulls of *S. osborni* (t-test=3.18, degrees of freedom=3, α=0.05). The most conspicuous feature of the skull is the solid, rod-like crest that extends posterodorsally from the skull roof and which projects beyond the squamosals in the largest specimens. In juveniles, the orbit is shaped like an inverted pear, but in adults it is posterodorsally reclined from the vertical and elongate. The

infratemporal fenestra forms a posterodorsally elongate ellipse and the supratemporal fenestra is elliptical.

*Premaxilla***.** The paired premaxillae form the anterior oral margin and contribute at least 50% of the length of the skull (measured from the anterior tip of the premaxilla to the posterior tip of the nasal crest). In lateral view, the body of the premaxilla is strongly upturned and the lateral margins are reflected although not as exaggerated as *Edmontosaurus regalis* (CMN 2288). In *S. osborni*, the dorsal margin of the premaxilla is straight in lateral view and the oral margin is only weakly reflected, similar to *Prosaurolophus*. The lateral premaxillary margins of *S. angustirostris* are perforated by numerous small foramina. Along the midline, the premaxillae meet to form a sharp sagittal keel that extends the length of the body of the premaxilla. The premaxillae fuse anteriorly only in adults. In articulated specimens viewed dorsally, the posterodorsal process of *S. angustirostris* is visible until it reaches the posterior margin of the external naris and attenuates posteriorly under the nasals. It extends posteriorly beyond this point, although its posterior terminus is obscured by the nasals. The posterodorsal process is triangular in cross-section for its entire length. The posterolateral process is plate-like. It extends posteriorly over the lacrimal without meeting the prefrontal, typical of most hadrosaurines except *Maiasaura* (Horner 1983) and *Brachylophosaurus* (CMN 8893), where it is notably shorter. The entire posterolateral process maintains a consistent width where it forms the ventral margin of the external narial foramen. It tapes gradually posterior to that foramen. The position of the anterior border of the prenarial fossa is ontogenetically variable. It forms a wide arc that is confluent with the anterior

border of the external narial foramen in adults (Fig. 3.2) but which is situated well forward of this foramen in juveniles. It is unclear if this character is ontogenetically variable in *S. osborni*, as only adult specimens are known. In *S. osborni* (AMNH 5221), the prenarial fossa extends anteriorly from the naris forming a long, narrow groove on the lateral surface of the premaxillary body. This extension is distinct from the broad arc seen in *S. angustirostris*.

*Maxilla***.** The outline of the maxilla forms a roughly symmetrical isosceles triangle in lateral view as in other hadrosaurines (Horner et al. 2004). The ventral margin is slightly concave ventrally and has more than 27 alveoli in ZPAL MgD-1/159 but more than 45 in the largest individuals (Table 1). Up to four (possibly five) teeth are present in each alveolus. The anterodorsal process is separated ventrally from the anterior tip of the maxilla by a sulcus. It is mediolaterally compressed and, in both juvenile and adult specimens, is visible through the external narial foramen where it almost reaches the anterior limit of that fenestra (Fig. 3.2). Equally long anterodorsal processes have been reported in *Maiasaura* (Horner 1983), *Brachylophosaurus* (Prieto-Marquez 2005; Cuthberson and Holmes 2010), and *Gryposaurus monumentensis* (see Gates and Sampson 2007). This process is either broken or is unprepared in specimens of *S. osborni* and therefore cannot be compared. The anterodorsal process abuts the underside of the premaxilla on its dorsomedially-inclined lateral surface. Dorsally, there is a prominent groove that migrates medially onto the distal end of the anterodorsal process that contacts the vomer (Horner 1992). Up to seven foramina, which decrease in diameter posteriorly, perforate the lateral surface of the maxilla. The most anterior foramen forms a notch in the anterodorsal edge of the maxilla. In

well-preserved specimens, the notch is partly covered by a tabular process on the lateral margin of the premaxilla. The contact with the premaxilla obscures a probable contact with the nasal in this region. The dorsal process lies at about the midlength of the maxilla. It contacts the lacrimal anteriorly and the jugal dorsally and laterally. The lateral contact for the jugal is furrowed ventrally and smooth dorsally. The posterior end of the maxilla cannot be fully viewed in any specimen, but is low and subrectangular in lateral view, as in *Prosaurolophus* and *Edmontosaurus* (Lambe 1920, Horner 1992).

Nasal.The nasals are the longest bones in the skull and are in contact for most of their length, meeting along their extensive, flat medial surfaces. The nasals remain unfused even in large specimens. Anteriorly, the nasals are mediolaterally flattened and separated by the posterodorsal processes of the premaxillae. Each nasal forms the entire dorsal margin of the external narial foramen and extends beyond the anterior limit of that foramen. This condition otherwise occurs only in *Prosaurolophus* (ROM 1928, CMN 2277), *Edmontosaurus* (CMN 8509, CMN 2288), and *S. osborni*. In all other hadrosaurines, the nasal does not extend the length of the naris and/or contributes along with the premaxilla to the dorsal margin of the narial opening. Posterior to the naris, the nasal is taller and wider, becoming triangular in cross-section. At the point where the nasal overlies the frontal and prefrontal, it extends posterodorsally to participate in the solid crest. The crest is roughly triangular in cross-section and extends beyond the posterior margin of the skull in the largest specimens. The proximal half of the crest is braced ventromedially by thin processes from the frontals and ventrolaterally by the prefrontals (Fig. 3.3). There are numerous longitudinal

grooves on the underside of the crest that likely served to strengthen this contact. In small and mid-sized specimens with short crests, the nasals are relatively straight in lateral view and the crest is consequently steeply elevated. In larger individuals, the crest extends beyond the posterior margin of the occiput and is less steeply elevated, which gives the nasal a 'bent' appearance in lateral view (Fig. 3.1A). Although an ontogenetic series is unknown for *S. osborni,* the nasals are straight and approximate the immature condition of *S. angustirostris* (Rozhdestvensky 1952, 1957); the crest is steeply angled and does not extend past the posterior margin of the skull (Fig. 3.1E). The distal end of the crest is unknown in *S. osborni*. In *S. angustirostris* the nasal terminates in a thickened bony 'swelling', which has been referred to as the posterior border of the circumnarial fossa (Maryańska and Osmólska 1979, Horner 1992, Godefroit et al. 2008). The dorsal surface of this distal swelling is marked by several posterolaterally-directed furrows. The anterior edge of the swelling is excavated, forming a cavity. A subtle, posterolaterally-oriented ridge on the anterior surface of the nasal extends to meet the lateral edge of the distal swelling. A second longitudinal ridge is present anteriorly near the anterior base of the crest. These ridges are synonymous with the longitudinal bony septum described by Maryańska and Osmólska (1979).

Jugal. The jugal is W-shaped in lateral aspect and forms the ventral borders of both the orbit and infratemporal fenestra. The anterior process is asymmetrical in small and medium sized animals, becoming more (but not entirely) symmetrical in the largest skulls (PIN 551-358, MPC 100/706). Medially, this process broadly overlies the maxilla and the ventral edge of the lacrimal. The

jugal does not reach the premaxilla as it does in *Edmontosaurus* (CMN 2288, CMN 8509). In lateral view, the anterior process tapers to an elongate spur that separates the maxilla and lacrimal for some distance (Figs. 3.1A, 3.4). This spur gives the ventral contour of the anterior process a sigmoidal outline similar to *Edmontosaurus*. This spur is consistently short in *S. osborni* and the ventral outline of the anterior process is subsequently more convex (Fig. 3.4; Gates and Sampson 2007). The straight postorbital process is angled posteriorly in *Saurolophus* and *Prosaurolophus*. In other hadrosaurines, this process is nearly vertical except in *Edmontosaurus* and *Brachylophosaurus* where it is strongly retroverted (Gates and Sampson 2007, Cuthbertson and Holmes 2010). The distal end of the postorbital process is anteroposteriorly flattened for contact with the posterior edge of the reciprocal process of the postorbital. The posterior process is tabular and the jugal flange only moderately developed as in *S. osborni*, *Prosaurolophus* (CMN 2277, ROM 1928), and *Edmontosaurus* (CMN 2288, CMN 8509). The posterior process overlies much of the quadratojugal, excluding it from the margin of the infratemporal fenestra.

Quadratojugal. The quadratojugal is subtriangular and incompletely separates the quadrate and the jugal. The ventral margin is concave and forms an acute angle with the posterior margin of the quadratojugal. This angle is about 77° in *S. osborni* (AMNH 5221) and *S. angustirostris* (MPC 100/706); wider than in *Brachylophosaurus* (66°, MOR 1071-7-15-98-218A). In *Edmontosaurus* (Lambe 1920), the posterior margin of the quadratojugal is so convex as to make this measurement equivocal. In contrast, the posterior margin in *Saurolophus* is

relatively weakly convex as in *Prosaurolophus* (ROM 787, ROM 1928). Posteromedially, the quadratojugal forms a lap joint with the corresponding facet on the quadrate. The quadratojugal is mediolaterally widest posteriorly and tapers anteriorly where it is covered laterally by the posterior process of the jugal. The quadratojugal of *S. osborni* is virtually identical to that of *S. angustirostris.*

Quadrate. The quadrate is rod-like and forms the posterior margin of the skull in lateral view. In all specimens of *S. angustirostris*, it is more strongly bowed in comparison to *S. osborni*, *Edmontosaurus* (CMN 8509, Lambe 1920), *Prosaurolophus* (Horner 1992), or *Gryposaurus* (Gates and Sampson 2007). In dorsal aspect, the squamosal articular facet of the quadrate is subtriangular in outline. The quadratojugal notch occupies approximately the middle third of the quadrate. It forms a shallow, symmetrical 'C' along its anterior margin that differs from the asymmetrical notch in *Gryposaurus* (Gates and Sampson 2007) and the deeply incised notch in *S. osborni* and *Edmontosaurus* (Fig. 3.5; Lambe 1920). Ventral to the quadratojugal notch, the quadrate is expanded mediolaterally to form a mandibular condyle that is roughly trapezoidal in dorsal section; the medial condyle is reduced and indistinct, typical of hadrosaurids (Horner et al. 2004). The pterygoid process extends anteromedially from the posteromedial surface of the quadrate. This process is slender, roughly triangular in lateral view, and extends nearly the entire height of the quadrate. The medial surface of the pterygoid process is covered by the quadrate processes of the pterygoid.

Squamosal. The squamosals forms the posterior border of the skull roof, including the posterior margin of the supratemporal fenestrae. There are four processes that originate posterolaterally. Extending medially and dorsally, the parietal process contacts its counterpart along the median sagittal plane to exclude the parietal from the posterior margin of the skull as in *Maiasaura* and Lambeosaurinae (Fig. 3.1B; Horner et al. 2004). Although this suture is not presently visible in any specimen of *S. osborni*, Brown (1912) indicated that the squamosals meet medially in this species also. In posterior view, the ventral margin of the parietal process is sinusoidal with the triangular dorsolateral corner of the exoccipital articulating ventrally. Extending ventrolaterally, the postquadratic process (paraoccipital process of the squamosal) flatly contacts the paraoccipital process of the exoccipital. The postquadratic process tapers distally, terminating short of the ventral tip of the paraoccipital process of the exoccipital. The quadrate cotylus is situated anterior to the postquadratic process and formed a synovial joint with the dorsal head of the quadrate (Horner et al. 2004). The cotylus is constrained anteriorly by a triangular prequadratic process that extends ventrally for a short distance along the anterior edge of the quadrate. The precotyloid fossa is best defined in adults; however, the posterodorsal margin remains indistinct as in *S. osborni*. This fossa is well defined in *Prosaurolophus* and *Gryposaurus* but is absent in *Edmontosaurus* (Gates and Sampson 2007). Anteriorly, the squamosal process of the postorbital contacts the postorbital process of the squamosal along a scarf joint that extends the length of both processes. At the posterior extent of this contact, two triangular prongs of the squamosal process of the postorbital are received within reciprocal depressions on the dorsal and lateral surfaces of the squamosal.

Postorbital. The postorbital is identical in both species of *Saurolophus*. In lateral aspect, it is T-shaped in small individuals, and Y-shaped in larger individuals. The postorbital of *S. osborni* is also Y-shaped in adults, but small individuals are unknown. In dorsal view, the prefrontal process is mediolaterally wide, contacting the supraorbital (palpebral of Maryańska and Osmólska 1979) anteriorly, frontal anteromedially, and the parietal posteromedially. Its ventral surface is concave but not deeply excavated as it is in *Edmontosaurus* and possibly *Shantungosaurus* (Horner et al. 2004). The lateral (orbital) margin of the prefrontal process is ontogenetically variable: it is smooth in all except the largest adult (PIN 551/358) in which it is dorsoventrally thickened and ornamented by a series of ridges and grooves. The cylindrical squamosal process tapers posteriorly where it laps the lateral surface of the postorbital process of the squamosal. The anteroventrally-directed jugal process tapers ventrally forming an anteroposteriorly flattened surface that loosely overlies the postorbital process of the jugal. Medial to the jugal process, a divot on the underside of the postorbital housed the dorsal head of the laterosphenoid.

Prefrontal-supraorbital complex. Maryańska and Osmólska (1979) demonstrated the ontogenetic fusion between the supraorbitals and prefrontal in *S. angustirostris*. There are two supraorbitals that form the anterodorsal orbital margin (Fig. 3.1). The anterior element (supraorbital I) is subrectangular and approximately twice as long as supraorbital II, which is tabular. The lateral (orbital) margins of both supraorbitals are coarsely striated in even the smallest specimens and are dorsolaterally flared. The suture between the supraorbitals is coarsely

interdigitating in ZPAL MgD-1/159 but is closed and indistinct in the larger specimen, PIN 551/359. Medially, they fuse to the prefrontal early in ontogeny (the sutures are visible ventrally in ZPAL MgD-1/159 and PIN 551/359) along a straight suture that prevents them from contacting the nasal. Contact between the prefrontal-supraorbital complex and the postorbital excludes the frontal from the orbital rim. Bell (2010) identified two supraorbitals in *S. osborni* that conform to the configuration in *S. angustirostris*. Although the supraorbital-prefrontal suture cannot be observed in the holotype of *S. osborni* (AMNH 5220), the suture between supraorbitals I and II is observable ventral to the orbital rim. In *S. osborni,* the lateral edges of the supraorbitals are upturned and sub-vertical compared to the relatively horizontally-lying supraorbitals in *S. angustirostris.* It is unclear whether this unusual condition in *S. osborni* is real or due to post-depositional deformation as it is only observable in the holotype; the supraorbitals are incomplete or not preserved in other specimens of *S. osborni*. Two supraorbitals are also present in *Maiasaura* (Horner 1983) and *Prosaurolophus* (Maryańska and Osmólska 1979).

The prefrontal is an elongate bone that lies parallel and ventral to the nasal. It is deepest laterally where it fuses with the supraorbitals. Anteriorly, an anteroventral process extends from the prefrontal ventral to the nasal and is braced ventrally by the anteroventral process of the frontal. The anterior limit of the prefrontal cannot be observed in any specimen but likely extended most of the length of the frontal platform. The anteroventral processes do not meet medially, but contribute to the lateral width of the frontal platform for the nasals. Posterodorsally, the prefrontal sends a sheet of bone (posterodorsal process of the prefrontal) along the underside of the lateral half of the nasal crest (Fig. 3.3).

Along its medial edge it contacts the posterodorsal process of the frontal. In juveniles (ZPAL MgD-1/159, PIN 551/359), the posterodorsal process of the prefrontal is weakly developed, formed by the upturned anteromedial edge of the prefrontal (Fig. 3.6). The posterodorsal process is broken in all observed specimens but may have been up to half the length of the crest based on the grooved pattern on the underside of the nasals. The suture between the prefrontal and nasal is loose even in the largest skulls (Maryańska and Osmólska 1981). Brown (1912) suggested the posterodorsal process in *S. osborni* fuses distally with the nasal; however, this could not be confirmed from the current mount of the holotype (Bell 2010). Only the base of this process is observable in *S. osborni* (CMN 8796), where it conforms to the morphology described for *S. angustirostris*.

Lacrimal. The outline of the lacrimal forms an isosceles triangle; the short side comprises part of the anterior orbital rim. In adults, the anterior tip reaches a point level with and ventral to the posterior margin of the external narial opening, although in juveniles it is dorsal and posterior to the naris. The dorsal apex is partially enclosed by supraorbital I in a loose bridle joint. The anterodorsal edge contacts the nasal along its length and, superficially, the lateral process of the premaxilla. Complete overlap by the posterolateral process of the premaxilla also occurs in *S. osborni* and *Brachylophosaurus* (Cuthbertson and Holmes 2010). However, the posterolateral process is shorter in *Gryposaurus* (Gates and Sampson 2007), *Prosaurolophus* (CMN 2277, ROM 1928), and *Edmontosaurus* (CMN 2288, CMN 8509), and incompletely overlaps the lacrimal. Ventrally, the lacrimal contacts the jugal posteriorly and the maxilla for a short

distance anteriorly. The relative length of the lacrimal-maxilla contact increases with skull length. The general shape of the lacrimal is closest to *S. osborni* and *Prosaurolophus*, but is similar also to *Maiasaura* (Horner 1983) and *Brachylophosaurus* (Prieto-Marquez 2005).

Neurocranial complex

Frontal. Each frontal is tripartite, consisting of a frontal body, an anteroventral process, and a posterodorsal process. In dorsal view, the frontal body is trapezoidal and flat lying in adults (Maryańska and Osmólska 1981). In juveniles, they are semicircular and domed (Fig. 3.6). Doming of the frontals is typical of adult lambeosaurines but is present also in *Lophorhothon* (Horner et al. 2004). Juvenile *S. osborni* are unknown, but the frontals are flat in adults. The frontal body is bounded posteriorly by the parietal, laterally by the postorbital, and anterolaterally by the prefrontal. Contact between the postorbital and prefrontal excludes the frontal from the orbital rim as in *S. osborni, Prosaurolophus* (CMN 2277, ROM 1928) and Lambeosaurinae. Ventrally, the cerebral cavity occupies the posteromedial quadrant of the frontal. This cavity is bounded anterolaterally by the presphenoid and posteriorly by the orbitosphenoid and laterosphenoid. The cerebral cavity narrows anteriorly for the passage of cranial nerve I. Lateral to the presphenoid contact, the orbital cavity continues as a shallow depression on the ventrolateral surface of the frontal body. The anteroventral process of the frontal is trapezoidal in anterior view and forms a platform the underlies the prefrontal and nasal. The surface of the frontal platform is smooth, forming a weak contact between these elements.

Anteromedially, the frontal platform continues posterodorsally as a strap-like posterodorsal process, which underlies the nasal crest (Fig. 3.3). Proximally, this process is buttressed along its lateral edge; elsewhere it is thin and usually broken even in well-preserved specimens. It extends approximately half the length of the crest in large animals. In juvenile specimens (ZPAL MgD-1/159, PIN 551/359), the posterodorsal process forms a blunt stub (contra Maryańska and Osmólska 1979, 1981) similar to that observed on juvenile *Parasaurolophus* (Fig. 3.6; Evans et al. 2007). This short process terminates within a depression on the underside of the nasal. As adults, however, the elongate posterodorsal process lies within a corresponding groove on the underside of the nasal. Contact between neighbouring posterodorsal processes is prevented in all specimens by a median ridge formed by the paired nasals. The short description of the posterodorsal process in *S. osborni* by Brown (1912) complies with that of *S. angustirostris*; however, it cannot be adequately observed in the holotype. In CMN 8796, the incompletely-preserved posterodorsal process is a finger-like process that is about as long as the frontal contribution to the skull roof. The preserved portion is equivalent in position and morphology to the lateral buttress on the posterodorsal process of *S. angustirostris.*

Parietals. Work by Horner and Currie (1994) shows the parietals form a single median element through the fusion of two embryonic elements. The parietals form a median, saddle-shaped element that defines the medial borders of the supratemporal fenestrae. The parietals are widest anteriorly where they contact the frontals and postorbitals laterally. A shallow triangular depression is present dorsally on the anterior half of the parietals. A medial spur separates the

frontals at their posteromedial border (Figs. 3.1, 3.6). This spur is wedge-shaped in ZPAL Mgd 1/159, but is virtually absent in PIN 551-359. This spur is also wedge-shaped in *Prosaurolophus* (Horner 1992, CMN 2277), and fingerlike in *Edmontosaurus* (AMNH 427, CMN 8509). It cannot be observed in *S. osborni* due to damage. In most hadrosaurines (except *Brachylophosaurus* [CMN 8893] and *S. osborni*), the parietals and frontals are flat-lying in lateral view. In *S. angustirostris*, the angle between these elements becomes more acute with age. The posterior two-thirds of the length of the parietals are mediolaterally constricted and form a sagittal crest, which becomes progressively taller in older animals. A tall sagittal keel and acute angle between the frontals and parietals are unique to *Saurolophus* spp. and Lambeosaurinae (Bell 2010). The sagittal crest posteriorly contacts the parietal processes of the squamosals, which exclude it from the posterior border of the skull. Ventrally, the parietals enclose the dorsal half of the cerebral cavity and are bounded anterolaterally by the laterosphenoid and presumably by the supraoccipital posterolaterally, although the latter cannot be seen in complete specimens.

Otoccipital. The exoccipital fuses with the opisthotic early in embryonic development (Horner and Currie 1994) forming a single element, the otoccipital. Together with the supraoccipital, the otoccipital forms the dorsal and lateral parts of the occiput. Ventrally, the club-like basioccipital process abuts the basioccipital to form the hemispherical occipital condyle. This union is dorsomedially inclined. In PIN 551/359, the basioccipital processes do not meet ventrally; a narrow portion of basioccipital completes the circumference of the foramen magnum. This is true for all hadrosaurines except *P. blackfeetensis* where

the basioccipital is apparently excluded from the foramen magnum (Horner 1992). In all other specimens of *S. angustirostris*, this relationship is obscured by fusion or diagenetic deformation.

Posterior to the crista tuberalis, three foramina penetrate the lateral wall of the basioccipital process in a sub-horizontal line. The posterior two correspond to the hypoglossal nerve (XII). The more anterior opening converges medially with a tract that exits laterally anterior to the crista tuberalis. Together they form a fossa on the medial wall of the otoccipital that housed the common root of cranial nerves IX, X, and XI (Fig. 3.7C, D). It is therefore equivocal whether cranial nerve X exited anteriorly with cranial nerve IX or posteriorly with the accessory nerve. The crista tuberalis extends anteroventrally onto the lateral face of the basioccipital, and posterodorsally, where it is continuous with the ventral margin of the paroccipital process. Anterior to the opening for cranial nerve IX, the fenestra ovalis opens medially into a spherical vacuity (otic vestibule) formed by the otoccipital and prootic (Fig. 3.7).

In posterior view, the paroccipital process extends dorsolaterally above the level of the supraoccipital before turning ventrolaterally and tapering to a rounded tip. The ventral limit of the paroccipital process is approximately level with the base of the basioccipital process, similar to the condition in *S. osborni* (AMNH 5221), *Gryposaurus* (Gates and Sampson 2007), and *Prosaurolophus* (CMN 2277, Horner 1992). The otoccipitals contact medially ventral to the supraoccipital along a straight, vertical suture that is visible as a low ridge in some specimens. Anteromedially, the exoccipital has a finely-ridged sutural contact with the supraoccipital. These ridges are parallel and angled ventromedially.

Supraoccipital. With the exoccipitals, the unpaired supraoccipital forms the dorsal margin of the occiput. In posterior view, it forms a trapezoidal bar ventral to the dorsal-most point of the exoccipitals, to which it is fused. The dorsal margin is concave. As it is only known from articulated complete specimens, the internal morphology of the supraoccipital is unknown. The supraoccipital is not observable in any specimen of *S. osborni*.

Basioccipital. Posteriorly, the convex margin of the unpaired basioccipital forms the ventral half of the occipital condyle. It is differentiated from the rest of the element ventrally by a transverse sulcus that is present in most hadrosaurines except *Brachylophosaurus* where it is variably present (Gates and Sampson 2007, Cuthbertson and Holmes 2010). Anterior to this sulcus, the basioccipital swells to meet the basisphenoid along a rugose, closed suture. Together, these elements form the paired basitubera, which are separated by a medial furrow. Dorsolaterally, the basioccipital contacts the otoccipital for most of its length. A contact with the prootic was likely present anterolaterally, although fusion has obscured this suture. Dorsally, a longitudinal furrow marks the position of the medulla. The basioccipital forms a minor part of the ventral margin of the foramen magnum but does not appear to participate in the formation of any additional cranial nerve foramina.

Basisphenoid. The basisphenoid fuses anteriorly with the parasphenoid early in embryonic development to form a single element (Horner and Currie 1994). It fuses posteriorly with the basioccipital and dorsally (from anterior to posterior) with the presphenoid, laterosphenoid, and prootic. Between the

presphenoid and laterosphenoid contacts, it forms the ventral part of a large neurovascular foramen. Maryańska and Osmólska (1981) suggested that cranial nerves III and VI exited via this foramen; however, in PIN 551/359 the foramen for cranial nerve III is visible as a distinct foramen on the laterosphenoid dorsal to the opening for the abducens nerve (CN VI; Fig. 3.8). In *S. osborni*, the foramina for cranial nerve III and VI are also separate and a distinct groove extends anteriorly from the foramen for cranial nerve III. In anteroventral aspect, the basisphenoid is triangular. The anterior apex of the basisphenoid extends to form the blade-like parasphenoid process (cultriform process). In lateral view, the parasphenoid process extends anteriorly and tapers to a point that terminates anterior to the presphenoid. This process is mediolaterally widest dorsally although it could not be determined if it is also dorsally concave as it is in *Brachylophosaurus* and *Maiasaura* (Prieto-Marquez 2005). Dorsally, at the base of this process, the median palatine artery emerged along a shallow, horizontal cleft between the basisphenoid and presphenoid. The pterygoid processes diverge posteroventrally from the posterolateral corners of the basisphenoid. Each finger-like pterygoid process ends in the angle formed by the quadrate process and basisphenoid process of the pterygoid. There is no medial prong on the transverse ridge that separates these processes; a condition shared only with *S. osborni* and *Prosaurolophus* (Gates and Sampson 2007). Just posterior to the base of each pterygoid process, a dorsoventral groove becomes the opening for the interior carotid artery (Figs. 3.7A, B, 3.8). This passageway extends dorsomedially and opens into the pituitary (hypophyseal) fossa. Within the pituitary fossa, dorsal to the foramina for the internal carotids and ventral to the dorsum sellae, a pair of smaller foramina marks the passage of cranial nerve VI.

These passageways extend posterodorsally emerging onto the floor of the endocranial cavity.

Laterosphenoid. The laterosphenoid is dorsoventrally elongate, with its dorsal terminus inserting into a cotylus on the ventral surface of the postorbital. The laterosphenoid extends ventrally to meet the basisphenoid posterior to the foramen for cranial nerve VI. The anterior contact with the orbitosphenoid is interdigitating in PIN 551/8, but is obliterated by fusion in MPC 100/706. Posteriorly, the laterosphenoid encloses the anterior margin of the foramen for cranial nerve V to exclude the basisphenoid from participating in the formation of that foramen. A tabular posterior extension of the laterosphenoid is present immediately dorsal to this foramen (Fig. 3.8), as in *Brachylophosaurus, Gryposaurus,* and *Prosaurolophus* (Gates and Sampson 2007), which contacts the parietal posterodorsally and the prootic posteroventrally. A ridge in this region in *S. osborni* may indicate a similar posterior extension of the laterosphenoid, but in most cases, fusion with the prootic makes interpretation difficult. This posterior extension is visible in PIN 551/357, but is indistinct in larger specimens due to fusion with the prootic. The ophthalmic branch of cranial nerve V lay in a longitudinal sulcus that separates the subcircular preotic pendant (alar process sensu Horner et al. 2004) from the rest of the laterosphenoid. The preotic pendant is appressed to the surface of the laterosphenoid and not wing-like as it is in *Brachylophosaurus* (Cuthbertson and Holmes 2010). The laterosphenoid of *S. osborni* is firmly co-ossified with the surrounding elements, hence its margins cannot be discerned.

Prootic. The prootic is best seen in PIN 551/359 and MPC 100/706. The anterior margin is invaginated at its mid-height to form most of the circumference of the foramen for the large trigeminal nerve (cranial nerve V). Dorsal to that foramen, the prootic forms an elongate triangle, the dorsal margin of which contacts the parietal. The posterior margin of the prootic is roughly parallel to the crista tuberalis but is visible only in PIN 551/357 (Fig. 3.8); it is indistinguishably fused with the otoccipital in MPC 100/706. The prootic contacts the basisphenoid ventral to the trigeminal foramen. Posteriorly, the prootic contacts the otoccipital and basioccipital ventrally. Along with the opisthotic, the prootic forms the fenestra ovalis and the anterior half of the otic vestibule. Cranial nerve VIII entered the otic vestibule from the medial wall of the prootic as in *Prosaurolophus* (Fig. 3.7C, D; Horner 1992). The small foramen for cranial nerve VII is between the fenestra ovalis and the trigeminal nerve foramen. In PIN 551/359, separate grooves for the palatine and hyomandibular branches extend ventrally and dorsally, respectively, from the foramen for the trigeminal nerve. In KID 476, however, the palatine branch groove is faint and that for the hypoglossal branch is absent altogether, as in *S. osborni* (AMNH 5221). Separating the position of cranial nerve VII from the fenestra ovalis is a ridge, the crista preotica. In PIN 551/359 the crista preotica is short, but in MPC 100/706 it extends posterodorsally to join the more robust crista prootica. The crista prootica is nearly horizontal, extending the anteroposterior length of the prootic onto the lateral face of the otoccipital. In *S. osborni*, the prootic is fused to other elements of the lateral wall of the braincase, hence its general outline is unknown. The other features do not differ from *S. angustirostris*.

Presphenoid. There is doubt regarding the identification and homology of the presphenoid in hadrosaurids (Evans 2006, Ali et al. 2008, McBratney-Owen 2008). Nevertheless, 'presphenoid' (=sphenethmoid in non-avian theropods, Ali et al. 2008) is used here for consistency in the hadrosaurid literature. The presphenoids are paired ossifications that together form a Y-shaped element in anterior view, attaching dorsally to the ventral surfaces of the frontals (Fig. 3.7E). The U-shaped dorsal component forms the canal for the olfactory bulbs and nerve (cranial nerve I). Ventral to this canal, the presphenoids meet to form the 'interorbital septum'. In lateral aspect, the presphenoid is roughly quadrangular in PIN 551/359, contacting the orbitosphenoid posteriorly and the basisphenoid posteroventrally as in *S. osborni* and *Prosaurolophus* (Horner 1992), but not *Brachylophosaurus* (Prieto-Marquez 2005). Anteroventrally, a cleft separates the presphenoid from the basisphenoid and transmitted the median palatine artery. The posteroventral margin of the presphenoid forms the anterior half of the foramen for cranial nerve IV (Fig. 3.8). This foramen is closed posteriorly by the orbitosphenoid.

Orbitosphenoid. The orbitosphenoid is a dorsoventrally tall, ovoid element. It is surrounded by the presphenoid anteriorly, the frontal dorsally, and the laterosphenoid posteriorly. Ventrally, it forms part of the dorsal wall for the anteroposteriorly elongate neurovascular foramen that included cranial nerve VI (Maryańska and Osmólska 1981). This fenestra separates the orbitosphenoid from the basisphenoid (Fig. 3.8). Posteroventrally, the orbitosphenoid is perforated by the foramen for cranial nerve II. A groove for that nerve extends anteriorly from the optic foramen. In most cases the anteroventral margin of the

orbitosphenoid forms the posterior margin of the foramen for the fourth cranial nerve. However, this foramen is not entirely enclosed posteriorly in PIN 551/359, and as a result, forms the anterior margin of the elongate neurovascular foramen that includes the foramen for cranial nerve VI (Fig. 3.8).

Palatal complex

The palatal bones are known only in complete specimens in which they are visible through the orbits and temporal fenestrae. Their complete morphology and relationships are therefore incompletely known. The strongly vaulted palate of ZPAL MgD-1/159 (Maryańska and Osmólska 1981) is the result of crushing. It is a broadly arcing complex consistent with other hadrosaurines (Heaton 1972).

Posteriorly, the pterygoid is loosely adhered to the medial surface of the pterygoid process of the quadrate. The dorsal quadrate process is triangular and posterodorsolaterally directed. The posteriorly directed ventral quadrate process is shorter and buttressed along its medial surface. Anterodorsally, the broad palatine process extends to meet the posterior margin of the palatine and medially to contact its counterpart. Together, the palatine processes form a vaulted palate typical of hadrosaurines; in contrast, the lambeosaurine palate is more steeply vaulted (Heaton 1972). The dorsal margin of the palatine process originates proximally on the medial surface of the dorsal quadrate process. At this contact, they form a deep sulcus that houses the pterygoid process of the basisphenoid (Fig. 3.1B). The ectopterygoid process is strongly buttressed,

extending ventrally to contact the posterior edge of the maxilla. The ectopterygoid partially overlaps the lateral surface of this process.

Part of the ectopterygoid is observable through the orbit of ZPAL MgD-1/159, as illustrated by Maryańska and Osmólska (1981, fig. 5). It extends, strap-like, along the posteroventral margin of the palatine, the ventrolateral surface of the palatine process of the pterygoid and the lateral surface of the ectopterygoid process of the pterygoid.

Anteroventrally, the palatine is mediolaterally expanded to contact the posteromedial surface of the anterior process of the jugal. The main body of the palatine rises dorsally into the interorbital cavity to form a blade-like extension that contacts its mate medially. The anterior edge is concave. In most hadrosaurines, the dorsal margin of this extension flares anteroposteriorly in lateral view; however, it tapers in *S. angustirostris* and possibly *S. osborni* (Heaton 1972). The palatine meets the pterygoid posteriorly. Ventrally, the contact with the maxilla is obscured by the ectopterygoid.

The dorsal apex of the vomer is visible in ZPAL MgD-1/159 just anterior to the palatine. At this point, the vomers are united and extend posteriorly between the paired palatines. Anteriorly, they are obscured by the nasals.

Mandibular complex

The single, median predentary is a horseshoe-shaped element that wraps around the mandibular symphysis. The posterolateral processes are dorsoventrally flattened and taper posteriorly. In MPC 100/706, the terminus is bifurcated. The posteromedial surface of the predentary has a dorsally placed

triangular process and more ventrally placed paired, tabular processes, both of which enclose the dental symphysis above and below, respectively. The oral margin is smooth in young animals, becoming more rugose in later ontogeny. It is perforated by five or six foramina on either side of the midline.

In lateral view, the dentary is straight along its ventral edge (Fig. 3.1) as in *S. osborni*, *Prosaurolophus* (CMN 2277, ROM 1928), and *Edmontosaurus* (CMN 2288, CMN 8509). The robust, distally-expanded coronoid process is procumbent and inserts into a space (adductor chamber) medial to the jugal. Medially, the dental battery is covered by a thin plate of bone (dental lamina) that is perforated by a row of special foramina (Edmund 1957). Each foramen corresponds to the base of a vertical tooth family and together they form a concave arc. Posterior to the dental battery, the dentary has a subconical process that contacts the lateral surface of the splenial. The splenial process is separated from the lateral wall of the dentary by a cleft (Meckelian fossa) that extends anteroventrally and forms the contact for the angular. The edentulous portion of the dentary constitutes 40% of the length of the dentary (irrespective of dentary length) and tapers anteriorly. The symphyseal region is offset medially and ventrally from the main body of the dentary, where it loosely abuts its neighbour. A vascular foramen exits anteroventrally near the symphysis and several smaller foramina open onto the lateral surface of the dentary.

The dentary houses at least 26 vertical tooth families in ZPAL MgD-1/159 and 50 in PIN 551/407. A high tooth count (>46 families) characterises *Edmontosaurus* and species of *Saurolophus*, but is linked to both ontogeny and absolute size. Up to six teeth are present within a single tooth family, although only one or two are functional for mastication at any one time. The enamelled

lingual surface is diamond shaped with a single, straight median carina. The teeth are typically hadrosaurine, being relatively short with a crown height that is close to twice the mesiodistal length. Marginal denticles are present only on the anterior-most teeth and are absent or poorly developed posteriorly (Fig. 3.9).

The largest element in the postdentary complex (Bell et al. 2009) is the surangular, which is U-shaped in lateral view. The dorsal surface is mediolaterally flared and excavated to receive the ventral condyles of the quadrate. A triangular process on the dorsolateral edge of the surangular restricts lateral movement in the jaw joint between the quadrate and the surangular. Posteriorly, the surangular is mediolaterally compressed; it contacts the articular medially. Anteriorly, the coronoid process of the surangular is thin and triangular and resides along the medial surface of the lateral wall of the dentary. The surangular contacts the angular ventromedially and the splenial medially.

The angular is straplike and forms the ventral edge of the postdentary complex. It extends anteriorly along the ventromedial surface of the dentary, where it is housed within a cleft. Posteriorly, it is contacted by the splenial dorsally and the surangular medially. The posterior half of the angular, in ventral aspect, is sinusoidal.

The splenial is a thin, subrectangular plate on the medial surface of the postdentary complex. It tapers posteriorly and contacts the angular ventrally and articular posterolaterally. The dorsal edge of the splenial is concave where it contacts the articular. Anteromedially, a V-shaped depression receives the corresponding splenial process of the dentary.

Wedged between the posterior ends of the surangular and splenial is the articular. The articular is a vertically-oriented ovate element that forms a part of the articulating surface of the jaw joint for the quadrate. In medial view, the dorsal half of this element is visible dorsal to the splenial, but is almost entirely obscured by the surangular in lateral aspect.

Accessory elements

Sclerotic ring. Three to five sclerotic plates, none of which is complete, are preserved in the right orbit of PIN 551/8 (Fig. 3.10). Three are in situ and the other two are broken and displaced. As preserved, these conform to the posterodorsal quadrant of the sclerotic ring. The plates are serially overlapping in an anti-clockwise direction; the posterior edge of a plate overlaps the leading edge of the following plate. The edges of the individual plates are finely crenulated, with the exception of the inner (i.e. toward the centre of the ring) margin, which is smooth. The overlapping portion is lobate (compared to the triangular processes in other hadrosaurids; Russell 1940, Ostrom 1961); however, the edges are incomplete. No plus or minus plates (sensu Lemmrich 1931) could be identified from the limited sample. Brown (1912) posited that the sclerotic plates in *S. osborni* were entirely serially overlapping; however, as pointed out by Russell (1940), this would be a unique arrangement. Reanalysis of the holotype AMNH 5220 confirms Russell's (1940) suspicions. The anterodorsal quadrant is composed of three serially overlapping plates in an anti-clockwise direction, where the triangular trailing edge of a plate is received in a reciprocal facet on the following plate. In the anteriormost plate, that facet is visible where the

preceding plate has become displaced. The adjacent, displaced plate lacks facets on its lateral surface, identifying it as a plus plate. A minus plate is present at the other end of the three aforementioned serially overlapping plates. If correct, this would confirm previous interpretations of a Lemmrich type A arrangement in *Saurolophus* (Russell 1940, Ostrom 1961).

Hyoid. The hyoid is visible only in the adult specimen PIN 551/357. It is rod-like, measuring 450mm long and 90mm high at the proximal (anterior) end. The proximal end is flattened and is triangular in cross-section. Each side of the triangle is concave and the shortest side is situated ventrally. The hyoid tapers gradually from the proximal end, becoming elliptical in cross-section. The hyoid is straight except for the distal third, which is offset posterodorsally. Left and right hyoids converge anteriorly at the ventromedial corner of their proximal ends. This convergence point is approximately ventral to the basisphenoid.

Phylogenetic analysis

The purpose of this analysis was to assess the position of *S. angustirostris* relative to *S. osborni,* rather than to comprehensively test the interrelationships of Hadrosaurinae as a whole. Forty-four cranial characters, as compiled from Weishampel et al. (1993), Godefroit et al. (2008), Bolotsky and Godefroit (2004), Horner et al. (2004), Prieto-Marquez (2005), and modified by Bell (2010) were used to evaluate the phylogenetic position of *S. angustirostris* (Table 3.2; Appendix 3.1). Ten ingroup and two outgroup taxa (*Iguanodon* and *Bactrosaurus*) were scored, with all characters assigned equal weight and unordered. A

heuristic search using parsimony with 1000 random addition sequence replicates performed using PAUP 4.0b10 (Swofford 2002) retrieved three most parsimonious trees with a length of 72 steps. These differed only in the relationships of *Kerberosaurus* and *Prosaurolophus* to *Saurolophus* spp. In the strict consensus tree (Fig. 3.11), these three genera form a polytomy; however, *S. angustirostris* is recovered as the sister taxon of *S. osborni*, confirming the similarity between these two species. *Saurolophus* is strongly united by the following unambiguous synapomorphies: a parietal that is excluded from the posterodorsal margin of the occiput by the squamosal (Character 1); secondary elongation of the frontal resulting in the backwards extension of the frontal platform (Character 7); a frontal platform that extends dorsal to the anterior portion of the supratemporal fenestra (Character 8); and a prefrontal that participates in the ventrolateral portion of the crest (Character 22). *Kerberosaurus, Prosaurolophus*, and *Saurolophus* are weakly united by one ambiguous character (frontal excluded from the orbital rim by the postorbital-prefrontal union; Character 5). General topology agrees well with those of Godefroit et al. (2008) and Bolotsky and Godefroit (2004) except that the current analysis recovered *Kerberosaurus, Prosaurolophus*, and *Saurolophus* in a polytomy. *Kerberosaurus* is the sister taxon to a clade that includes *Prosaurolophus* and *Saurolophus* in the analyses of Bolotsky and Godefroit (2004) and Godefroit et al. (2008). The only previous study to incorporate both species of *Saurolophus* in a phylogenetic analysis is that of Prieto-Marquez (2010). Although the current analysis is limited in terms of both taxa and cranial characters (compared to the extensive list of cranial and postcranial characters used by Prieto-Marquez 2010), both studies recovered a monophyletic *Saurolophus* clade; however, Prieto-Marquez (2010)

also resolved *Kerberosaurus* as the sister taxon to the clade comprising *Saurolophus* and *Prosaurolophus*.

Discussion

The most characteristic feature of the skull in *Saurolophus* is the nasal crest and the involvement of the prefrontals and frontals in its construction. Although a posterodorsal process of the frontal was described for *S. osborni* by Brown (1912), the inaccessibility of the mount led to doubt of its existence (Ostrom 1961, Horner 1992, Horner et al. 2004). The absence of a posterodorsal process of the frontal was used by Horner (1992) to differentiate *S. osborni* from *S. angustirostris*; however, Bell (2010) has demonstrated its presence in both species. Brown (1912, p. 135) described this process in the holotype of *S. osborni* as "broad"; however, in the only specimen where it is currently observable (CMN 8796), it is broken and forms a short, nearly conical spike that matches the equivalent region in *S. angustirostris*. Maryańska and Osmólska (1981) also suggested the posterodorsal process of the prefrontal may be relatively longer in *S. osborni,* but this cannot be demonstrated given that the crest is incomplete in all specimens of that species. Regardless, the prefrontal-frontal contribution to the crest in *Saurolophus* is peculiar among hadrosaurines. In other crested hadrosaurines, the prefrontals and frontals are not simultaneously involved in supporting the crest. In *Maiasaura*, however, where the frontals contribute to the crest, they extend dorsally to form a transverse, anterodorsally-inclined ridge that forms the posterior and dorsal parts of the crest (Horner 1983). Similar to most lambeosaurines, the frontals of *Brachylophosaurus* provide a wide embayment and

extensive sutural contact for the nasals (Prieto-Marquez 2005, Evans et al. 2007). The posterodorsal process of the frontal in *Saurolophus* is reminiscent of the dorsal promontorium in *Charonosaurus* and *Parasaurolophus* (Godefroit et al 2001, Evans et al. 2007, Bell 2010). In *Charonosaurus* and *Parasaurolophus,* the underside of the crest is braced by elongate processes of the prefrontals and frontals; those from the prefrontals are longer than the frontal processes (Sullivan and Williamson 1999, fig. 17). As in *Parasaurolophus* (Evans et al. 2007), development of the 'dorsal promontorium' in *Saurolophus* is ontogenetically variable. In ZPAL MgD-1/159, the posterodorsal processes of the frontal and prefrontal are short stubs, although the crest is already well developed at this early stage. An equivalent-sized *Parasaurolophus* braincase described by Evans et al. (2007) has a similar degree of development of the dorsal promontorium. As adults, the posterodorsal processes in *Saurolophus* extend up to half the length of the crest; longer (both relatively and absolutely) than the analogous region in *Parasaurolophus*.

Saurolophus is the only dinosaur genus currently recognised from penecontemporaneous beds of both Asia and North America. Despite the fact that there are well-preserved specimens of both species, they have not been described or compared in detail, generating confusion about their cranial anatomy and the validity of the Mongolian taxon (Norman and Sues 2000). Bell (2010) redescribed *S. osborni*; however, the descriptions of *S. angustirostris* provided by Rozhdestvensky (1952, 1957) and Maryańska and Osmólska (1981) were insufficient to permit a comprehensive comparison. The supplementary description and phylogenetic results presented here confirm the close relationship of *S. angustirostris* and *S. osborni*. Although it may be prudent to

consider these taxa as separate genera given the considerable geographical separation, a sister group relationship does not require the renaming of either taxon and the genus name, *Saurolophus* is retained. In addition, it is the author's opinion that the seven cranial differences listed here do not constitute a difference significant enough to justify distinction at the generic level.

Maryańska and Osmólska (1981) described six cranial characters, which supposedly differentiate the species of *Saurolophus*. However, several of these differences are likely a consequence of comparing juvenile *S. angustirostris* to adult material of *S. osborni*; specifically, that *S. angustirostris* possesses a relatively shorter lacrimal and external naris, and a relatively longer maxilla. When adult specimens are compared, the proportions of these structures are identical in all cases. This study corroborates two other differences suggested by Maryańska and Osmólska (1981): *S. angustirostris* possesses a more strongly bowed quadrate, and there is a spur on the anterior process of the jugal that separates the lacrimal and maxilla. Although quadrate curvature is difficult to quantify, it is accepted that hadrosaurines typically possess straight quadrates compared to lambeosaurines, which are curved (Horner et al. 2004). Although *S. osborni* conforms to the usual hadrosaurine condition, the quadrate in *S. angustirostris* is bowed as in Lambeosaurinae. The elongate spur on the anterior process of the jugal of *S. angustirostris* is well developed on even the smallest specimen giving the ventral margin of the anterior process a sigmoidal outline. In *S. osborni* this spur is smaller and the ventral margin of the anterior process is convex. Moreover, these differences are maintained across all observed specimens and ontogenetic stages, and therefore are unrelated to preservation or individual

variation (contra Norman and Sues 2000). A list of ontogenetic changes identified for *S. angustirostris* in this study are shown in Fig. 3.12.

Maryańska and Osmólska (1979, 1981) referred to ridges (longitudinal bony septa) on the dorsal surfaces of the nasals in the region of the crest. These were not described for *S. osborni* (Brown 1912), and Maryańska and Osmólska (1981) tentatively regarded this as a specific difference. Although the distal end of the crest is not preserved in *S. osborni*, Bell (2010) did note a series of grooves and ridges on the preserved anterior surface of AMNH 5220, which likely correspond to the ridges described by Maryańska and Osmólska (1981). Longitudinal bony septae, therefore, probably do not distinguish between species of *Saurolophus*.

Palaeobiogeography

As discussed by Bolotsky and Godefroit (2004), the palaeobiogeography of *Saurolophus* is complex. Fragmentary and scarce hadrosaurine remains from the Amur Region, Russia, have been referred to an apparently closely related form, *Kerberosaurus manakini* (see Bolotsky and Godefroit 2004). *K. manakini* differs from *S. angustirostris* in having a straight quadrate in lateral view; a circumnarial fossa limited posterodorsally by a ridge on the nasal around the naris; a mediolaterally compressed frontal that lacks a posterodorsal process; and a crescent-shaped prefrontal lacking a posterodorsal process. Bolotsky and Godefroit (2004) identified *Kerberosaurus* as 'middle' to late Maastrichtian and placed it as the sister taxon to *Saurolophus* and *Prosaurolophus* on account of the frontal being excluded from the orbital rim (Character 5). Results of the phylogenetic analysis

presented here place these three taxa in a polytomy, although the apparent absence of a crest in *Kerberosaurus* does indicate a primitive state relative to both *Prosaurolophus* and *Saurolophus*. The geologically oldest of these three taxa, *Prosaurolophus*, is from the late Campanian of Alberta and Montana. *Saurolophus osborni* is known only from the lower Maastrichtian beds of the Horseshoe Canyon Formation, Alberta (Eberth and Deino 2005, Bell 2010). The Nemegt Formation has not been tightly constrained biostratigraphically, and radiometrically-datable beds are absent. The Nemegt Formation is considered Maastrichtian based on superposition and imprecise biostratigraphy (Jerzykiewicz and Russell 1991, Jerzykiewicz 2000, Shuvalov 2000), but more specific chronostratigraphy is unavailable.

The Beringian land bridge between North America and Asia, which opened during the Aptian–Albian, provided a major dispersal route for terrestrial vertebrates throughout the Late Cretaceous (Russell 1993). The predominant dispersal direction was from west to east, with many Late Cretaceous dinosaur groups—including Neoceratopsia (You and Dodson 2003), Ankylosauridae (Vickaryous et al. 2004), Hadrosauridae (Godefroit et al. 2008), Tyrannosauridae (Sereno et al 2009), and Troodontidae (Russell and Dong 1993)—supposedly originating in Asia. At higher taxonomic levels, however, dispersal patterns become more complex. Within the Hadrosaurinae, evolution of the clade containing *Kerberosaurus*, *Prosaurolophus*, and *Saurolophus* underwent at least two major dispersal events between Asia and North America. Following the phylogenetic hypothesis of Bolotsky and Godefroit (2004), ancestors of *Kerberosaurus* must have crossed into Asia at or prior to the early late Campanian. Assuming a direct relationship between *Prosaurolophus* and *Saurolophus osborni*, a

second dispersal must have taken place at or prior to the earliest Maastrichtian, leading to the evolution of *S. angustirostris*. Alternatively, but less parsimoniously, the most recent common ancestor of *Prosaurolophus* and *Saurolophus* dispersed to Asia at or prior to the early late Campanian and a third dispersal from west to east occurred before the end of the Campanian.

The evolutionary and biogeographic relationship between *S. angustirostris* and *S. osborni* remains unresolved. Therefore, it is unclear which of the two species is more primitive and from which direction the final dispersal took place. Regardless, it is reasonable to suppose that related forms should be present in penecontemporaneous beds in those intervening regions (particularly Alaska, and far eastern Russia and China) that will help elucidate the evolutionary sequence between species of *Saurolophus*.

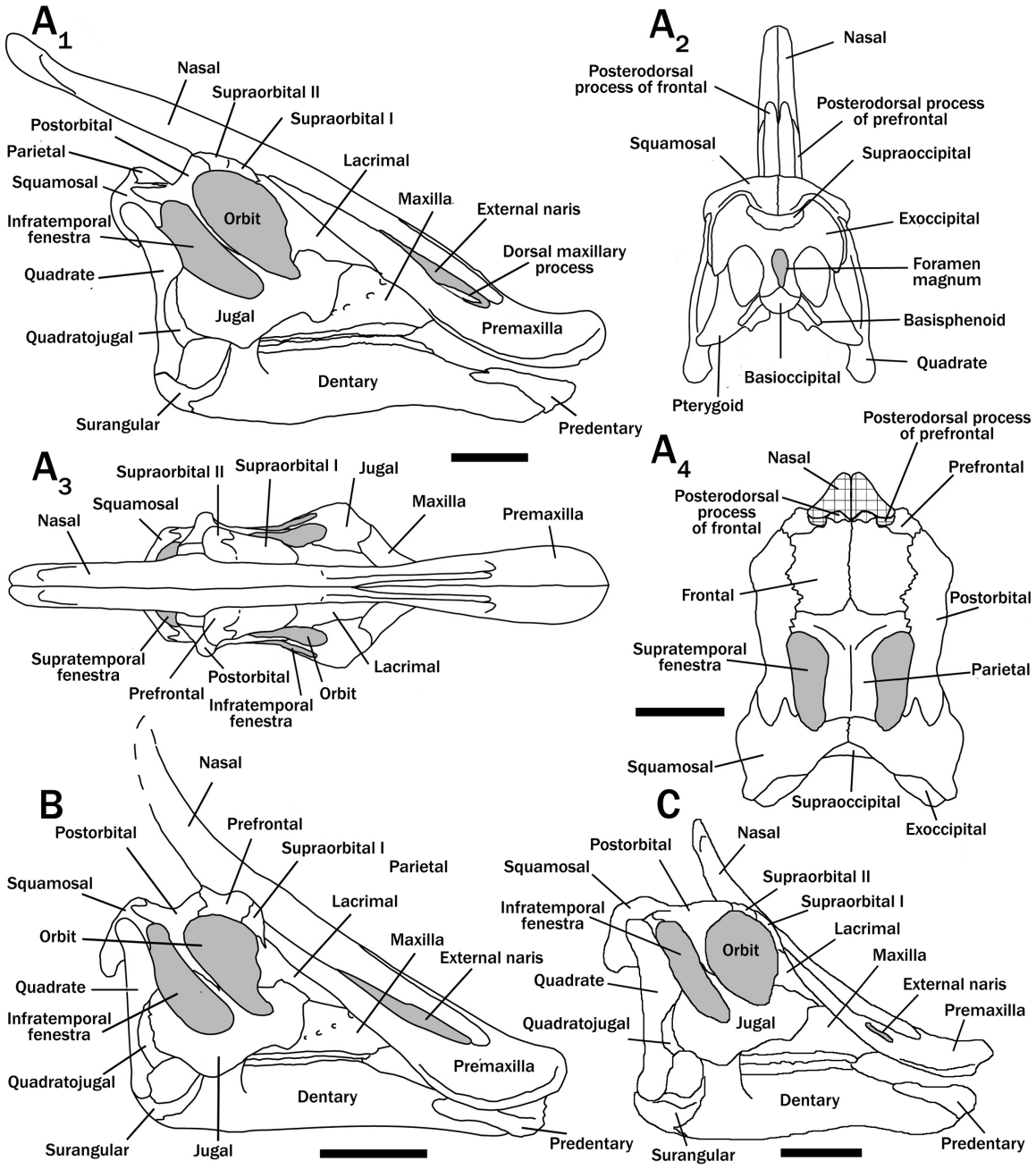

Figure 3.1. Adult *Saurolophus* skulls compared. *S. angustirostris* (based on MPC 100/706) in lateral (A), posterior (B), and dorsal (C) view. (D) Skull roof with crest removed as denoted by cross-hatching. Skull of *Saurolophus osborni* (AMNH 5220) in lateral view (E). Not to scale. Dashed lines imply inferred margins.

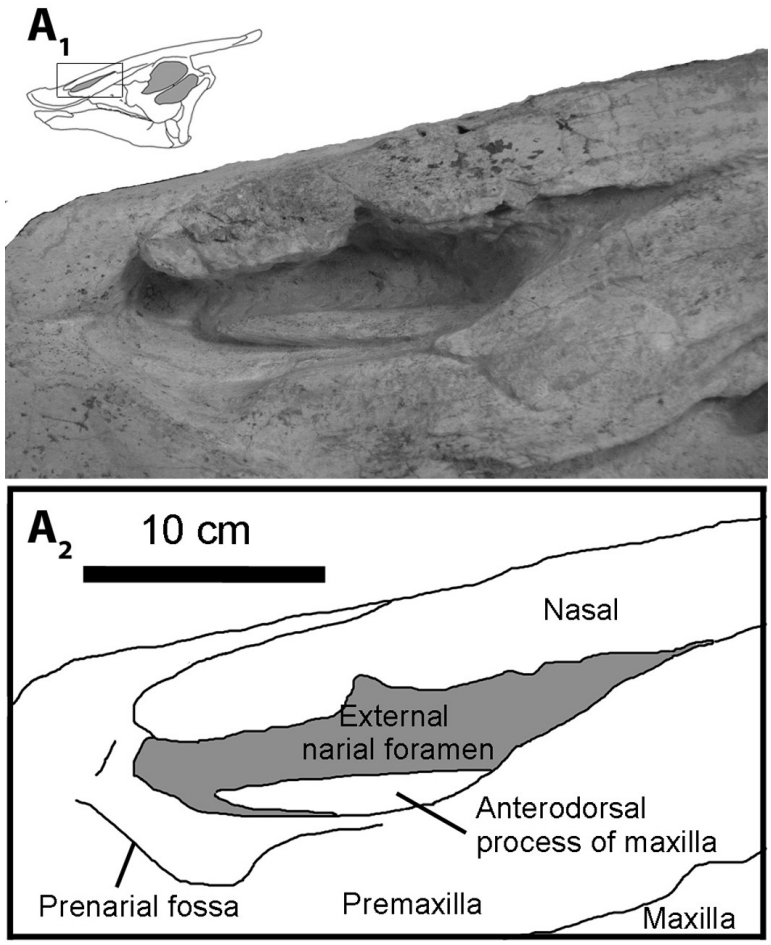

Figure 3.2. Details of the left narial region in an adult *S. angustirostris* (MPC 100/764) showing the elongate anterodorsal process of the maxilla. Grey indicates matrix. Anterior to left; dorsal is up.

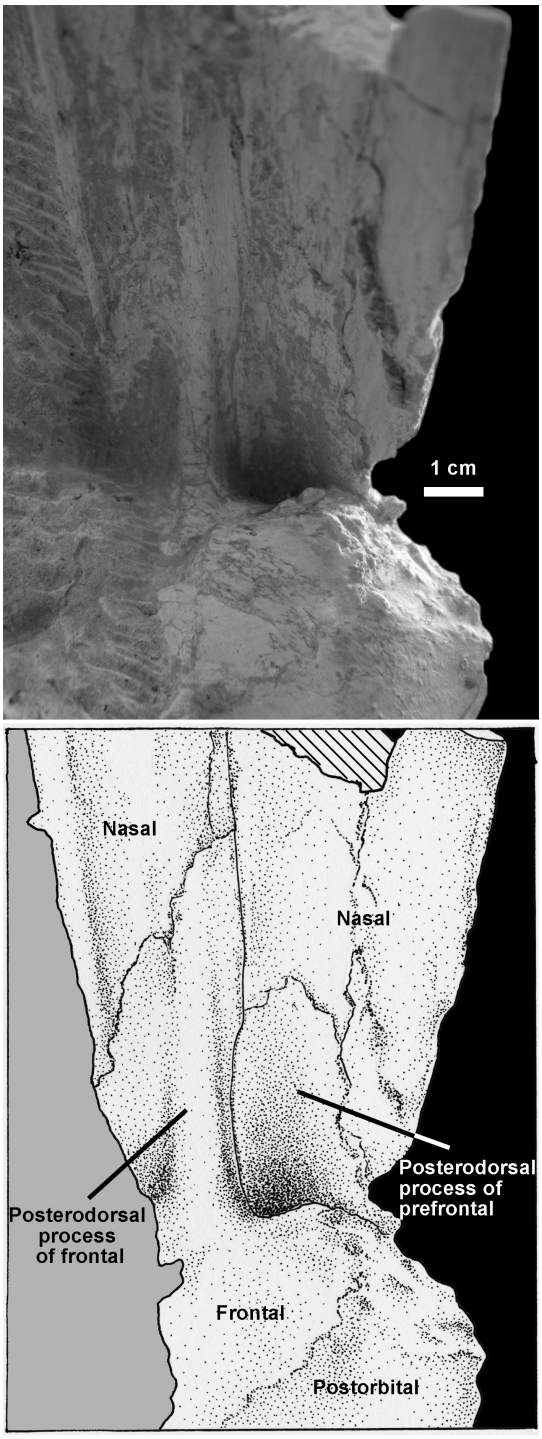

Figure 3.3. Posterior view of the proximal crest in MPC 100/764; right side. Shading indicates matrix. Cross-hatching indicates broken cross-section of nasal. Dorsal is up.

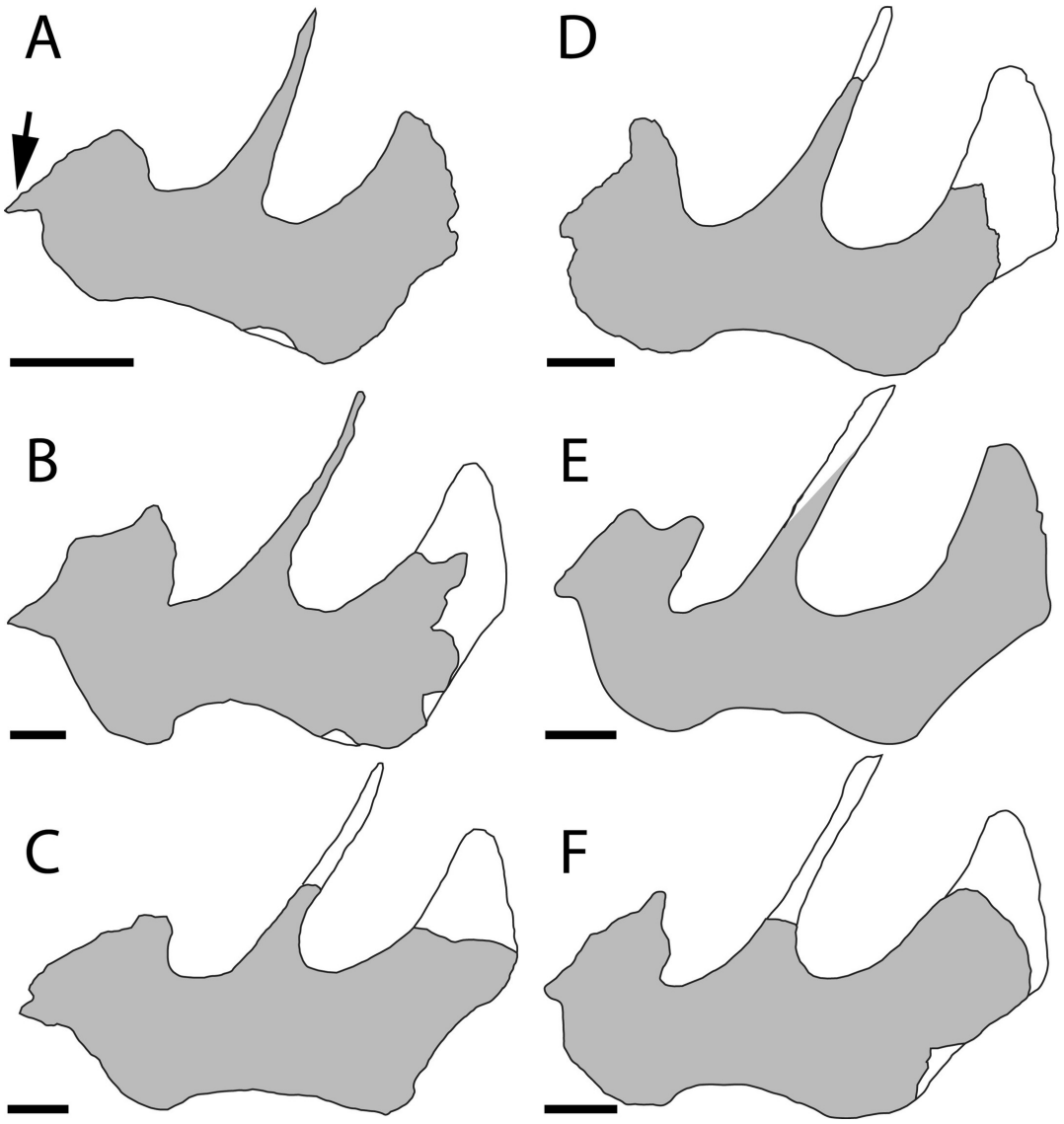

Figure 3.4. Jugals of *Saurolophus angustirostris* (A–C) and *Saurolophus osborni* (D–F). (A), ZPAL MgD-1/159 juvenile; (B), MPC 100/706 adult; (C) MPC 100/764 adult; (D), AMNH 5221 adult, reversed; (E), AMNH 5220 adult, reversed; (F), CMN 8796 adult, reversed. Note the anteriorly-directed spur on the anterior process in *S. angustirostris* is prominent in even the juvenile. This process is reduced in *S. osborni*. White represents reconstructed areas.

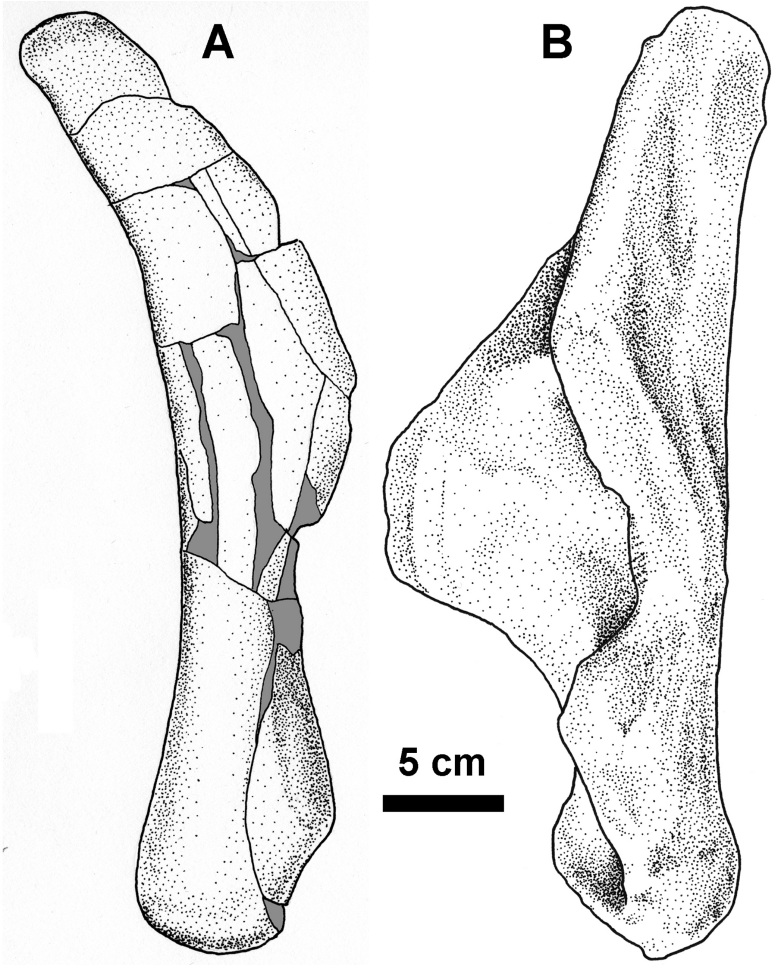

Figure 3.5. Comparison of quadrates of *Saurolophus* in lateral view: (A) Right quadrate of *S. angustirostris* (ZPAL MgD-1/163). (B) Left quadrate of *S. osborni* (AMNH 5220). B modified from Bell (2010). Grey regions indicate broken surfaces. Dorsal is up.

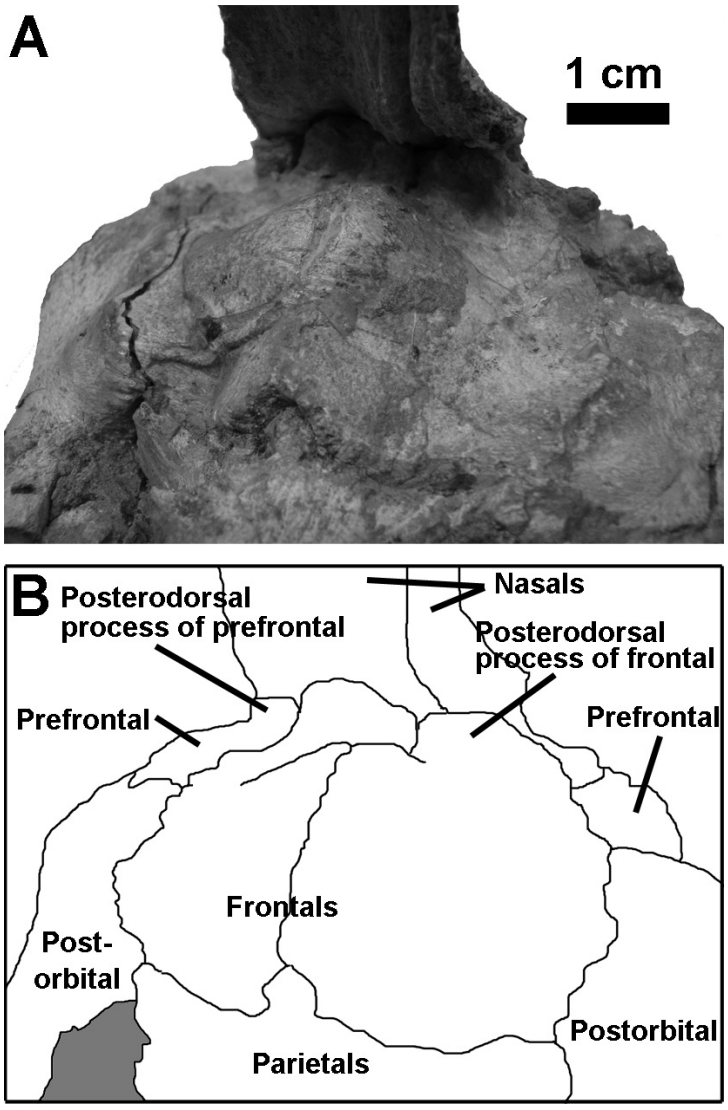

Figure 3.6. Dorsal oblique view of juvenile *S. angustirostris* (ZPAL MgD-1/159) skull roof. Photo (A) and interpretive drawing (B). Shading indicates matrix.

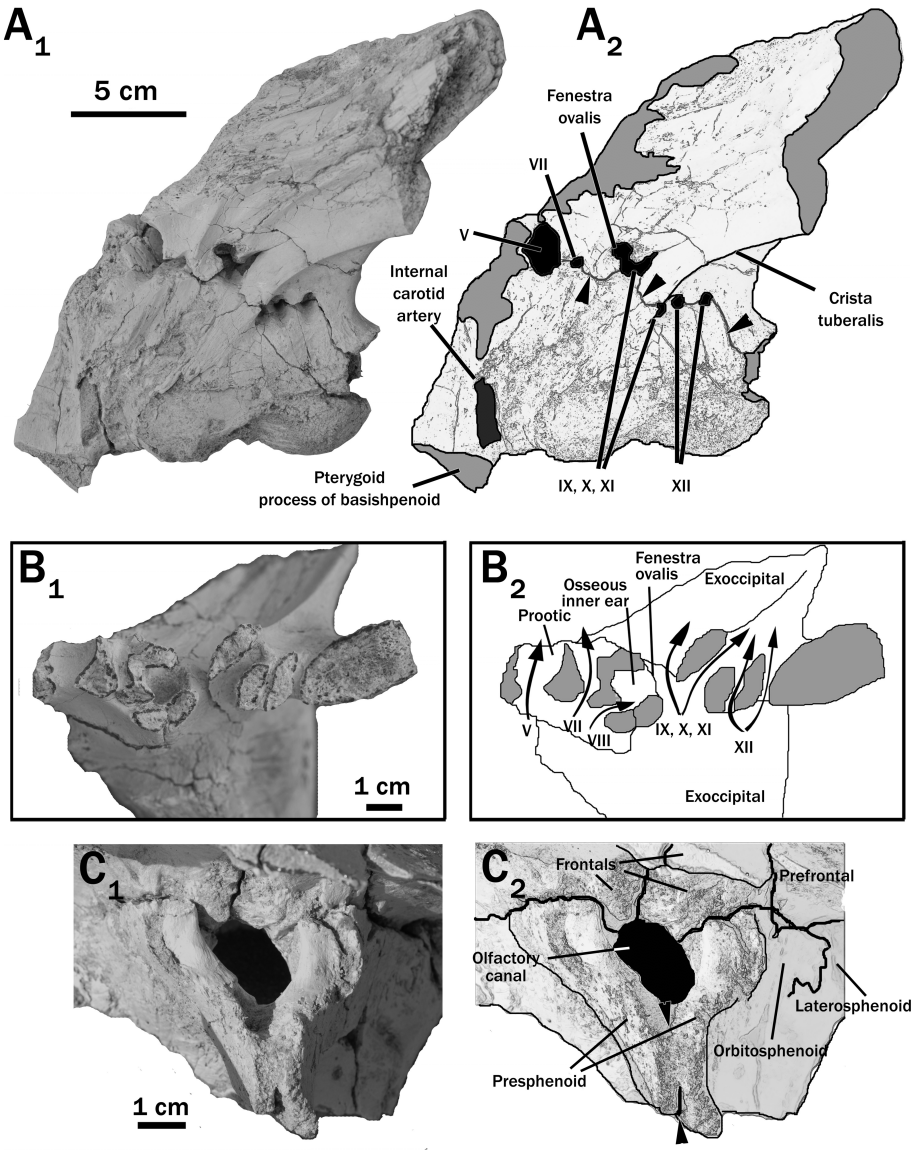

Figure 3.7. Partial braincase of adult *S. angustirostris* (KID 476). (A, B) Left lateral view of otoccipital, basioccipital, prootic, and basisphenoid. (C, D) Ventral view of left otoccipital and prootic across broken surface denoted by arrowheads in B. (E) Anterior view of braincase showing the paired presphenoids. The inter-presphenoid suture is indicated by arrowheads. Grey regions indicate broken surfaces. Cranial nerves are indicated with roman numerals.

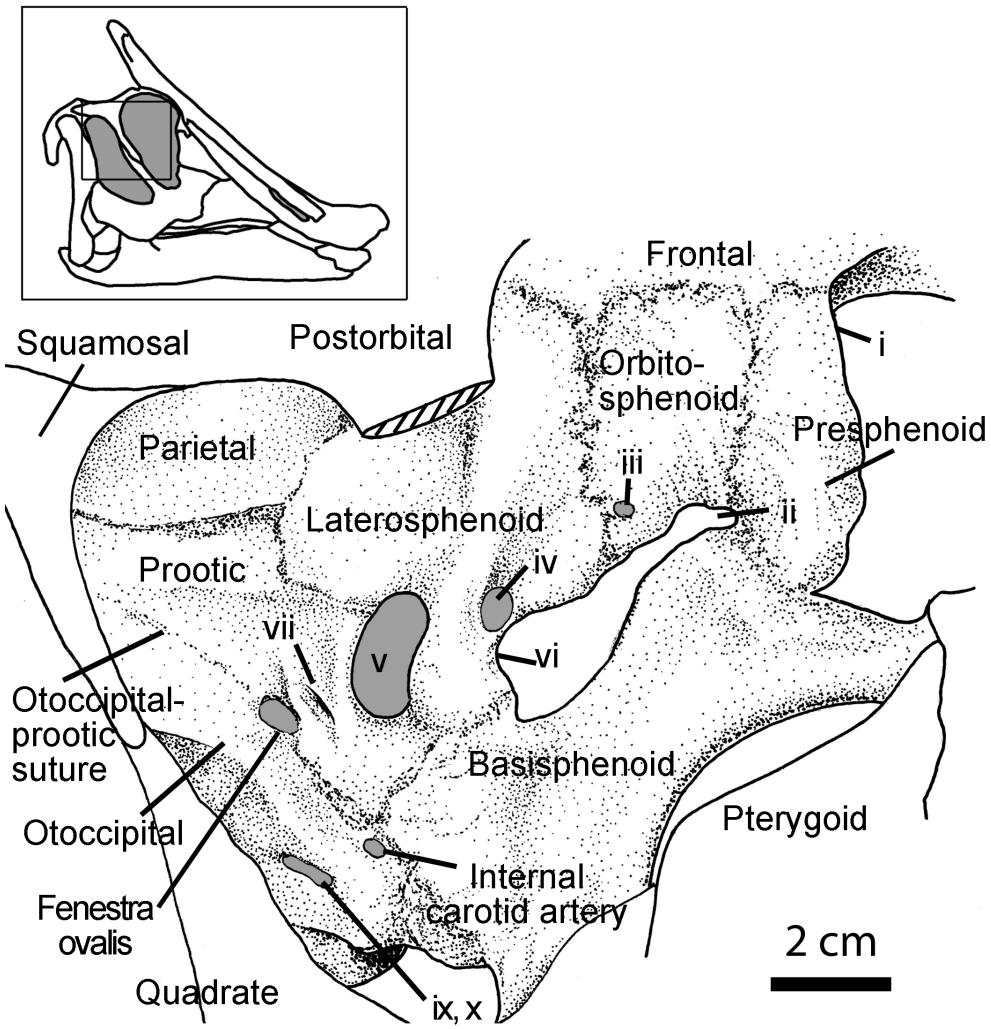

Figure 3.8. Right lateral view of juvenile braincase (PIN 551/359) with postorbital and jugal processes removed (cross hatching). Grey regions denote neurovascular openings.

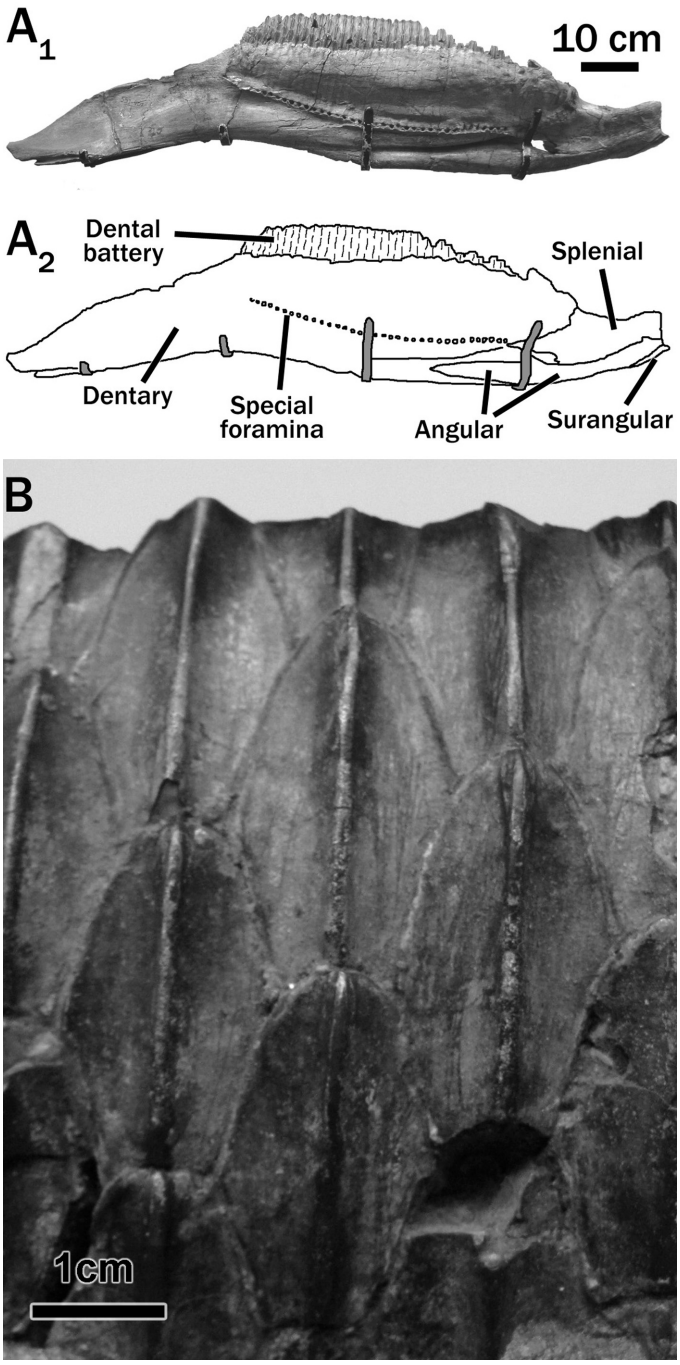

Figure 3.9. Right dentary of *S. angustirostris* (PIN 551/407) in lingual view. A_1 photograph and A_2 interpretive illustration. B. Lingual view of dentary teeth from the middle of the tooth row. Anterior is left. Note the coronoid process is missing in this specimen.

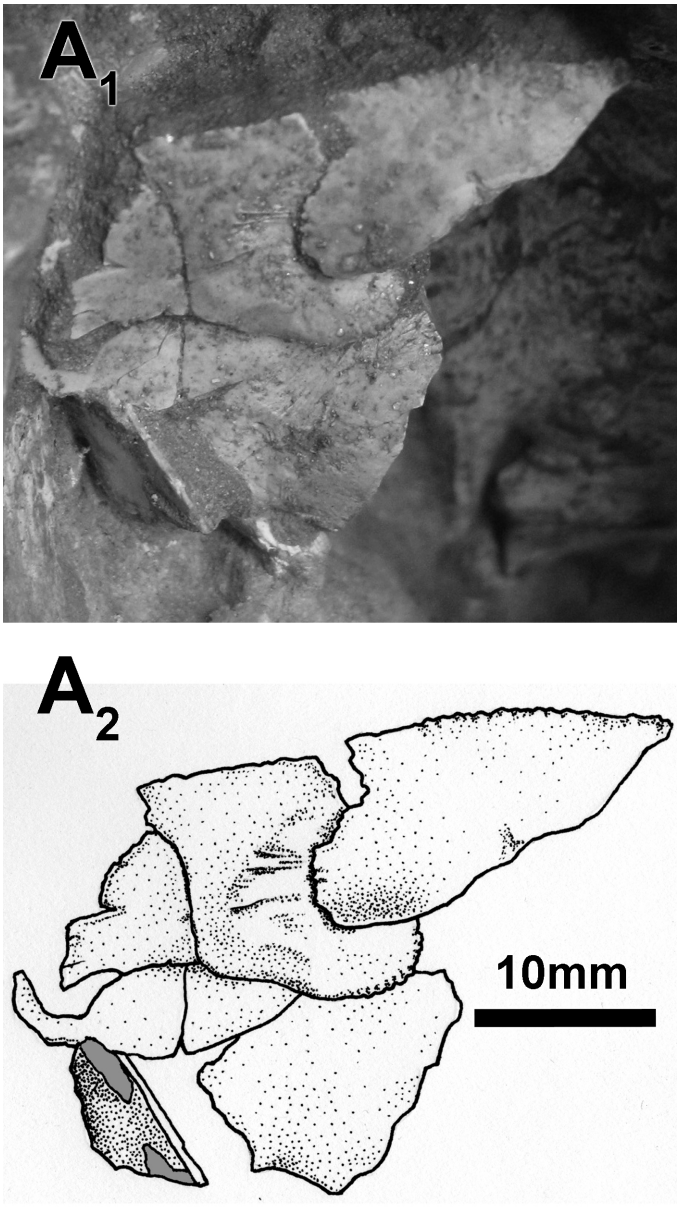

Figure 3.10. Photograph (A) and interpretive illustration (B) of partial sclerotic ring in right orbit of PIN 551/8. Grey regions in B denote matrix. Dorsal is up.

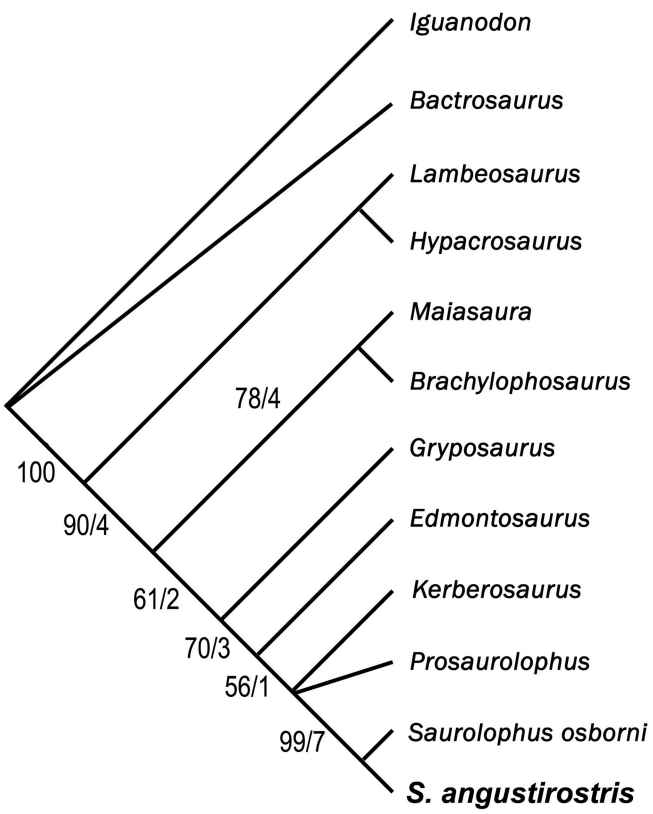

Figure 3.11. Strict consensus tree showing the phylogenetic position of *Saurolophus angustirostris*. RI= 0.87, CI= 0.84, and RCI= 0.74. Values at the base of nodes refer to bootstrap and decay indices, respectively.

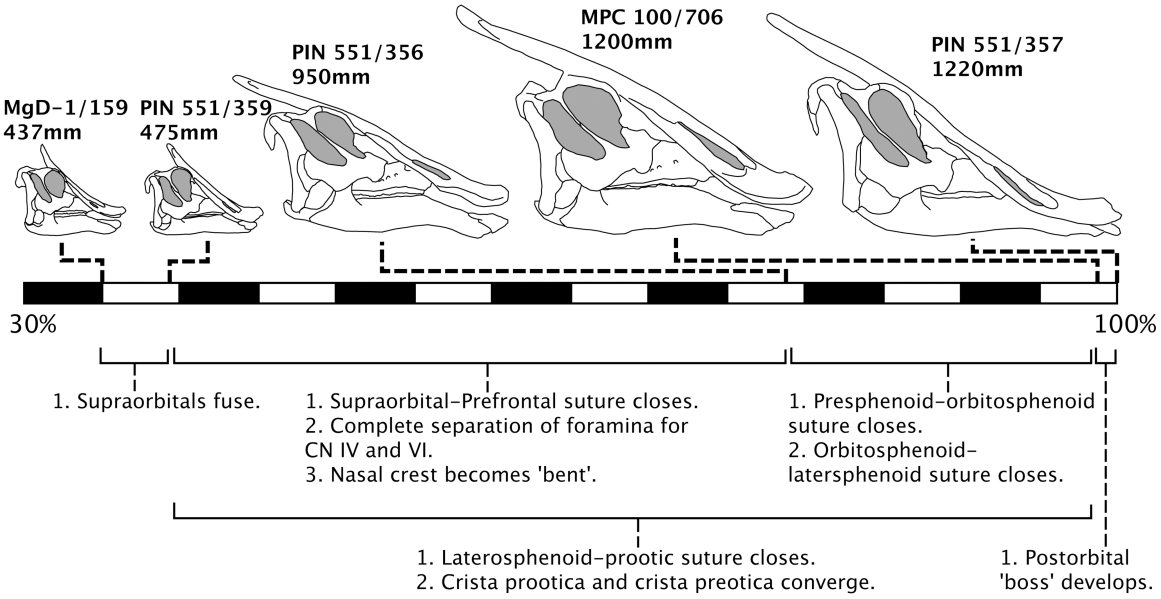

Figure 3.12. Ontogenetic series of *Saurolophus angustirostris* skulls with associated neurocranial (and select dermatocranial) changes. Specimens are placed on the scale bar as a percentage of length of the largest specimen. Specimens are to scale.

	S. angustirostris									*S. osborni*		
	PIN 551/356 (type)	**PIN 551/359**	**PIN 551/357**	**UALVP 49067**	**MPC 100/706**	**MPC 100/764**	**MgD-1/159**	**MgD-1/162**	**PIN 551/358**	**AMNH5220 (type)**	**AMNH5221 (para)**	**CMN 8796**
length (premax to quadrate)	950	575	1220	580	1200		437		1025	1000b		945
length (premax to tip of crest)	1350	670		740	1770		485			1170b		950#
Premaxilla: length	760	380	~900	375	890#		255		~1210	780i	660	680
Premaxilla: length of dorsal ramus from naris	340	145		165	510	380	50		370	324i	230#L,260#R	>285
Premaxilla: length of ventral ramus from naris	495	260	~650	240	700#	650	149		~890	548i	450	430
Quadrate: height	395	260	460	240	485		215	395	545	365	375	385*
Crest: length	405	200			570		150			307i		115#
Naris: length	230	90	165	160	370	215	55		195	352i		
Mandible: length	955	565		600	1120		415		1260	951i		910
Dentary: length	770	450	1025	440	940		335		1030		425#L, 370#R	730
Dentary: length of edentulous portion	330	170	450	160	380		130		450			290
Dentary: tooth count					46	>29	>26				43#L, 43#R	
Maxilla: ventral length		290	580		590			390			450	450
Maxilla: tooth count		>35	>50			>44	>27				46^	
Nasal: length	~170	580		625	1495		378		1020#	994i#		780*
Frontal: length posterodorsal process	105				220		~10					
Jugal: length	345	230		185	400	390	183	307	410	340	315	340

i = Image J
b = Brown 1912
# = incomplete
* = reconstructed
~ = approximate
L = left
R =Right
> = more than
^ based on 6teeth per 5cm. Tooth row length 390mm

Table 3.1. Select cranial measurements (mm) for *Saurolophus angustirostris* and *S. osborni.*

	1-5	6-10	11-15	16-20	21-25	26-30	31-35	36-40	41-44
Iguanodon	00000	00000	00000	00000	00000	00000	00000	00000	0000
Bactrosaurus	00000	00000	00000	00000	00000	00000	00000	00000	0000
Lambeosaurus	01011	11110	10110	20110	11101	00011	10111	21111	1211
Hypacrosaurus	01011	11110	10110	20120	11101	00011	10111	21111	1211
Maiasaura	00100	00011	01000	01002	10011	00012	21110	01111	2210
Brachylophosaurus	00100	00011	01001	01201	10011	00012	21110	11121	2210
Gryposaurus	00100	00012	01001	01000	10001	10013	11110	01111	1210
Kerberosaurus	001?1	000??	?????	?2??0	10001	1?013	11110	?11??	?2?0
Prosaurolophus	00101	00012	01001	12001	10001	10013	11110	01121	1210
Edmontosaurus	00100	00013	01001	12000	10001	11013	11110	21131	1310
Saurolophus osborni	10111	02212	01001	12202	1210?	?0013	11110	01121	?210
Saurolophus angustirostris	10111	02202	01001	12202	12101	10013	111?0	01121	1310

Table 3.2. Character-taxon matrix for phylogenetic analysis performed in this study. Character numbers and definitions correspond to those provided by Bell (2010).

References

Ali, F., Zelenitsky, D.K., Therrien, F., and Weishampel, D.B. 2008. Homology of the "ethmoid complex" of tyrannosaurids and its implications for the reconstruction of the olfactory apparatus of non-avian theropods. *Journal of Vertebrate Paleontology* 28: 123–133.

Bell, P.R. 2010. Redescription of the skull of *Saurolophus osborni* Brown 1912 (Ornithischia: Hadrosauridae). *Cretaceous Research.* Doi:10,1016/j.cretres.2010.10.002

Bell, P.R. and Evans, D.C. 2010. Revision of the status of *Saurolophus* from California. *Canadian Journal of Earth Sciences* 47: 1417–1426.

Bell, P.R., Snively, E., and Shychoski, L. 2009. A comparison of the jaw mechanics in hadrosaurid and ceratopsid dinosaurs using finite element analysis. *Anatomical Record* 292: 1338–1351.

Bolotsky, Y.L. and Godefroit, P. 2004. A new hadrosaurine dinosaur from the Late Cretaceous of far eastern Russia. *Journal of Vertebrate Paleontology* 24: 351–365.

Brown, B. 1912. A crested dinosaur from the Edmonton Cretaceous. *Bulletin of the American Museum of Natural History* 31: 131–136.

Currie, P. J. 2009. Faunal distribution in the Nemegt Formation (Upper Cretaceous), Mongolia. In: Y.-N. Lee (ed.), *Annual Report 2008, Korea-Mongolia International Dinosaur Project*. Korean Institute Geology and Mineralogy, Seoul, Korea, pp. 143–156.

Cuthbertson, R.S. and Holmes, R.B. 2010. The first complete description of the holotype of *Brachylophosaurus canadensis* Sternberg, 1953 (Dinosauria:

Hadrosauridae) with comments on intraspecific variation. *Zoological Journal of the Linnean Society* 159: 373–397.

Edmund, A.G. 1957. On the special foramina in the jaws of many ornithischian dinosaurs. *Royal Ontario Museum Division of Zoology, Palaeontological Contributions* 48: 1–14.

Eberth, D.A. and Deino, A. 2005. New $^{40}Ar/^{39}Ar$ ages from three bentonites in the Bearpaw, Horseshoe Canyon and Scollard formations (Upper Cretaceous-Paleocene) of southern Alberta, Canada. In: D.R. Braman, F. Therrien, E.B. Koppelhus and W. Taylor (eds.), Dinosaur Park Symposium, Short Papers, Abstracts, and Program, Royal Tyrrell Museum, Drumheller, Alberta, September 24-25, 2005, Special Publication of the Royal Tyrrell Museum, pp. 23–24.

Evans, D.C. 2006. Nasal crest homologies and cranial crest function in lambeosaurines dinosaurs. *Paleobiology* 32: 109–125.

Evans, D.C. 2010. Cranial anatomy and systematics of *Hypacrosaurus altispinus*, and a comparative analysis of skull growth in lambeosaurine hadrosaurids (Dinosauria: Ornithischia). *Zoological Journal of the Linnean Society* 159: 396–434.

Evans, D.C., Reisz, R.R., and Dupuis, K. 2007. A juvenile *Parasaurolophus* (Ornithischia: Hadrosauridae) braincase from Dinosaur Provincial Park, Alberta, with comments on crest ontogeny in the genus. *Journal of Vertebrate Paleontology* 27: 642–650.

Gates, T.A. and Sampson, S.D. 2007. A new species of *Gryposaurus* (Dinosauria: Hadrosauridae) from the late Campanian Kaiparowits Formation, southern Utah, USA. *Zoological Journal of the Linnean Society* 151: 351–376.

Godefroit, P., Zan, S., and Jin, L. 2001. The Maastrichtian (Late Cretaceous) lambeosaurine dinosaur *Charonosaurus jiayinensis* from north-eastern China. *Bulletin de l'Institut royal des Sciences naturelles de Belgique, Sciences de la Terre* 71: 119–168.

Godefroit, P., Hai, S., Yu, T., Lauters, P. 2008. New hadrosaurid dinosaurs from the uppermost Cretaceous of northeastern China. *Acta Palaeontologica Polonica* 53: 47–74.

Heaton, M.J. 1972. The palatal structure of some Canadian Hadrosauridae (Reptilia: Ornithischia). *Canadian Journal of Earth Sciences* 9: 185–205.

Horner, J. 1983. Cranial osteology and morphology of the type specimen of *Maiasaura peeblesorum* (Ornithischia: Hadrosauridae), with discussion of its phylogenetic position. *Journal of Vertebrate Paleontology* 3: 29–38.

Horner, J. 1992. Cranial morphology of *Prosaurolophus* (Ornithischia: Hadrosauridae) with descriptions of two new hadrosaurid species and an evaluation of hadrosaurid phylogenetic relationships. *Museum of the Rockies Occasional Paper* No. 2, 119 pp.

Horner, J.R. and Currie, P. J. 1994. Embryonic and neonatal morphology and ontogeny of a new species of *Hypacrosaurus* (Ornithischia, Lambeosauridae) from Alberta and Montana. InL K. Carpenter, K.F. Hirsch, and J.R. Horner (eds.) *Dinosaur Eggs and Babies*, Cambridge University Press, Cambridge, UK, pp. 312–336.

Horner, J.R., de Ricqles, A., and Padian, K. 2000. Long bone histology of the hadrosaurid dinosaur *Maiasaura peeblesorum*: growth dynamics and physiology based on an ontogenetic series of skeletal elements. *Journal of Vertebrate Paleontology* 20: 115–129.

Horner, J.R., Weishampel, D.B., and Forster, C.A. 2004. Hadrosauridae. In: D.B. Weishampel, P. Dodson, and H. Osmólska (eds.), *The Dinosauria*, (Second Edition). University of California Press, Berkeley, California, pp. 438–463.

Jerzykiewicz, T. 2000. Lithostratigraphy and sedimentary settings of the Cretaceous dinosaur beds of Mongolia. In: M.J. Benton, M.A. Shishkin, D.M. Unwin, and E.N. Kurochkin (eds.), *The Age of Dinosaurs in Russia and Mongolia*. Cambridge University press, Cambridge, UK, pp. 279–296.

Jerzykiewicz, T. And Russell, D.A. 1991. Late Mesozoic stratigraphy and vertebrates of the Gobi Basin. *Cretaceous Research* 12: 345–377.

Lambe, L. 1920. The hadrosaur *Edmontosaurus. Geological Survey of Canada, Memoir* 120:1–79.

Lemmrich, W. 1931. The sclerotic ring of birds (in German). *Jenaische Zeitschrift für Naturwissenschaft* 65: 514–586.

Maryańska, T. and Osmólska, H. 1979. Aspects of hadrosaurian cranial anatomy. *Lethaia* 12: 265–273.

Maryańska, T. and Osmólska, H. 1981. Cranial anatomy of *Saurolophus angustirostris* with comments on the Asian Hadrosauridae (Dinosauria). *Palaeontologia Polonica* 42: 5–24.

Maryańska, T. and Osmólska, H. 1984. Post-cranial anatomy of *Saurolophus angustirostris* with comments on other hadrosaurs. *Palaeontologia Polonica* 46: 119–141.

McBratney-Owen, B., Iseki, S., Bamforth, S.D., Olsen, B.R., and Mossiss-Kay, G.M. 2008. Development and tissue origins of the mammalian cranial base. *Developmental Biology* 322: 121–132.

Morris, W.J. 1973. A review of Pacific coast hadrosaurs. *Journal of Paleontology* 47: 551–561.

Norman, D. and Sues, H.-D. 2000. Ornithopods from Kazakhstan, Mongolia and Siberia. In: M.J. Benton, M.A. Shishkin, D.M. Unwin, and E.N. Kurochkin (eds.), *The Age of Dinosaurs in Russia and Mongolia*. Cambridge University Press, Cambridge, UK, pp. 462–479.

Ostrom, J.H. 1961. Cranial morphology of the hadrosaurian dinosaurs of North America. *Bulletin of the American Museum of Natural History* 122: 33–186.

Prieto-Marquez, A. 2005. New information on the cranium of *Brachylophosaurus canadensis* (Dinosauria, Hadrosauridae), with a revision of its phylogenetic position. *Journal of Vertebrate Paleontology* 25: 144–156.

Riabinin, A.N. 1930. Towards a problem of the fauna and age of dinosaur beds on the Amur River [in Russian with English summary]. *Russkoe Paleontologicheskoe Obshchestva, Monografy* 11: 41–51.

Rozhdestvensky, A.K. 1952. A new representative of duckbilled dinosaurs from the Upper Cretaceous deposits of Mongolia [in Russian]. *Doklody Akademic SSSR* 86: 405–408.

Rozhdestvensky, A.K. 1957. The duck-billed dinosaur *Saurolophus* from the Upper Cretaceous of Mongolia [in Russian].*Vertebrate PalAsiatica* 1: 129–149.

Rozhdestvensky, A.K. 1965. Growth changes in Asian dinosaurs and some problems of their taxonomy [in Russian]. *Paleontologicheskii Zhurnal* 3: 95–109.

Russell, D.A. 1993. The role of central Asia in dinosaurian biogeography. *Canadian Journal of Earth Sciences* 30: 2002–2012.

Russell, D.A. and Chamney, T.P. 1967. Notes on the biostratigraphy of dinosaurian and microfossil faunas in the Edmonton Formation (Cretaceous), Alberta. *National Museum of Canada Natural History Papers* 35, 22 p.

Russell, D.A. and Dong, Z.-M. 1993. A nearly complete skeleton of a new troodontid dinosaur from the Early Cretaceous of the Ordos Basin, Inner Mongolia, People's Republic of China. *Canadian Journal of Earth Science* 30: 2163–2173.

Russell, L.S. 1940. The sclerotic ring in the Hadrosauridae. *Royal Ontario Museum Palaeontology Contributions* 3: 1–7.

Sereno, P.C., Tan, L., Brusatte, S.L., Kriegstein, H. J., Zhao, X., Cloward, K. 2009. Tyrannosaurid skeletal design first evolved at small body size. *Science* 326: 418–422.

Shuvalov, V.F. 2000. The Cretaceous stratigraphy and palaeobiogeography of Mongolia. In: M.J. Benton, M.A. Shishkin, D.M. Unwin, and E.N. Kurochkin (eds.), *The Age of Dinosaurs in Russia and Mongolia*. Cambridge University Press, Cambridge, UK, pp. 256–278.

Sullivan, R.M. and Williamson, T.E. 1999. A new skull of *Parasaurolophus* (Dinosauria: Hadrosauridae) from the Kirtland Formation of New Mexico and a revision of the genus. *New Mexico Bulletin of Natural History and Science* 15, 52p.

Swofford, D.L. 2002. *Phylogenetic analysis using parsimony (and other methods). Version 4.0b10*. Sinauer Associates, Sunderland, Massaschusetts, 40 pp.

Vickaryous, M.K., Maryańska, T., Weishampel, D.B. 2004. Ankylosauria. In: D.B. Weishampel, P. Dodson, and H. Osmólska (eds.), *The Dinosauria*, (Second Edition). University of California Press, Berkeley, California, pp. 363–392.

Weishampel, D.B. and Horner, J.R. 1990. Hadrosauridae. In D. Weishampel, P. Dodson, and H. Osmólska (eds.) *The Dinosauria*. University of California Press, Berkeley, pp. 534–561.

Weishampel, D., Barrett, P., Coria, R., Le Loeuff, J., Xu, X., Zhao, X., Sahni, A., Gomani, E., and Noto, C. 2004. Dinosaur distribution. In: D. Weishampel, P. Dodson, and H. Osmólska (eds.) *The Dinosauria*, (Second edition). University of California Press, Berkeley, California, pp. 517–606.

You, H.-L. And Dodson, P. 2003. Redescription of neoceratopsian dinosaur *Archaeoceratops* and early evolution of Neoceratopsia. *Acta Palaeontologia Polonica* 48: 261–272.

Young, C.C. 1958. The dinosaurian remains of Laiyang, Shantung. *Palaeontologia Sinica* 16: 53–138.

Appendix 3.1: Character Descriptions

1. Parietal: participates in occipital aspect of skull (0); completely excluded from the occiput (1).
2. Parietal: "length/minimal width" >2 (0); <2 (1).
3. Parietal: sagittal crest short, <2/3 the length of parietal (0); long, >2/3 the length of the parietal (1).
4. Parietal: midline ridge straight to slightly downwarped along length (0); strongly downwarped to below the level of the postorbital-prefrontal joint (1).
5. Frontal: participates in the orbital rim (0); excluded by postorbital-prefrontal joint (1)
6. Hollow supracranial crest: absent (0); present (1).
7. Frontal: long, "caudal length/maximal width" ratio >0.74 (0); very shortened, "caudal length/maximal width" ratio <0.6 (1); secondary elongation resulting in the backwards extension of the frontal platform (2).
8. Frontal platform: absent (0); occupying the rostral part of the frontal in adult (1); extends above rostral portion of the supratemporal fenestra (2).
9. Premaxilla: narrow, expanded laterally less than two times width at post-oral constriction, margin oriented nearly vertically (0); expanded transversely to more than two time post-oral constriction, margin flared laterally into a more horizontal orientation (1).
10. Premaxilla: reflected rim absent (0); deflected at anterolateral corner and posteriorly reflected (1); reflected along entire rim and narrow (2); reflected along entire rim, but thickened at anteroventral corner (3).
11. Premaxillary foramen present (0); absent (1).
12. Premaxilla: auxillary narial fossa absent (0); present (1).
13. Posterior premaxillary process: short, not meeting the lateral premaxillary process posterior to external naris (0); long, meets the lateral premaxillary process behind external naris to exclude the nasal, nasal passage enclosed ventrally by folded, divided premaxillae.
14. Lateral premaxillary process stops at level of lacrimal (0); continues further backward above skull roof (1).
15. External naris/basal skull length ratio <0.2 (0); >0.2 (1).
16. external naris: posterior apex formed entirely by nasal (0); formed by nasal (dorsally) and premaxilla (ventrally) (1); formed entirely by premaxilla (2).
17. Circumnarial depression absent (0); light depression incised into nasal and premaxilla (1); marked by a well-developed ridge and sometime invaginated (2).
45. Nasal: restricted to area rostral to braincase, *cavum nasi* small (0), retracted caudally to lie over braincase in adults resulting in convoluted, complex narial passageway, *cavum nasi* enlarged (1); retracted caudally to lie over braincase, narial passageway simple (2). Extra character state added to match condition in *S. osborni* and *B. canadensis*.
46. Nasal: does not participate in hollow crest (0); participates in small part of the hollow crest and is excluded from the caudodorsal margin of the crest (1); participates in half of the crest or more and forms the caudodorsal aspect of the crest (2).

47. Solid supracranial crest: absent (0); formed by nasals only (1); formed by nasals and frontals with or without contribution from prefrontals (2).
48. Supraorbital free in adults (0); fused to prefrontal (1).
49. Prefrontal: caudal portion oriented horizontally (0); participates in the lateroventral portion of the hollow crest (1); participates in the lateroventral portion of the solid crest (2). State added to match condition in *S. osborni.*
50. Squamosal: medial ramus lower than paroccipital process (0); higher than paroccipital process (1).
51. Squamosal: prequadratic process strikingly longer than rostrocaudal length of quadrate cotylus (0); only slightly longer than rostrocaudal length of quadrate cotylus (1).
52. Supraoccipital: posterior surface nearly vertical (0); steeply inclined forwardly at an angle of about 45° (1).
53. Supraoccipital/exoccipital shelf limited (0); very extended (1) above foramen magnum.
54. Postorbital pouch absent (0); well developed (1).
55. Postorbital: dorsal surface flat (0); thickened to form a dorsal promontorium (1).
56. Jugal: rostral process tapering in lateral view to fit between maxilla and lacrimal (0); dorsoventral expanded (1).
57. Jugal: rostral process angular and slightly asymmetrical in lateral view (0); rounded and symmetrically very expanded (1); isosceles-triangle shaped (2); asymmetrically strongly upturned (3).
58. Jugal flange: slightly developed, dorsoventral depth of jugal from ventral border of infratemporal fenestra to ventral edge of flange approximately equal to minimum dorsoventral depth of rostral segment of jugal between rostral and postorbital process (0); dorsoventral depth of jugal from ventral border of infratemporal fenestra to ventral edge of flange less than twice minimum depth of rostral segment of jugal between rostral and postorbital process (1); strongly projected ventrally into semicircular boss, dorsoventral depth of jugal from ventral border of infratemporal fenestra to ventral edge of flange twice or nearly twice minimum dorsoventral depth of rostral segment of jugal between rostral and postorbital process (2).
59. Maxilla: apex caudal to centre (short caudal portion of maxilla) (0); at or rostral to centre (long and robust caudal portion of maxilla) (1).
60. Maxillary foramen: situated rostrolaterally (0); on dorsal maxilla and on premaxilla-maxilla suture (1).
61. Maxilla: ectopterygoid ridge faintly developed and inclined caudally (0); strongly developed and nearly horizontal (1).
62. Maxilla: rostromedial process present (0); wide sloping maxillary shelf (1).
63. Lacrimal-maxilla contact: present (0); extremely reduced, only anterior sharp tip of lacrimal contacting maxilla (1); lost or covered as result of jugal-premaxilla contact (2).
64. Paraquadratic foramen: present (0); absent (1).
65. Quadrate: distal head transversely expanded (0); dominated by a large hemispherical lateral condyle (1).
66. Dentary: diastema between first dentary tooth and predentary short, no more than width of 4 or 5 teeth (0); moderate, equal to approximately 1/5 to ¼ of

tooth row (1); long, more than 1/3 of tooth row but less than 1/2 (2); extremely long, more than 1/2 of tooth row (3).

67. Dentary: coronoid process sub-vertical (0); inclined rostrally (1).
68. Predentary: rostral mediolateral width less than or equal to rostrocaudal length of lateral process (0); greater than or equal to rostrocaudal length of lateral process (1); greater than twice rostrocaudal length of lateral process (2).
69. Dentary: number of tooth positions in adult specimen, ≤30 (0); 34–40 (1); 42–45 (2); ≥47 (3).
70. Dentary: tooth crowns broad with dominant ridge and secondary ridges (0); miniaturised with or without faint secondary ridges (1).
71. Dentary: median carina of teeth straight (0); sinuous (1).

CHAPTER 4

REVISION OF THE STATUS OF *SAUROLOPHUS* (HADROSAURIDAE) FROM CALIFORNIA.

A version of this chapter was published as Bell, P. R. and Evans, D. C. 2010. Revision of the status of *Saurolophus* (Hadrosauridae) from California. *Canadian Journal of Earth Sciences* 48:1417-1426

Introduction

During the Late Cretaceous, hadrosaurids had a near cosmopolitan distribution, and were among the most common and diverse dinosaurs in both inland and coastal environments (Horner et al. 2004). Despite a rich fossil record from areas of western North America east of the Rocky Mountains, the remains of hadrosaurs from the west coast remain rare (Morris 1973; Horner et al. 2004). The best record of Late Cretaceous vertebrates in this region is from California, U.S.A. and Baja, Mexico (Morris 1973). In California, numerous isolated elements have been recovered from the Point Loma, Ladd, Williams, and Moreno formations, yet few have revealed significant insights into the diversity of hadrosaurs in this region.

The Moreno Formation records the shoaling of the central San Joaquin basin to shelf depths during the late Maastrichtian to Paleocene (70–61 Ma; McGuire 1988). Shelf sediments were derived from the Sierra Nevada magmatic arc and transported across the alluvial plain before being deposited in the fore arc basin (McGuire 1988). The shallow marine deposits of the Moreno Formation have yielded abundant remains of marine reptiles, specifically mosasaurs and plesiosaurs, and rare, transported remains of hadrosaurs are also known.

In the summers of 1939 and 1940, two incomplete hadrosaurid skeletons, both including partial skulls, were collected by Chester Stock and his crews (California Institute of Technology) from the Moreno Formation, Panoche Hills, Fresno County. The first skeleton (LACM/CIT 2670) consists of most of the skull and several pelvic girdle and limb bones in a poor state of preservation. The second specimen (LACM/CIT 2852) is reported to be better preserved and

includes a nearly complete skull and skeleton. In a private communication to Stock, A.C. Drescher commented on the likeness of this specimen (Hilton 2003) to *Saurolophus osborni*. However, it was not until 1973 that this identification was formalised in the scientific literature by Morris (1973). In his review of the Hadrosauridae from California, Morris (1973) assigned both specimens, plus a third partial postcranial skeleton (UCMP 32944), to cf. *Saurolophus.* The 'spatulate premaxillae' (p. 555), proportions of the quadrate, and relatively deep skull, appeared to him to be closer to *S. osborni* than they were to *Prosaurolophus*.

The assignment of LACM/CIT 2852 to *Saurolophus* has important implications for hypotheses of Late Cretaceous dinosaur biogeography, as it extends the geographic range of *Saurolophus* considerably southward from its type locality in Alberta, Canada, and west of the Rocky Mountains. Although much of the skull and skeleton of the best of these three specimens (LACM/CIT 2852) is in a poor state of preservation, enough anatomical information is present in the cranial elements to provide new anatomical and phylogenetic information.

Systematic Palaeontology

Dinosauria Owen, 1842

Ornithischia Seeley, 1887

Ornithopoda Marsh, 1881

Hadrosauridae Cope, 1869

Hadrosaurinae Lambe, 1918

Genus and species indet.

Material

LACM/CIT 2852 consists of a moderately complete, but poorly preserved skeleton. The skull consists primarily of the right side of the face and includes the premaxillae, maxillae, jugal, quadratojugal, quadrate, paroccipital process, ?postorbital, both dentaries, predentary, and parts of the angular, surangular, and splenial, but lacks the majority of the braincase (including the frontals) and most of the nasals (Fig. 4.1). The postcranium consists of a large number of vertebrae from all regions of the column (except the sacrum) and numerous ribs. Shafts of limb bones and many phalanges are also present from the fore- and hind limbs, but pelvic girdle material is missing.

Locality and Horizon

Strata of the Moreno Formation crop out in the Panoche Tumey Hills of Fresno County, California on the western edge of the San Joaquin basin (Fig. 4.2). At the type section (Escarpado Canyon, Panoche Hills), the formation comprises approximately 800 m of dark brown, grey, and maroon shales and mudstones (McGuire 1988). Although the exact location of the quarry of LACM/CIT 2852 within the Moreno Formation is unknown, it most likely comes from the upper part (Marca Member, Payne 1941), where deposits represent facies more proximal to the paleoshoreline. The only biostratigraphic study of the Moreno Formation to include dinosaurs is that of Ford (2006) who included only two hadrosaurid localities, both of which were from the Marca Member. The

underlying Tierra Loma Member is rich in mosasaur and plesiosaur fossils; however, dinosaurs have not been recovered from this unit. McGuire (1988) describes the Marca Member as a finely-laminated, diatomaceous shale that is overlain by the Paleocene Dos Palos Member, suggesting that the Marca Member is late Maastrichtian in age. That interval has been interpreted as an oxygen-deficient upper slope facies within an overall shoaling sequence of the San Joaquin basin (McGuire 1988).

Description

Premaxilla. The paired premaxillae were found in union; however, they have suffered from post-depositional deformation. The left premaxilla has rotated medially so that its medial process now partially overlaps the medial process on the right premaxilla and the midline suture towards the front of the beak can be seen in right lateral view (Fig. 4.3*a*). The premaxillae form an edentulous beak that was likely covered by a keratinous ramphotheca in life (Sternberg 1935). Medially and ventrally, the oral margin is lined with a series of coarse domical nodes (Fig. 4.3*b*). Although crushed, the prenarial body is elongated as in *Edmontosaurus*; however, in dorsal view, they do not appear to have flared mediolaterally like *Edmontosaurus* but rather form a spatulate arrangement as in *Prosaurolophus* and *Saurolophus.* The dorsal border of the premaxillary body is rather straight as in *Saurolophus osborni* but not *S. angustirostris.* The entire oral margin appears upturned as in *Prosaurolophus* and *Saurolophus* but the bones are clearly distorted. Although incomplete, the naris appears to have been dilated dorsoventrally as in most hadrosaurines, with the

exception of *Prosaurolophus* and *Saurolophus*, which have slit-like external nares. The posterolateral premaxillary process is plate-like and extends posteriorly to overlie the anterodorsal edge of the maxilla. A broken length of what may be the posterolateral process of the right premaxilla measures 22 cm (Fig. 4.3). Although fragmentary, it would have extended along the anterodorsal length of the maxilla to the level of the lacrimal-maxillary contact.

Maxilla. The maxilla is low and slender. It measures 45 cm long and is roughly symmetrical in lateral aspect as in Hadrosaurinae. At least three poorly preserved maxillary foramina form a horizontally oriented row just ventral to the jugal suture (Figs. 4.4*c*, *e*). The sutural surface for the jufal is at about the midlength of the maxilla on the lateral surface of the dorsal process. The dorsal process appears to be low and poorly defined, unlike the prominent triangular processes seen in most hadrosaurines, including *Edmontosaurus* and the saurolophines, although this may be due to breakage and wear. The right maxilla preserves the jugal in articulation. The premaxilla rests on the anterodorsal surface of the maxilla in the typical hadrosaurine configuration (Horner 1992). A short length of the posterolateral premaxillary process is preserved on the anterior-most portion of the right maxilla (Figs. 4.4*c*, *e*). More than fifty tooth families are present with up to five teeth per family. This condition occurs only in *Saurolophus* and *Edmontosaurus* among hadrosaurids. The occlusal surface of the tooth row forms a slightly sinusoidal profile in lateral view. Medially, there is a horizontal row of special dental foramina (Edmond 1957), which lie close to the dorsal margin of the maxilla. Each foramen corresponds to the base of each alveolus; however, not all foramina are preserved (Figs. 4.4*d*, *f*).

Jugal. The right jugal is preserved in union with the maxilla (Figs. 4.4*c–f*). The anterior process is symmetrical, rounded anteriorly, and only weakly expanded dorsoventrally; however, its contours are almost certainly due to erosion. The dorsal half of the anterior process was apparently devoted to contact with the lacrimal, which is not preserved; the ventral half meets the dorsal process of the maxilla. The postorbital process is robust and strongly retroverted proximally, becoming more vertically oriented distally such that the anteroventral corner of the infratemporal fenestra appears 'pinched', as in *Edmontosaurus*. The posterior process of the jugal is only weakly expanded and the ventral margin is almost straight. It seems that the jugal would have continued further posteriorly and expanded dorsally to cover the lateral surface of the quadratojugal. There is no prominent ventral flange on the posterior process as there is in *Gryposaurus, Brachylophosaurus*, or *Maiasaura.* The jugal resembles the general morphology seen in specimens of *Edmontosaurus*, *Prosaurolophus*, and *Saurolophus*.

Quadratojugal. The right quadratojugal is preserved in contact with the jugal (Fig. 4.4). It is poorly preserved; the original outline of the element is unknown as most of its margins are damaged. As preserved, it is ovoid and higher than it is long. As the jugal is broken, it is unclear whether the quadratojugal participated in the border of the infratemporal fenestra. The posterior margin of the quadratojugal is only weakly curved where it fits into the reciprocal notch in the quadrate.

Nasal. A short midline segment of the conjoined left and right nasals is preserved (Fig. 4.3). Each nasal fragment is straight in lateral view with parallel ventral and dorsal borders. Although the exact position of the segment is unknown, it most likely formed the dorsal narial borders posterior to the contact with the medial processes of the premaxillae. There is no indication of a gryposaur- or saurolophine-like crest.

Quadrate. The preserved portion of the quadrate resembles a slender and slightly recurved rod. Ventrally, it is weakly expanded to form the condyle for articulation with the lower jaw; however, it is crushed and the lateral and medial condyles are indistinct. The quadratojugal notch is open and forms an obtuse angle such that the ventral extent of the notch does not wrap around the posterior edge of the quadratojugal. Therefore it is not C-shaped as it is in *Saurolophus, Prosaurolophus,* and *Edmontosaurus* (Fig. 4.5). It is possible that this shape is an artefact of preservation. The pterygoid process is missing; however, a broken ridge on the medial surface of the dorsal half of the quadrate delineates its origin (Fig. 4.5*b*).

Postorbital. An unusual bone may represent the right postorbital that is potentially fused to lateral portions of the frontal and/or the prefrontal (Fig. 4.6). The anteriorly projecting prefrontal process is missing. The elongate jugal process is ornamented by several strong transverse and oblique ridges that give the entire process a distinct robustness. The medial surface of the jugal process is buttressed by a thin ridge that extends the length of that process. Ventrally, the jugal process has a slightly expanded, almost spoon-shaped termination. The

angle between the jugal process and the squamosal process is obtuse, which would have formed the anterodorsal margin of the infratemporal fenestra. The bone surface in this region is rugose. The angle between the jugal process and the base of the prefrontal process appears to have rather spacious similar to the postorbital pouch in *Edmontosaurus* (Horner et al. 2004); however, not enough of this element is preserved to confirm the presence of this feature. Much of the medial surface of this element has been eroded to expose the trabecular bone within.

Paroccipital process. A large, crescentic conglomeration of two incomplete, flat bones may represent the paroccipital process. Only the postcotyloid process of the squamosal is preserved. It is mediolaterally compressed and in union with the anterior surface of the paraoccipital process of the exoccipital (Fig. 4.5*a*). In lateral view, the postcotyloid process has the same anteroposterior length for its entire height and is bowed to conform to the curvature of the paraoccipital process, terminating in a rounded knob ventrally. A number of parallel ridges on its posterolateral surface extend nearly the entire height of the postcotyloid process. The paraoccipital process of the exoccipital is preserved with the squamosal fragment (Fig. 4.5). It is broadly C-shaped and is in contact with but slightly longer than the postcotyloid process of the squamosal. The ventral terminus of the paraoccipital process is damaged but appears to taper to a rounded point.

Mandible. The predentary is relatively well-preserved, but it is crushed. The horseshoe-shaped predentary wraps around the dentary symphysis and is of

typical hadrosaurid design (Figs. 4.7*c*, *h*; Horner et al. 2004). Ventrally, two small, tab-shaped medial processes meet the dentary symphysis. Several small foramina perforate the ventral surface of the predentary. The oral margin lacks the fine projections present in *Prosaurolophus* and is lined with a row of low, domical nodes that probably bore a keratinous sheath in life to facilitate occlusion with the premaxilla.

The dentary is the longest of the preserved bones in the skull of LACM/CIT 2852. Although both dentaries are preserved, they are in such poor condition that the left dentary was originally mistaken for a femur and mounted as such in the historical mount of this specimen (Figs. 4.7*a*, *b*). The dentary ramus is straight and the dorsal and ventral margins are parallel as in *Edmontosaurus*. The edentulous portion of the dentary comprises half of the length of that bone. The edentulous portion does not appear to be significantly deflected ventrally, but tapers where it meets the predentary. The coronoid process slopes anterodorsally and its dorsal terminus is anteroposteriorly expanded and spatulate, as in Hadrosauridae. No teeth were preserved in situ and the alveolar grooves are entirely obliterated.

The angular is a strap-like element that extends along the medioventral surfaces of the dentary, surangular, and splenial. The posterior third of the angular, is preserved in LACM/CIT 2852 (Figs. 4.7*f*, *g*). It is of roughly even dorsoventral height for the anterior two thirds of the preserved length, behind which it tapers sharply whereit overlays the splenial dorsally and surangular ventrally.

A single partial splenial is preserved in LACM/CIT 2852 but lacks the anterior and posterior extremities and the dorsal margin. As preserved, it is a

mediolaterally compressed plate of bone that would have occupied the typical hadrosaurid position on the medial surface of the surangular just dorsal to the angular. Ventrally, the splenial is mediolaterally thickened where it contacts the strap-like angular. There is a broad depression on the lateral surface, which extends for most of the preserved length of the splenial (Fig. 4.7*j*).

The surangular is the largest of the postdentary bones and forms the glenoid for the ventral condyle of the quadrate (Figs. 4.7*d*, *e*). The open glenoid occupies much of the dorsal surface of the surangular, which is mediolaterally expanded around the glenoid. Posteriorly, the surangular tapers in both height and width where it forms a flat, vertical surface for contact with the articular. The anterior part of the surangular is mediolaterally compressed and expanded dorsoventrally. The coronoid process of the surangular is not preserved in this specimen.

Teeth. The maxillae still retain complete batteries of teeth although they are not as well preserved. There are at least fifty tooth families with up to five teeth per family. One or two teeth contribute to the occlusal surface in any given family. The maxillary teeth are narrower and smaller than the dentary teeth.

Although no teeth were preserved in situ in the dentaries, large numbers of isolated and amalgamated teeth were found in association with the skull (Fig. 4.8). Dentary teeth are arranged in vertical families of at least three teeth of which two may be active at any one time (Fig. 4.8*b*). The height of each crown (roughly diamond shaped in lingual view) is little more than twice its anteroposterior length. A prominent, straight median carina bisects the height of each crown. There are no accessory ridges or papillae. Especially in the complete lack of

papillae, the dentary teeth closely resemble those of *Edmontosaurus*. The crown-root angle is 130°, within the expected range of other hadrosaurines (Horner et al. 2004). The wear surfaces are concave and medially inclined.

Hyoid. The single partial hyoid found in LACM/CIT 2852 is of typical hadrosaurid design (Fig. 4.9). Anteriorly, it is expanded and club-shaped, terminating in a flat surface perpendicular to the long axis of the hyoid. The medial surface of the anterior end has weak longitudinal striations. The hyoid tapers posteriorly; however, its complete length is not preserved.

Phylogenetic Analysis

In order to assess the taxonomic identification and systematic position of the California hadrosaurid, the data matrix of Godefroit et al. (2008) was utilized. LACM/CIT 2852 was scored based on the morphological information presented in this paper (Table 1). The first analysis using the entire dataset of Godefroit et al. (2008) confirms that LACM/CIT 2852 is a hadrosaurine. Lambeosaurinae was therefore collapsed into a single terminal taxon using *Corythosaurus* as the representative of the clade. The final dataset consists of ten in-group hadrosaurine operational taxon units (nine genera plus LACM/CIT 2852) plus *Corythosaurus* (representing Lambeosaurinae) and *Bactrosaruus*. *Bactrosaurus* was specified as the outgroup to polarize characters and root the trees. Due to the fragmentary nature of LACM/CIT 2852, it could only be coded for 20 characters

(36% of the total dataset). In using *Corythosaurus* as a single terminal outgroup taxon, only 19 of the 56 character dataset are parsimony-informative.

The data matrix was constructed in MacClade 4.08 (Maddison and Maddison, 2005) and analyzed phylogenetically with PAUP 4.0b10 using the Branch-and-Bound algorithm (Swofford, 2002). Unlike the original analysis of Godefroit et al. (2008), all characters were treated as unordered. Both ACCTRAN and DELTRAN character optimizations were conducted, and characters that do not change placement under both optimizations are considered unambiguous. Standard bootstrap analysis (1000 replicates using the Branch-and-Bound algorithm performed in PAUP) and Bremer decay values were calcuated in order to assess the stability of the maximum parsimony tree topologies.

Results

Phylogenetic analysis of the data matrix resulted in two most parsimonious trees (MPTs) of 70 steps (Fig. 4.10). Each tree has a Consistency Index of 0.929 (excluding parsimony uninformative characters CI= 0.861), a Rescaled Consistency Index of 0.806, and a Retention Index of 0.868. The MPTs differ only in the placement of LACM/CIT 2852. In one MPT, LACM/CIT 2852 is posited as the sister taxon to the *Edmontosaurus-Anatotitan* clade. In the other, it is the sister-taxon to *Saurolophus* within a clade that includes *Kerberosaurus* and the 'saurolophs'. In both scenarios, the placement of LACM/CIT 2852 is supported by one unambiguous synapomorphy: the high number of tooth families that make up the dental batteries (47[3]). This character is homoplastic and is inferred to have evolved independently in the *Saurolophus* and *Edmontosaurus-Anatotitan*

lineages. The number of teeth has a definite link to skull size in hadrosaurids, and may simply reflect the large size of these three taxa.

Bremer and bootstrap values indicate that the phylogenetic hypothesis presented here is weakly supported. All nodes have bremer decay indices that are less than 2, and bootstrap values are generally weak. The sister-group relationship between LACM/CIT 2852 and either *Saurolophus* or the *Edmontosaurus+Anatotitan* clade is poorly supported, with bootstrap values less than 50%, reflective of zero decay value support for either grouping.

Discussion and Conclusions

LACM/CIT 2852 is a large hadrosaurine hadrosaurid, with a skull that likely measured over one meter in length. Although the postcranial skeleton is poorly preserved, enough anatomical information is obtainable from the skull to determine its phylogenetic affinities. LACM/CIT 2852 can be identified as a hadrosaurine based on several derived cranial apomorphies, including a symmetrical maxilla with the jugal facet at about its midlength, and a reflected oral margin of the premaxilla, a unique character of hadrosaurines that is not included in the dataset of Godefroit et al. (2008). A number of features of the dentition (reduced papillae, absence of secondary ridges on the enamel face, and low aspect ratio tooth crowns) also indicate hadrosaurine affinities.

Although it can be confirmed that the specimen represents a large hadrosaurine, the original suggestion Morris' (1973) that LACM/CIT 2852 represents a species of *Saurolophus* cannot be unequivocally substantiated.

LACM/CIT 2852 appears to differ from *Saurolophus* in lacking a well-developed dorsal process of the maxilla (assuming this region is not broken), and despite deformation, the premaxilla seems to suggest that external naris was not slit-like. Moreover, some of these differences (a relatively dilated external naris in comparison to saurolophs [a plesiomorphy]; a low, elongate maxilla with a reduced dorsal process; and low aspect ratio dentary tooth crowns that lack marginal papillae) are more similar to edmontosaurs like *Edmontosaurus* and *Anatotitan*. LACM/CIT 2852 differs from *Edmontosaurus* in lacking a strongly reflected oral margin to the premaxillae; in this feature LACM/CIT 2852 is closer to *Prosaurolophus* and *Saurolophus*. However, it must be stressed that the premaxillae are so diagenetically deformed as to make characters derived from this element ambiguous at best. The morphology of the nasals suggests the absence of "Roman nose" characteristic of *Gryposaurus*. However, the nasals are so fragmentary that this and the presence of a pseudonarial crest (as in *Saurolophus, Prosaurolophus, Brachylophosaurus*, and *Maiasaura*) cannot be ruled out.

The possible presence of an *Edmontosaurus*-like hadrosaurid from the Maastrichtian of California is not unexpected considering the geographic range of that genus (Bell and Snively 2008). The separation of the western coastal alluvial plains from the Western Interior Seaway by the Sierra Nevada magmatic arc may have acted as a significant dispersal boundary to many land vertebrates, including dinosaurs. Therefore it is also possible that LACM/CIT 2852 represents a separate taxon from its more eastern relatives; however, at this stage, hadrosaur remains from the Moreno Formation (including LACM/CIT 2852) are

too poorly preserved to permit conclusive specific assignment and LACM/CIT 2852 must be considered Hadrosaurinae indet.

North American hadrosaur diversity reached its acme during the Campanian, perhaps most spectacularly within the Belly River Group of Alberta and Montana. In comparison, Maastrichtian hadrosaur faunas were relatively depauperate, represented by four genera (*Saurolophus, Hypacrosaurus, Edmontosaurus,* and *Anatotitan*) although indeterminate hadrosaurid material is known from Alaska and northern Canada to Mexico (Weishampel et al. 2004). The present study cannot confirm the widely-cited southern occurrence of *Saurolophus* (Morris 1973; Weishampel and Horner 1990; Horner et al. 2004; Gates and Farke 2009). It is equally possible that LACM/CIT 2852 represents an *Edmontosaurus*-like hadrosaurine from the western coastal plains of California. In either case, it has important biogeographical implications for one of these two wide-ranging Maastrichtian lineages. The only other reasonably complete hadrosaurid from the Moreno Formation (LACM/CIT 2670) is substantially smaller than LACM/CIT 2852 and may be a lambeosaurine (T. Ford, pers. comm., 2009); however, further preparation and study of this specimen is required to qualify its systematic position. ?*Lambeosaurus laticaudus* from the 'El Gallo Formation' of Baja California (Mexico) is significantly older (Campanian) than LACM/CIT 2852 (Morris 1973, 1981). All other hadrosaurid remains from west of the cordillera are too fragmentary or poorly preserved to allow further taxonomic assignment.

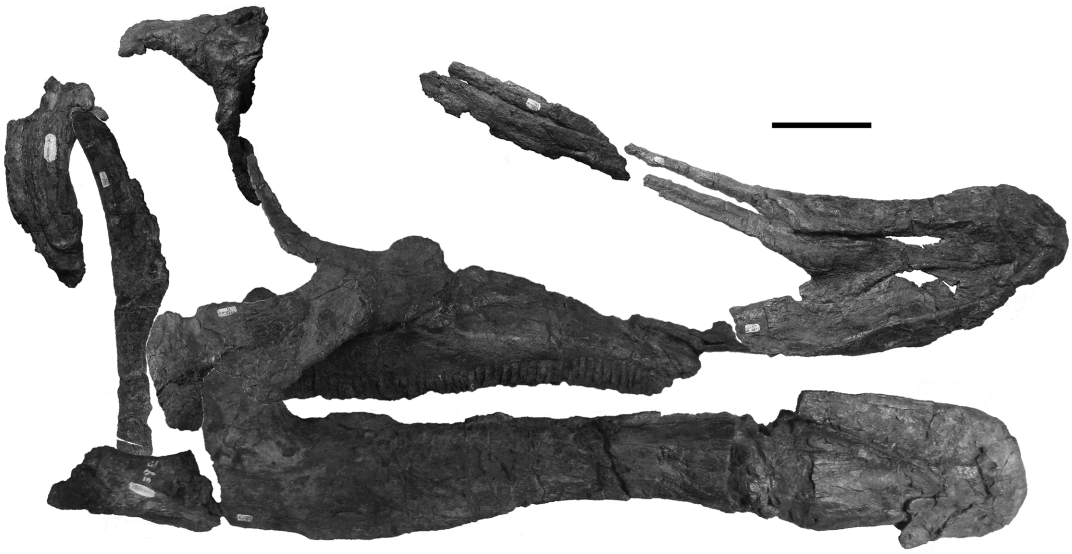

Figure 4.1. Partial skull of LACM/CIT 2852. Scale = 10 cm.

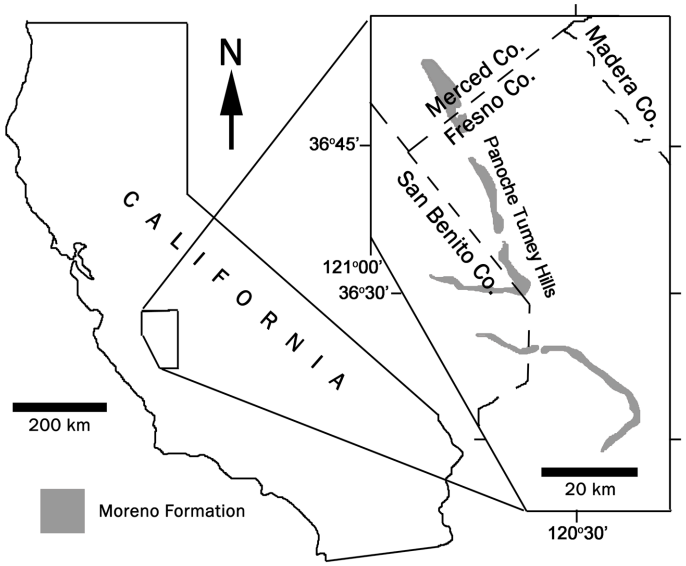

Figure 4.2. Locality map of the Panoche Tumey region in central California. Modified from http://geology.usgs.gov (accessed 31 March, 2009).

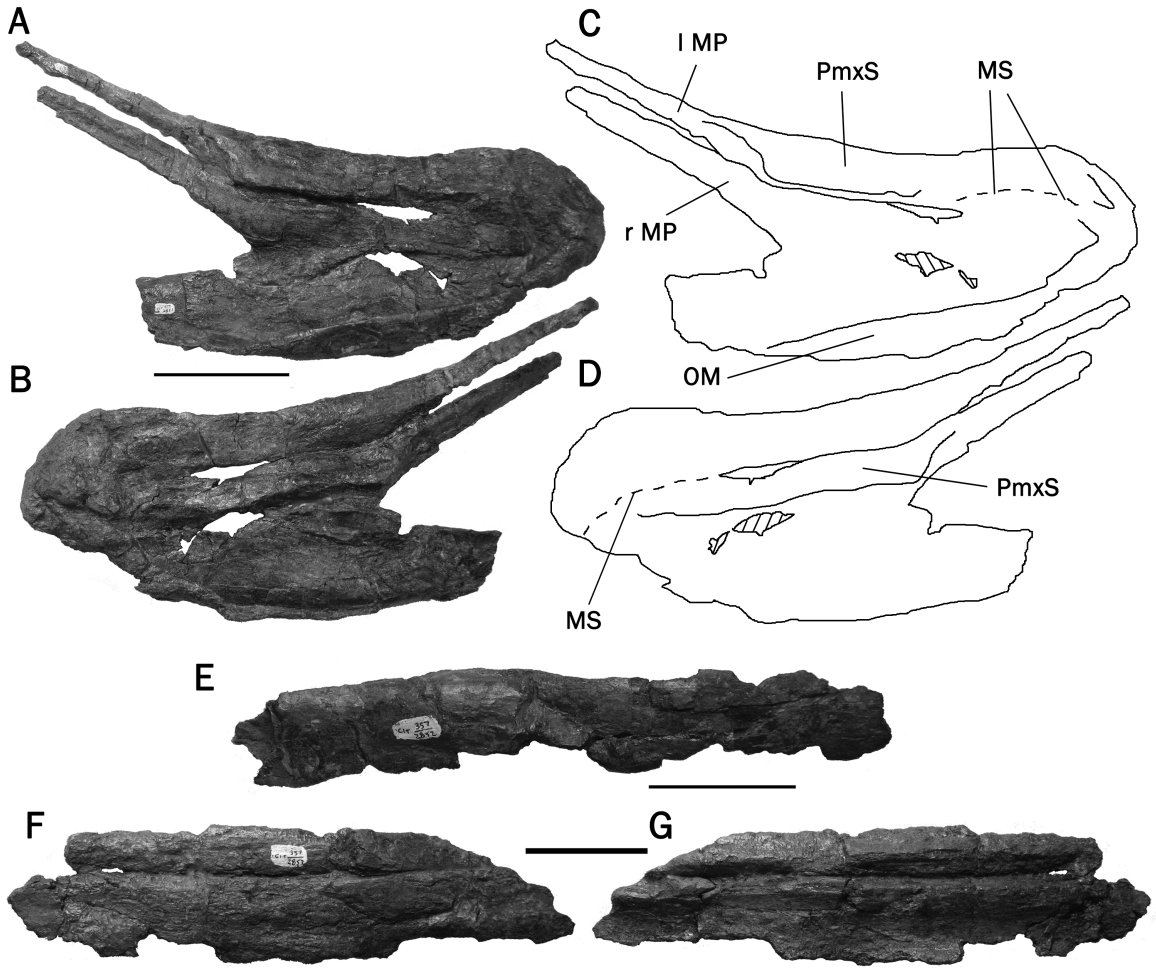

Figure 4.3. Cranial elements of LACM/CIT 2852. Premaxilla in right lateral (A) and medial aspects (B). C and D are interpretive drawings of the same views. E. shaft of bone interpreted as the lateral process of the right premaxilla. Left and right nasal fragment (LACM/CIT 2852) in dorsal (F) and ventral (G) views. Scale = 10 cm (A–D), 5 cm (E–G). MP, medial process; MS, midline suture.

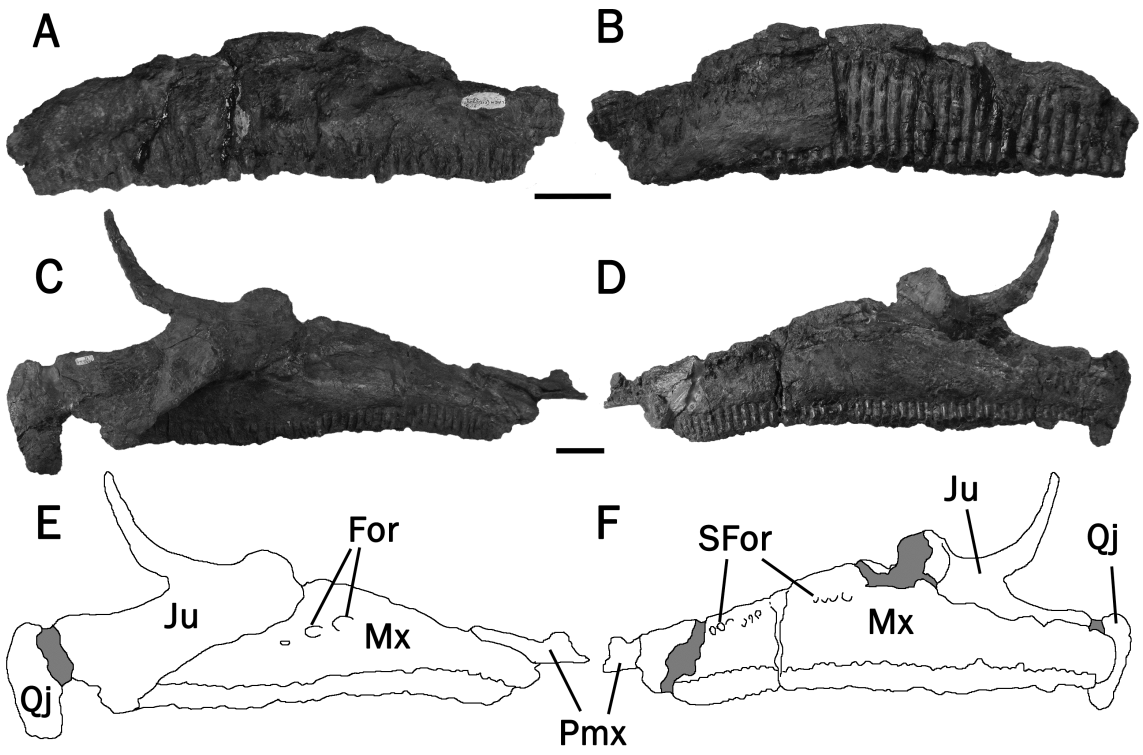

Figure 4.4. Left maxilla of LACM/CIT 2852 in lateral (A) and medial (B) views. Right maxilla, jugal, and quadratojugal in lateral (C) and medial (D) views. E and F, interpretive drawings of C and D, respectively. For, maxillary foramina; Ju, jugal; Mx, maxilla; Pmx, lateral process of the premaxilla; Qj, quadratojugal; SFor, special mental foramina. Shading denotes reconstructed areas. Scale bars = 5 cm.

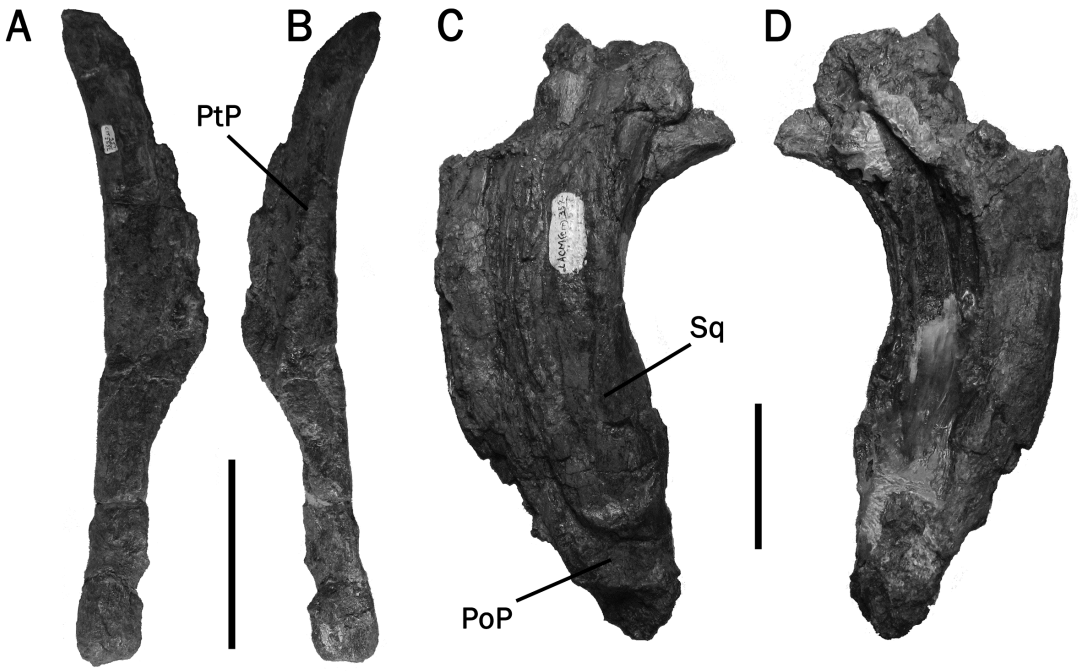

Figure 4.5. Right quadrate in lateral (A) and medial (B) aspects. Scale = 10 cm. Exoccipital and squamosal in anterior (C) and posterior (D) aspects. Scale = 5 cm. PoP, paraoccipital process; PtF, base of pterygoid flange; Sq, squamosal.

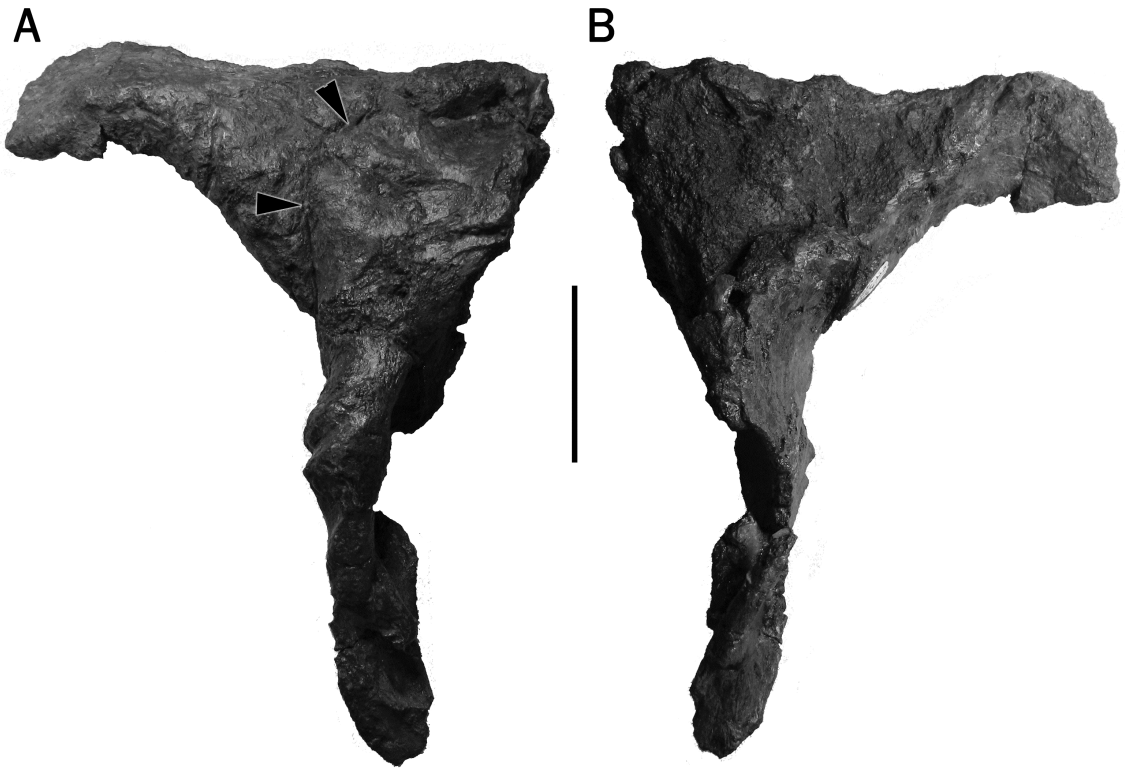

Figure 4.6. Right (?)postorbital of LACM/CIT 2852 in lateral (A) and medial (B) aspects. Arrows indicate possible line of fusion between two elements. Scale = 5 cm.

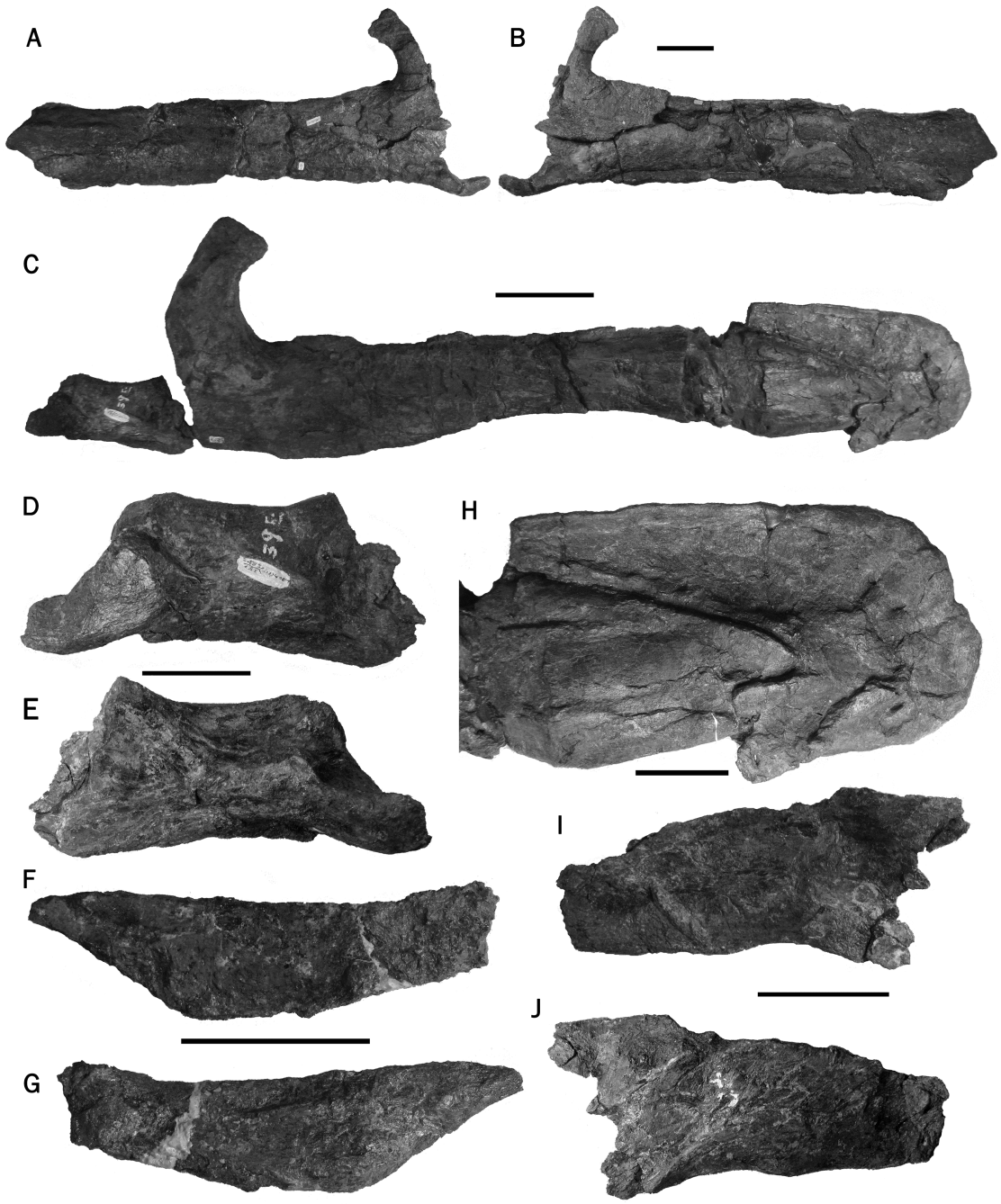

Figure 4.7. Lower jaw elements of LACM/CIT 2852. Left dentary in lateral (A) and medial (B) aspects; C. lateral view of right mandible; right surangular in lateral (D) and medial (E) view; right angular in lateral (F) and medial (G) views; H. predentary; right splenial in medial (I) and lateral (J) views. Scale bars for A, B, and C equal 10 cm. All others equal 5 cm.

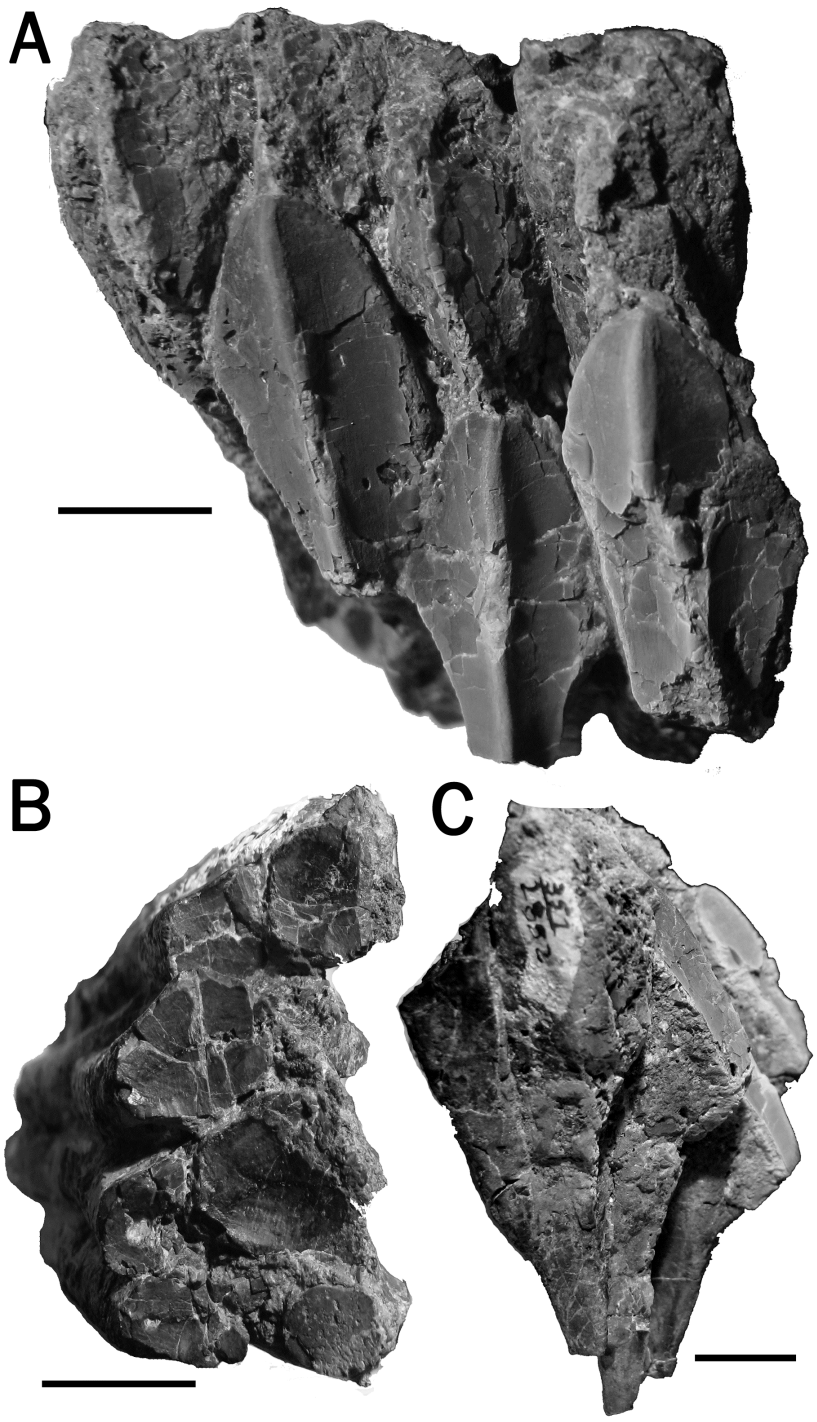

Figure 4.8. Dentary teeth of LACM/CIT 2852 in lingual (A), occlusal (B), and anteroposterior (C) aspects. Scale bars = 1 cm.

Figure 4.9. Hyoid of LACM/CIT 2852 in lateral (A) and medial (B) aspects. Scale = 5 cm.

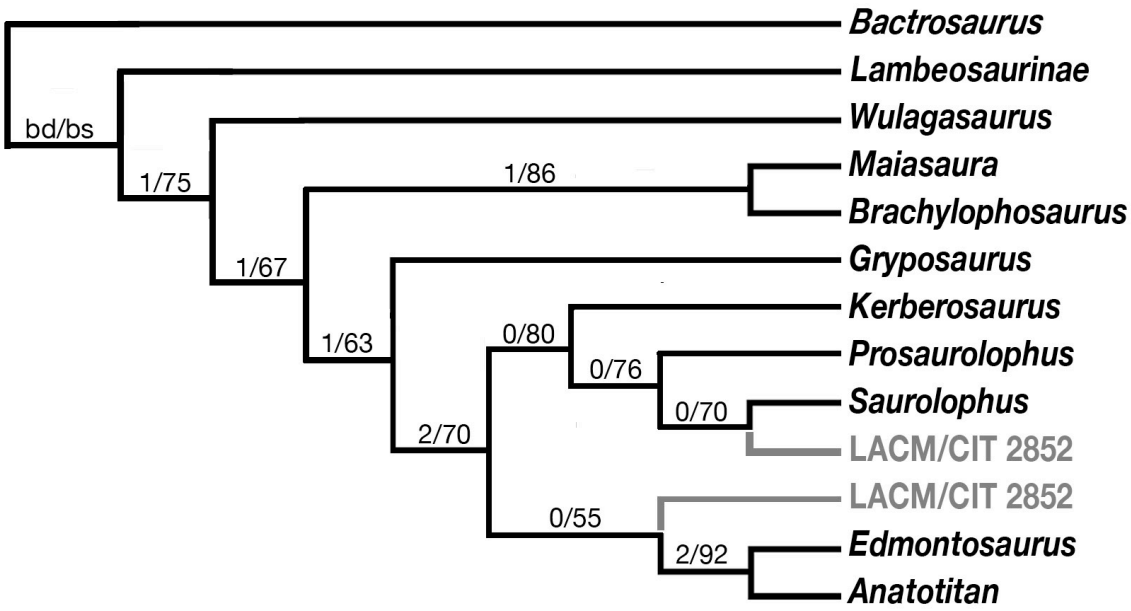

Figure 4.10. Summary of the two most parsimonious trees recovered in the phylogenetic analysis of Hadrosaurinae based on the dataset of Godefroit et al. (2008). The alternate phylogenetic positions of LACM/CIT 2852 in the otherwise identical most parsimonious tree topologies are denoted in gray. Abbreviations: bd, bremer decay values; bs, bootstrap values.

LACM/CIT 2852	?????	???02	??0??	??00?	?????	???13	1111?	1?211	310??	1????	?????	0

Table 4.1. Character matrix for LACM/CIT 2852 based on the dataset of Godefroit et al. (2008).

References

Bell, P.R., and Snively, E. 2008. Polar dinosaurs on parade; a review of dinosaur migration. Alcheringa, **32**: 271–284.

Edmond, A.G. 1957. On the special foramina in the jaws of many ornithischian dinosaurs. Royal Ontario Museum Division of Zoology and Palaeontology Contributions, **48**: 1–14.

Ford, K.W. 2006. Stratigraphic positions of marine reptile and dinosaur specimens in the Moreno Formation, in the Tumey Hills and Panoche Hills, Fresno County, California. New Mexico Museum of Natural History and Sciences Bulletin, **35**: 407–410.

Gates, T.A., and Farke, A.A. 2009. Biostratigraphic implications of a hadrosaurid (Ornithopoda: Dinosauria) from the Upper Cretaceous Almont Formation of Wyoming, USA. Cretaceous Reseach, **30**: 1157–1163.

Godefroit, P., Hai, S., Yu, T., and Lauters, P. 2008. New hadrosaurid dinosaurs from the uppermost Cretaceous of northeastern China. Acta Palaeontologica Polonica, **53**: 47–74.

Hilton, R.P. 2003. Dinosaurs and other Mesozoic Reptiles of California. California University Press, Berkeley, Calif.

Horner, J. 1992. Cranial morphology of Prosaurolophus (Ornithischia: Hadrosauridae) with descriptions of two new hadrosaurid species and an evaluation of hadrosaurid phylogenetic relationships. Museum of the Rockies Occasional Paper No. 2, 119 pp.

Horner, J.R., Weishampel, D.B., and Forster, C.A. 2004. Hadrosauridae. *In* The Dinosauria, second edition. *Edited by* D. Weishampel, P. Dodson, and H. Osmólska. University of California Press, Berkeley, Calif. pp. 438–463.

Maddison, D.R., and Maddison, W.P. 2005. MacClade 4: analysis of phylogeny and character evolution. Version 4.08. Sinauer Associates, Sunderland, Massachusetts.

McGuire, D.J. 1988. Depositional framework of the Upper Cretaceous-lower Tertiary Moreno Formation, central San Joaquin basin, California. *In* Studies of the Geology of the San Joaquin Basin. *Edited by* S.A. Graham and H.C. Olson. Society of Economic Paleontologists and Mineralogists, Los Angeles, Calif. pp. 173–188.

Morris, W.J. 1973. A review of Pacific coast hadrosaurs. Journal of Paleontology, **47**: 551–561.

Morris, W.J. 1981. A new species of hadrosaurian dinosaur from the Upper Cretaceous of Baja California: ?Lambeosaurus laticaudus. Journal of Paleontology, **55**: 453–462.

Payne, M.B. 1941. Moreno Shale, Panoche Hills, Fresno County, California. Geological Society of America Bulletin, **52**: 1953–1954.

Sternberg, C.M. 1935. Hooded hadrosaurs of the Belly River series of the Upper Cretaceous: a comparison with description of new species. Bulletin of the American Museum of Natural History, **77**: 1–37.

Swofford, D.L. 2002. Phylogenetic analysis using parsimony (and other methods). Version 4.0b10. Sinauer Associates, Sunderland, Massachusetts, 40pp.

Weishampel, D.B., and Horner, J.R. 1990. Hadrosauridae. *In* The Dinosauria, *Edited by* D. Weishampel, P. Dodson, and H. Osmólska. University of California Press, Berkeley, Calif. pp. 534–561.

Weishampel, D.B., Barrett, P.M., Coria, R.A., Le Louff, J., Xu, X., Zhao, X., Sahni, A., Gomani, E.M.P., and Noto, C.R. 2004. Hadrosauridae. *In* The Dinosauria, second edition, *Edited by* D. Weishampel, P. Dodson, and H. Osmólska. University of California Press, Berkeley, Calif. pp. 517–606.

Appendix 2: Permission to publish

I, David C. Evans, hereby grant permission for Phil R. Bell to include a version of the co-authored paper:

Bell, P. R. and Evans, D. C. 2010. Revision of the status of *Saurolophus* (Hadrosauridae) from California. *Canadian Journal of Earth Sciences* 48:1417-1426

as a chapter of his PhD thesis to be submitted at the University of Alberta.

Sincerely,

David C. Evans
DATE: January 10, 2011

CHAPTER 5

THE INTEGUMENT OF THE LAURASIAN HADROSAUR, *SAUROLOPHUS*, AND A NEW TERMINOLOGY FOR SCALE DESCRIPTION.

This chapter has been submitted as Bell, P.R. and Currie, P.J. 'The integument of the Laurasian hadrosaur *Saurolophus* and a new terminology for scale description' to the Hadrosaur Symposium at the Tyrrell Museum of Palaeontology, September 22-23, 2011 and will be published in the forthcoming volume.

Introduction

Dinosaur integument is known from most major groups, including theropods, sauropods, thyreophorans, and cerapodans (Osborn 1911, 1912, Lambe 1914a, b, Horner 1984, Briggs et al. 1997, Czerkas 1992, 1997, Dodson et al. 1998, Ji and Bo 1998, Xu et al. 1999a, b, 2001, Coria and Chiappe 2007, Siber and Möckli 2009). Hadrosaurid integument is particularly well known due in part to several remarkable 'mummies' from North America including those of *Corythosaurus, Edmontosaurus,* and *Brachylophosaurus*. Such specimens preserve not only skin impressions, but epidermal microstructure, vestiges of the musculature, and the keratinous coverings of the 'beak' and terminal pedal phalanges (Osborn 1911, 1912, Brown 1916, Murphy et al. 2006, Manning et al. 2009).

Hadrosaurid scales, like those of many dinosaurs, differ from most modern reptiles in that they are tubercle-like and non-imbricating, similar to extant varanid and helodermatid lizards (Osborn 1912). Unlike many small theropods, there is no evidence to suggest a filamentous covering in adult hadrosaurs; however, skin has not yet been found associated with hatchlings, or nestlings. Hadrosaurids possessed an intricate and often mosaic arrangement of epidermal scales along the length of the body. The cervical vertebrae were held within a thick and muscular neck quite unlike the slender and sinuous morphology reflected by the bones themselves. *Maiasaura* apparently also possessed a throat wattle (dewlap) that might have been brightly coloured and used for display (Czerkas 1997). The ramphothecae that lined the predentary and premaxillae provided an ever-growing and resistant surface for food

procurement. Enlarged, tabular scales along the dorsal midline in some taxa may have been used for visual display (Horner 1984). The manus was enclosed within a fleshy 'mitten' that restricted movement of the metacarpals and phalanges. This design may have been useful for swimming and/or afforded the forelimb greater weight-bearing capacity (Osborn 1912, Currie 1983, Czerkas 1997).

Despite the relatively rich fossil record of hadrosaurid integument, few attempts have been made to synthesise what is currently known of these structures (Lull and Wright 1942). Nevertheless, preliminary studies suggest the taxonomic utility of hadrosaurid scale morphology (Brown 1916, Lull and Wright 1942, Negro 2001).

In 1947, the Russian Palaeontological Expedition led by I. A. Efremov to Mongolia's Gobi Desert, discovered a bonebed of the giant hadrosaurine, *Saurolophus angustirostris* Rozhdestvensky 1952 in the Nemegt Formation. The bonebed became known as the "Dragon's Tomb" from which numerous articulated skeletons, many with skin impressions, were recovered. The reliability of this site as a producer of well-preserved, articulated dinosaur skeletons has unfortunately made it a favourite target for poachers, and untold numbers of *Saurolophus* specimens have destroyed in the process. Regardless, the Dragon's Tomb continues to yield spectacular skin impressions, and many undescribed specimens have been deposited in museums around the world.

Although not as extensive, skin impressions were found with the holotype (AMNH 5220) and paratype (AMNH 5221) of *Saurolophus osborni* Brown 1912 from the upper Horseshoe Canyon Formation in southern Alberta, Canada. These specimens, collected by B. Brown and P. Kaisen in 1911 included skin impressions from the jaw, pelvis, pes, and tail but were never mentioned in the

original descriptions (Brown 1912, 1913) of that species and have subsequently evaded study. A third specimen (AMNH 5271), also collected by Brown, preserves extensive skin impressions along the tail. This specimen lacks the skull but is attributed to that taxon on account of the relatively low neural spines on the dorsal vertebrae, which differentiate it from *Hypacrosaurus altispinus*, the only other hadrosaur known from that stratigraphic level.

The preserved integument on the two species of *Saurolophus* provides a unique opportunity to investigate the taxonomic utility of hadrosaur scale morphology at the species level. The purpose of this paper is threefold: 1. to propose a system of terminology that will facilitate standardised descriptions of dinosaur scale morphology; 2. to describe the integument of *S. osborni* and *S. angustirostris,* and 3. to provide a comparison of the soft tissues between these two species and elucidate for the first time areas of soft tissue not previously observed among hadrosaurs.

Suggested terminology for scale morphology

In an attempt to simplify and standardise terminology used for describing scale morphology and general arrangement, a terminology is herein proposed. This system is not intended to be comprehensive for the Dinosauria; however, certain terms and definitions will, and do apply to groups outside of the Hadrosauridae although they will not be elaborated on here. The proposed system is intended as a starting point to be built upon and refined by other workers as new specimens and scale morphologies are found.

Herein, the terms 'matrix' or 'matrix-scales' are used to describe the scales that form the major part of the integumentary surface. Collections of similar-sized matrix-scales in a mosaic-like arrangement were described as 'cluster areas' by Osborn (1912, p.42) and this terminology is followed here. Matrix-scales form the background pattern onto which larger and sporadically arranged scales are often imposed (Fig. 5.1A). These larger scales are frequently (but not invariably) of different morphology to the matrix-scales and are referred to as 'feature-scales'. One or more type of feature scale may be present in a single anatomical region (e.g., hindlimb) on a single individual but may be absent altogether. Feature scales present along the dorsal midline above the neural spines (as in *Gryposaurus incurvimanus*, *Brachylophosaurus canadensis,* and ?*Edmontosaurus* sp., Horner 1984) are termed 'midline feature-scales'. 'Interstitial-tissue' refers to the integument between the scales and presumably afforded the skin its ability to flex and fold.

Several types of scale morphologies are recognised in the integument of *Saurolophus* and are defined as follows:

Polygonal scales may range from four- to six-sided. Although three-sided and greater-than-six sides have not been observed, they would also fall into this category. Sizes range from ~2mm to more than 10mm in greatest dimension and may be symmetrical or asymmetrical. Polygonal scales may form matrices, feature-scales, or both.

Pebbly scales, or pebbles, are always small and form a matrix of closely-packed, rounded nodes (Fig. 5.1B). They are apparently the smallest of the scales, typically measuring only about 1mm in diameter.

Shell scales are asymmetrical, and somewhat trapezoidal in shape (Fig. 5.1C). Shells form matrices that are often imbricated to some degree. The most critical feature are the anteroposteriorly oriented corrugations that give each scale the overall appearance of some bivalvular mollusc shells from which the name is derived.

Scales without obvious geometrical sides are termed irregular. Often, the circumference is wavy or indistinct. These are of variable size (>2mm in diameter) and may form matrix- or feature-scales. Irregular scales can also have radial striae (corrugations), giving them a "wrinkled" appearance, which add to their irregular outline (Fig. 5.1D).

Shield scales are circular or ovoid and interspersed among the surrounding scales as feature-scales (Fig. 5.1A). Consequently, they are notably larger than the surrounding matrix-scales ranging from 7 mm to several centimetres in diameter and have been referred to as "limpet-like" by some authors (Brown 1916, Evans and Reisz 2007). Shields are typically flat or domical and their surfaces may be smooth or corrugated. A variation of shield includes a series of triangular points around the circumference of the central shield and is referred to as a multi-pointed shield. The individual points tend to intervene between adjacent matrix-scales or may lie in a wide area of interstitial tissue.

Anatomical directions such as dorsal or ventral reference the scales' relationship relative to the axial midline of the animal as they appear in most two-dimensional fossils. In the case of a three-dimensional animal, the ventral edge of a scale underhanging the belly where the outer (superficial) surface faced the ground refers to the edge that may have been facing somewhat medially in life.

Methods

Due to the immense quantity of material available at the Dragon's Tomb, only a limited number of specimens were collected. Collection was further hindered due to the extreme hardness of the entombing rock. Where possible, small hand samples were collected that had been previously unearthed and broken by poachers. In order to obtain voucher specimens that represent different body parts, two methods of molding were also employed in the field. Initial attempts used quick-setting modelling clay, which was applied directly on to the rock surface. The clay was pressed onto the impressions and removed before it had time to set (less than five minutes). Cyanoacrylate and/or acryloid was then applied to strengthen the molds. Despite good results, shrinkage and the fragility of the final product rendered this method less than ideal. A second method using liquid two-part silicone (Dragon's Skin ™) provided excellent results. Dragon's Skin ™ was poured directly onto the skin impressions and allowed to cure overnight before being removed. Anti-adhesive sprays were not used as the silicone peels did not penetrate the heavily indurated sandstone and separated easily from the rock surface. All observations and measurements were taken from the original specimens and supplemented by the casts. Measurements were taken using a measuring tape and/or callipers from the original specimens to avoid discrepancies on the molds from shrinkage due to drying, which was apparent in the larger clay molds. For all other specimens (i.e., not from the Dragon's Tomb locality), only the actual specimens were used.

Description

Skull and mandible

Skin from the face of *Saurolophus osborni* is known from a single fragment from the right dentary of AMNH 5220. It measures 14cm anteroposteriorly and 5.5cm dorsoventrally (Fig. 5.2). Matrix-sales on the posteroventral surface are anteroposteriorly longer than high (5x3 mm) with no apparent variation. They form rounded, vaguely diamond-shaped, raised tubercles. More dorsally situated scales are diamond or hexagonal in shape, anteroposteriorly longer than high, ranging from 5–6 mm long and 3–4 mm high. Scales appear to increase in size anteriorly and feature-scales are absent.

At least two patches of faintly preserved skin are present on a juvenile specimen of *Saurolophus angustirostris* (MgD-I/159). Skin is preserved on the right quadrate-quadratojugal-jugal contact (40x50 mm) and the left infratemporal fenestra (30x40 mm). Scales comprise of small (1mm), closely-packed, hexagonal-to-subcircular pebbles. These are uniformly distributed with no apparent pattern or variation.

Axial region

Integument from the over the rib cage of *Saurolophus* is not well known and is present only in *S. angustirostris*. Matrix-scales in a subadult specimen from the Dragon's Tomb (Fig. 5.3) appear somewhat distorted. Individual scales are 2-to-3 mm in diameter and best described as pebbly or irregular in outline;

however, their low relief and small size make observations difficult. There does not appear to be any variation in size or morphology. Juveniles (represented by isolated patches of integument on the ribs of MgD-1/159) appear to follow a similar integumentary pattern.

Skin is best represented on the tails of both species of *Saurolophus*. The holotype of *S. osborni* retains skin impressions in two areas. One block measuring 18 cm long contains two fairly complete caudal vertebrae with neural spines. Both centra are 7cm in length, and probably represent caudal vertebrae six and seven where the tail has been broken on the original specimen (Brown 1913, pl LXIII) presumably to facilitate removal during excavation. Unfortunately, few individual scales are actually distinguishable despite a relatively extensive veneer of integumentary impression across the specimen. Those that are discernable on the centra appear hexagonal (2.5mm in diameter) and separated from each other by 1mm wide bands of interstitial tissue. Scales on the neural spines are larger and hexagonal although they are difficult to discern. One measurable scale at the base of the neural spine is 4mm in diameter. It is possible that these scales were arranged into cluster areas, although the poor preservation prevents definite identification of these associations.

A second fragment from an unidentified area on the tail of AMNH 5220 measures 14cm x 9cm. Scales are hexagonal and of variable size. Although no directional data was available, scales measure 6x6mm, 6x9mm, 5x4mm, and 6x7mm and are arranged haphazardly. At least one incompletely-preserved feature-scale measures ~25mm long; its edges are drawn into tapering points to form a multi-pointed star. Each point fits between the edges of two adjacent

regular hexagonal scales. When complete, as many as fifteen points probably surrounded the large scale.

The caudal series of AMNH 5271 preserves the most extensive tracts of integument of any specimen of *S. osborni* spanning the entire length of the tail, albeit discontinuously (Fig. 5.4). The most proximal vertebrae, retain the latticework of ossified tendons along the flanks of the elongate neural spines. Matrix-scales on the centra are arranged into cluster areas of small (1–2mm diameter) and large (4–5mm) scales (Fig. 5.4C, D). These patches grade into one another. Individual scales are typically hexagonal although others are irregular. Scales on the neural spines appear to follow this general pattern where they are less well preserved. The skin apparently did not extend high above the tips of the neural spines by way of a dorsal 'frill' and there is no indication of midline feature-scales; however, it is possible that this area was lost during recovery of the specimen. More distally, the scales are variably hexagonal, pentagonal, or may be irregular (Fig. 5.4E, F). Scales are vaguely corrugated and are typically 4–6mm in diameter. Rare feature scales 6–8mm long are found close to the chevrons. These differ from the regular matrix-scales in that they are irregularly shaped and dorsoventrally taller than they are long.

Scales on the most distal part of the tail are evenly spaced, regular-sided hexagons and pentagons 3mm in diameter with slightly depressed centres (Fig. 5.4G, H).

Integument from the tail of *S. angustirostris* varies considerably along its length. Proximally, matrix-scales are arranged into alternating, dorsoventrally-oriented bands, herein referred to as zones A and B (PIN 3738, PIN 3747, UALVP 52787; Fig. 5.5). Zone A bands are approximately 60 mm wide and consist of

regular polygonal scales ranging from 4–6mm in diameter. Slightly larger scales (10mm) of the same morphology are unevenly interspersed throughout the matrix-scales. Other feature-scales are smooth, sometimes multi-pointed, domical shields 25–30mm in diameter. Shield feature-scales are arranged into a grid-like pattern with individual scales set approximately 4cm from the neighbouring shield feature-scales. Some variation exists in their arrangement, presumably as a result of stretching/wrinkling of the original skin. Zone A grades into zone B, which is immediately recognisable by smaller matrix-scales and the absence of feature scales. Zone B bands are relatively narrow (approximately 20-30 mm wide) and are composed of irregular, corrugated matrix-scales 3–4 mm in diameter. Midline feature-scales form a near continuous series dorsal to the neural spines along the caudal vertebrae (Fig. 5.6). Individual scales do not correspond perfectly with the tip of each neural spine. As skin impressions are not known from the cervical region or above the dorsal vertebrae, it is unclear whether or not the midline feature-scales continue along these regions. In the largest individuals (UALVP 52748), midline feature-scale can measure up to 80 mm long and 40 mm high (Fig. 5.6C, D). The lateral surfaces of the midline feature-scales have several dorsoventrally oriented ridges and grooves (Fig. 5.6G) similar to those described for cf. *Edmontosaurus* (Horner 1984).

The distal half of the tail in *S. angustirostris* is devoid of distinct dorsoventral bands or zones and lacks feature-scales. Instead, the integument is comprised of an even covering of polygonal matrix-scales. Midline feature-scales continue distally and appear to be present almost to the tip of the tail (UALVP 52824).

Appendicular regions

Although skin is not known from the forelimb of *S. osborni,* the entire forelimb of *S. angustirostris* (UALVP 52781, UALVP 52786) was covered in a uniform arrangement of 1-2 mm wide pebbles even in relatively large individuals (Fig. 5.7). This pattern persisted over the shoulder joint, humerus, and forearm; however, skin from the manus of *Saurolophus* is unknown. There are apparently no feature-scales, cluster areas or variation within the forelimb.

In *S. osborni*, only AMNH 5220 retains skin impressions from the pelvic region. Three fragments from the body of the ilium show a matrix of regular hexagonal scales 3x4 mm (Fig. 5.8A, B). There is no indication of any variation in these scales and no feature-scales were observed. A fragment measuring 10cm long and 7cm wide, taken from the shaft of the ischium preserves a non-uniform arrangement of irregular, multi-pointed matrix-scales. The number of points is variable and difficult to discern because of the imperfect preservation. Individual scales are not regularly shaped; scales may be equi-dimensional, constricted at their midpoint, or pinched on one end.

Skin from the pelvic region of *S. angustirostris* is known only from a small patch between the sacral ribs of a subadult individual (Fig. 5.8C, D). Matrix-scales are irregular and measure 5 mm in diameter. Feature-scales and other variations are absent; however, the extent of skin is too small to confirm the presence/absence of variation or feature-scales.

Skin from the hindlimb of *S. osborni* is unknown except for the metatarsus and pes. In the holotype (AMNH 5220), anterior surface of the left metatarsus was covered in regularly-spaced pebbles approximately 2 mm in diameter.

Although most scales are sub-circular in outline, others appear to be hexagonal (Fig 5.9A). The pes is represented by a block containing two of the pedal unguals that were not installed as part of the panel mount. The pes was partially disarticulated after death (as seen on the original panel mount) and one ungual is rotated behind the other; therefore it cannot be said exactly where the skin fragment is from, but is likely from the top of the foot. Skin impressions over the dorsal surface of the digit measure 19x10 cm in total area. The matrix-scales are slightly elongated hexagons (6x7 mm). Smaller scales are also present but their positioning is apparently random. A portion of skin that lies adjacent to the ungual is separated from the remainder of the impressions by a shallow depression. Scales on this surface are small, irregular pebbles 2–3 mm in diameter, which may represent a displaced portion of the digital pad or the lateral surface of the digit (Fig 5.9B).

The hindlimb integument of *S. angustirostris* is known from both juveniles and subadult specimens. The proximal region of left femur of the juvenile MgD-1/159 preserves three discrete patches of skin. The largest is 140x65 mm on the anterior aspect between the head and the greater trochanter. On the anterolateral edge of the greater trochanter is a second patch that adheres closely to the bone and can be traced faintly for most of the preserved length of the element (~180 mm). A third patch, anterior to the greater trochanter, measures 90x45 mm. In all three areas, matrix-scales are corrugated and irregular. Most measure 3–4mm in greatest dimension but are interspersed with smaller 1mm wide pebbles. Relief is minimal, although some scales have small keels and other presumed feature-scales (4–5mm across) are more domical and elevated relative to the surrounding scales. There is no distributional pattern evident for these feature-scales.

The distal half of the femur and proximal tibia was dominated by irregular-to-subcircular matrix-scales 3mm in diameter. Arranged at intervals of 2–3cm are larger feature-scales ~7mm across (Fig. 5.10). These are circular and domical and the periphery of each shield is ornamented by a series of fine, radiating grooves and ridges. The shields are further arranged into rows 20–25 mm apart and each row is staggered relative to the two adjacent rows. A single multi-pointed shield close to the distal end of the femur is imperfectly preserved but measures 40mm across (Fig. 5.10C). This shield feature-scale is strongly domed but is otherwise smooth. The central shield is 20mm across and is surrounded by at least four triangular points spaced at irregular intervals, but may have been surrounded by as many as eight points.

Skin around the ankle joint and dorsal surface of the pes is comparatively simple, consisting of a matrix of uniform pebbles 1-2 mm in diameter devoid of variation or feature-scales (UALVP 52785).

Miscellaneous. (Fig. 5.11)

Several blocks of integument of unknown anatomical origin were found associated with the type and paratype of *S. osborni.* These are described here as they represent otherwise unknown morphologies and/or provide insight into the variation of the integumentary covering of this species.

Three patches of miscellaneous skin from AMNH 5220 were identified. One patch measuring 13x8cm preserves four-to-six-sided, polygonal matrix-scales ranging from 1–3mm in diameter. Scales are arranged into a mosaic of similar-sized scales although the specimen is too small to permit identification of

the outline of these patches. One patch of large (3mm) scales is 30mm in maximum dimension.

Two other blocks measuring 13.5x10cm and 11.5x7cm display a matrix of regular hexagonal scales 9–11mm in diameter, which show some degree of imbrication. The posterior, or 'free' edges of the scales are 'stepped' and show wrinkles perpendicular to the truncated edge. The surfaces of the scales are roughened. Matrix-scales in one specimen increase in size until they abut a single shield feature-scale at the edge of the block. The shield measures approximately 35x45mm however some of its edges are damaged and its full extent cannot be ascertained. Where it is better preserved, its edges occupy the space between neighbouring matrix-scales to form a multi-pointed star.

A single miscellaneous block from AMNH5221 measures 8.5x9cm. The skin is wrinkled and the weakly pentagonal or hexagonal matrix-scales are variably sized (4x5mm, 2x3mm, 6x4mm) probably owing to the stretching and constriction of the skin. There is up to 2mm of interstitial material between individual scales. A single preserved shield feature-scale measures 15mm in diameter. Curiously, it is multi-pointed on one hemisphere whereas the other edge is a relatively smooth (non-pointed) arc.

Discussion

Comparison of S. osborni *and* S. angustirostris

As with earlier studies of hadrosaur skin impressions (Lull and Wright 1942), comparisons are necessarily incomplete as equivalent regions of the

integument are uncommon between specimens (Fig. 5.12). Nevertheless, several comparisons and observations can be made to permit some generalisations about the differences and similarities in the scale architecture between species of *Saurolophus*.

The area of most overlap between species of *Saurolophus* is undoubtedly the tail. The presence of cluster areas of matrix-scales in *S. osborni* is markedly different to the complex patterning in *S. angustirostris.* The latter species is typified by vertical bands of differentiated matrix-scales and shield feature-scales at the base of the tail and a more homogeneous covering of polygonal matrix-scales distally. Moreover, the midline feature-scales observed in both juvenile and adult *S. angustirostris* cannot be confirmed in *S. osborni*; however, this region is less well known in *S. osborni*.

Multi-pointed shield feature-scales are apparently unique to both species of *Saurolophus* (see following discussion on interspecific variation) having been observed on the hindlimb of *S. angustirostris* and from the tail and unidentified areas of *S. osborni.* At this stage, the multi-pointed shield morphologies are too rare to understand their distribution over the body.

Integumentary patterns in *S. angustirostris* appear to have remained relatively unchanged throughout ontogeny. The presence of domical shield feature-scales from the tail and hindlimb of immature and larger, more mature *S. angustirostris*, suggests at least some consistency in the scale morphology of this taxon. Similarly, midline feature-scales are present on both small and large individuals. Admittedly, the areas of overlap between young and old individuals are limited, so consistent scale architecture between age groups cannot be argued with certainty. In addition, the skin of hatchling and 'yearling' *Saurolophus* is as

yet unknown. If true, however, the presence of similar markings between young and old individuals may have helped with intra- and inter-species recognition.

Comparison with other hadrosaur skin impressions.

Although a comprehensive comparison with other hadrosaurid skin impressions is beyond the scope of this paper, excellent descriptions of the integument are available for *Edmontosaurus annectens* (Osborn 1912) and *Corythosaurus casuarius* (Brown 1916). Additional skin impressions are also known from *Brachylophosaurus canadensis* (Murphy et al. 2007), *Maiasaura peeblesorum* (Trexler 1995) *Prosaurolophus maximus* (TMP 1998.50.01), *Gryposaurus incurvimanus* (Parks 1920), *Parasaurolophus walkeri* (Lull and Wright 1942), *Lambeosaurus magnicristatus* (Evans and Reisz 2007), *Lambeosaurus lambei* (Lull and Wright 1942) as well as a number of other unidentified hadrosaurids. Such specimens permit some comparisons and generalisations to be made about hadrosaurid integument.

Skin impressions from the cranium and mandibles are notably rare among hadrosaurids. In addition to those of *Saurolophus,* facial skin impressions have been observed on only two other specimens (Osborn 1912, Wegweiser et al. 2006). Osborn (1912) described scale patterns preserved on the quadrate and the region immediately posterior to it in *E. annectens* (AMNH 5060,). These consisted of cluster areas of polygonal scales interspersed within a larger area of pebbly matrix-scales. Pebbly matrix-scales were observed in *S. angustirostris*; however, there is no evidence of cluster areas of morphologically distinct scales. Admittedly, the patches of skin in *S. angustirostris* (MgD-1/159) are too small to

conclusively dismiss the presence of cluster areas on the skull of this taxon. Nevertheless, cluster areas were not observed on any other part of the body so there is little reason to believe they existed on the skull of *S. angustirostris.* Wegweiser et al. (2006) described the scales from the anterior part of the dentary of an indeterminate (possibly lambeosaurine) hadrosaur from the Lance Formation. The scales are polygonal, several millimetres in diameter, and ornamented by fine corrugations that fan out from the ventral margin. Although *S. osborni* also possessed polygonal scales on the dentary, ornamentation such as described by Wegweiser et al. (2006) is absent.

Scales from the shoulder girdle and forelimb of *S. angustirostris* differs from other hadrosaurids. In *S. angustirostris,* this entire region is populated with a uniform matrix of pebbles. In *E. annectens,* pebbly matrix-scales are present on the ventral surface of the forearm and medial surface of the humerus; however, the humerus also bears small cluster areas of polygonal matrix-scales (Osborn 1912). The dorsal surface of the entire arm in *E. annectens* and the ventral surface of the forearm in *B. canadensis* were covered in a uniform matrix of polygonal scales up to 10 mm in diameter (Osborn 1912, Murphy et al. 2006). Undifferentiated polygonal matrix-scales are also present on the anterior surface of the humerus of *Lambeosaurus magnicristatus* (Evans and Reisz 2006).

Lull and Wright (1942) recognised two categories of scale patterns on the flanks. The first is comprised of an undifferentiated covering of polygonal matrix-scales (*C. casuarius, L. lambei, G. incurvimanus,* and *Parasaurolophus walkeri*). The second form consists of a mosaic of similar-sized scales arranged into cluster areas seen only in *E. annectens* (Osborn 1912). The scale configuration over the thoracic ribs of *S. angustirostris* appears to conform to the first category. Thoracic

integument is unknown from *S. osborni.* An undescribed juvenile specimen of *Prosaurolophus maximus* (RTMP 1998.50.01) demonstrates a third unique category: polygonal matrix-scales are punctuated by shield feature-scales loosely set into longitudinal rows. Although this arrangement has not been observed in the thoracic region of other hadrosaurs, it is present on the abdomen of *C. casuarius* in the vicinity of the ischium as well as the hindlimb and proximal part of the tail of *S. angustirostris*. It is notable that this arrangement of shield feature-scales is similar to some ceratopsids (Lambe 1914a, Brown 1917, Sternberg 1925) and also *Carnotaurus* (Czerkas 1997).

The scale architecture of hadrosaurs is best represented along the tail and demonstrates the morphological diversity of integument in this group. Cluster areas on the proximal caudal region of *S. osborni* are reminiscent of the body covering of *E. annectens,* but the multi-pointed and irregular feature-scales from other parts of the tail are unlike previously described hadrosaur integument. Undifferentiated, polygonal matrix-scales are found on *C. casuarius* and *L. lambei*, which is similar to the distal tail of *S. angustirostris.* Proximally, the caudal integument of *S. angustirostris* bears some resemblance to that of an incomplete skeleton from the Dinosaur Park Formation (‘*Trachodon marginatus’*, Lambe 1914a). The tail of ‘*T. marginatus*’ was covered in polygonal matrix-scales along with sparse, radially-ornamented shield feature-scales (Lambe 1914a). The vertical banding (as described here for *S. angustirostris*) is absent in ‘*T. marginatus*’ and all other described hadrosaurid specimens. Polygonal matrix-scales with faint radial ornamentation have been described in an unidentified hadrosaur from the Kaiparowits Formation (Gillette et al. 2002). Broad areas of irregular matrix-scales from the tail of an indeterminate hadrosaur from the Late

Campanian of New Mexico show ornate radial ornamentation and include radially-ornamented shield feature-scales (Anderson et al. 1998). Horner (1984) also described midline feature-scales on the tail of an unidentified hadrosaur (possibly *Edmontosaurus*) and these are also present in *Gryposaurus incurvimanus* (Parks 1920), *Brachylophosaurus canadensis* (Murphy et al. 2007), and *S. angustirostris* (this study). They are unknown in *Corythosaurus*. Vertical striations on the lateral surfaces of the midline scales described by Horner (1984) are also present in *S. angustirostris.*

Pelvic and abdominal skin of *Saurolophus* appears to have been uniform but differed between species in the contours of the matrix-scales. *S. osborni* apparently consisted of regular hexagonal matrix-scales along the ilium and irregular matrix-scales along the ischium. In its relatively uniform arrangement, pelvic skin of *S. osborni* most closely resembles that of *Gryposaurus notabilis* and *Lambeosaurus magnicristatus*, both of which had an undifferentiated matrix of polygonal scales (Lambe 1914b, Evans and Reisz 2007). Only two other taxa preserve skin in this region, both of which differ from *S. osborni. E. annectens* retained a mosaic of cluster areas that was present elsewhere on the body (Osborn 1912) and *C. casuarius* possessed a matrix of polygonal scales interrupted by shield feature-scales arranged into close-set rows. The single patch of irregular scales associated with *S. angustirostris* differ from the polygonal scales in most other taxa, except *S. osborni* but this patch is too small to permit detailed comparisons.

Aside from the pes of *C. casuarius* (AMNH 5240), very little is known of the integument from the hind limbs of hadrosaurids. MgD-1/159 (*S. angustirostris*) therefore provides the most complete picture of the hind leg of any

hadrosaur described to date. Skin from the front of the proximal femoral region of *Lambeosaurus lambei* (=*L. clavinitialis,* CMN 8703; Sternberg 1935) consists of small, polygonal matrix-scales devoid of feature scales. This pattern is similar to patches of skin preserved on the fibula of *E. annectens*. Skin from the hindlimb of *S. angustirostris* differs markedly from these specimens: the proximal femur consists of irregular, radially-corrugated scales and sporadically-placed shield feature-scales. More distally, the existence of larger shield feature scales over the knee and a large, multi-pointed shield on the distal femur appear unique to this species. The arrangement of polygonal and pebbly scales associated with the pes of both *S. angustirostris* and *S. osborni* is not unlike that observed on *C. casuarius* (Brown 1916).

Conclusions

Hadrosaurid skin impressions are relatively common yet scale morphology can only be considered well known in a limited number of taxa. Extensive skin impressions of *Saurolophus angustirostris* from the Dragon's Tomb locality in southern Mongolia permit the opportunity to reconstruct the soft tissue anatomy of that taxon. *S. angustirostris* is typified by considerable variation in scale design across the body. Scales over the shoulders and forelimbs consisted of small, pebbly scales, similar to rare skin impressions found posterior to the orbits. The flanks and distal part of the tail were covered in undifferentiated polygonal scales although tabular feature-scales were also present along the entire dorsal midline of the tail as in *Gryposaurus incurvimanus*, *Brachylophosaurus canadensis*, and ?*Edmontosaurus* (Horner 1984). The hindlimbs and base of the tail

supported a grid-like arrangement of large, shield feature-scales dispersed among the smaller matrix-scales. Matrix-scales on the proximal tail were further differentiated in vertical bands of polygonal and shell matrix-scales. It is not unreasonable to suppose that regions of differentiated scales also sported different colours (Osborn 1912). Preliminary evidence suggests that juveniles of *S. angustirostris* had similar integumentary patterns to the adults at least in the presence of midline feature-scales and the distribution of shield feature-scales over the abdominal region.

Comparisons of *S. angustirostris* scale architecture with the lesser-known integument from *S. osborni* provide a test of the taxonomic utility of scale morphology between closely related dinosaur species. Comparisons suggest that these species differed from one another, most notably in the tail region. In fact, *S. osborni* was more similar to *Edmontosaurus annectens* in the presence of cluster areas on the tail and apparent lack of midline feature-scales.

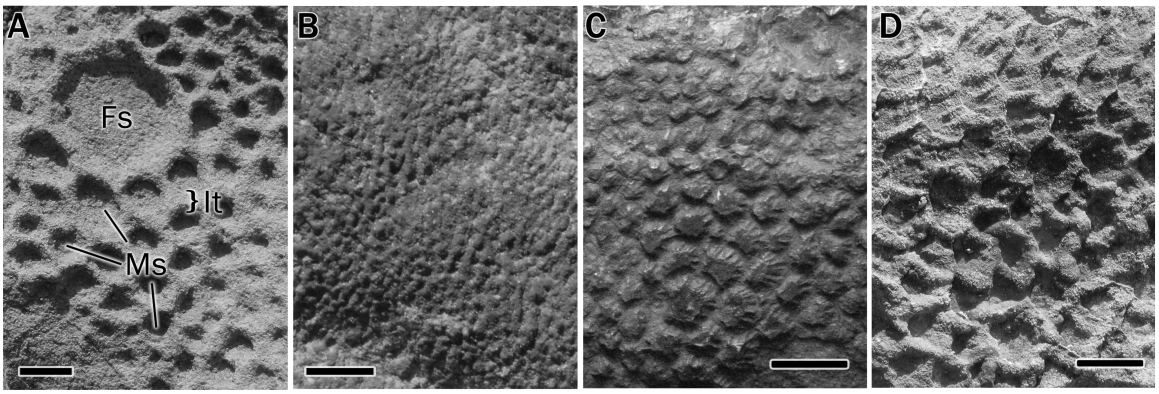

Figure 5.1. Hadrosaur scale morphology. A. Polygonal matrix-scales (Ms) with a shield feature-scale (Fs). Interstitial tissue (It) occurs between scales (*Saurolophus angustirostris*); B. Pebbles (*S. angustirostris*); C. Radially-ornamented, irregular matrix-scales (*Edmontosaurus annectens* ROM 801); D. Imbricated shell matrix-scales (*S. angustirostris*). Scale bars = 1 cm.

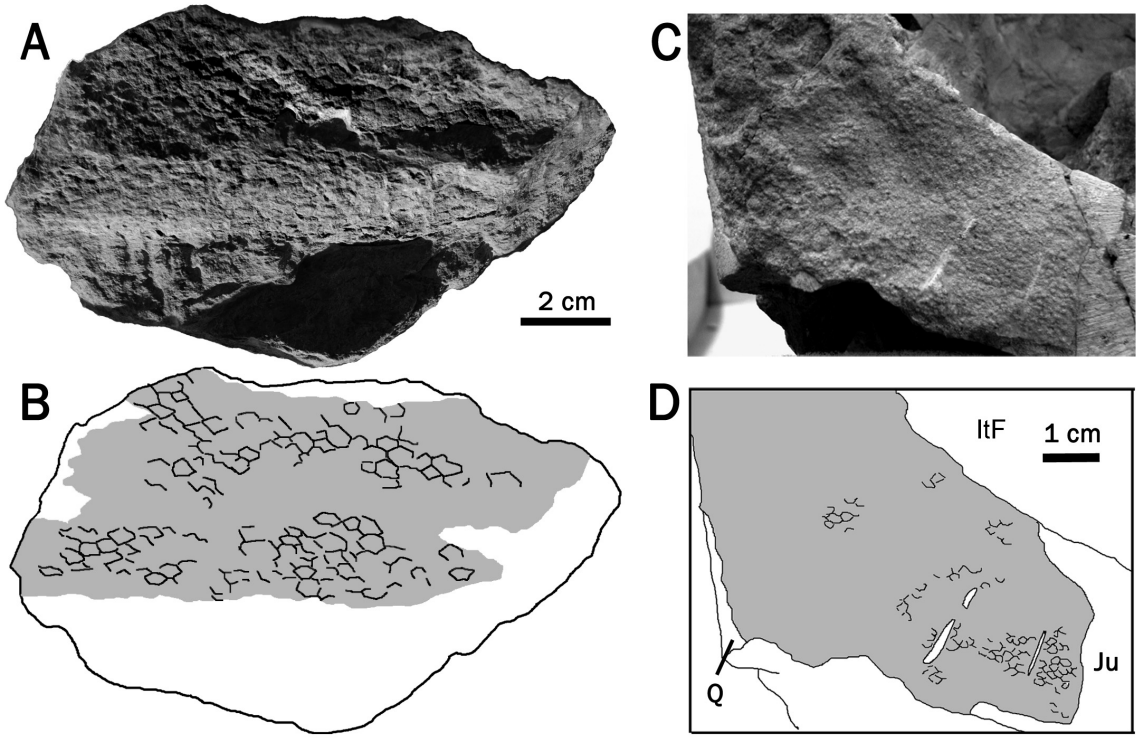

Figure 5.2. Cranial integument. A, B. *Saurolophus osborni* (AMNH 5220) right dentary. C, D. Juvenile *S. angustirostris* (MgD-1/159). Itf, infratemporal fenestra; Ju, jugal; Q, quadrate. Grey areas denote regions of skin impressions.

Figure 5.3. Field photograph of the integument over the ribs of a subadult *S. angustirostris*. Note impressions of the ribs. Scale bar in cm.

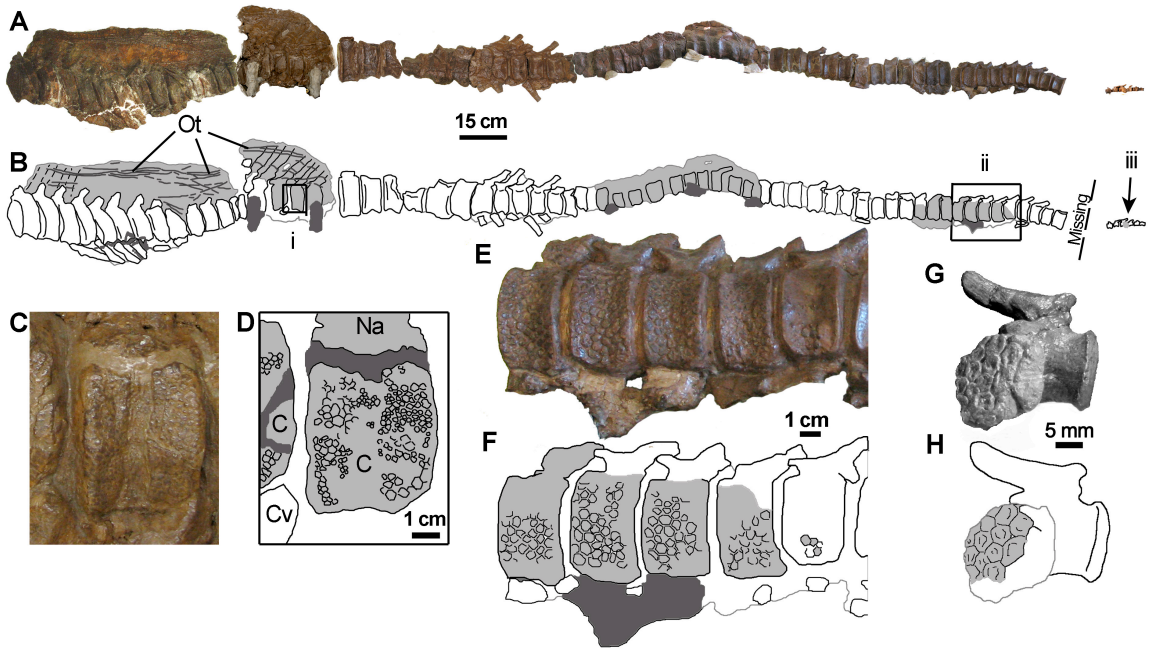

Figure 5.4. Tail integument of *S. osborni* (AMNH 5271). Composite photograph (A) and interpretive drawing (B) of caudal series. Note a section of distal vertebrae is missing. *i, ii,* and *iii* identify enlarged images in (C, D), (E, F), and (G, H), respectively. Light grey regions denote areas of skin impressions. Dark grey indicates plaster reconstruction. C, centrum; Cv, chevron; Na, neural arch; Ot, ossified tendons.

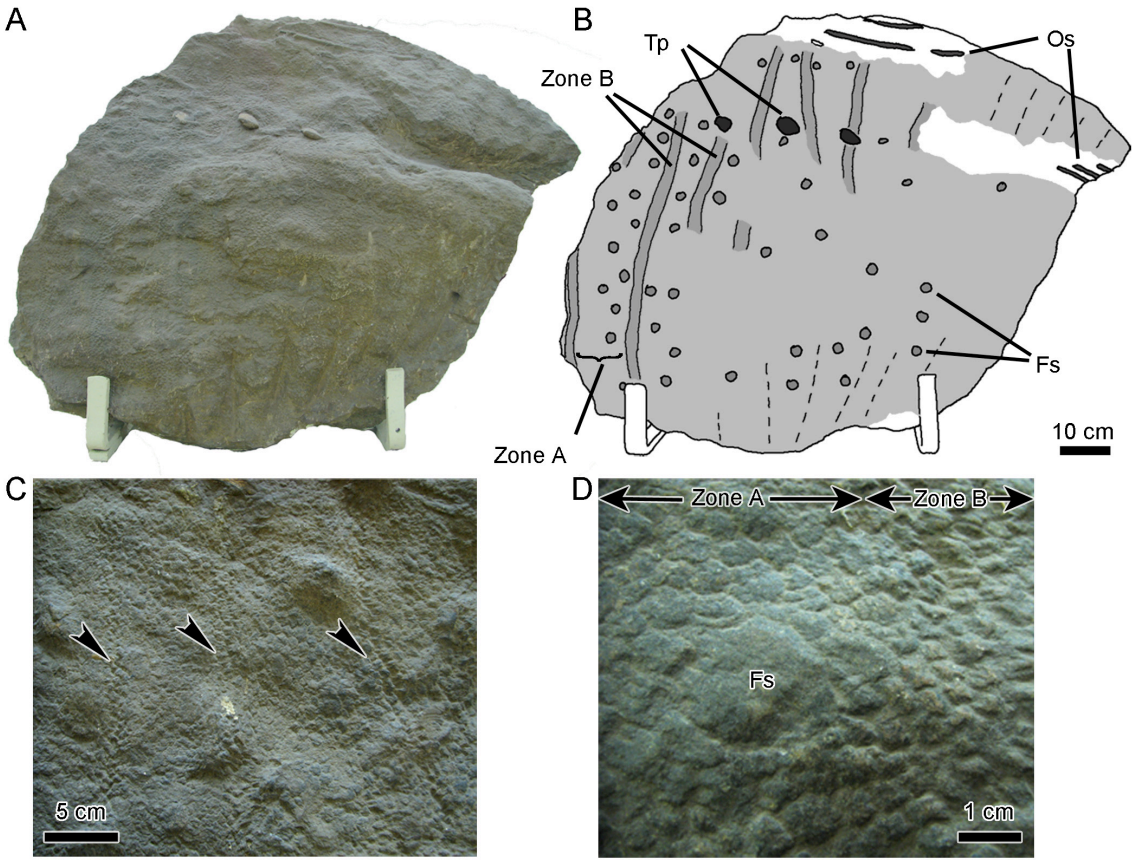

Figure 5.5. Proximal-most tail integument of an adult *S. angustirostris* (PIN 3738), photograph (A) and interpretive illustration (B). Light grey indicates extent of preserved integument. Dashed lines denote wrinkles in the skin. C. Close-up showing narrow vertical bands of zone B scales (arrowheads). D. Detail of transition between polygonal matrix-scales in zone A and shell matrix-scales of zone B. Fs, feature-scale; Os, ossified tendon; Tp, transverse processes of caudal vertebrae.

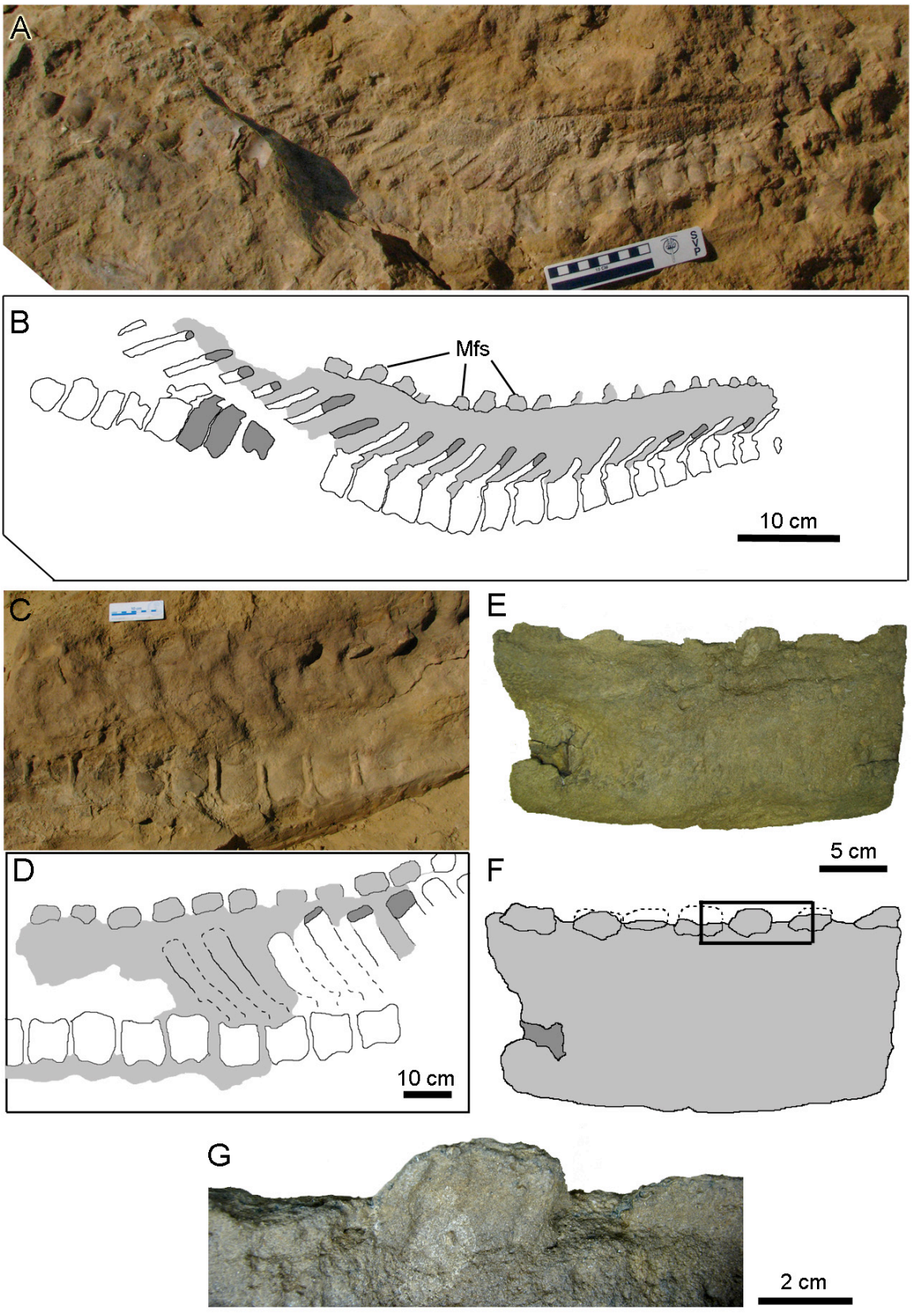
A
B
Mfs
10 cm
C
D
10 cm
E
5 cm
F
G
2 cm

Figure 5.6. Tail integument of *S. angustirostris*. A, field photograph and B. interpretive illustration of a juvenile caudal series showing distribution of midline feature-scales (Mfs). C, D, Adult proximal-mid caudal series showing enlarged midline feature-scales. E, F, Three dimensional skin preservation on mid-distal caudal series of subadult PIN 4216/49. G. close-up of midline feature-scales indicated by boxed region in F. Light grey indicates extent of skin impressions. Dark grey denotes bone. Dashed lines are inferred outlines of structures.

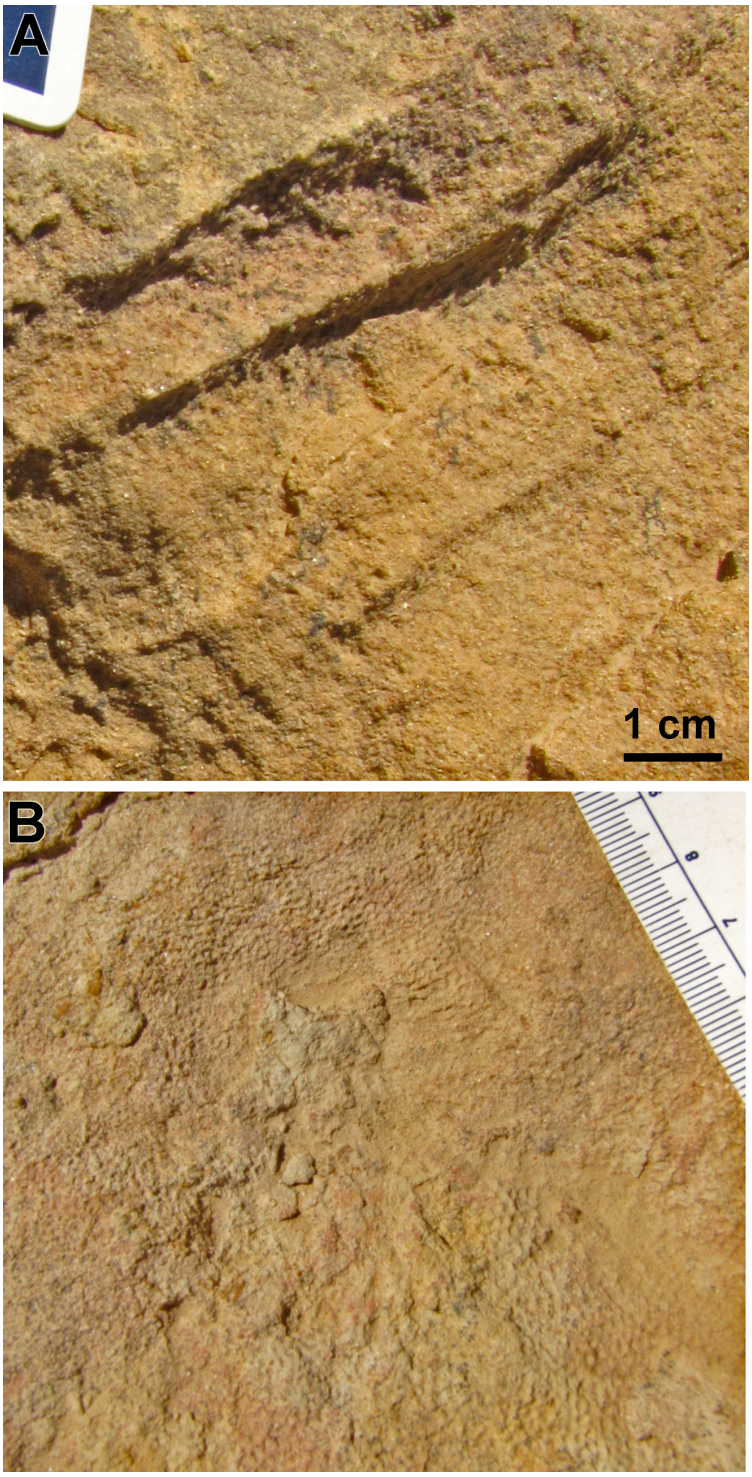

Figure 5.7. Field photographs of pebbly matrix-scales in *Saurolophus angustirostris* forearm (A) and shoulder girdle, superficial to the scapula (B). Longitudinal ridges in A are folds in the integument; distal is to the right.

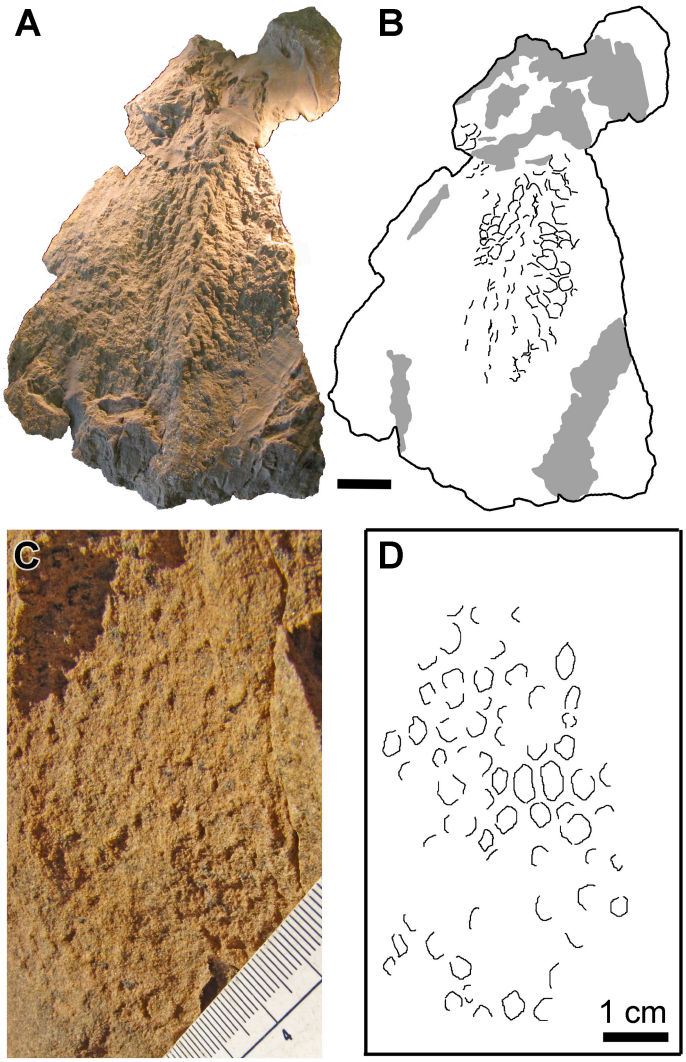

Figure 5.8. Pelvic integument of *Saurolophus.* A, B. *S. osborni* (AMNH 5220) from the lateral surface of the iliac body. C, D. Field photograph of *S. angustirostris* integument preserved between the sacral ribs of a subadult individual. Grey areas denote areas obscured by plaster.

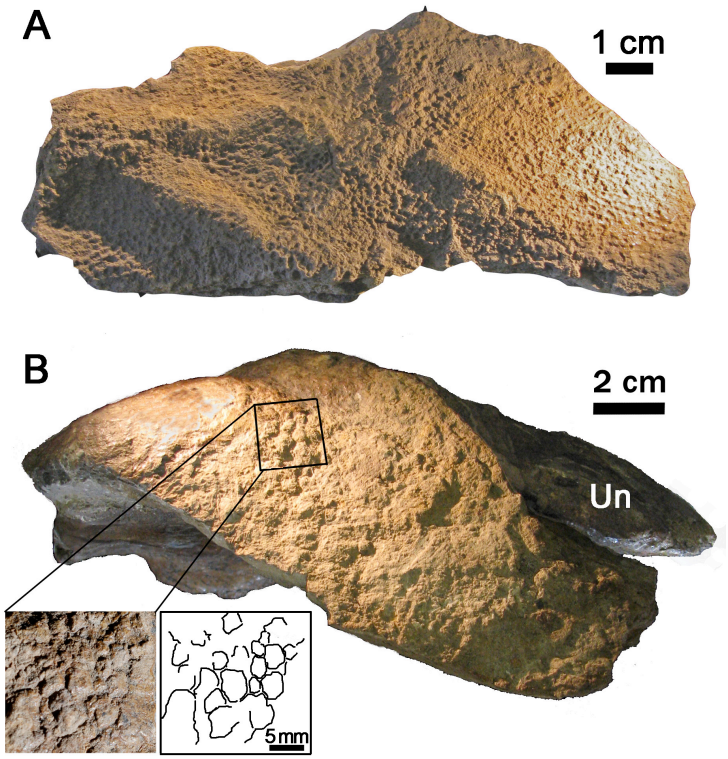

Figure 5.9. Skin impressions from the left pes of *S. osborni* (AMNH 5220). A. Skin from the anterior surface of the metatarsus. B. ?Lateral view of an unidentified pedal digit with the ungual (Un) still intact showing irregular scales (inset).

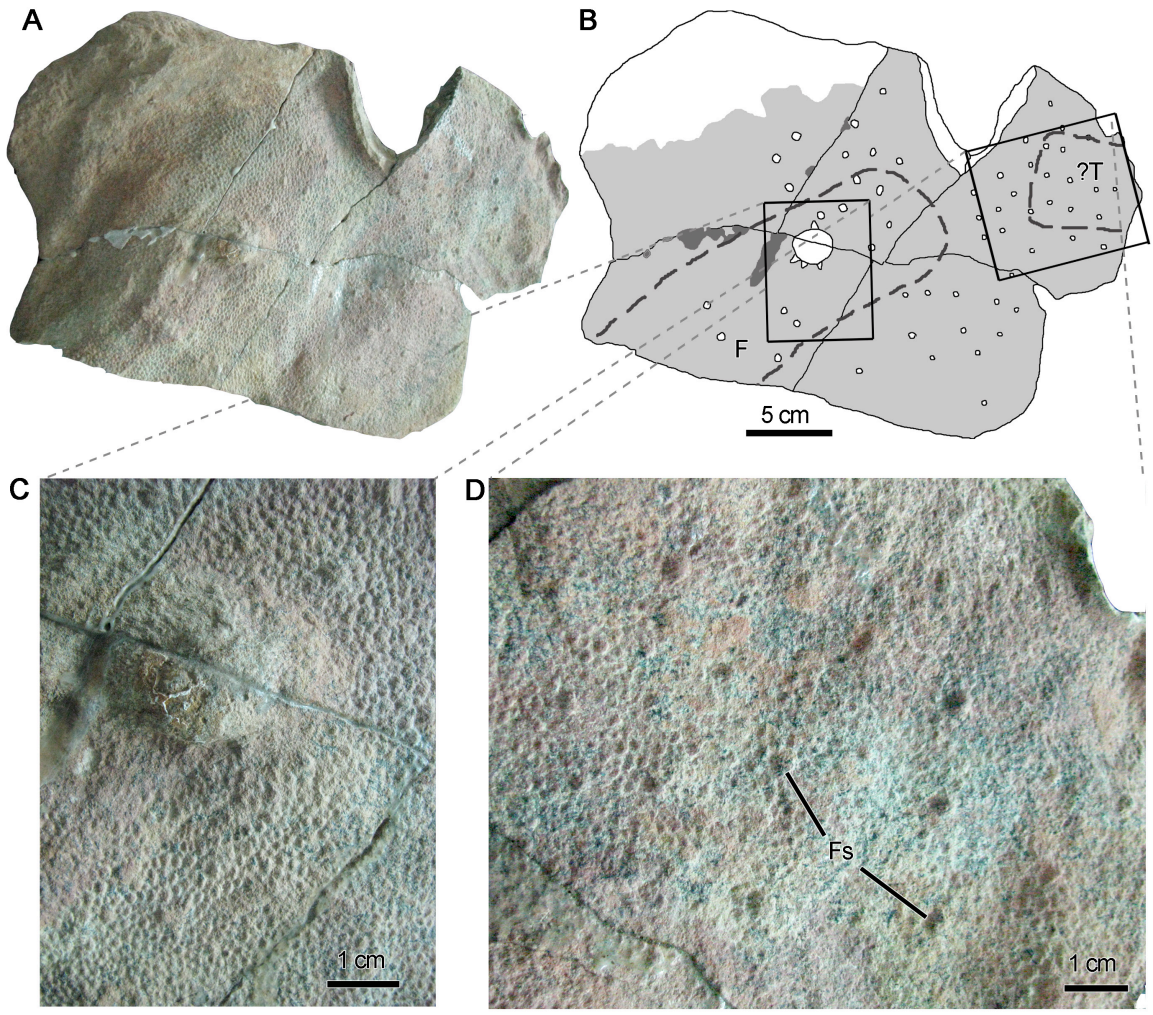

Figure 5.10. Right leg of juvenile *S. angustirostris* (MgD-1/159). Photograph (A) and interpretive drawing (B) showing distribution of shield feature-scales (Fs). Thick dashed line indicates outline of femur (F) and ?tibia (?T) exposed on the opposite surface of the block. C. Close-up of large multi-pointed shield feature-scale. D. Detail of integument.

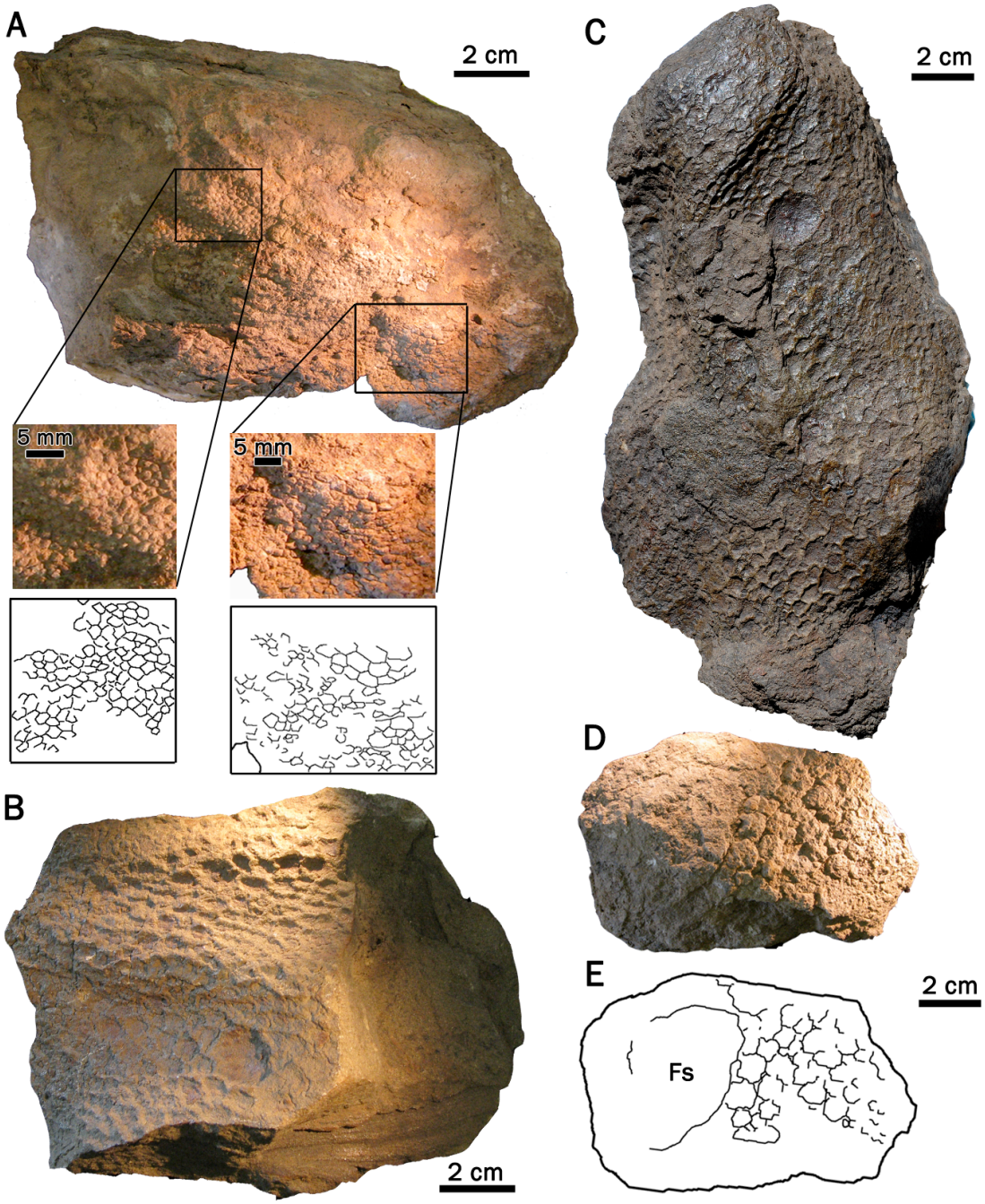

Figure 5.11. Miscellaneous skin impressions of *S. osborni* A., AMNH 5220; B AMNH 5221; C. AMNH 5221; D. AMNH 5220. Fs, feature scale.

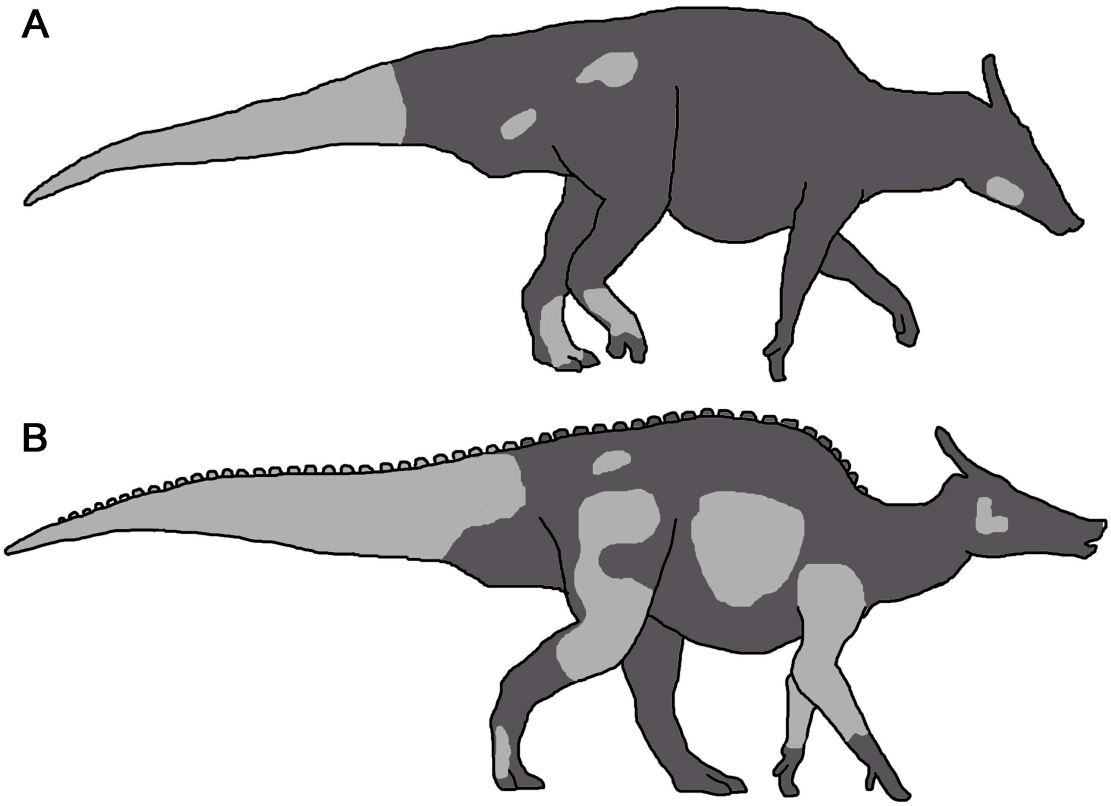

Figure 5.12. Regions of skin impressions (light grey) currently known for *S. osborni* (A) and *S. angustirostris* (B).

References

Anderson, B.G., Lucas, S.G., Barrick, R.E., Heckert, A.B., and Basabilvaso, G.T. 1998. Dinosaur skin impressions and associated skeletal remains from the Upper Cretaceous of southwestern New Mexico: new data on the integument morphology of hadrosaurs. Journal of Vertebrate Paleontology 18: 739–745.

Briggs, D. E. G., Wilby, P. R., Pérez-Moreno, B. P., Sanz, J. L., and Fregenal-Martínez, M. 1997. The mineralisation of dinosaur soft tissue in the Lower Cretaceous of Las Hoyas, Spain. Journal of the Geological Society, London 154:587–588.

Brown, B. 1916. *Corythosaurus casuarius*: skeleton, musculature and epidermis. Bulletin of the American Museum of Natural History 35:709–723.

Brown, B. 1917. A complete skeleton of the horned dinosaur *Monoclonius*, and description of a second skeleton showing skin impressions. Bulletin of the American Museum of Natural History 37:281–306.

Currie, P.J. 1983. Hadrosaur trackways from the Lower Cretaceous of Canada. Acta Palaeontologica Polonica 28:63–73.

Currie, P. J., Langston Jr., W., and Tanke, D. H. 2008. A new species of *Pachyrhinosaurus* (Dinosauria, Ceratopsidae) from the Upper Cretaceous of Alberta, Canada. In P. J. Currie, W. Langston Jr., and D. H. Tanke (eds.) A new horned dinosaur from an Upper Cretaceous bone bed in Alberta. NRC Research Press, Ottawa, Ontario, pp. 1–108.

Coria, R. A. and Chiappe, L. M. 2007. Embryonic skin from Late Cretaceous sauropods (Dinosauria) of Auca Mahuevo, Patagonia, Argentina. Journal of Paleontology 81:1528–1532.

Czerkas, S. A. 1992. Discovery of dermal spines reveals a new look for sauropod dinosaurs. Geology (Boulder) 20:1068–1070.

Czerkas, S. A. 1997. Skin. In P. J. Currie and K. Padian (eds.) The Encyclopedia of Dinosaurs. Academic Press, California, pp. 669–675.

Dodson, P., Krause, D. W., Forster, C. A., Sampson, S. D., and Ravoavy, F. 1998. Titanosaurid osteoderms (Sauropoda) osteoderms from the Late Cretaceous of Madagascar. Journal of Vertebrate Paleontology 18:563–568.

Evans, D. and Reisz, R.R. 2007. Anatomy and relationships of *Lambeosaurus magnicristatus*, a crested hadrosaurid dinosaur (Ornithischia) from the Dinosaur Park Formation, Alberta. Journal of Vertebrate Paleontology 27:373–393.

Fanti, F. and Currie, P. J. 2007. A new *Pachyrhinosaurus* bonebed from the Late Cretaceous Wapiti Formation. Ceratopsian Symposium, Program, Abstracts, and Short Papers, Royal Tyrrell Museum of Palaeontology September 22–23, 2007, Drumheller, Alberta, Canada.

Gillette, D.D., Albright III, L.B., Titus, A.L., and Graffam, M.H. 2002. Skin impressions from the tail of a hadrosaurian dinosaur in the Kaiparowits Formation (Upper Cretaceous), Grande Staircase-Escalante National Monument. Abstracts with Programs – Geological Society of America 34:6.

Horner, J. R. 1984. A 'segmented' tail frill in a species of hadrosaurian dinosaur. Journal of Paleontology 58:270–271.

Ji, S.-A. and Bo, H.C. 1998. Discovery of the Psittacosaurid skin impressions and its significance. Geological Review 44: 603–606.

Ji, S. 1999. Initial report of fossil psittacosaurid skin impressions from the uppermost Jurassic of Sihetun, northeastern China. Earth Science 53:314–316.

Lambe, L. 1914a. On the fore-limb of a carnivorous dinosaur from the Belly River Formation of Alberta, and a new genus of Ceratopsia from the same horizon, with remarks on the integument of some Cretaceous herbivorous dinosaurs. Ottawa Naturalist 27:129–135.

Lambe, L. 1914b. On *Kritosaurus notabilis*, a new genus and species of trachodont dinosaur from the Belly River Formation of Alberta, with a description of the skull of *Chasmosaurus belli*. Ottawa Naturalist 27:145–155.

Larson, P., Larson, M., Ott, C., and Bakker, R. 2007. Skinning a *Triceratops*. Journal of Vertebrate Paleontology 27:104A.

Manning, P.L., Morris, P.M., McMahon, A., Jones, E., Gize, A., Macquaker, J.H.S., Wolff, G., Thompson, A., Marshall, J., Taylor, K.G., Lyson, T., Gaskell, S., Reamtong, O., Sellers, W.I., van Dongen, B.E., Buckley, M., and Wogelius, R.A. 2009. Mineralized soft-tissue structure and chemistry in a mummified hadrosaur from the Hell Creek Formation, North Dakota (USA). Proceedings of the Royal Society B 276: 3429–3437.

Mayr, G., Peters, S., Plodowski, G. and Vogel, O. 2002. Bristle-like integumentary structures at the tail of the horned dinosaur *Psittacosaurus*. Naturwissenschaften 89:361–365.

Murphy, N.L., Trexler, D., and Thompson, M. 2006. "Leonardo", a mummified *Brachylophosaurus* from the Judith River Formation. In K. Carpenter (ed.) Horns and Beaks: Ceratopsian and Ornithopods Dinosaurs. Indiana University Press, Bloomington, Indiana, pp. 117–133.

Osborn, H. F. 1911. A dinosaur mummy. American Museum Journal 2:7–11.

Osborn, H. F. 1912. Integument of the iguanodont dinosaur *Trachodon.* American Museum of Natural History Memoir, Part II:33–54.

Parks, W.A. 1920. The osteology of the trachodont dinosaur *Kritosaurus incurvimanus*. Transactions of the Royal Society of Canada 13:5–76.

Siber, H.J. and Möckli, U. 2009. The Stegosaurs of the Sauriermuseum Aathal. Sauriermuseum Aathal, Switzerland.

Sternberg, C.M. 1925. Integument of *Chasmosaurus belli*. Canadian Field Naturalist 39:108–110.

Sternberg, C.M. 1935. Hooded hadrosaurs of the Belly River Series of the Upper Cretaceous. National Museum of Canada Bulletin 77:1–38.

Trexler, D. 1995. Detailed description of newly discovered remains of *Maiasaura peeblesorum* (Reptilia: Ornithischia) and a revised diagnosis of the genus. Unpublished MS thesis, University of Calgary, Calgary, Alberta, 217 p.

Wegweiser, M.D., Hartman, S.A., and Lovelace, D.M. 2006. Duckbill dinosaur chin scales: ups, downs and arounds of surficial morphology of Upper Cretaceous Lance Formation dinosaur skin. New Mexico Museum of Natural History and Science Bulletin 35:119–125.

Xu, X., Tang, Z.-L., and Wang, X.-L. 1999a. A therizinosaurid with integumentary structures from China. Nature 399:350–354.

Xu, X., Wang, X.-L, and Wu, X.-C. 1999b. A dromaeosaurid dinosaur with a filamentous integument from the Yixian Formation of China. Nature 401:262–266.

Xu, X., Zhou, Z.-H., and Prum, R. O. 2001. Branched integumental structures in *Sinornithosaurus* and the origin of feathers. Nature 410:200–204.

CHAPTER 6

THE DRAGON'S TOMB: A *Saurolophus* (HADROSAURIDAE) BONEBED FROM THE LATE CRETACEOUS OF MONGOLIA, WITH COMMENTS ON THE PUTATIVE HADROSAURINE, *Barsboldia*.

This chapter is part of a larger study under the authorship of M.J. Ryan, D.C. Evans, P.R. Bell, and D. Badamgarav, which includes the taphonomy of the Dragon's Tomb.

Introduction

Hadrosaurids are best known from the Late Cretaceous of North America, although recent discoveries demonstrate an equally diverse and abundant Asian fauna. Recent fieldwork in central Asia, particularly in Kazakhstan and the Amur region of far eastern Russia and China, have provided new information on existing taxa and yielded a number of important new taxa including *Charonosaurus jiayinensis* (Godefroit et al. 2000, 2001), *Olorotitan aharensis* (Godefroit et al. 2003), *Kerberosaurus manakini* (Bolotsky and Godefroit 2004), *Sahaliyania elunchunorum* (Godefroit et al. 2008), and *Wulagasaurus dongi* (Godefroit et al. 2008). Extensive monodominant bonebeds of *Charonosaurus* (Godefroit et al. 2000), *Amurosaurus* (Godefroit et al. 2004a, Lauters et al. 2008), and *Sahaliyania* (Godefroit et al. 2008) are known from this region and at least two other species (*K. manakini, W. dongi*) comprise minor components of some of these bonebeds. The proliferation of new basal Asian taxa has also bolstered support for an Asian origin for both hadrosaurines and lambeosaurines (Godefroit et al. 2003, 2004a, b, 2008).

The fossil-rich, late Campanian-?Maastrichtian beds of Mongolia preserve only two hadrosaurid taxa, both from the Nemegt Formation; a crested hadrosaurine, *Saurolophus angustirostris*, and the enigmatic *Barsboldia sicinskii*. *Barsboldia* is known from a single, partial postcranial skeleton with unusually tall neural spines and keeled sacral vertebrae. Maryańska and Osmólska (1981a) originally assigned this taxon to Lambeosaurinae; however, a recent revision of the Hadrosauridae placed it amongst Hadrosaurinae (Prieto-Marquez 2010). *Saurolophus* is known from at least fifteen skeletons (Norman and Sues 2000) and

represents approximately 25% of the total number of dinosaurs collected from the Nemegt Formation (Currie 2009). It is characterised by a solid, posterodorsally-directed, spike-like crest that is constructed of the nasals, frontals, and prefrontals (Maryańska and Osmólska 1981b, Bell in press)

In 1948, members of the Russian-Mongolian expedition to Mongolia's Gobi Desert, discovered an accumulation of well-preserved skeletons of *Saurolophus* in badlands exposed at Altan Uul II. An account of the discovery given in Russian by Efremov (1958) noted seven nearly complete articulated skeletons exposed on the surface. Many of the specimens preserved skin impressions and the 'sepulchral embankment' (Efremov 1958, pg. 208) on which they were preserved led them to name the locality, 'the Dragon's Tomb'. This remarkable locality has received only passing mentions in the English literature (Colbert 1968, Maryańska and Osmólska 1984, Coy 1997, Kurochkin and Barsbold 2000, Norman and Sues 2000). Unfortunately, the reliability of this locality for yielding complete skulls and skeletons of *S. angustirostris* has made it attractive to poachers, and in recent years untold numbers of specimens have been collected, plundered, destroyed and/or sold.

This study is the result of two excursions to the Dragon's Tomb as parts of the Korean International Dinosaur Project (2008) and Nomadic Expeditions (2010). The purpose of this chapter is to document the excavation history and the effects of poaching at this important site. The ontogenetic series of *Saurolophus* available from the Dragon's Tomb (supplemented by additional material from nearby localities within the Nemegt Basin) supplies new information concerning the validity of *Barsboldia*.

Locality and Geology

The Dragon's Tomb (N 100' 33.664; E 43' 36.192) occurs in rocks of the Nemegt Formation exposed at Altan Uul II on the southern flank of Altan Uul in south-central Mongolia (Fig. 6.1). The Nemegt Formation (Gradzinski and Jerzykiewicz 1974) is a 320m thick package of upward-fining sandstones and mudstones with locally-abundant reworked caliche pebbles. These sediments have been interpreted as overbank, lacustrine and channel fill deposits that were laid down on an alluvial floodplain analogous to the present-day Okavango Delta in south-central Africa (Jerzykiewicz and Russell 1991, Jerzykiewicz 2000). Locally abundant bivalves within the Nemegt Formation occur in coarse-grained fluvial deposits, which have been interpreted as largely lacustrine in origin. Rocks of the Nemegt Formation mark the wettest conditions in a progressively wetter sedimentary sequence that extended through the underlying Bayanshiree and Baruungoyot Formations (Jerzykiewicz and Russell 1991).

A two metre thick sedimentary section exposed on the edge of the embankment at the Dragon's Tomb is divisible into four lithological units (Fig. 6.2). A yellowish-grey sandy siltstone greater than 100 cm thick forms the base of this section (unit A). Invertebrate burrows are common in the upper part of the exposed thickness where they are preserved in bold relief. Unit A is conformably overlain by a laminar bedded mudstone approximately 22 cm thick (unit B), interpreted here as an overbank floodplain deposit. Unit C conformably overlies unit B and comprises more than 25 cm of tangential trough cross-bedded fine sandstone with abundant reworked clay and caliche pebbles up to 3 cm in diameter. These are typical of basal lags within palaeochannels in the Nemegt

Formation (Eberth et al. 2009). Clasts are of variable size, typically rounded but may be angular, and evenly distributed through this layer. The bonebed host layer (unit D) is a bench-forming coarse sandstone up to 45 cm thick. It is strongly indurated and laterally extensive for at least 200 m. Unit D is composed of tangential, trough cross-beds with individual beds measuring between ~1–2 cm in thickness. The base of unit D truncates the bedding planes in unit C. Articulated and disarticulated vertebrate remains are found within a fossiliferous band approximately 45 m wide (Fig. 6.3) although the overall lateral extent of unit D is greater than this. Petrified logs measuring approximately 30 cm in diameter are found along the western edge of the bonebed but were not observed directly associated with the bones (Fig. 6.3). Sedimentary features and overall geometry of unit D, when considered within the sedimentary context of the Nemegt Formation, are consistent with the interpretation of a pointbar deposit within a meandering fluvial system (Gradzinski et al. 1977, Eberth et al. 2009).

History

Following World War II, an agreement between the former Soviet Union and Mongolia permitted the first major palaeontological expedition to Outer Mongolia since the Central Asiatic Expeditions in the 1920's. The Russian-Mongolian Expeditions (1946, 1948–9) were led by Ivan A. Efremov under the auspices of the Palaeontological Institute (Moscow).

The Dragon's Tomb was discovered in May 1948 by V. Pronin, one of the expedition drivers, at the foot of Altan Uul ("Golden Mountain") in the Nemegt Basin. Efremov (1958) described six skeletons of *Saurolophus* lying close together

and somewhat intertwined with one another on a broad sandstone ledge. Despite several attempts to get vehicle access to the site, they were forced to transport the specimens by camel some 500m to their transports. Over several weeks, the expedition collected parts of at least four skeletons (PIN 551/356, PIN 551/357, PIN 551/358, PIN 551/259) from animals ranging from 6 to 9m in length (Efremov 1958). In a short description, Rozhdestvensky (1952) chose the best of those specimens (PIN 551/356) and erected a new species, *Saurolophus angustirostris,* based on its close similarity to the North American taxon, *Saurolophus osborni*. In addition, numerous blocks of articulated postcranial elements with superb skin impressions (e.g. PIN 3738, PIN 3747/1, PIN 3747/2, PIN 4216/48, PIN 4216/49) were also collected but never described. Following preparation of the remaining material, Rozhdestvensky (1957) redescribed the skull and postcranium of *Saurolophus angustirostris* and commented on the ontogeny of the species (Rozhdestvensky 1957, 1965). Strangely, Rozhdestvensky did not mention the Dragon's Tomb in any of his publications. Furthermore, his earliest reports (Rozhdestvensky 1952, 1957) refer only to Nemegt as he regarded Altan Uul and Nemegt as the same locality (V. Alifanov pers. comm. 2010). The Russian specimens are currently on display at the Palaeontological Institute, Moscow.

In September 2001, Dr. Rinchen Barsbold led a team from Nomadic Expeditions (a Mongolian tour operative) to the Dragon's Tomb. The site was revisited again in August 2003 and 2004 by a team led by P.J. Currie (then at the Royal Tyrrell Museum of Palaeontology) and coordinated by Nomadic Expeditions. The team, which included members of the historic Polish-Mongolian Expeditions (1965–1971) collected several blocks of skin impressions

that are now curated at the Mongolian Palaeontological Centre. Although several other groups (including the Polish-Mongolian Expeditions and the Hayashibara Museum of Natural Sciences) have worked in the area, they did not intrude on the site.

The locality was visited briefly by members of the Korean International Dinosaur Project on 16 September 2008 during which several small samples bearing skin impressions were collected. In some cases, molds were made of impressions that were not practical to remove. These molds are curated at the University of Alberta. Comparison of the site with photos from the Nomadic Expeditions earlier visits clearly demonstrate the devastating impact of poachers in the interim. In 2009, an expedition run jointly by Drs. M. Ryan (Cleveland Museum) and D. Evans (Royal Ontario Museum), in cooperation with the Geological Research Authority (Ulaan Baatar), Nomadic Expeditions, and Montesori High School (Cleveland, Ohio) was initiated to restore the site and recover anything of scientific value. That year, expedition members attempted to clear the site of rubble and bone fragments left by the poachers in order to get down to the bedrock. Although no excavations were made, the expedition collected one small, almost complete *Saurolophus* skull (Fig. 6.3) that had been poached but not taken. They also recovered a partial *Tarbosaurus* braincase that has been poached from the juvenile *Tarbosaurus* at the site, but which was discarded. These collections are now at the Mongolian Palaeontological Centre (Ulaan Baatar). In addition, documentation was made of all significant skeletal elements left behind by poachers. The following August, a small Nomadic Expeditions crew returned in to map *in situ* exposures of the bonebed and to document the extensive skin impressions from the site and to gather additional

taphonomic information. These skin impressions, curated at the University of Alberta, are described in chapter 5. The taphonomy of this site is currently under study by other authors (e.g. M. Ryan and D. Evans) and will be described elsewhere.

Poaching

Although excellent dinosaur specimens have been collected from Mongolia for nearly a century, fossil poaching has become particularly troublesome in only the last ten to fifteen years. Primarily, poachers are concerned with easily recognizable and saleable elements such as skulls, teeth, and claws. Because the fossil-bearing rocks are heavily indurated, excavations at the Dragon's Tomb are not easily undertaken. Nevertheless, the richness of this locality and the high-quality fossilized remains has prompted poachers to use dynamite to extract the well-preserved bones (Fig. 6.4). Drill holes, and blast craters are still visible and discarded quarry garbage (glue bottles, dynamite cord, tools, etc.) still litter the site. Blasting has been to such an extent that much of the original 45 metre wide exposure is pockmarked with craters and few areas remain *in situ* (Fig. 6.5). Efremov (1958) described six skeletons lying in repose when they discovered the site, four of which were collected, either partly or wholly. The obvious ramifications of imprecise drilling and blasting include the wholesale destruction and loss of scientifically valuable material. The entire exposure is now covered in boulders of often-articulated elements from an unknown number of additional individuals. The majority of this poached debris still retains extensive skin impressions. Frequently, the blasted material is too

badly broken to be of use to the poachers and is subsequently left behind but unknown numbers of specimens have also be plundered and presumably sold. Paradoxically, it is this illegal activity that has uncovered several important, yet damaged specimens, including the only known *Tarbosaurus* from the Dragon's Tomb. Poachers have also uncovered excellent skin impressions that cover entire body parts (such as the trunk, tail, and forelimbs) and three-dimensional integumentary structures that may represent preserved muscle bulk (Murphy et al. 2006). Poaching at the Dragon's Tomb did not start until some time after September 2001 (P. J. Currie, unpublished field notes). Although poaching in Mongolia has certainly escalated within recent years, renewed poaching activity was not observed between 2008 and 2010.

Gregariousness in *Saurolophus*

The Dragon's Tomb qualifies as a monodominant bonebed (Eberth and Getty 2005). Based on numbers reported by Efremov (1958), at least six individuals are present in the assemblage ranging in length from 6 to 9m. At least four individuals were collected including two large, mature individuals (PIN 551/356, PIN 551/357), a late-stage subadult (PIN 551/358), and the skull of a juvenile animal (PIN 551/359). Based on the sketch maps in Efremov (1955), the remaining two individuals were (or close to) full size.

Actuoexperiments strongly suggest that multi-individual bonebeds are not created artificially in fluvial systems but represent pre-existing (either intrinsic or extrinsic) accumulations (Rogers and Kidwell 2007 and references therein). In addition, Eberth et al. (2007) argued that most monodominant

bonebeds are the result of mass mortality events, which supports the interpretation that intrinsic biological factors (i.e. gregariousness) are responsible for their genesis. It must be noted that in the absence of a thorough taphonomic analysis, a possible intrinsic biological origin for the Dragon's Tomb assemblage must be considered with some caution. However, if such an interpretation is correct, the Dragon's Tomb represents the only known example of gregarious behaviour in *Saurolophus angustirostris*. Although the minimum number of individuals is too small for robust statistical analysis, the herd preserved at the Dragon's Tomb appears to represent all size classes except for hatchlings/yearlings. Perhaps more importantly, the Dragon's Tomb is the only known bonebed in the world that preserves dinosaur 'mummies'. Although skin impressions, even so-called dinosaur 'mummies', are known from around the world (Sternberg 1953, Martill 1991, Murphy et al. 2007), in no case have they been found in association with more than one individual within a single quarry. Indeed, all 'mummies' represent exquisite, albeit isolated cases. Other famous localities that have repeatedly yielded soft tissue structures (such as the Jianshangou Bed of the Yixian Formation in Liaoning, China) preserve such specimens over a given stratigraphic interval rather than a single event horizon (Chen et al. 2005). Skin impressions associated with dinosaur remains are usually preserved as trace fossils (Sternberg 1953, Martill 1991, Murphy et al. 2007) although three-dimensional skin structure has also been reported (Kellner 1996, Briggs et al. 1997, Manning et al. 2009). Few studies have directly addressed the process of skin preservation although Wegweiser et al. (2004) demonstrated that usual mummification processes (such as desiccation or decay-inhibiting chemicals) are not necessary for the fossilisation of dinosaur integument. Instead,

rapid replacement of soft tissues by minerals in mineral-rich groundwater can take place within a period of weeks or months following death (Wegweiser et al. 2004, Manning et al. 2009). The taphonomic implications of skin impressions found at the Dragon's Tomb have yet to be addressed; however, their presence (see also Chapter 5) further underscores the importance of this site.

Hadrosaurid bonebeds are well known from the Late Cretaceous of North America and Asia. Although bonebed formation is not the result of any one factor, it is generally accepted that hadrosaurid (particularly monodominant) bonebeds represent intrinsic biogenic accumulations resulting from gregarious behaviour (Varricchio and Horner 1993, Rogers and Kidwell 2007). Such mass accumulations are critical to understanding intraspecific variation, ontogenetic change, relative growth rates, aggregation behaviour, palaeoecology, and even predator-prey relationships (Brinkman et al. 2007). Bonebeds are not a ubiquitous feature among hadrosaurids although a variety of hadrosaurines (*Brachylophosaurus* [Larock et al. 2000], *Edmontosaurus* [Derstler 1995], *Maiasaura* [Varricchio and Horner 1993], *Prosaurolophus* [Varricchio and Horner 1993]) and lambeosaurines (*Charonosaurus* [Godefroit et al. 2001], *Amurosaurus* [Lauters et al. 2008], *Sahaliyania* [Godefroit et al. 2008], *Hypacrosaurus* [Bell, unpubl. data]) appear to have been gregarious (Varricchio and Horner 1993). A 'family' of four *Corythosaurus* recovered from a single quarry (quarry #11) at Dinosaur Provincial Park implies some degree of socialism for this genus also (Dodson 1971). The Dragon's Tomb provides the first evidence of gregarious behaviour in *Saurolophus*; there is, as yet, no evidence to support a similar lifestyle in *Saurolophus osborni*. Although taxonomically widespread, when superimposed on to the hadrosaurid family tree (Fig. 6.6), herding behaviour inferred from

bonebeds shows no clear phylogenetic signal; however, as new bonebeds will no doubt be found, this diversity cannot be said to represent all hadrosaurids.

Variation in *Saurolophus* and the validity of *Barsboldia*.

Barsboldia sicinskii was erected based on a single partial skeleton (ZPAL MgD 1/110) from the Nemegt Formation (Quarry 23 on fig. 1 of Gradzinski and Jerzykiewicz 1972) at the Nemegt locality. Maryańska and Osmólska (1981a) diagnosed it as a lambeosaurine based on the relatively high neural spines of the posterior dorsal, sacral, and anterior caudal vertebrae in addition to keeled sacral vertebrae. They further diagnosed *Barsboldia* by club-like neural spines of the anterior caudals and a deep ilium dorsal to the acetabulum. Keeled sacral vertebrae and relatively tall neural spines, while common among lambeosaurines (Horner et al. 2004), have also been observed in non-lambeosaurine hadrosaurids (e.g., *Tanius sinensis, Pararhabdodon isonensis*; Prieto-Marquez et al. 2006). Prieto-Marquez (2010) reassigned *Barsboldia* to the Hadrosaurinae (Saurolophinae of Prieto-Marquez 2010) based on a single feature of the ilium. This character is defined as a poorly delineated posterodorsal margin of the ilium that appears discontinuous with the dorsal margin of the proximal part of the postacetabular process, because of the lack of a well-demarcated posterodorsal ridge [character 240(1) of Prieto-Marquez 2010]. Furthermore, the apparent differences listed by Maryańska and Osmólska (1981a) between *Saurolophus* and *Barsboldia* are almost certainly due to comparison of immature with mature individuals, respectively. The holotype, and only specimen of *Barsboldia* is represented by a large and mature individual as evidenced from the closed neurocentral sutures and the

presence of nine fused sacral vertebrae (Maryańska and Osmólska 1981a, Horner et al. 2004). The ilium itself is over one metre in length, and individual centra measure up to 205 mm in height (table 1, Maryańska and Osmólska 1981a). Comparisons in Maryańska and Osmólska (1981a) relied heavily on specimens easily available to them, especially ZPAL MgD-1/159, which is the smallest known specimen of *Saurolophus angustirostris.* Although large *Saurolophus* (MPC 100/706, PIN 551/357, PIN 551/358) within the size range of ZPAL MgD 1/110 have been collected, their postcrania are unprepared. The only available published description of a large individual is that of the holotype (PIN 551/356, Rozhdestvensky 1957), which is approximately 33% smaller than the largest individuals of *Saurolophus* based on skull length. Moreover, Maryańska and Osmólska (1981a) were unable to view the holotype of *Saurolophus angustirostris* directly and therefore were reliant on the illustrations in Rozhdestvensky (1957) to provide meaningful comparisons. As stated in Maryańska and Osmólska (1981a, p. 250), they used Rozhdestvensky's skeletal reconstruction of *Saurolophus angustirostris* (fig. 5 in Rozhdestvensky 1957) to compare with the ilium and sacrum of *Barsboldia.* Unfortunately, this figure can only be described as schematic. Firsthand observation of PIN 551/356 also confirms that the ends of some of the sacral neural spines have been reconstructed. Therefore comparison of ZPAL MgD-1/159 and PIN 551-356 to *Barsboldia* must be done cautiously because of potential ontogenetic differences.

The ontogenetic series of *Saurolophus angustirostris* available from the Dragon's Tomb, with the addition of other specimens, permits reconstruction of the developmental sequence of some of these features, including the relative and absolute heights of the neural spines, and transverse expansion of the distal

neural spines. Juveniles (ZPAL MgD-1/159) possess transversely flattened neural spines on both sacral and proximal caudal vertebrae that are equally long anteroposteriorly for their entire height. The neural spines on the most proximal caudal vertebrae are approximately 10 cm high or twice the height of the corresponding centrum. In large subadults (PIN 551/356), the distal ends of the neural spines become transversely expanded and the neural spine approaches heights of 2.5 times the height of the respective centrum. Transverse expansion is even more pronounced in the largest individuals (PIN 3741-1; Fig 6.7) with neural spine height exceeding 45 cm or approximately 3.5 times the height of the corresponding centrum. In both PIN 551/356 and PIN 3741-1, these measurements represent incomplete neural spines and/or correspond to (approximately) the fifth, or greater, caudal vertebrae. Therefore, they do not represent the maximum heights attained by the neural spines on these individuals. In *Barsboldia,* the neural spines of both sacral and anterior caudal vertebrae are three times the height of the corresponding centrum and reached maximum heights of 62 cm over the sacrum (Maryańska and Osmólska 1981a). Although vertebrae of *Saurolophus* have not been measured at the same absolute size of *Barsboldia,* it is clear that absolute and relative height, as well as transverse expansion of the neural spines is a function of ontogeny in *Saurolophus*. Moreover, the heights of the sixth to tenth caudal vertebrae of *Barsboldia* compare well in all dimensions to those of the large *Saurolophus* specimens (PIN 551/356, PIN 3741-1). It is also noteworthy that, despite the specimen richness of the Nemegt Formation, more than 60 years of intensive fieldwork in this region (including the Dragon's Tomb) has failed to recover any definitive Lambeosaurine material. Based on these observations, it is considered prudent to

assign ZPAL MgD 1/110 to *Saurolophus angustirostris* and regard *Barsboldia* as a junior synonym of *Saurolophus angustirostris*.

Conclusions

The Dragon's Tomb represents a monodominant bonebed of the hadrosaurine, *Saurolophus angustirostris.* Well-preserved, articulated skeletons were preserved on pointbar deposit within the fluviolacustrine context of the Nemegt Formation. At least six individuals, ranging from 6–9m in length were observed when the site was first discovered in 1948. The Russians collected parts of at least four individuals, which included the holotype skull and skeleton of *Saurolophus angustirostris*. More recent visits by research groups have been followed by periods of poaching. Poaching has dramatically altered the Dragon's Tomb and unknown numbers of specimens have subsequently been destroyed, lost, and presumably sold. Nevertheless, the Dragon's Tomb still represents one of the most important and unique palaeontological sites in Mongolia. The Dragon's Tomb is the only known example of a bonebed that preserves skin impression from multiple individuals. In addition, it provides the best evidence for gregarious behaviour in *Saurolophus.* The presence of different size classes sheds light on some ontogenetic features in the postcrania. The only other possible hadrosaurid from the Nemegt Formation is *Barsboldia sicinskii*, which was defined by its 'club-like' neural spines and neural spines that are up to three times the height of the corresponding centrum in the sacral and proximal caudal vertebrae (Maryańska and Osmólska 1981a). These features were unsuccessful in distinguishing *Barsboldia* in a recent review of the Hadrosauridae (Prieto-

Marquez 2010). Evaluation of *Saurolophus* postcrania from the Dragon's Tomb reveals ontogenetic changes in the relative height of the neural spines in the proximal-most tail (sacral vertebrae could not be appraised due to the absence of appropriate material) and concomitant mediolateral widening of the dorsal ends of the neural spines reminiscent of the conditions in *Barsboldia*. In the absence of more diagnostic material, *Barsboldia* is here considered a junior sysnonym of *Saurolophus angustirostris.*

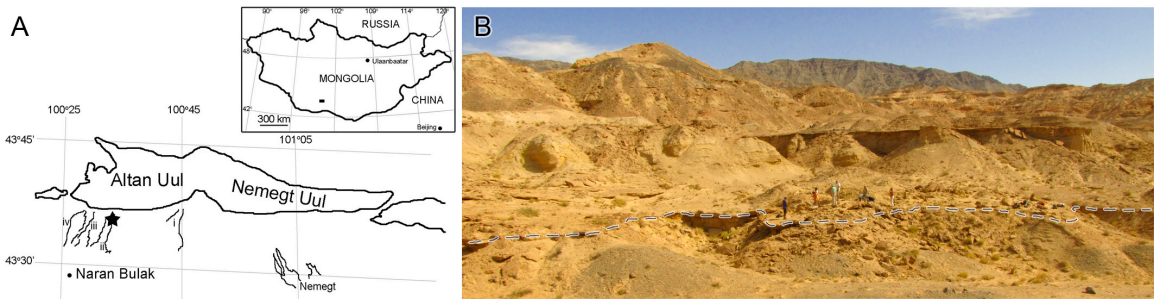

Figure 6.1. Location of the Dragon's Tomb at Altan Uul II within the Nemegt basin of Mongolia (A). B. Panorama looking north at the Dragon's Tomb. The top of the bone-bearing unit is marked by a dashed line. Note the large slabs of sandstone on the lower slope, many of which were displaced by poachers. People for scale. Photo by D. Lloyd.

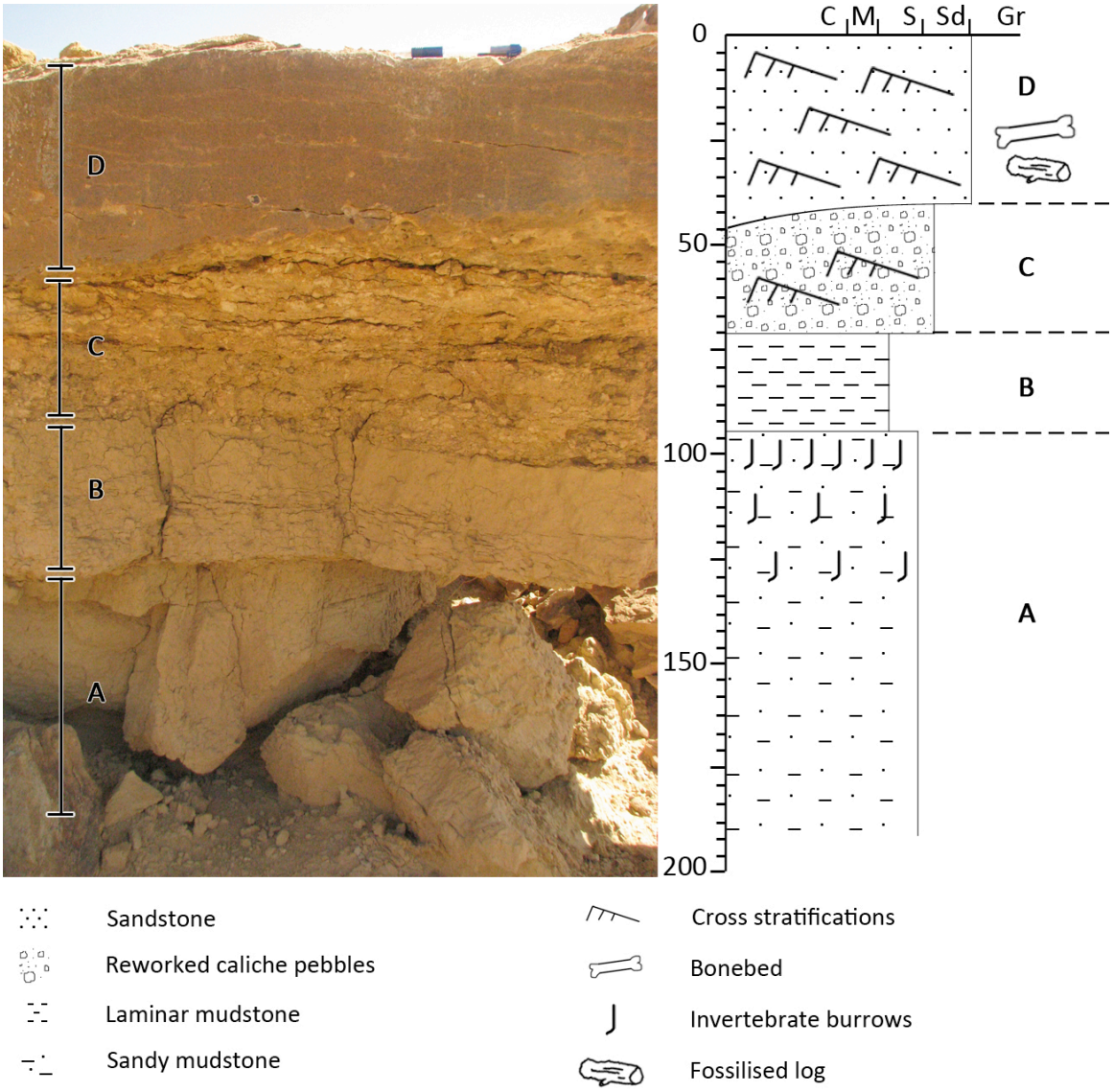

Figure 6.2. Stratigraphic section of the Dragon's Tomb. Scale in centimetres.

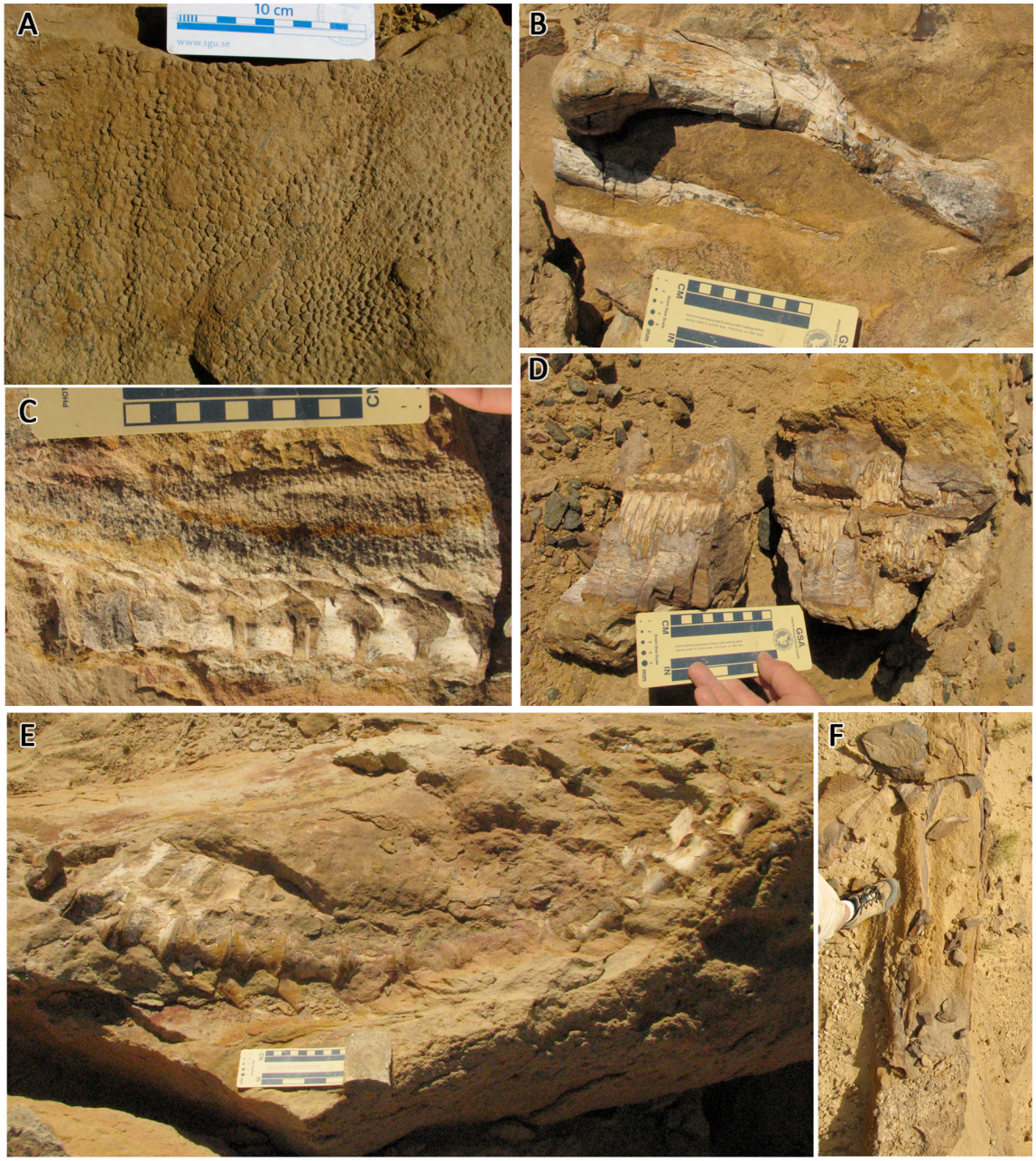

Figure 6.3. Preservation quality at the Dragon's Tomb. A. *Saurolophus* skin impressions; B. articulated forelimb of subadult individual; C. articulated juvenile tail with skin impressions; D. articulated subadult skull and jaws destroyed by poachers; E. articulated tail of subadult *Tarbosaurus*; F. Large petrified log. Approximate width of trunk equals 30 cm. All other scales as indicated.

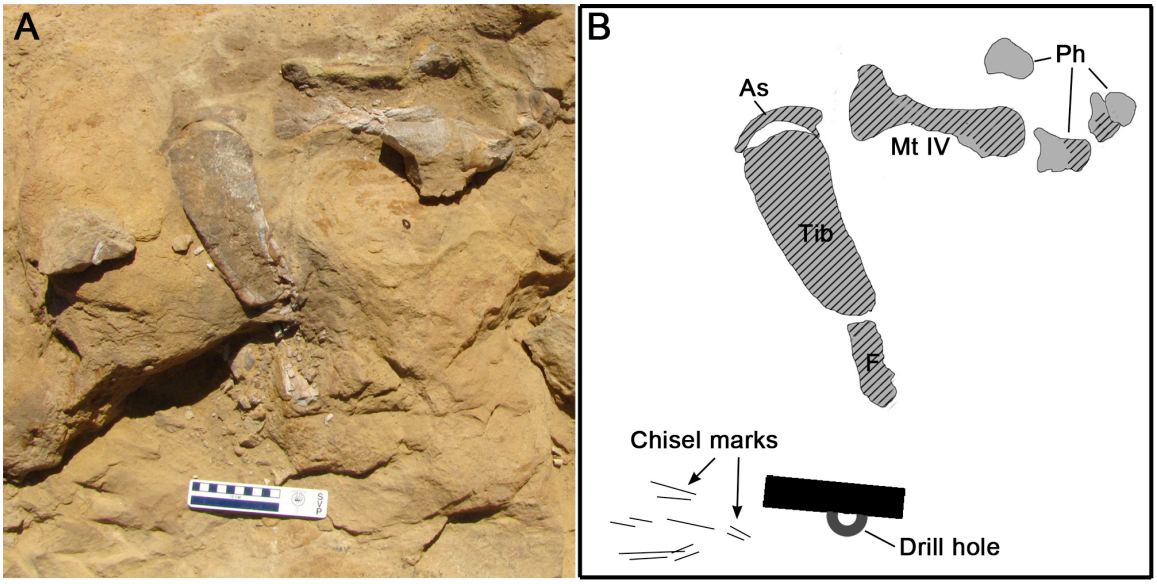

Figure 6.4. Photograph (A) and illustration (B) of a poached articulated hindleg of *Saurolophus*. Hatching indicates broken bone surface. A drill hole (partly obscured by the scale) is visible into which dynamite would have been packed. As, astragalus; F, fibula; Mt, metatarsal; Ph, phalanges; Tib, tibia. Photo by D. Lloyd.

Figure 6.5. Expedition members survey the effects of poaching at the Dragon's Tomb in 2010. The boulders in the fore- and middle-ground have been torn up by poachers. Most contain both bones and skin impressions. Photo by D. Lloyd.

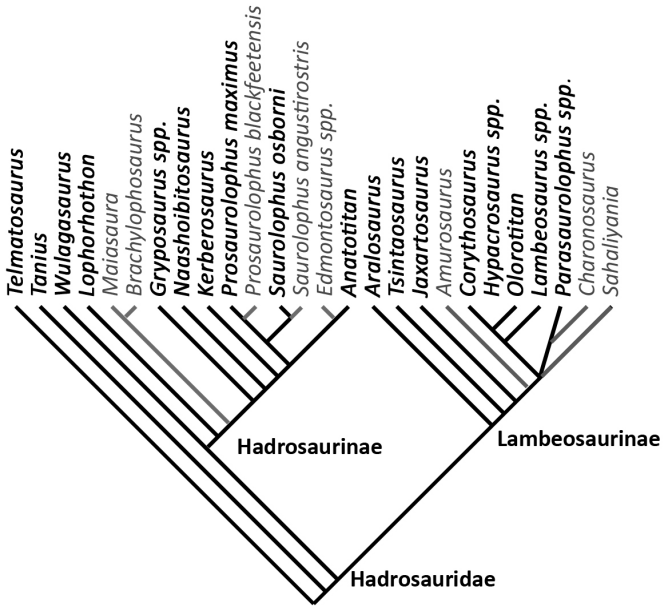

Figure 6.6. Cladogram showing the distribution of gregariousness (grey) across Hadrosauridae as determined from bonebed data. Tree topology adapted from Godefroit et al. (2008)

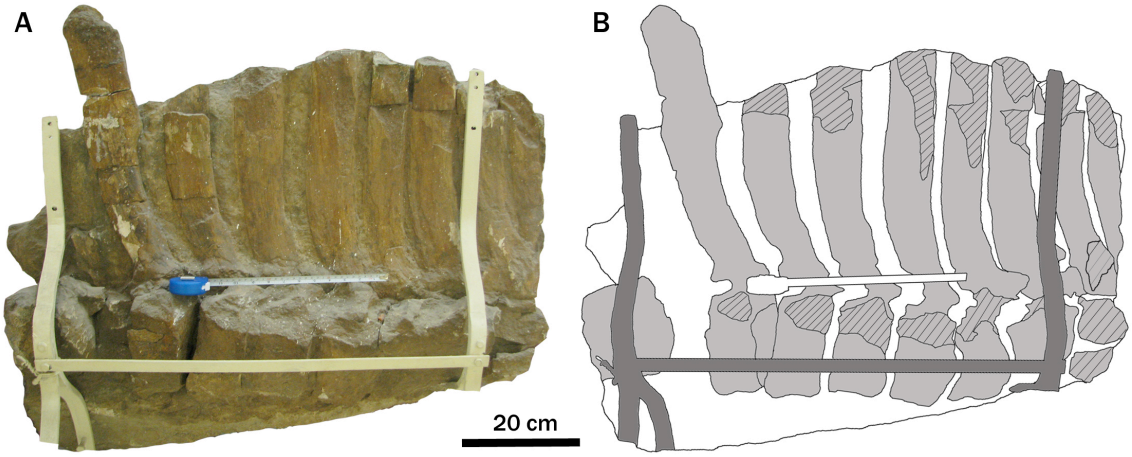

Figure 6.7. Proximal-most caudal vertebrae of *Saurolophus angustirostris* (PIN 3747-1). Photograph (A) and interpretive drawing (B). Hatching represents broken bone surface. Support armature is in dark grey.

References

Bell, P.R. in press. Cranial osteology and ontogeny of *Saurolophus angustirostris* from the Late Cretaceous of Mongolia with comments on *Saurolophus osborni* from Canada. Acta Palaeontologica Polonica doi:10.4202/app.2010.0061

Bolotsky, Y.L. and Godefroit, P. 2004. A new hadrosaurine dinosaur from the Late Cretaceous of far eastern Russia. Journal of Vertebrate Paleontology 24, 351–365.

Briggs, D.E.G., Wilby, P.R., Pérez-Moreno, Sanz, J.L., and Fregenal-Martínez, M. 1997. The mineralization of dinosaur soft tissue in the Lower Cretaceous of Las Hoyas, Spain. Journal of the Geological Society 154: 587–588.

Brinkman, D. B., Eberth, D.A, and Currie, P. J. 2007. From bonebeds to paleobiology: applications of bonebed data. In R. R. Rogers, D.A. Eberth, and A. R. Fiorillo (eds.), Bonebeds; Genesis, Analysis, and Paleobiological Significance. University of Chicago Press, Chicago, pp. 221–264.

Chen, P., Wang, Q. Zhang, H., Cao, M., Li, W., Wu, S. and Shen, Y. 2005. Jianshangou Bed of the Yixian Formation in west Liaoning, China. Science in China 48: 298–312.

Colbert, E.H. 1968. Men and Dinosaurs – the Search in Field and Laboratory. E.P. Dutton and Co., New York, 283 pp.

Coy, C. 1997. Soviet-Mongolian Palaeontological Expeditions. In P.J. Currie and K. Padian (eds.) Encyclopedia of Dinosaurs. Academic Press, San Diego, pp. 691–692.

Currie, P. J. 2009. Faunal distribution in the Nemegt Formation (Upper Cretaceous), Mongolia. In Y.-N. Lee (ed.), Annual Report 2008, Korea-Mongolia International Dinosaur Project. Korean Institute Geology and Mineralogy, Seoul, Korea, pp. 143–156.

Derstler, K. 1995. The dragon's grave: an *Edmontosaurus* bonebed containing theropod eggshells and juveniles, Lance Formation (uppermost Cretaceous), Niobrara Co., Wyoming. Journal of Vertebrate Paleontology 15: 26A.

Dodson, P. 1971. Sedimentology and taphonomy of the Oldman Formation (Campanian), Dinosaur Provincial Park, Alberta (Canada). Palaeogeography, Palaeoclimatology, Palaeoecology 10:21-74

Eberth, D.A., and Getty, M.A. 2005. Ceratopsian bonebeds: occurrence, origins, and significance. In P.J. Currie and E.B. Koppelhus (eds.) Dinosaur Provincial Park; a Spectacular Ancient Ecosystem Revealed, Indiana University Press, Bloomington, Indiana, pp. 501–536.

Eberth, D.A., Shannon, M., and Noland, B.G. 2007. A bonebed database: classification, biases, and patterns of occurrence. In R.R. Rogers, D.A. Eberth, and A.R. Fiorillo (eds.) Bonebeds: Genesis, Analysis, and Paleobiological Significance. University of Chicago Press, Chicago, Illinois, pp.103–220.

Eberth, D.A., Badamgarav, D., and Currie, P.J. 2009. The Baruungoyot-Nemegt transition (Upper Cretaceous) at the Nemegt type area, Nemegt Basin, south central Mongolia. Journal of the Palaeontological Society of Korea 25: 1–15.

Efremov, I. A. 1955. Burial of dinosaurs in Nemegt (South Gobi, MPR). *In* Voprosy Geologii Azii. Izdatel'stvo Akademii Nauk SSSR, Moscow: 789–809 (in Russian).

Efremov, I.A. 1958. *Road of Winds* [in Russian]. The All-Union Uchebno-pedagogical publishing house, Moscow, 360 pp.

Godefroit, P., Zan, S., and Jin, L. 2000. *Charonosaurus jiayinensis* n.g., n.sp., a lambeosaurine dinosaur from the Late Maastrichtian of north-eastern China. Comptes rendus de l'Académie des Sciences de Paris, Sciences de la Terre et des Planètes 330: 875–882.

Godefroit, P., Zan, S., and Jin, L. 2001. The Maastrichtian (Late Cretaceous) lambeosaurine dinosaur *Charonosaurus jiayinensis* from north-eastern China. Bulletin de l'Institut royal des Sciences naturelles de Belgique, Sciences de la Terre 71, 119–168.

Godefroit, P., Bolotsky, Y., and Alifanov, V. 2003. A remarkable hollow-crested hadrosaur from Russia: an Asian origin for Lambeosaurines. Comptes Rendus Palevol 2: 143–151.

Godefroit, P., Bolotsky, Y., and Van Itterbeeck, J. 2004a. The lambeosaurine dinosaur *Amurosaurus riabinini*, from the Maastrichtian of Far Eastern Russia. Acta Palaeontologica Polonica 49: 585–618.

Godefroit, P., Alifanov, V., and Bolotsky, Y. 2004b. A re-appraisal of *Aralosaurus tuberiferus* (Dinosauria, Hadrosauridae) from the Late Cretaceous of Kazakhstan. Bulletin de l'Institut royal des Sciences naturelles de Belgique, Sciences de la Terre 74:139–154.

Godefroit, P., Hai, S., Yu, T., Lauters, P. 2008. New hadrosaurid dinosaurs from the uppermost Cretaceous of northeastern China. Acta Palaeontologica Polonica 53: 47–74.

Gradzinski, R. and Jerzykiewicz, T. 1972. Additional geographical and geological data from the Polish-Mongolian Palaeontological Expeditions. Palaeontologica Polonica 27: 17-30.

Gradzinski, R. and Jerzykiewicz, T. 1974. Sedimentation of the Barun Goyot Formation. Palaeontologica Polonica 30: 111–146.

Gradzinski, R., Keilan-Jaworowska, Z., and Maryanska, T. 1977. Upper Cretaceous Djadokhta, Barun Goyot and Nemegt formations of Mongolia, including remarks on previous subdivisions. Acta Geologica Polonica 27: 281–317.

Jerzykiewicz, T. 2000. Lithostratigraphy and sedimentary settings of the Cretaceous dinosaur beds of Mongolia. In: M.J. Benton, M.A. Shishkin, D.M. Unwin, and E.N. Kurochkin (eds.), The Age of Dinosaurs in Russia and Mongolia. Cambridge University press, Cambridge, UK, pp. 279–296.

Jerzykiewicz, T. and Russell, D. A. 1991. Late Mesozoic stratigraphy and vertebrates of the Gobi Basin. Cretaceous Research 12: 345–377.

Kellner, A.W.A. 1996. Fossilised theropod soft tissue. Nature 379: 32.

Kurochkin, E.N. and Barsbold, R. 2000. The Russian-Mongolian expeditions and research in vertebrate palaeontology. In: M.J. Benton, M.A. Shishkin, D.M. Unwin, and E.N. Kurochkin (eds.), The Age of Dinosaurs in Russia and Mongolia. Cambridge University press, Cambridge, UK, pp. 235–255.

Larock, J.W., Schmitt, J.G., and Horner, J.R. 2000. A Cretaceous paleo-logjam: taphonomy and sedimentology of a dinosaur bonebed from the Upper

Cretaceous Judith River Formation, northcentral Montana. Geological Society of America 32: 220A.

Lauters, P., Bolotsky, Y.L., Van Itterbeeck, J., and Godefroit, P. 2008. Taphonomy and age profile of a latest Cretaceous dinosaur bonebed in far eastern Russia. Palaios 23: 153–162.

Manning, P.L., Morris, P.M., McMahon, A., Jones, E., Gize, A., Macquaker, J.H.S., Wolff, G., Thompson, A., Marshall, J., Taylor, K.G., Lyson, T., Gaskell, S., Reamtong, O., Sellers, W.I., van Dongen, B.E., Buckley, M., and Wogelius, R.A. 2009. Mineralized soft-tissue structure and chemistry in a mummified hadrosaur from the Hell Creek Formation, North Dakota (USA). Proceedings of the Royal Society B 276: 3429–3437.

Martill, D.M. 1991. Organically preserved dinosaur skin: taphonomic and biological implications. Modern Geology 16: 61–68.

Maryańska, T. and Osmólska, H. 1981a. First lambeosaurine dinosaur from the Nemegt Formation, Upper Cretaceous, Mongolia. Acta Palaeontologica Polonica 26: 243–255.

Maryańska, T. and Osmólska, H. 1981b. Cranial anatomy of *Saurolophus angustirostris* with comments on the Asian Hadrosauridae (Dinosauria). Palaeontologia Polonica 42: 5–24.

Maryańska, T. and Osmólska, H. 1984. Postcranial Anatomy of *Saurolophus angustirostris* with comments on other hadrosaurs. Acta Palaeontologica Polonica 46: 119–141.

Murphy, N.L., Trexler, D., and Thompson, M. 2006. “Leonardo”, a mummified *Brachylophosaurus* from the Judith River Formation. In K. Carpenter (ed.)

Horns and Beaks: Ceratopsian and Ornithopods Dinosaurs. Indiana University Press, Bloomington, Indiana, pp. 117–133.

Norman, D. and Sues, H.-D. 2000. Ornithopods from Kazakhstan, Mongolia and Siberia. In: M.J. Benton, M.A. Shishkin, D.M. Unwin, and E.N. Kurochkin (eds.), The Age of Dinosaurs in Russia and Mongolia. Cambridge University press, Cambridge, UK, pp. 462–479.

Prieto-Marquez, A. 2010. Global phylogeny of Hadrosauridae (Dinosauria: Ornithopoda) using parsimony and Bayesian methods. Zoological Journal of the Linnean Society 159: 435-502.

Prieto-Marquez, A., Gaete, R., Gonzalo, R., Galobart, A., and Boada, M. 2006. Hadrosaurid dinosaurs from the Late Cretaceous of Spain: *Pararhabdodon isonensis* revisited and *Koutalisaurus kohlerorum*, gen. et sp. nov. Journal of Vertebrate Paleontology 26: 929-943.

Rogers, R.R. and Kidwell, S.M. 2007. A conceptual framework for the genesis and analysis of vertebrate skeletal concentrations. In R.R. Rogers, D.A. Eberth, and A.R. Fiorillo (eds.) Bonebeds: Genesis, Analysis, and Paleobiological Significance. University of Chicago Press, Chicago, Illinois, pp. 1–64.

Sternberg, C.M. 1953. A new hadrosaur from the Oldman Formation of Alberta, discussion of nomenclature. Canadian Department of Resource Development Bulletin 128: 275–286.

Varricchio, D. J. and Horner, J.R. 1993. Hadrosaurid and lambeosaurid bone beds from the Upper Cretaceous Two Medicine Formation of Montana: taphonomic and biologic implications. Canadian Journal of Earth Science 30: 997–1006.

Wegweiser, M.D., Breithaupt, B.H., Matthews, N.A., Sheffield, J.W., and Skinner, E.S. 2004. Quo vadis? Paleoenvironmental and diagenetic constraints on Late Cretaceous dinosaur skin from western north America. Sedimentary Record 2: 4–8.

CHAPTER 7

TAPHONOMY OF AN *EDMONTOSAURUS* (HADROSAURIDAE) BONEBED FROM THE HORSESHOE CANYON FORMATION, ALBERTA.

A future publication based on this chapter is anticipated to appear in PALAIOS by P.R. Bell and P.J. Currie under the same title.

Introduction

Bonebeds are an important source of paleontologic, paleobiologic, and taphonomic information (Straight and Eberth, 2002; Eberth, 2002a). The dinosaur bonebeds of southern Alberta, particularly in the Dinosaur Park Formation, are famous for their extent and number and have received much attention (Currie and Dodson, 1984; Visser, 1986; Ryan, 1992, 2003; Getty et al., 1997, 1998; Ryan and Russell, 2005; Eberth and Getty, 2005). In the Dinosaur Park Formation, all monodominant bonebeds are exclusively ceratopsid dominated. In contrast, the monodominant bonebeds from the slightly younger (late Campanian to early Maastrichtian) Horseshoe Canyon Formation are composed of hadrosaurids and have received only cursory attention in the literature (Ryan et al., 1995). Several *Edmontosaurus* bonebeds are known from the lower Horseshoe Canyon Formation. An *Albertosaurus* bonebed (Currie, 1998) and at least one undescribed *Hypacrosaurus* bonebed are also known from the upper units of the formation.

The Horseshoe Canyon Formation crops out in southern and central Alberta between Edmonton and Drumheller where they represent an overall regressive sequence dominated by parasequences and parasequence sets deposited during the final major regression of the Bearpaw Sea (Hamblin, 2004; Eberth, 1996, 2002b, 2004). To date, the majority of paleontological studies have focused on the lower 135 m (i.e. unit 1) of the Horseshoe Canyon Formation in the Drumheller area, where strata are widely and well exposed (Ryan et al., 1995; Baszio, 1997; Straight and Eberth, 2002; Straight et al., 2004). Hadrosaur-dominated bonebeds in this unit are associated with vertically-aggrading,

organic- to coal-rich mudstones and channel-dominated horizons in high-accommodation settings (Eberth, 2002a).

In the Edmonton region, exposures of the Horseshoe Canyon Formation are limited to localised areas of moderate relief and erosion, particularly along the banks of the North Saskatchewan River and its tributaries. Although dinosaur remains are relatively plentiful in this area, they have received virtually no attention in the scientific literature. From a taphonomic perspective, isolated bones dominate, although vertebrate microfossils, footprint localities, and at least one bonebed (described herein) are also present.

This study addresses the taphonomic history of an *Edmontosaurus* sp. bonebed from the mid-to-upper part of unit 1 in the Horseshoe Canyon Formation near Edmonton. This report provides the first formal description of hadrosaurid-dominated bonebed from the Horseshe Canyon Formation and helps advance the understanding of the genesis of these accumulations. Improved knowledge of such bonebeds also provides insight into the paleobiology of *Edmontosaurus*.

Excavation history of the Danek Bonebed

The Danek Bonebed (University of Alberta [UALVP] loc. # L2379) was discovered on March 31st 1989 by a local collector, Danek Mozdzenski. It occurs on the southern bank of Whitemud Creek, south of Edmonton, some 300 km north of the better-known Drumheller exposures (Fig 1A). Initial excavations in April of that year by the Royal Tyrrell Museum of Palaeontology led to the recovery of disarticulated and articulated remains from at least four hadrosaurs.

The large size of the bones and a single diagnostic frontal became the basis for identifying the animal as *Edmontosaurus.* This quarry is herein referred to as the *Edmontosaurus* Quarry.

In 2006, the site was reopened by the University of Alberta and a second quarry (Small Quarry) on the south bank was opened 55 m upstream of the original excavation. The following year, new exposures of the bone-bearing horizon between the two existing quarries were explored and a third quarry (Middle Quarry) was opened (Fig. 7.1B). Since 2006, excavations at these sites have been conducted each summer by crews from the University of Alberta and continue to supply a near inexhaustible supply of bones.

Geological Setting

Regional Geology

The Horseshoe Canyon Formation is the lowest member of the Edmonton Group forming an eastward-thinning, clastic wedge deposited during the final major regression of the Western Interior Seaway (Eberth, 2004). It overlies the marine Bearpaw Formation and is overlain by the Battle and Scollard Formations. In the Drumheller region, where it is best exposed, it is up to 275m thick and spans the period from approximately 73–67 Ma (Eberth, 2004). The Horseshoe Canyon Formation is equivalent to Units 4–5 of the Wapiti Formation in northwestern Alberta and the Blood Reserve and St. Mary River Formations in the southern Alberta (Fanti, 2007).

Eberth (2004) divided the formation into five informal units based mainly on the presence/absence of coals and sandstone stacking patterns: Unit 1 (Midland tongue of Hamblin, 2004) is 135m thick succession of channel sandstones, laterally extensive mudstones and well-developed coal seams (#0–9). It records the vertical transition from marine to non-marine deposited in a warm and wet paleoenvironment (Rahmani 1989, Ainsworth, 1994; Eberth, 1996, 2002b, 2004; Hamblin, 2004). Unit 2 is 30m thick and contains coal #10 and the Drumheller Marine Tongue. A bentonite layer just above coal #10 revealed an age of 70.44±0.17 Ma, which is roughly equivalent to the Campanian-Maastrichtian boundary (Eberth and Deino, 2005). Units 3 and 4 are non-coaly intervals that grade from channel sandstone-dominated (Unit 3) to sub-equal paleochannel-overbank ratios (Unit 4). The paleoclimate for Units 2–4 is interpreted as cool and dry. Unit 5 is dominated by thick channel sandstones, extraformational pebbles, and contains coal seams #11 and 12 thus recording a return to wetter but cool environment.

Local Geology

The geology at L2379 is well exposed along the southern river bank directly below the excavations. The stratigraphic section, up to six metres thick, can be divided into seven easterly-dipping, Cretaceous-age horizons (A–G) plus one overlying Quaternary horizon (H) (Fig. 7.2).

The lowest horizon in the section is an immature coal seam (horizon A), which is only observable when water levels on Whitemud Creek are low. Eberth (unpub. data) places the coals in the south of Edmonton at the level of coal seams

#6 or #7 (Weaver coal zone) in the Drumheller region. This correlation places the bonebed and associated deposits within the mid- to-upper part of Unit 1.

Overlying horizon A is a bench-forming sandstone (horizon B). This horizon preserves low-angle, tangential cross bedding and conformably overlies horizon A. It is directly overlain by a 40 cm thick mudstone horizon (C). Rare planar laminations and minor sandy lenses are interrupted by common root traces and soft-sediment deformation structures.

The transition between horizon C and D is marked by a thin, fine-grained sandy layer that is the first of several sandy lenses between intervening mudstone layers. Rare, poorly-defined planar laminations are the only indication of geometry in the sandstones. Root traces and vertical, unbranched invertebrate burrows are common. The entire horizon is approximately 90 cm thick and grades into horizon E, which is differentiated by the lack of sandy interbeds. Horizon E is a 145 cm thick planar-laminated sandy claystone. *In situ* root traces are abundant. Soft-sediment deformation is evidenced from slickensides and ball-and-pillow structures.

Horizon F conformably overlies Horizon E and consists of an alternating succession of interbedded very-fine sandstone-siltstone couplets. Individual strata range from millimetre- to centimetre-scale laminae at the base, and become increasingly thicker (multi-centimetre thick beds) toward the top of the succession. At the top of the horizon, modern pedogenic features have overprinted and obscured sedimentological information. Laminar beds at the base are replaced by long-wavelength ripples at the top of the horizon. Organic fragments (stems, seeds, leaf fragments) are abundant in the mudstone interbeds and can be seen on bedding surfaces in hand samples. Burrows and roots often

intersect several interbeds at a time. Horizon F is up to 80 cm thick but it is almost completely truncated by down cutting of the bone layer (horizon G) where the bone layer is at its thickest.

Horizon G is a black, highly fissile, organic-rich siltstone that is the bonebed host unit. Because of the dip of the entire stratigraphic section in relation to the modern topography, the unit is approximately 70 cm thick at the Small Quarry but over 200 cm thick at the *Edmontosaurus* Quarry. These sediments take on a reddish hue when exposed at the surface. Downcutting by the overlying Quaternary horizon has completely removed parts of horizon G giving the false impression that it is composed of several lenses. Exposures of horizon G are traceable for over 70 m downstream where it is eventually lost under vegetation. No indication of bedding or flow direction is observable from the sediments in outcrop or in thin section. Minor inclusions of amber up to 5 mm across and charcoal fragments up to 30 mm were observed; however, there is no evidence of scorching on the bones. Plant fragments and coalified logs up to and exceeding 20 cm in diameter are common and found in close association with the bones. Abundant hadrosaurid bones at the base of this horizon are normally graded through the lower 50 cm of horizon G. 'Suspended' bioclasts (bones and teeth) are up to approximately 15 cm in greatest dimension and orientations ranged from horizontal to steeply plunging. Bones at the base of the horizon are horizontal, measuring up to and exceeding 120 cm in length, and show no preferred orientation (see results). Slickensides frequently form in the sediments around bioclasts.

Handsamples were taken from the base of horizon G in close association with fossil bones in each of the three excavation sites (Fig. 7.3). Each displays

randomly- oriented organic fragments, which range from millimetre-to-decimetre in length. Millimetre-to-centimetre scale amber fragments and angular clay clasts are found dispersed throughout the matrix. Although organic detritus sometimes displays a laminar fabric, vertical- and subvertically oriented fragments are also present in the same samples, which can be attributed in some cases to root traces and invertebrate burrows (M. Gingras, personal communication, 2010). Other bedding structures (e.g. cross stratification, ripple cross laminations, laminar stratification) are absent. Pedogenic structures such as peds and soil horizons are also absent.

The bone layer is erosionally and unconformably overlain by a poorly sorted and unlithified Quaternary horizon (H) up to 56 cm thick. Rip-up bioclasts of hadrosaur bones in this layer are horizontally-to-vertically oriented and can occasionally be recombined with the remainder of the bone from horizon G.

Environmental Interpretation

The Cretaceous section preserved at L2379 records a fining-upwards succession between horizons B–E. Warm and wet conditions permitted peat formation in the lowest part of the succession during which time vegetation must also have been abundant (McCabe, 1984). The low-angle cross beds of horizon B are interpreted as a downstream migration of channel dunes in an upper flow regime (Boggs, 2001). Horizon C and E represent deposits furthest from the channel as evidenced by the small grain size and laminar bedding. Root traces and invertebrate burrows indicate primary colonisation was possible intermittently following deposition of these beds.

The pattern of alternating sandstone and siltstones in horizons D and F record fluctuations in fluvial influence on the floodplain. Long ripple wavelengths in horizon F indicate high flow velocities associated with the deposition of sandstone interbeds. Root traces and invertebrate burrows indicate colonisation by terrestrial biota occurred in between periods of inundation. Both units are interpreted as proximal floodplain deposit recording periods of intermittent bank avulsions (crevasse splays; Boggs, 2001). The vertical increase in thickness of individual sandstone beds in horizon F represents a progressively closer proximity to the fluvial system.

Coalified logs and plant detritus in horizon G indicate the area was well vegetated. Oxygen levels were low (dysoxic), as evidenced by coal formation and well-preserved dinosaur bones (McCabe, 1984). The fine-grained, organic-rich sediments of horizon G are interpreted as an overbank deposit. It cannot be excluded that horizon G represents a stacked mudstone sequence in which bedding planes were overprinted by bioturbation. Uniform weathering and abrasion values indicate burial of vertebrate remains occurred in a single event (Behrensmeyer, 1991; see Results section). Small bones and bone fragments 'suspended' within the matrix imply reworking of bioclasts by a sediment-laden and semi-cohesive fluid that prevented settling of entrained particles (Boggs, 2001; Gangloff and Fiorillo, 2010). Petrographic sampling suggests an intrabasinal provenance for the sediments in horizon G. The apparent pinching out of this horizon up-dip (i.e. to the west) is more than likely affected, or at very least enhanced, by the erosional nature of the overlying horizon H.

Materials and Methods

The standardised taphonomic procedure developed by Behrensmeyer (1991) and advocated by Eberth et al. (2007) and Blob and Badgley (2007) is followed. Taphonomic data are grouped into three broad categories; assemblage data, quarry data, and bone modification (Table 1) and each subcategory was assessed as per outlined by Behrensmeyer (1991).

Specimen counts follow definitions adapted from Badgley (1986) and Blob and Badgley (2007) where a specimen is defined as a single, partial or complete bone or tooth fragment regardless of degree of articulation. In this definition, fused bones (e.g. a neural spine attached to a centrum) are regarded as a single 'specimen', however, if they are unfused and lying separate to each other, they are considered as two specimens. Similarly, a fused sacrum would be counted as one specimen but an articulated series of five vertebrae for example, would be recorded as five specimens. A 'body part' is an articulated series of bones and may comprise a number of specimens e.g. forelimb, pes, caudal series. All recovered bone fragments (down to ~10 mm in greatest dimension) were also mapped and counted, regardless of size or preservation quality.

Minimum number of individuals (MNI) and number of identified specimens (NISP) were used for abundance counts (Badgley, 1986; Blob and Badgley, 2007). MNI was calculated from the lengths of right femora. Left femora were included if they were differed in length by more than 50mm from the nearest-sized right femur. Two tibiae were also included as they did not correspond to the expected femur-tibia length ratio for any of the collected femora.

Skeletal representation is often measured using Voohries (1969) groups; however, use of this method has been criticised for many extinct groups (especially dinosaurs) regarding the hydraulic equivalence between the study taxon and the taxa that were used in flume experiments to determine these categories (Eberth et al., 2007; Britt et al., 2009). Nevertheless, the bones of large and small animals differ enough in relative dispersal as to allow segregation of traditional Voohries groups (Behrensmeyer, 1975), and it is the proportion of (rather than absolute values) these groups that is of relevance (Ryan, 2003; Ganloff and Fiorillo, 2010). Behrensmeyer (1975) has demonstrated these categories hold for hippopotami, whose bones approximate those of large ornithischians. This assumption has been successfully applied to a number of North American dinosaur bonebeds (Lehman, 1982; Ryan, 1992, 2003; Ralrick and Tanke, 2008; Gangloff and Fiorillo, 2010). This method is followed here and represented graphically as a ternary plot (Fiorillo, 1988).

Patchiness was calculated using Lloyd's (1967) index of patchiness, which can be defined as:

$$\text{Patchiness} = \text{Mc}/\text{Md}$$

where *Mc* (Lloyds crowding index) is calculated as:

$$\text{Mc} = \text{Md} + ([\sigma^2/\text{md}]-1)$$

where *Md* is the mean density, and o^2 is the variance within the sample set. Variance is defined as:

$$\sigma^2 = [\Sigma\ (\alpha\text{-}x)^2]/n$$

where α is any value in a set of values for which the variance is being found, x is the mean of those values, and n is the total number of values in that set. Where

patchiness is ≤1, distribution of elements is random. If there is clumping of elements, patchiness >1. For the *Edmontosaurus* Quarry, the TMP and UA excavations were considered together. Quadrats with no bones were omitted as they all fell at the edges of the quarries and were considered incompletely excavated at the time of writing.

Individual bones were ranked using Behrensmeyer's (1978) stages for weathering following revision by Fiorillo (1988) and the abrasion series developed by Fiorillo (1988) was used. Readers are referred to these references for a full explanation of these techniques.

Orientation data was measured directly from the bonebed maps and the rose diagrams and associated statistics were calculated using GEOrient 9.2 (Holcombe, 1994). Dip data was not included because elements were predominantly horizontal; however, plunge was noted where elements deviated from this pattern.

Results

Assemblage Data

Sample size.—306 specimens were analysed, including unidentifiable fragments, teeth and partial-to-complete bones.

# of individuals.—At least nine individuals are present in the bonebed (eight *Edmontosaurus* and one tyrannosaurid) (Table 2). The tyrannosaurid *Albertosaurus* is represented by a single right maxilla (TMP 1989.17.53, Fig. 7.4). A partial ectopterygoid (TMP 1989.17.51) and distal caudal vertebra

(UALVP50965), all of which were recovered from the *Edmontosaurus* quarry, may be part of the same individual.

# of species.—At least three vertebrate taxa are present in the assemblage. *Edmontosaurus* sp. is identified based on a large hadrosaurine frontal (TMP 1989.17.45, Fig. 7.5) and all other hadrosaur material conservatively follows this diagnosis. Tyrannosaurid elements are attributable to an adult individual of *Albertosaurus* cf. *A. sarcophagus*. Shed tyrannosaurid teeth and rare skeletal components (TMP 1989.17.51, UALVP50965) are tentatively also identified as *Albertosaurus* sp. A single shed velociraptorine tooth was recovered during preparation; however it was unfortunately lost before it could be catalogued. No other vertebrate microfossil remains (turtles scutes, fish scales etc.) were recovered.

Relative abundance.—The frequency of the remains of hadrosaurs and theropods based NISP is approximately 6:1 and 8:1 for MNI. Shed tyrannosaurid teeth (cf. *Albertosaurus*) contributed to the inflation of tyrannosaurid NISP.

Body size.—Although no complete skeletons have been recovered, a fully grown *Edmontosaurus*, as represented by the largest femur (UALVP47920), probably reached 12 m in length and weighed approximately three metric tonnes (Paul, 1997). The smallest femur (UALVP431343) is 40% of the length of the largest femur and is estimated to have come from an animal approximately two metres long.

Age spectrum (Demographics).—Based on hadrosaur tibiae and femora (Table 2), five of the eight individuals fall within 'subadult' size (femur length, 700–1099 mm) category; one juvenile (femur length <699 mm) and two adults

(femur length >1010 mm) are also present. Insufficient data exist to create a statistically significant demographic profile for the Danek Bonebed.

Bone articulation.—Only a single body part was found in articulation; TMP 1989.37.1 is an articulated series of four mid caudal vertebrae including both neural spines and haemal arches. A partial skeleton (TMP 1991.63.1) was noted in the collection records of the TMP, but the jacket has never been opened to verify this, and there is no indication from the quarry maps to suggest articulation.

Skeletal parts (Voohries groups).—A Voohries grouping of the skeleton of *Edmontosaurus* is given in Table 3. Voohries groupings from the bonebed were plotted on a ternary diagram (Fig. 7.6), which shows an apparent enrichment in VG III elements from all three quarries. A χ^2 goodness of fit statistical test demonstrates that this enrichment is statistically significant; however, this analysis did not take into account the numerous unidentifiable fragments collected from the bonebed.

The maximum lengths of individual bones were measured (irrespective of completeness or preservation quality) in order to evaluate the size distribution of specimens within the assemblage. Figure 7 shows that over half of specimens are less than 10 cm in maximum dimension, and most are fragmentary (see section on bone modification).

Quarry Data

Size of accumulation.—Based on the extent of outcrop and the positions of the current excavations, the total bonebed area is estimated to be a minimum of

400 m^2. The total excavation area (57 m^2) from which a MNI of nine individuals have been recovered suggests approximately 70 individuals may be present in the assemblage.

Spatial Density.—In plan view, the Small Quarry has a maximum bone density of 14 bones/m^2 with a mean of 7.7 bones/m^2. Individual quadrats range from 0-14 bones/m^2 (Fig. 7.8); however quadrats devoid of or with only one bone were conspicuously along the edge of the quarry or were not fully excavated and therefore excluded from statistical analysis. The Middle Quarry has maximum values of 14 bones/m^2 with a mean of 8.25 bones/ m^2. At the *Edmontosaurus* Quarry, individual quadrats exhibit bone densities up to 22 bones/m^2. 78% of quadrats have between one and ten bones with an overall mean of 4.8 bones/m^2.

Spatial Arrangement.—Results for spatial arrangement were considered in three perspectives; plan view, profile, and patchiness.

i. In Plan View. The orientations of bones with a distinct long axis were measured directly from the quarry maps (Fig. 7.9). Polarity was not included. Orientations of 36 bones from the Small Quarry and 58 bones from the Middle Quarry had a mean resultant trend of 136-316° and 30-210°, respectively (Fig. 7.10).

Orientation of bones from the *Edmontosaurus* Quarry were tabulated separately for the UALVP (n=24, Fig. 7.10C) and TMP (n=87, Fig. 7.10D) collections due to the absence of compass bearings on the TMP maps. An approximate northing was used for the TMP maps, which does not alter the circular variance. Mean resultant direction for the two datasets are 155-335° and 21-201°, respectively.

ii. In profile. Bones were recovered from the lower part of horizon G in all three quarries with a notable concentration of large elements (decimeter scale or larger) at, or close to the base. Smaller bones and fragments (<10cm) were normally graded and were found up to 50cm above the base of that horizon. Although dip data were not recorded during excavation, most bones showed no obvious plunge; however, specimens that sat relatively high in section (i.e. usually smaller, graded bones and bone fragments) were often steeply-inclined. Several worn bones were also found in the overlying horizon H where it had down cut the bone-bearing horizon.

iii. Patchiness. Patchiness values for the *Edmontosaurus*, Small, and Middle Quarries, respectively, were 1.50, 1.06, and 1.23.

Bone Modification

Breakage.—Complete bones within the entire assemblage are rare; the majority of the assemblage being made up of fragmentary and partial bones (Fig. 7.11). Complete bones are most common at the *Edmontosaurus* Quarry; however it is likely this is a consequence of collecting bias within the TMP collection, as taphonomically important fragments were probably not collected.

Despite the preponderance of broken bones, greenstick (spiral) fractures could only be confidently attributed to two specimens (UALVP48031, UALVP48979). Nearly all breakages occurred after death, as evidenced by their irregular surfaces (Currie and Dodso, 1984; Lyman, 1994; White and Folkens, 2005). Greenstick fractures are conspicuous on even the largest bones (e.g. femora, ilia) of very large, or adult individuals.

Weathering.—Homogenous weathering stages across several individuals from a bonebed are a good indication of both autochthony and relatively sudden death of a group of animals (Behrensmeyer, 1991). Over 90% of all specimens from each quarry showed no sign of weathering (rank 0; Fig. 7.12) suggesting bones were rapidly interred (< 1 year, Behrensmeyer, 1978).

Abrasion/polish.—Low levels of abrasion (ranks 1–2, Fiorillo, 1988) were found throughout the bonebed at each quarry (Fig. 7.13). The degree of rounding exhibited by a bone is often cited as product of hydraulic intensity and the distance travelled generally as a result of fluvial or marine reworking (e.g. Christians 1992, Laudet and Antoine 2005); however, it has been demonstrated that bones and teeth can undergo extensive transport with a minimum of abrasion (Argast et al., 1987; Bartlett et al., 2003). In fact, abrasion may be more indicative of sediment grain size and weathering state (Bartlett et al., 2003) or trampling (Brain, 1967). As such, abrasion still provides a measure of the time or intensity of reworking. 97% of the assemblage at the Danek Bonebed specimen showed low levels of abrasion.

Bite marks.—Predation traces are common at L2379 and consist almost entirely of tooth gouges, parallel tooth marks, and serration traces (Fig. 7.14). Bite marks were recorded on 24.5% of specimens; tyrannosaurs accounting for well over half (62.7%) of these marks. Incidence of tyrannosaur versus small theropod feeding traces was consistent across the three quarry assemblages, although bones from the Middle Quarry experienced lower overall degree of scavenging (Fig. 7.15). Ribs suffered the most damage (n=19) followed by tendons (n=8) and unidentified bone fragments (n=8) (Fig. 7.16). Serration scoring on one ossified tendon fragment (UALVP47896, Fig. 7.14B) was measured. Individual serrations

measure 0.415 mm in diameter (~2.4 denticles/mm) and are broadly U-shaped corresponding to the denticle morphologies of *Dromaeosaurus albertensis* or juvenile tyrannosaurs (Currie et al., 1990). Eight specimens exhibited bite marks from both large and small theropods consistent with sequential feeding patterns in modern scavengers (Gomez et al., 1994). One dentary (UALVP47919) shows numerous parallel and sub-parallel tooth marks from a small theropod below the coronoid process on its lateral surface (Fig. 7.14D).

Parallel striae.—Parallel striae is the term used here to define scoring derived from a sedimentary source. Parallel striae characteristically form when a bone is pressed into the substrate (bioturbation) causing individual grains to abrade the surface of the bone (Behrensmeyer et al., 1986; Fiorillo, 1988, 1989). 60% of the entire assemblage (not including teeth) shows parallel striae. Multiple episodes of trampling/abrasion are apparent from 'overprinting', where distinct series of parallel striae intersect with other series of parallel striae.

Discussion

The remains of at least eight *Edmontosaurus* and one tyrannosaurid were deposited on a periodically inundated floodplain represented by horizon F. Aslan and Behrensmeyer (1996) have demonstrated that bones, once introduced into a stream channel, are rarely redeposited on the floodplain, therefore the animals presumably died at or near their present location. Lack of preferential alignment may result from insufficient flow velocity or taphonomic overprinting (e.g. scavenging/trampling, Fiorillo 1989, Rogers and Kidwell 2007). Aquatic vertebrates (e.g. champsosaurs, turtles, crocodiles, fishes) are conspicuously

absent from the deposit, again suggestive that the remains were not washed in from a fluvial or marine source (Fastovsky et al., 1995).

Age class distribution is usually an important indicator of the mode of accumulation (i.e. mass mortality or attrition). All size classes of hadrosaur were recorded except for hatchling-sized animals, ranging from ~2–12 metres in length. The preponderance of mid-sized animals ('subadults') at the Danek Bonebed is suggestive of a single mass mortality event of a life assemblage (Lyman, 1994), although it is acknowledged that the MNI is too small to be statistically robust. Support for a non-selective mechanism can also be found in the mixed faunal composition (hadrosaurs and tyrannosaurs), which illustrates that the cause of mortality was not restricted to herbivorous animals (Behrensmeyer, 1991). Rare greenstick fractures indicate a traumatic perimortem history for some animals; however, injury does not appear to be the main cause of fatality for the group. The uniformly low weathering ranks (rank 0) from all three quarries suggest that the time between death and burial was limited. Eberth et al. (2007) summarised the problem of equating weathering stages with a set time interval because of the complex interplay of environmental and climatic conditions. Instead, it can only be inferred that exposure time was relatively brief and that all other biostratinomic processes must have occurred during this period.

Carcasses were heavily scavenged by tyrannosaurids and small theropods prior to the deposition of horizon G as evidenced by common shed teeth and the high incidence of tooth-marked bones. Bite marks were encountered most commonly on ribs and fragments of ossified tendon indicating that theropods were feeding primarily on the viscera and muscles along the spine and tail. A

recurrent feature of very large bonebed accumulations (hundreds to thousands of individuals) is uniformly low incidences of bitemarks (Christians, 1992; Eberth and Getty, 2005; Ryan and Russell, 2005; Ralrick and Tanke, 2008; Gangoff and Fiorillo, 2010). Gangloff and Fiorillo (2010) suggested that the overwhelming number of carcasses preserved in such deposits diluted the effect of scavengers. This may explain the relatively common feeding traces on bones at the Danek Bonebed, that is, the Danek Bonebed is a smaller assemblage and the effects of scavenging are therefore more obvious. The same may be assumed for a second *Edmontosaurus* bonebed from the Horseshoe Canyon Formation near Drumheller where approximately 50% of bones show evidence of scavenging (Ryan et al., 1995). The high incidence of bite marks on broken tendons and unidentifiable bone fragments at the Danek Bonebed suggests scavenging also played an important role in the disarticulation and breakage of skeletons. While most greenstick fractures, abrasion, and parallel striae occurred from trampling by scavengers (e.g. tyrannosaurs), it is conceivable that fractures and abrasion were also incurred during the deposition of horizon G; however, this cannot be demonstrated conclusively. The forces required to break the largest elements in the assemblage such as femora and ilia would clearly have been substantial (McGowan, 1999) and trampling is the most plausible agent.

The statistically significant enrichment of Voohries group III elements is indicative of (selective) removal of smaller, more easily transported specimens, but it is acknowledged that this analysis did not take into account the large number of small, fragmentary and often unidentifiable bones, which dominate the entire assemblage. The large numbers of small fragments, which are found alongside the largest and least damaged bones, more likely indicate that

trampling and fragmentation of specimens was most effective on smaller (Voohries groups I and II) bones and/or some winnowing took place prior to the fragmentation of the remaining specimens (Eberth and Getty, 2005). Selective transport by scavengers is another, but untestable, possibility.

While patchiness values indicate clumping of specimens within both the Middle and *Edmontosaurus* Quarries, there is no direct evidence that these represent associations of bones from single individuals. Furthermore, these values may be influenced by low bone counts within incompletely excavated quadrats, whereas the random arrangement of bones in the Small Quarry was calculated from completely excavated subset of quadrats (as controlled by the author during excavation) and is probably more representative of the entire deposit.

With the exception of a series of four caudal vertebrae (TMP 1989.37.1), all specimens were found disarticulated. In some environments, disarticulation of a skeleton occurs fairly rapidly after death (between weathering stages 0-2, or 0-6 years) although small or juvenile animals may be disarticulated more quickly (Hill and Behrensmeyer, 1984). This process is expedited under fluvial conditions (Varricchio et al., 2005). Low weathering rates, however, indicate that burial probably occurred within 12 months of death.

Rapid disarticulation was probably achieved by a combination of predation/scavenging, trampling, and final burial as already discussed. The hypothetical sequence of sedimentation, mortality event, and final deposition is shown in figure 17.

Comparison With Other Bonebeds

Hadrosaur bonebeds are a relatively common taphonomic feature of Late Cretaceous strata in North America. Monodominant *Edmontosaurus* bonebeds occur throughout the Western Interior from the North Slope of Alaska to South Dakota and Wyoming; however, the majority of published accounts provide only preliminary data (Christians, 1992; Derstler, 1995; Ryan et al., 1995; Eberth, 2002a; Colson et al., 2004; Chadwick et al., 2005; Gangloff and Fiorillo, 2010). In all reported cases (including the Danek Bonebed), these represent intrinsic biogeneic concentrations (Rogers and Kidwell, 2007) of life assemblages that reflect gregarious behavior of up to 10 000 individuals or more (Christians, 1992; Chadwick et al., 2005). In addition, *Edmontosaurus* bonebeds have only been reported within overbank mudstones. Similar intrinsic biogenic concentrations are known for both hadrosaurines (*Brachylophosaurus* [Larock et al., 2000], *Prosaurolophus* [Rogers, 1990; Varricchio and Horner, 1993], *Maiasaura* [Varricchio and Horner, 1993], *Saurolophus* [Bell, unpub. data]) and lambeosaurines (*Hypacrosaurus* [Bell, unpubl. data], *Charonosaurus* [Godefroit et al., 2001], *Amurosaurus* [Lauters et al., 2008], *Sahaliyania* [Godefroit et al., 2008]) suggesting gregariousness was widespread among the Hadrosauridae (Varricchio and Horner, 1993); however, taphonomic modes vary widely. From a taphonomic perspective, the Danek Bonebed is most similar to the temporally equivalent Liscomb Bonebed from the Prince Creek Formation (late Campanian-Maastrichtian) of Alaska (Gangloff and Fiorillo, 2010). Both bonebeds were formed as a result of intrinsic biogenic accumulations of skeletal remains on a fluvially-dominated floodplain, which remained exposed for a relatively short

period before being interred in overbank muds. Bones are disarticulated, primarily fragmentary, randomly oriented, and normally graded within the matrix as a result of viscous flow. Moreover, hadrosaur teeth are virtually absent in both sites whereas theropod teeth are relatively common. The Liscomb Bonebed differs in that it is: (1) a larger accumulation (~3500 m^2; MNI=36 but may contain thousands of individuals); (2) enriched in Voohries' Group III elements; (3) dominated by juveniles; (4) less heavily scavenged and abraded; (5) and preserved within a relatively thin host unit.

Laterally extensive and prolific ceratopsian bonebeds in southern Alberta, significantly from the Campanian deposits of Dinosaur Provincial Park (DPP), are comparatively well-studied where both sandstone- and mudstone-hosted bonebeds are common (Ryan et al. 2001, Eberth and Getty 2005). In DPP, nine of the twenty known bonebeds are mudstone hosted, while the remainder are associated with channel sandstone deposits. Of the nine mudstone-hosted bonebeds, eight are associated with overbank mudstones and one occurs in a splay deposit (Getty et al., 1997, 1998; Ryan, 2003; Eberth and Getty, 2005). All other reported bonebeds from western Canada have been cited as fluvial in origin or have not yet received adequate taphonomic treatment (Ryan et al., 1995; Ryan, 2003; Ryan and Russell, 2005; Fanti and Currie, 2007; Currie et al., 2008; Ralrick and Tanke, 2008).

Notable similarities in taphonomic (particularly sedimentary) signature between the mudstone-hosted bonebeds of DPP and the Danek Bonebed are apparent. All share (1) organic-fragment-rich sandy claystone to siltstone host sediment; (2) the lower boundary surface of the host deposit is sharp and sometimes contorted; (3) matrix is massive to contorted throughout; (4) fossil

remains are normally graded; (5) bones are typically horizontal but occasional steeply inclined bones are present; (6) in all but one bonebed (BB030), bones are randomly oriented; (7) enrichment of large (VG III) specimens; and (8) skeletons are completely disarticulated. Similar levels of weathering and abrasion are also present in both deposits. The Danek Bonebed, however, does differ in some aspects: (1) large trees are found in association with bones; (2) absence of rooting structures in the host unit; (3) the host unit is appreciably (75%) thicker than the thickest bonebed deposit in DPP; (4) low number of greenstick fractures; and (5) abundant feeding traces. The thickness of the bonebed host horizon at L2379 (up to 2 m) does not comply with trampling as a cause of grading of bioclasts (as is the case in DPP; Ryan et al. 2001, Eberth and Getty 2005) as they are simply too deep. Given both diagenetic compaction (Perrier and Quiblier 1974) and the erosional upper boundary, 2 m should be regarded as a minimum estimate of the original thickness of horizon H. The vertical thickness through which bioclasts are distributed (i.e. the basal 50 cm) is similarly conservative. A fluvial origin to grading at the Danek Bonebed is therefore most likely.

Conclusions

The Danek Bonebed is interpreted as a catastrophic death assemblage of a herd of least eight *Edmontosaurus*. Extrapolation over the total estimated area of the bonebed suggests more than 70 individuals may be present in the taphocoenosis. Cause of death is equivocal but the demographic spread, taxonomic composition, uniform abrasion and weathering ranks, and rare greenstick fractures are all indicative of a single, non-selective, mass-mortality

event. Carcasses amassed on a vegetated floodplain and remained exposed to scavengers and other subaerial processes for up to a year. Scavenging by both large and small theropods contributed significantly to the disarticulation, fragmentation and possibly also selective removal of body parts. The effect of scavenging was probably amplified as a result of the relatively small size of the thanatocoenosis. Incipient but common abrasion and parallel striae suggests trampling (presumably also by scavengers) was also important in the disassociation and break-up of skeletons. Soft-part deterioration appears to have been virtually complete prior to entombment. The remaining skeletal debris was buried within a semi-cohesive flow more viscous than typical flood deposits, crevasse splays or interchannel ponds and lakes (Gangloff and Fiorillo, 2010). Small bones and fragments were entrained within sediment-laden floodwater that prevented settling out offollowing quiescence of the flow.

Although bonebeds are not a ubiquitous taphonomic feature of hadrosaurids, considerable evidence suggests that members of both Hadrosaurinae and Lambeosaurinae were gregarious from time to time, forming herds many thousands strong. The Danek Bonebed shares similar taphonomic signatures with the Liscomb Bonebed and mudstone-hosted ceratopsid bonebeds from Dinosaur Provincial Park suggesting a common mechanism of preservation. Comparison with other published descriptions of *Edmontosaurus* bonebeds from the Western Interior of North America reveals that these animals were periodically subject to mass kills of up to thousands of individuals and frequently preserved in overbank flood deposits.

Figure 7.1. A. Locality map of Alberta showing the extent of the Horseshoe Canyon Formation (grey). The Danek Bonebed lies within the city limits of Edmonton; B. Photograph looking east-southeast at the south bank of Whitemud Creek showing the relative positions of the three quarries (arrows). From left to right: *Edmontosaurus* Quarry, Middle Quarry, Small Quarry. Note person in Small Quarry for scale.

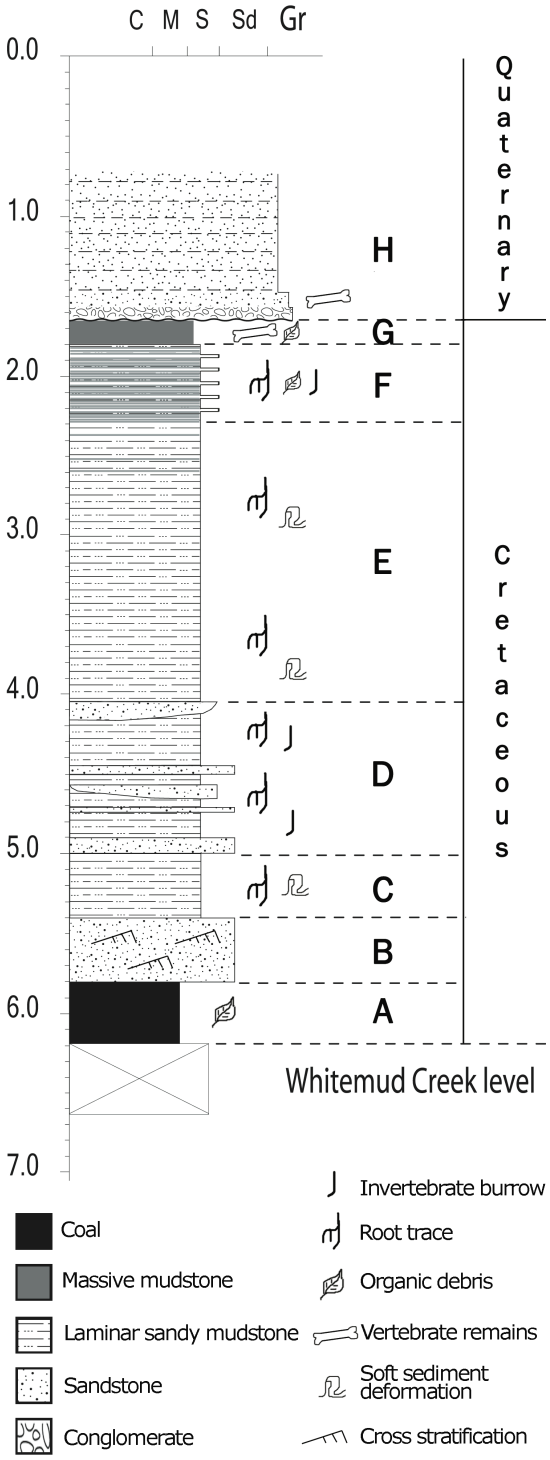

Figure 7.2. Stratigraphic section of the Small Quarry at the Danek Bonebed. Deposits were subdivided into discrete horizon (A–H) based on lithology and depositional environment. Scale is in metres.

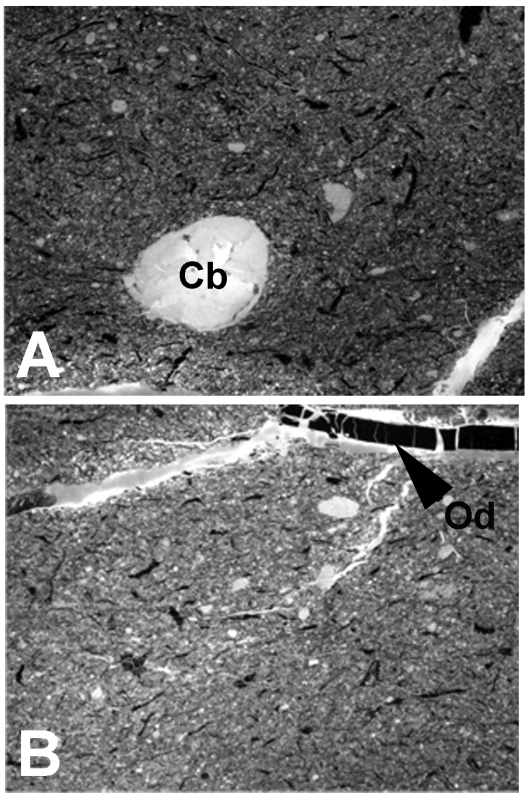

Figure 7.3. Petrographic thin-sections of horizon G from the *Edmontosaurus* Quarry (A), Middle Quarry (B), and Small Quarry (C). Cb, clay ball; Od, organic debris. Field of view = 15 mm.

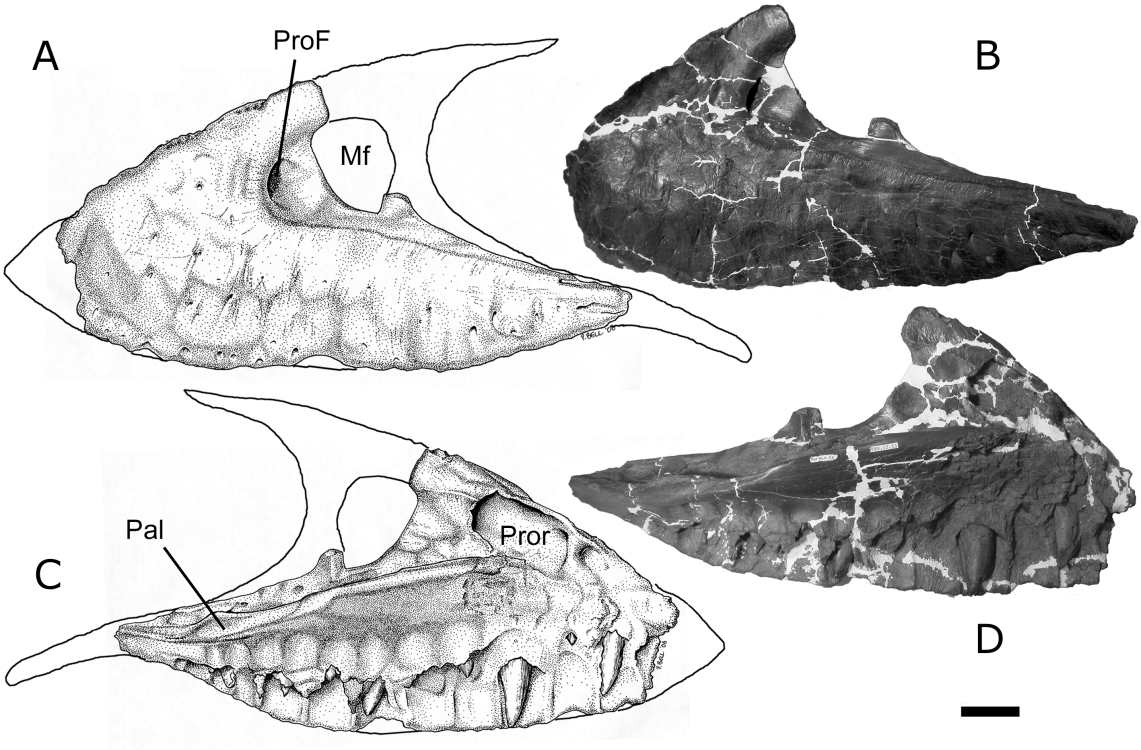

Figure 7.4. *Albertosaurus* sp. maxilla (TMP 1989.17.53) from the *Edmontosaurus* Quarry in lateral (A, B) and medial (C, D) views. Mf, maxillary fenestra; Pal, palatal shelf; ProF, promaxillary fenestra; Pror, promaxillary recess. Scale = 5 cm.

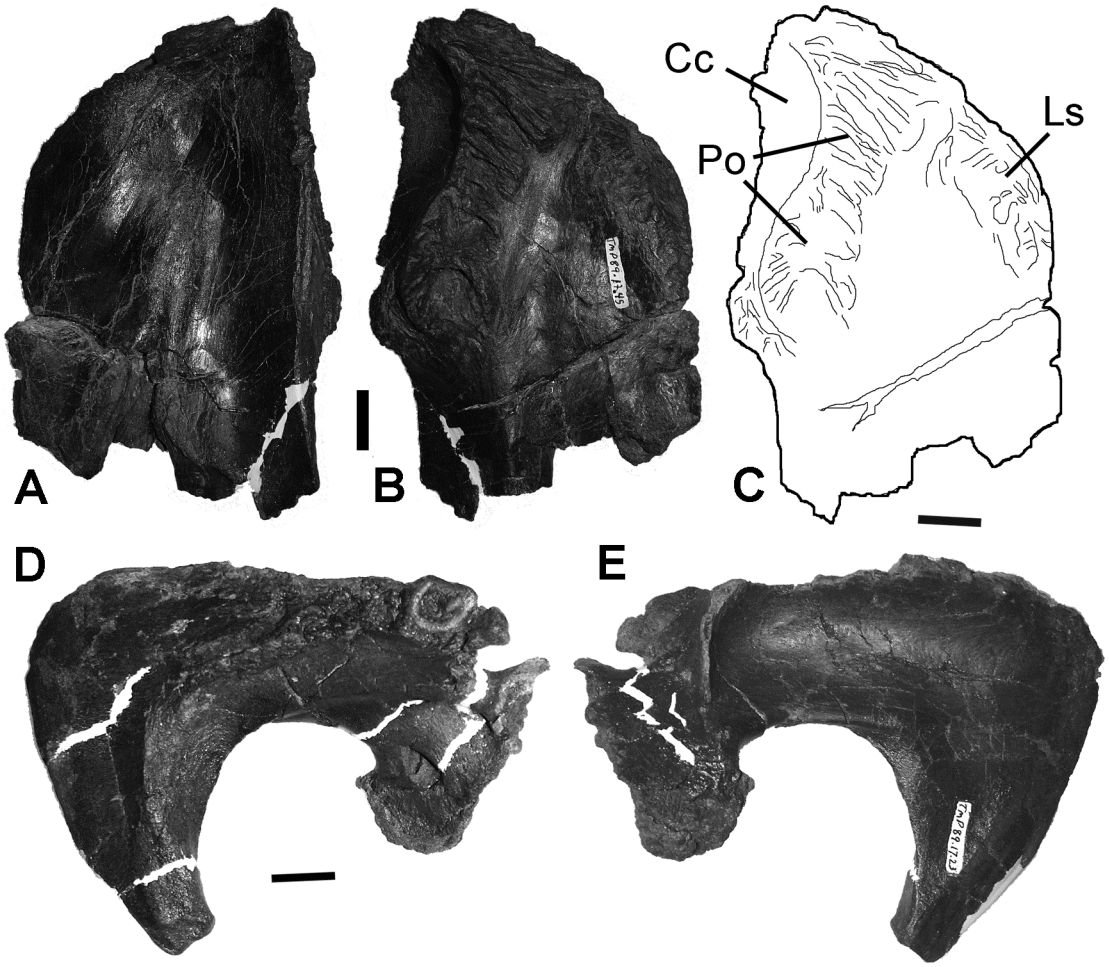

Figure 7.5. Cranial elements of *Edmontosaurus*. Frontal (TMP 1989.17.45) in dorsal (A) and ventral (B) views. C. interpretive drawing of B. Exoccipital (TMP 1989.17.23) in rostral (D) and caudal (E) aspects. Scale = 2 cm.

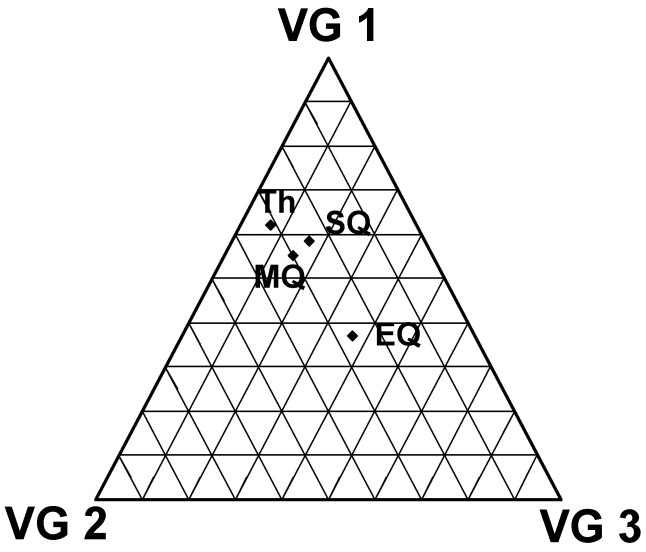

Figure 7.6. Ternary plot of Voohries group distributions in the Small Quarry (SQ), Middle Quarry (MQ), and *Edmontosaurus* Quarry (EQ) compared to the theoretical value (th) of complete *Edmontosaurus* skeleton as calculated from Table 3.

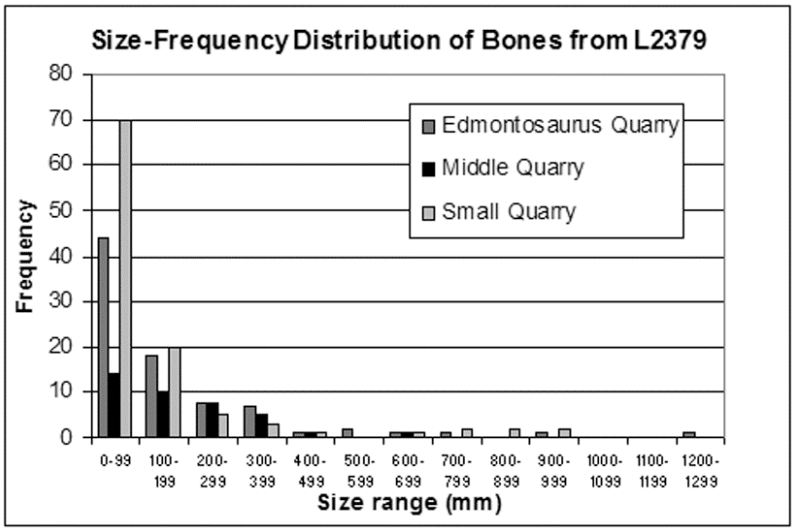

Figure 7.7. Size-frequency distribution of bones from L2379.

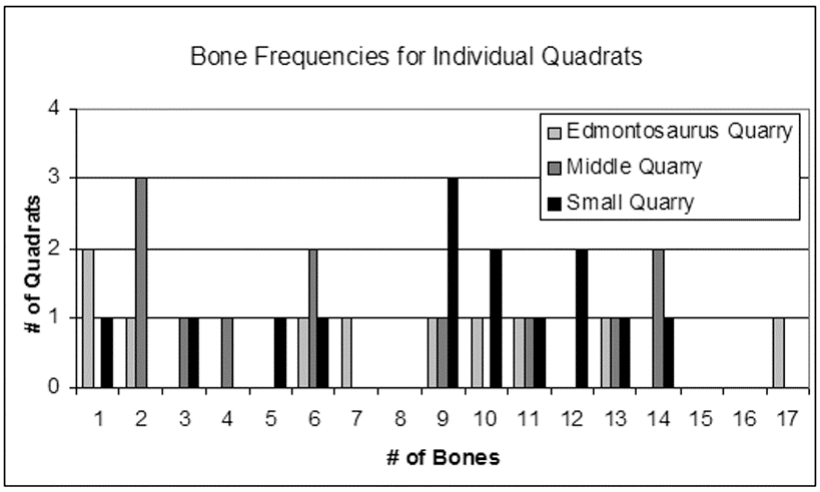

Figure 7.8. Bone frequencies measured for individual quadrats from L2379.

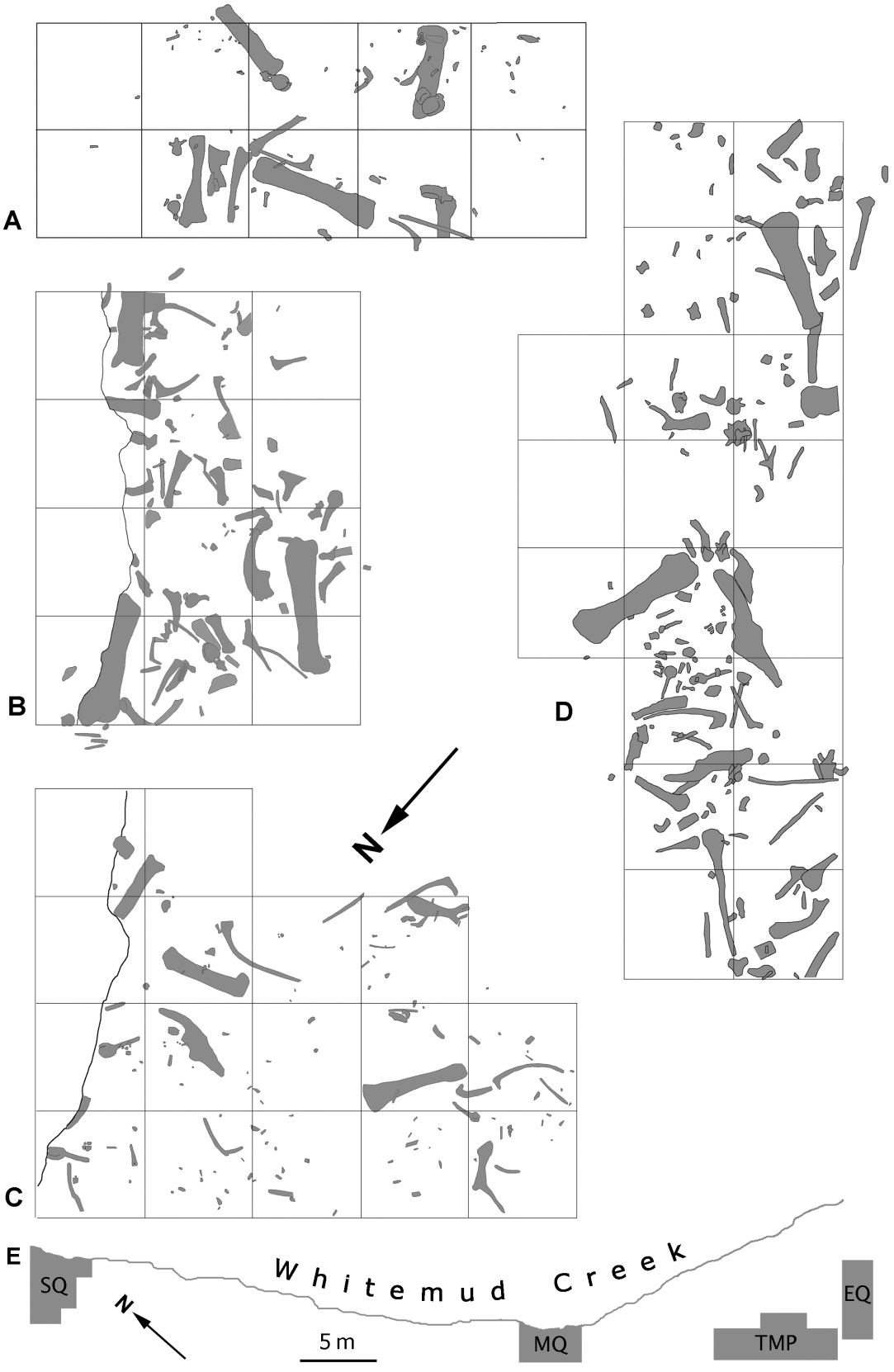
A
B
C
D
N
E
SQ
N
Whitemud Creek
5 m
MQ
TMP
EQ

Figure 7.9. Quarry maps of the A. *Edmontosaurus* Quarry (EQ), B. Middle Quarry (MQ), C. Small Quarry (SQ), and D. TMP excavations. Individual quadrats are 1 m^2. E. Aerial view of L2379 showing relative position of the excavations. The position and orientation of the TMP quarry is approximate.

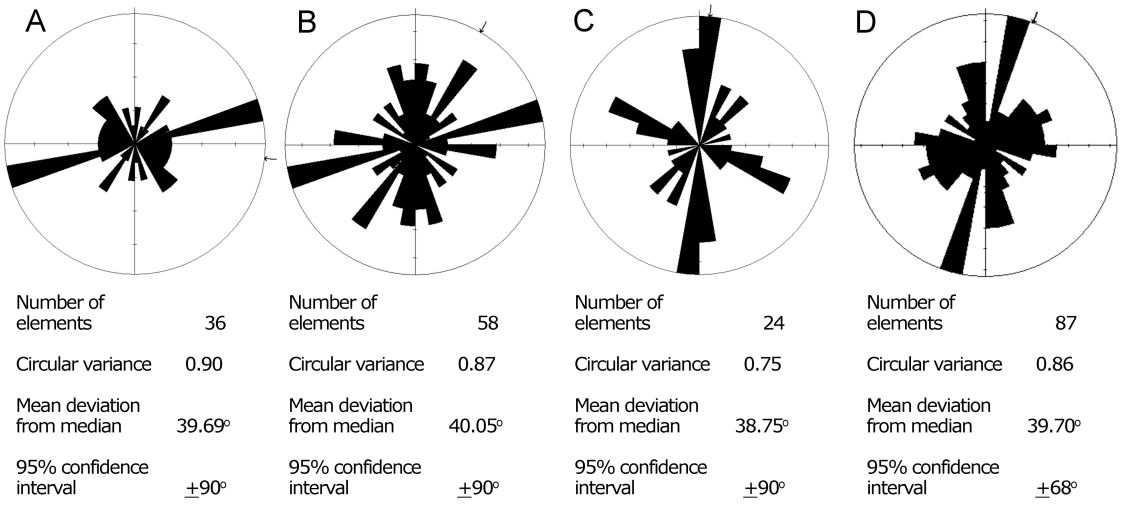

Figure 7.10. Rose diagrams showing the overall orientation of long bones from A. Small Quarry, B. Middle Quarry, C. *Edmontosaurus* Quarry, and D. Royal Tyrrell Museum excavations. Arrows indicate the mean resultant orientation. Note the high circular variance in each quarry.

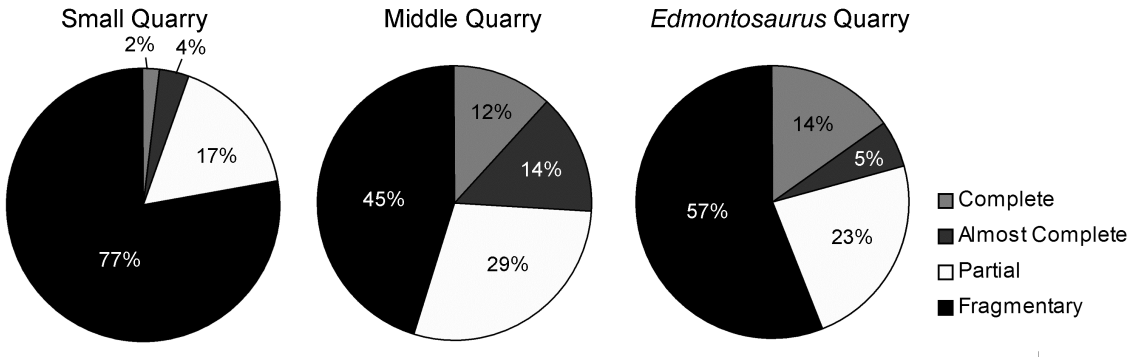

Figure 7.11. Completeness/breakage graphs for the Danek bonebed. Individual bones were ranked as follows; Complete: undamaged or with only superficial damage; Almost complete: bones that were less than complete to 90% complete by volume; Partial: bones between 50 and 90% complete by volume; Fragmentary: bones less than 50% complete by volume.

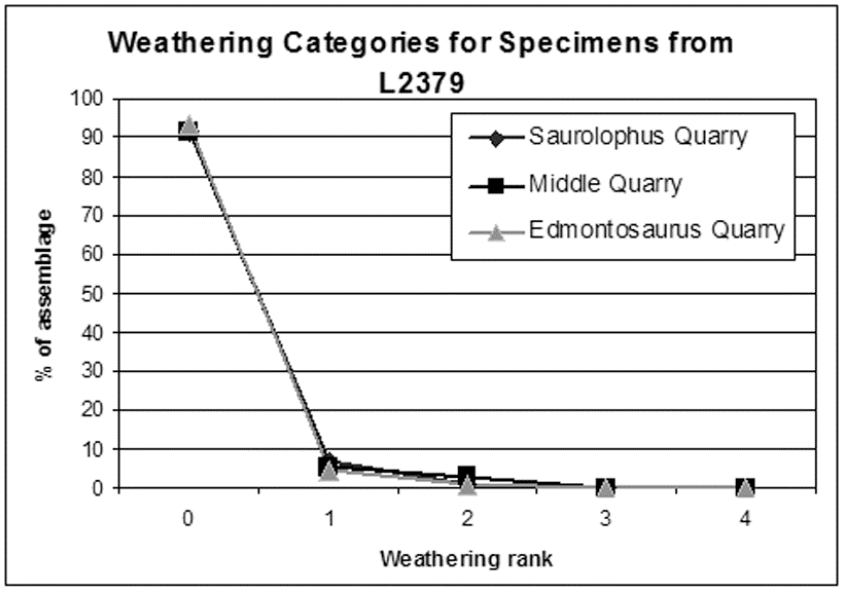

Figure 7.12. Weathering ranks for the Danek Bonebed. Note the similar weathering profile between all three quarries. Values from the *Edmontosaurus* Quarry include data from the TMP excavations. Ranks follow definitions of Behrensmeyer's (1978) and Fiorillo (1988).

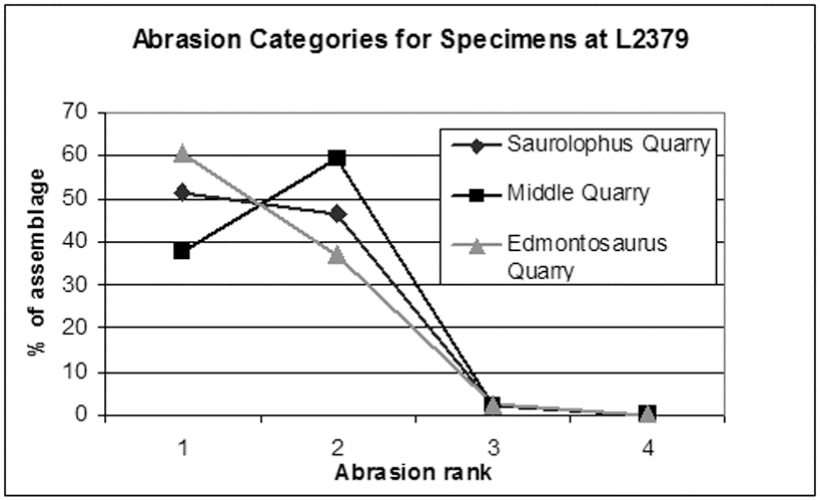

Figure 7.13. Abrasion ranks for the Danek Bonebed. Values from the *Edmontosaurus* Quarry include data from the TMP excavations. Ranks follow definitions of Fiorillo (1988).

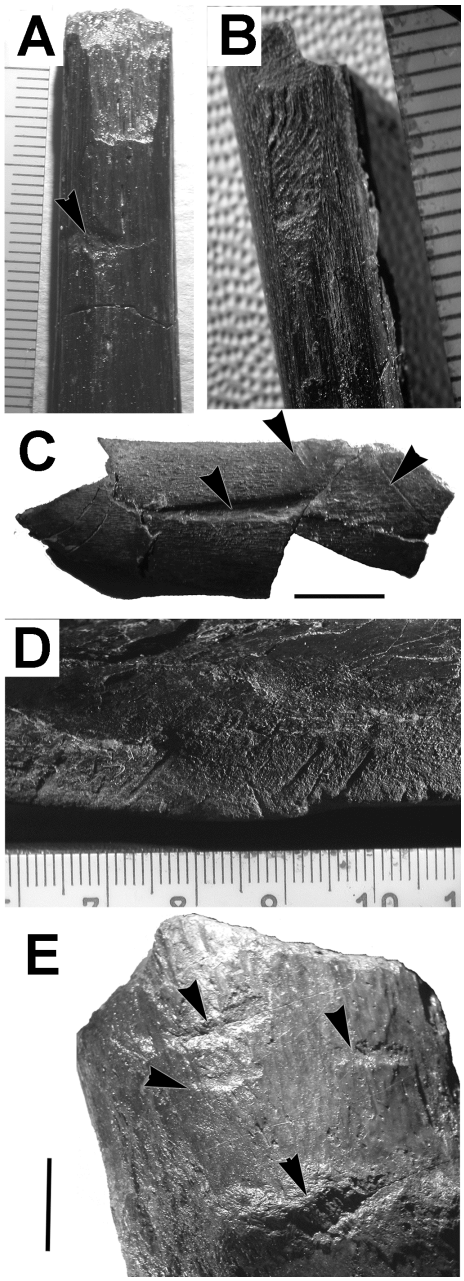

Figure 7.14. Bite marked hadrosaur bones. A. ossified tendon (UALVP48955); B. ossified tendon (UALVP47896) with serration marks; C. unidentified bone fragment (UALVP47945); D. close up of ventral edge of dentary (UALVP47919) showing multiple, parallel cut marks; E. close up of neural spine of proximal caudal vertebra (UALVP47910). Scale bars in C and E = 1 cm. All other scales are 1 mm increments.

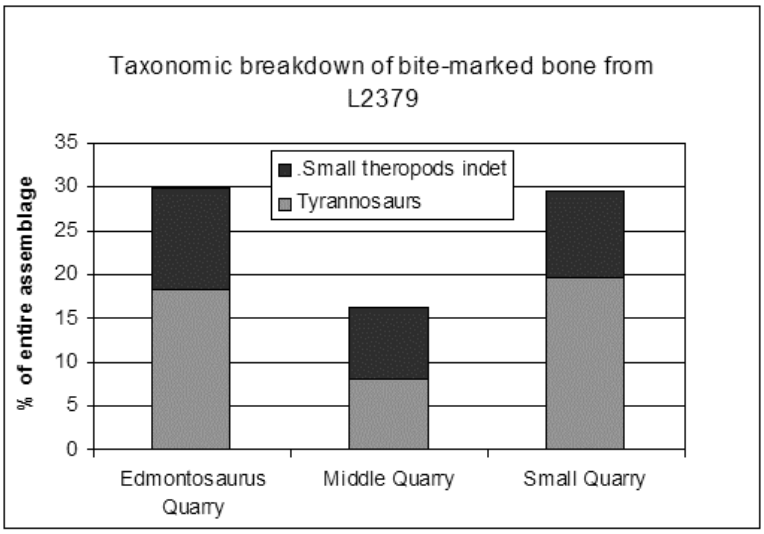

Figure 7.15. Taxonomic subdivision of bite-marked bone from L2379.

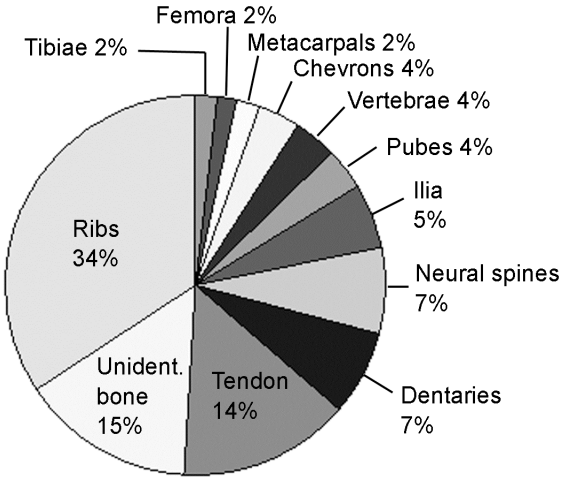

Figure 7.16. Incidence of bite-related trauma on skeletal elements from L2379.

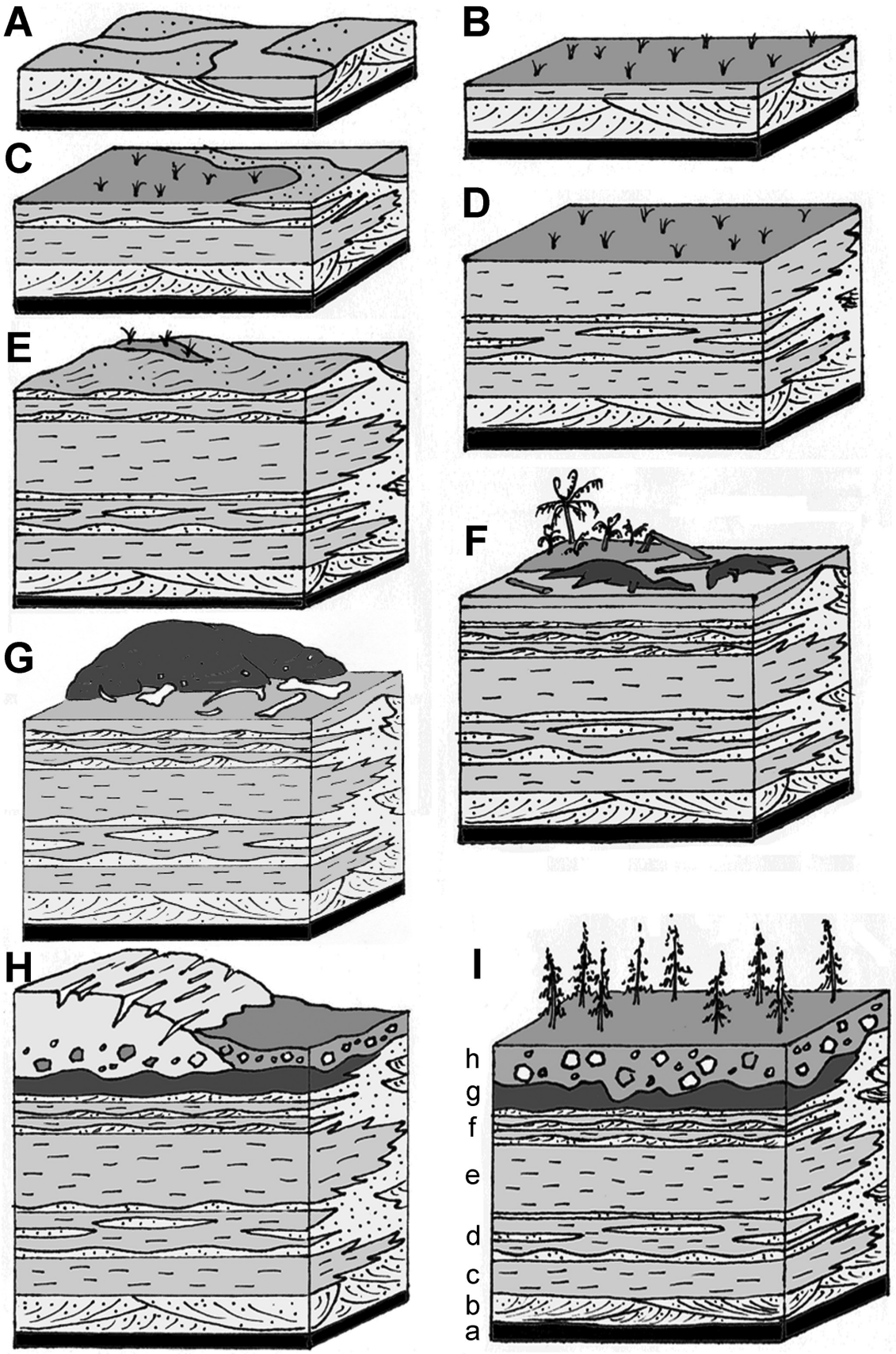
A
B
C
D
E
F
G
H
I
h
g
f
e
d
c
b
a

Figure 17. Hypothetical sequence of sedimentation and depositional environments of stratigraphic horizons A-I at the Danek Bonebed. A. downstream-migrating dunes form on the river bed forming horizon B; B. partly vegetated floodplain (horizon C); C. partly vegetated proximal floodplain with occasional channel avulsions and crevasse splays (horizon D); D. partly vegetated floodplain (horizon E); E. partly vegetated floodplain (horizon F) recording periodic washover events; F. catastrophic death of a herd of *Edmontosaurus* and at least one *Albertosaurus.* Remains were heavily scavenged on the floodplain (top of horizon F) where they remained exposed for a relatively short period; G. Semi-cohesive flow (horizon G) entombs the thanatocoenosis and entrains smaller bioclasts; H. extensive glaciation in the Pleistocene erased the post-Cretaceous sedimentary record leaving a capping tillite (horizon H); I. present day. Lowercase letters refer to the horizons described in section 3.1. Not to scale.

Assemblage Data	→				
Sample size	1	10	100	1000	10,000
# of individuals	1	10	100	1000	
# of species	1	10	20		
Relative abundance to species	All individuals/one species			equal individuals	
Body size (kg)	1	10	100	1000	10,000
Age spectrum	juveniles only			adults only	
Bone articulation	articulated	disarticulated	associated + isolated but associated	dispersed	
Skeletal parts	unsorted	sorted	one part only		
Quarry Data					
Size of accumulation					
Spatial Density (per m^2)	<0.1	0.1	1	10	
Spatial arrangement					
In plan view orientation	random	preferred			
In profile	horizontal				
dipping Patchiness	even	uneven	highly patchy		
Bone Modification					
Size distribution					
Breakage	complete only	fragments only			
Weathering Stages 0-3	Stage 0	Stage 1	Stage 2		
Abrasion/polish Stages 0-3	Stage 0	Stage 1	Stage 2		
Bite marks (%)	0	50	100		
Hackett tunnels (%)	0	50	100		
Corrosion (%)	0	50	100		
Parallel striae (%)	0	50	100		

Table 7.1. The standardised taphonomic approach followed in this study (modified from Behrensmeyer 1991). Information for each category is recorded on a sliding scale to produce a taphogram.

Element	Taxon	Specimen No.	Length (mm)
Femur	*Edmontosaurus*	UALVP 48930	775
Femur	*Edmontosaurus*	RTMP 1989.17.55	~820
Femur	*Edmontosaurus*	UALVP 431343	510
Femur	*Edmontosaurus*	UALVP 47920	1270
Femur	*Edmontosaurus*	UALVP 47878	820
Femur	*Edmontosaurus*	UALVP 50964	905
Tibia	*Edmontosaurus*	UALVP 47898	905
Tibia	*Edmontosaurus*	UALVP 49554	975
Tibia	*Edmontosaurus*	UALVP 47931	585
Tibia	*Edmontosaurus*	UALVP 47933	905
Maxilla	*Albertosaurus*	RTMP 1989.17.53	490

Table 7.2. Hindlimb and cranial elements used to determine the minimum number of individuals.

VOOHRIES GROUP 1		VOOHRIES GROUP II		VOOHRIES GROUP III	
element	**#**	**element**	**#**	**element**	**#**
Caudal vertebrae	50	Coracoids	2	Sacrum	1
Cervical vertebrae	13	Dorsal vertebrae	18	Ilia	2
Ischia	2	Fibulae	2	Femora	2
Metapodials	14	Pubes	2	Tibiae	2
Phalanges	48	Radii	2	Scapulae	2
		Ribs	36	Humeri	2
		Ulnae	2	Skull	1
				Dentaries	2
total	**127**	**total**	**64**	**total**	**14**
% of Assemblage	62.0%	% of Assemblage	31.2%	% of Assemblage	6.8%

Table 7.3. Inventory of bones found in an *Edmontosaurus* skeleton. Note: all values are actual numbers except for caudal vertebrae, which is poorly known in *Edmontosaurus*; the most complete skeleton shows 29 vertebrae, however hadrosaur tails are know to anywhere between 50 and 70 vertebrae (Horner et al. 2004). Therefore, a conservative estimate of 50 is given.

References

Ainsworth, R.B., 1994, Marginal marine sedimentology and high resolution sequence analysis; Bearpaw-Horseshoe Canyon transition, Drumheller, Alberta, Canada: Bulletin of the Canadian Petroleum Geologists, v. 42, p. 26–54.

Argast, S., Farlow, J.O., Gabet, R.M., and Brinkman, D.L., 1987, transport-induced abrasion of fossil reptilian teeth: Implications for the existence of Tertiary dinosaurs in the Hell Creek Formation, Montana: Geology, v. 15, p. 927–930.

Aslan, A., and Behrensmeyer, A.K., 1996, Taphonomy and time resolution of bone assemblages in a contemporary fluvial system: the East Fork River, Wyoming: PALAIOS, v. 11, p. 411–421.

Badgley, C., 1986, Counting individuals in mammalian fossil assemblages from fluvial environments: PALAIOS, v. 1, p. 328–338.

Bartlett, J., Coulson, A., Woodward, H., and Straight, W., 2003, Comparing transport-induced abrasion of fresh and fossilized skeletal remains: Geological Society of America – Abstracts with Programs v. 35, p. 63.

Baszio, S., 1997, Palaeo-ecology of dinosaur assemblages throughout the Late Cretaceous of South Alberta: Courier Forschungsinstitut Senckenberg, v. 196, p. 1–32

Behrensmeyer, A.K., 1975, The taphonomy and paleoecology of Plio-Pleistocene vertebrate assemblages east of Lake Rudolf, Kenya: Bulletin of the Museum of Comparative Zoology, Harvard University, v. 146, p. 474–578.

Behrensmeyer, A.K., 1978, Taphonomic and ecological information from bone

weathering: Palaeobiology, v. 4, p. 150–162.

Behrensmeyer, A.K., 1991, Terrestrial vertebrate accumulations, *in* Allison, A., and Briggs, D.E.G., eds., Taphonomy: Releasing the Data Locked in the Fossil Record: Plenum Press, New York, NY, p. 291–335.

Behrensmeyer, A.K., 2007, Bonebeds through time, *in* Rogers, R.R., Eberth, D.A., and A.R. Fiorillo, A.R., eds., Bonebeds: Genesis, Analysis, and Paleobiological Significance: University of Chicago Press, Chicago, p. 65–102.

Behrensmeyer, A.K., Gordon, K.D., and Yanagi, G.D., 1986, Trampling as a cause of bone surface damage and pseudo-cutmarks: Nature, v. 319, p. 768–771.

Blob, R.W., and Badgley, C., 2007, Numerical methods for bonebed analysis, *in* Rogers, R.R., Eberth, D.A., and A.R. Fiorillo, A.R., eds., Bonebeds: Genesis, Analysis, and Paleobiological Significance: University of Chicago Press, Chicago, p. 333–396.

Boggs, S., 2001, Principles of Sedimentology and Stratigraphy, third edition: Prentice Hall, Upper Saddle River, New Jersey, 688 p.

Brain, C.K., 1967, Bone weathering and the problem of bone pseudotools: South African Journal of Science, v. 63, p. 97–99.

Britt, B.B., Eberth D.A., Scheetz, R.D., Greenhalgh, B.W., and Stadtman, K.L., 2009, Taphonomy of debris-flow-hosted bonebeds at Dalton Wells, Utah (Lower Cretaceous, Cedar Mountain Formation, USA): Palaeogeography, Palaeoclimatology, Palaeoecology, v. 280, p. 1–22.

Chadwick, A.V., Spencer, L.A., and Turner, L.E. Taphonomic windows into an Upper Cretaceous *Edmontosaurus* bonebed: Geological Society of America – Abstracts with Programs, v. 37, p. 159.

Christians, J.P., 1992, Taphonomy and sedimentology of the Mason Dinosaur Quarry, Hell Creek Formation: Unpublished M.Sc. thesis, University of Wisconsin, Madison, USA.

Colson, M.C., Colson, R.O., and Nellermoe, R., 2004, Stratigraphy and depositional environments of the upper Fox Hills and lower Hell Creek Formations at the Concordia hadrosaur site in northwestern South Dakota: Rocky Mountain Geology, v. 39, p. 93–111.

Currie, P.J., 1998, Possible evidence of gregarious behavior in tyrannosaurids: Gaia, v. 15, p. 272–277.

Currie, P.J., and Dodson, P., 1984, Mass death of a herd of ceratopsian dinosaurs. In: W.E. Reir, F. Westphal, F., eds., Third Symposium on Mesozoic Terrestrial Ecosystems, Short Papers; Royal Tyrrell Museum, Drumheller, Alberta, pp. 61–66.

Currie, P.J., Rigby, J.R., and Sloan, R.E., 1990, Theropod teeth from the Judith River Formation of southern Alberta, Canada, *in* Carpenter, K., and Currie, P.J., eds., Dinosaur Systematics: Perspectives and Approaches: Cambridge University Press, p. 107–125.

Currie, P. J., Langston Jr., W., and Tanke, D. H., 2008, A new species of *Pachyrhinosaurus* (Dinosauria, Ceratopsidae) from the Upper Cretaceous of Alberta, Canada, *in* Currie, P.J., Langston Jr., W., and Tanke, D.H., eds., A new horned dinosaur from an Upper Cretaceous bone bed in Alberta: NRC Research Press, Ottawa, Ontario, p. 1–108.

Derstler, K. 1995, The Dragon's Grave; an *Edmontosaurus* bonebed containing theropod eggshells and juveniles, Lance Formation (uppermost

Cretaceous), Niobrara County, Wyoming: Journal of Vertebrate Paleontology, Supplement, v. 15, p. 26.

Eberth, D.A., 1996, Origin and significance of mud-filled incised valleys (Upper Cretaceous) in southern Alberta, Canada: Sedimentology, v. 43, p. 459–477.

Eberth, D.A., 2002a, Taphonomic modes of large dinosaurs in the Horseshoe Canyon Formation (Campanian-Maastrichtian) of southern Alberta, Canada: Journal of Vertebrate Paleontology, Supplement, v. 22, p. 50–51A.

Eberth, D.A., 2002b, Review and comparison of Belly River Group and Edmonton Group stratigraphy and stratigraphic architecture in the southern Alberta plains. 75th Anniversary of CSPG Convention: Canadian Society of Petroleum Geologists, Calgary, Alberta, June 3–7, 2002, p. 1–6.

Eberth, D.A., 2004, A revised stratigraphy for the Edmonton Group (Upper Cretaceous) and its potential sandstone reservoirs. CSPG-CHOA-CWLS Joint Conference: Calgary, Alberta, May 31-June 4, 2004; Pre-Conference Field Trip #7, Sunday, May 30, 44 p.

Eberth, D.A., and Deino, A., 2005, New $^{40}Ar/^{39}Ar$ ages from three bentonites in the Bearpaw, Horseshoe Canyon, and Scollard Formations (Upper Cretaceous–Paleocene) of southern Alberta, Canada, *in* Braman, D.R., Therrien, F., Koppelhus, E.B., and Taylor, W., compilers, Dinosaur Park Symposium, Short Papers, Abstracts, and Program: Royal Tyrrell Museum, Drumheller, Alberta, September 24–25, p. 23–24.

Eberth, D.A., and Getty, M.A., 2005, Ceratopsian bonebeds: occurrence, origin and significance, *in*: Currie, P.J., and Koppelhus, E.B., eds., Dinosaur

Provincial Park; a Spectacular Ancient Ecosystem Revealed: Indiana University Press, Indianapolis, p. 501–536.

Eberth, D.A., Rogers, R.R., and Fiorillo, A.R., 2007, A practical approach to the study of bonebeds, *in* Rogers, R.R., Eberth, D.A., and A.R. Fiorillo, A.R., eds., Bonebeds: Genesis, Analysis, and Paleobiological Significance: University of Chicago Press, Chicago, p. 265–331.

Fanti, F., 2007, Unfolding the geological history of the North: new comprehensive survey of the Wapiti Formation, Alberta, Canada, *in* Braman, D.R., compiler, Ceratopsian Symposium, Program, Abstracts, and Short Papers: Royal Tyrrell Museum of Palaeontology, September 22–23, 2007, Drumheller, Alberta, Canada, p. 33–38.

Fanti, F., and Currie, P. J., 2007, A new *Pachyrhinosaurus* bonebed from the Late Cretaceous Wapiti Formation, *in* Braman, D.R., compiler, Ceratopsian Symposium, Program, Abstracts, and Short Papers: Royal Tyrrell Museum of Palaeontology, September 22–23, 2007, Drumheller, Alberta, Canada, p. 39–43.

Fastovsky, D.E., Clark, J.M., Strater, N.H., Montellano, M.R., Hernandez, and R., Hopson, J.A., 1995, Depositional environments of a Middle Jurassic terrestrial vertebrate assemblage, Huizachal Canyon, Mexico: Journal of Vertebrate Palaeontology, v. 15, p. 561–575.

Fiorillo, A.R., 1988, Taphonomy of Hazard Homestead Quarry (Ongalla Group), Hitchcock County, Nebraska: Contributions to Geology, v. 26, p. 57–97.

Fiorillo, A.R. 1989, Taphonomy and paleoecology of the Judith River Formation (Late Cretaceous) of south-central Montana: Unpublished Ph.D dissertation, University of Pennsylvania, Philadelphia, PA, 298 p.

Gangloff, R.A., and Fiorillo, A.R., 2010, Taphonomy and paleoecology of a bonebed from the Prince Creek Formation, North Slope, Alaska: PALAIOS, v. 25, p. 299–317.

Getty, M., Eberth, D.A., Brinkman, D.B., Tanke, D., Ryan, M., and Vickaryous, M., 1997, Taphonomy of two *Centrosaurus* bonebeds in the Dinosaur Park Formation, Alberta, Canada: Journal of Vertebrate Paleontology, supplement, v. 17, p. 48–49A.

Getty, M., Eberth, D.A., Brinkman, D.B., and Ryan, M., 1998, Taphonomy of three *Centrosaurus* bonebeds in the Dinosaur Park Formation, Alberta: Journal of Vertebrate Paleontology, supplement, v. 18, p. 46A.

Godefroit, P., Zan, S., and Jin, L., 2001, The Maastrichtian (Late Cretaceous) lambeosaurine dinosaur *Charonosaurus jiayinensis* from north-eastern China: Bulletin de l'Institut royal des Sciences naturelles de Belgique, Sciences de la Terre, v. 71, p. 119–168.

Godefroit, P., Hai, S., Yu, T., and Lauters, P., 2008, New hadrosaurid dinosaurs from the uppermost Cretaceous of northeastern China: Acta Palaeontologica Polonica, v. 53, p. 47–74.

Gomez, L.G., Houston, D.C., Cotton, P., and Tye, A., 1994, The role of greater yellow-headed vultures *Cathartes melambrotus* as scavengers in neotropical forest: Ibis, v. 136, p. 193-196.

Hamblin, A.P., 2004, The Horseshoe Canyon Formation in southern Alberta: surface and subsurface stratigraphic architecture, sedimentology, and resource potential: Geological Survey of Canada, Bulletin, v. 578, 180 p.

Hill, A., and Behrensmeyer, A.K., 1984, Disarticulation patterns in some modern East African mammals: Palaeobiology, v. 10, p. 366-376.

Holcombe, R., 1994, GEOrient – an integrated structural plotting package for MS-Windows: Geological Society of Australia, Abstracts, v. 36, p. 73–74.

Van Itterbeeck, J., Bolotsky, Y., Bultynck, P., and Godefroit, P., 2005, Stratigraphy, sedimentology and palaeoecology of the dinosaur-bearing Kundur section (Zeya-Bureya Basin, Amur region, far eastern Russia): Geology Magazine, v. 142, p. 735–750.

Larock, J.W., Schmitt, J.G., and Horner, J.R., 2000, A Cretaceous paleo-logjam: taphonomy and sedimentology of a dinosaur bonebed from the Upper Cretaceous Judith River Formation, northcentral Montana: Geological Society of America – Abstracts with Programs, v. 32, p. 220.

Laudet, F., and Antoine, P.-O., 2005, Caraterisation d'une taphocoenose médiolittorale moderne à méso-mammifères terrestres: Paléontologie Sytématique, v. 4, p. 203-208 (in French).

Lauters, P., Bolotsky, Y.L., van Itterbeeck, J, and Godefroit, P., 2008, Taphonomoy and age profile of a latest Cretaceous dinosaur bonebed in far eastern Russia: PALAIOS, v. 23, p. 153–162.

Lehman, T.M., 1982, A ceratopsian bonebed from the Aguja Formation (Upper Cretaceous) Big Bend National Park, Texas: Unpublished M.Sc. thesis, University of Texas, Austin, Texas, 210 p.

Lloyd, M., 1967, Mean crowding: Journal of Animal Ecology, v. 36, p. 1–30.

Lyman, R.L., 1994, Vertebrate Taphonomy: Cambridge University Press, New York, 524 p.

McCabe, P.J., 1984, Depositional environments of coal and coal-bearing strata. In: R.A. Rahmani, R.M. Flores (Eds.), Sedimentology of Coal and Coal-

Bearing Sequences: International Association of Sedimentologists Special Publication, v. 7, p. 13–42.

McGowan, C., 1999, A Practical Guide to Vertebrate Mechanics: Cambridge University Press, Cambridge, U.K., 316 p.

Paul, G.S., 1997, Dinosaur models: the good, the bad, and using them to estimate the mass of dinosaurs, *in* Wolberg, D.L., Stump, E., Rosenberg, G.D., eds., Dinofest International: Proceedings of a Symposium Held at Arizona State University: The Academy of Natural Sciences, Philadelphia, p. 129-154.

Perrier, R. and Quiblier, J., 1974, Thickness changes in sedimentary layers during compaction history; methods for quantitative evaluation: American Association of Petroleum Geologists Bulletin, v. 58, p. 507–520.

Rahmani, R.A., 1989, Cretaceous tidal estuarine and deltaic deposits, Drumheller, Alberta, Second International Research Symposium on Clastic Tidal Deposits Field Trip Guidebook: Canadian Society of Petroleum Geologists, Calgary, Alberta, 55 p.

Ralrick, P.E., and Tanke, D.H., 2008, Comments on the quarry map and preliminary taphonomic observations of the *Pachyrhinosaurus* (Dinosauria: Ceratopsidae) bonebed at Pipestone Creek, *in* Currie, P.J., Langston Jr., W., and Tanke, D.H., eds., A new Horned Dinosaur from an Upper Cretaceous Bone Bed in Alberta: NRC Research Press, Ottawa, Ontario, p. 109–116.

Rogers, R.R., 1990, Taphonomy of three dinosaur bonebeds in the Upper Cretaceous Two Medicine Formation of northwestern Montana: Evidence for drought-related mortality: PALAIOS, v. 5., 394–413.

Rogers, R.R., and Kidwell, S.M., 2007, A conceptual framework for the genesis and analysis of vertebrate skeletal concentrations, *in* Rogers, R.R., Eberth,

D.A., and A.R. Fiorillo, A.R., eds., Bonebeds: Genesis, Analysis, and Paleobiological Significance: University of Chicago Press, Chicago, p. 1–64.

Ryan, M.J., 1992, The Taphonomy of a *Centrosaurus* (Reptilia: Ornisthischia) Bone Bed (Campanian), Dinosaur Provincial Park, Alberta, Canada: Unpublished M.Sc. thesis, University of Calgary, Calgary, Alberta, 526 p.

Ryan, M.J., 2003, Taxonomy, systematics and evolution of centrosaurine ceratopsids of the Campanian western interior basin of North America: Unpublished Ph.D. dissertation, University of Calgary, Calgary, Alberta, 578 p.

Ryan, M.J., and Russell, A.P., 2005, A new centrosaurine ceratopsid from the Oldman Formation of Alberta and its implications for centrosaurine taxonomy and systematics: Canadian Journal of Earth Sciences, v. 42, p. 1369–1387.

Ryan, M.J., Bell, J.G., and Eberth, D.A., 1995, Taphonomy of a hadrosaur (Ornithischia: Hadrosauridae) bonebed from the Horseshoe Canyon Formation (Early Maastrichtian), Alberta, Canada: Journal of Vertebrate Paleontology, supplement, v. 15, p. 51A.

Ryan, M.J., Russell, A.P., Eberth, D.A., and Currie, P.J., 2001, The taphonomy of a *Centrosaurus* (Ornithischia: Ceratopsidae) bonebed from the Dinosaur Park Formation (upper Campanian), Alberta, Canada, with comments on cranial ontogeny: PALAIOS, v. 16, p. 482–506.

Straight, W.H., and Eberth, D.A., 2002, Testing the utility of vertebrate remains in recognising patterns in fluvial deposits: an example from the lower Horseshoe Canyon Formation, Alberta: PALAIOS, v. 17, p. 472–490.

Straight, W.H., Barrick, R.E., and Eberth, D.A., 2004, Reflections of surface water, seasonality, and climate in stable oxygen isotopes from tyrannosaurid tooth enamel: Palaeogeography, Paleoclimatology, Paleoecology, v. 206, p. 239–256.

Varricchio, D. J. and Horner, J.R., 1993, Hadrosaurid and lambeosaurid bone beds from the Upper Cretaceous Two Medicine Formation of Montana: taphonomic and biologic implications: Canadian Journal of Earth Sciences, v. 30, p. 997–1006.

Varricchio, D., Jackson, F., Scherzeer, B., and Shelton, J., 2005, Don't have a cow, man! It's only actualistic taphonomy on the Yellowstone River of Montana: Journal of Vertebrate Paleontology, supplement, v. 25, p. 126A.

Visser, J., 1986, Sedimentology and taphonomy of a *Styracosaurus* bonebed in the Late Cretaceous Judith River Formation, Dinosaur Provincial Park, Alberta: Unpublished M.Sc. thesis, University of Calgary, Calgary, Alberta, 150 p.

Voohries, M.R., 1969, Taphonomy and population dynamics of an early Pliocene vertebrate fauna, Knox County, Nebraska: Contributions to Geology, Special Paper, v. 2, p. 1-69.

White, T.D., and Folkens, P.A., 2005, The Human Bone Manual: Academic Press, San Diego, CA, 464 p.

CHAPTER 9

GENERAL CONCLUSIONS

The hadrosaurid genus, *Saurolophus* is represented by two species, *Saurolophus osborni* and *Saurolophus angustirostris* from Canada and Mongolia, respectively. Both species are represented by multiple, excellent specimens but since the discovery of *Saurolophus osborni* nearly a century ago, details of its anatomy have been misrepresented or overlooked. Moreover, a thorough description of *Saurolophus osborni* has not been available, leading to confusion regarding certain anatomical peculiarities. Most critical is the construction of the solid cranial crest, which is the most obvious defining character of this species and for which the genus was named (Brown 1912). Despite a number of descriptive works (Rozhdestvensky 1952, 1957, 1965, Maryańska and Osmólska 1979, 1981b, 1984), *Saurolophus angustirostris* has not been adequately described or compared to *Saurolophus osborni.* Where comparisons have been made, they have been based on inappropriate material and/or descriptions that would by regarded as insufficient by modern standards. The sum of this previous work has unfortunately resulted in a lack of consensus concerning the validity of *Saurolophus angustirostris* (Norman and Sues 2000). Those authors posited that the diagnostic characters listed by Maryańska and Osmólska (1981b, 1984) may fall within the realm of intraspecific variation. Resolution of this concern is central to understanding the complex palaeobiogeographical history of this genus.

Detailed redescriptions in chapters 2 and 3 of both species confirm their status as distinct taxa and permit diagnosis of the genus. *Saurolophus* can be primarily distinguished from all other hadrosaurines by the presence of a solid, posterodorsally-directed cranial crest. The crest is formed by posterodorsal extensions of the nasals that are buttressed posteriorly and posterolaterally by the frontals and prefrontals, respectively. Exaggeration of crest development in

Saurolophus (when compared to other crested hadrosaurines: *Brachylophosaurus, Maiasaura,* and *Prosaurolophus*) has led to several convergences with lambeosaurines, most notably *Parasaurolophus* and *Charonosaurus* (Godefroit et al. 2001, Evans et al. 2007). These can be summarized as: 1. Posterodorsal and anteroventral extension of the frontals to form a frontal platform (dorsal promontorium); 2. Exclusion of the parietal from the posterodorsal margin of the occiput by the squamosals, and 3. 'Down-warping' of the frontal-parietal suture to form an obtuse angle between those elements in lateral view.

In addition to its greater absolute size, *Saurolophus angustirostris* is differentiated from *Saurolophus osborni* by having an upturned premaxillary body, a more strongly dorsally reflected oral margin of the premaxilla, lacking an anterior notch in the prenarial fossa, having a sigmoidal contour of the ventral margin of the anterior process of the jugal compared to the arcuate margin in *Saurolophus osborni*, having a relatively shallow quadratojugal notch on the quadrate, and by having a more strongly bowed quadrate in lateral view.

The availability of extensive skin impressions suggests species of *Saurolophus* can be distinguished based solely on scale architecture. This is notable as it is the first time that intrageneric differences have been identified for a dinosaur based soft tissue preservation. Whereas identifications of extant taxa rely almost entirely on soft tissue characters, palaeontologists are rarely privy to such evidence. Although the taxonomic utility of scale morphology has been suggested within the Hadrosauridae (Brown 1916, Lull and Wright 1942, Negro 2001), this question has not been previously addressed in any detail. Furthermore, resolution has not been available at the species level. Results in Chapter 5 show *Saurolophus angustirostris* can be differentiated from *Saurolophus*

osborni by the presence of tabular midline feature-scales along the length of the tail and a banded pattern of scales on the base of the tail. The hindlimb and proximal part of the tail of *Saurolophus angustirostris* were also covered in circular shield feature-scales that were set in a grid-like arrangement. Repetition of scale morphologies and patterns between specimens (i.e. individuals) confirms the observed characteristics do not differ significantly between individuals of the same species. Preliminary results suggest these patterns were also ontogenetically stable in *Saurolophus angustirostris*. Characterisation of scale architecture in a single species of dinosaur based on multiple individuals has not been previously achieved. Future characterisations, however, may also be possible for *Edmontosaurus annectens* for which multiple 'mummies' are known. *Saurolophus osborni* shares similarities with *Edmontosaurus* in the presence of cluster areas of similarly-sized scales on the tail. Comparisons with other hadrosaurids suggest widespread morphological variability in scale architecture, especially in the caudal region where most skin impressions are preserved. The taxonomic importance of scale morphology is evident; however, more specimens are required before they can be incorporated fully into species diagnoses.

Phylogenetic analysis of osteological characters corroborates a sister taxon relationship between *Saurolophus angustirostris* and *Saurolophus osborni*. *Saurolophus* itself is recovered as most closely related to the Laurasian taxa *Prosaurolophus* and *Kerberosaurus* in an unresolved trichotomy. As the only confirmed dinosaur genus common to both North America and Asia, *Saurolophus* is of considerable palaeobiogeographic importance. Yet few attempts have been made to comment on the dispersal history of this genus (Bolotsky and Godefroit 2004). Unfortunately, phylogenetic resolution between *Saurolophus,*

Prosaurolophus, and *Kerberosaurus* was not forthcoming from the analysis in Chapter 3. Although the palaeobiogeographic history of *Saurolophus* remains unresolved, this study confirms at least two dispersal events must have taken place across Beringia during the late Cretaceous leading to the evolution of the *Saurolophus-Prosaurolophus-Kerberosaurus* clade. The first dispersal, from west to east, must have occured at or prior to the early late Campanian with the ancestors of *Kerberosaurus.* Assuming a direct relationship between *Prosaurolophus* and *Saurolophus osborni* (Bolotsky and Godefroit 2004, Prieto-Marquez 2010a), the second dispersal event occurred at or prior to the earliest Maastrichtian leading to the evolution of *Saurolophus angustirostris.* The evolutionary history of this group illustrates the rapid evolution and complexity of hadrosaurine palaeobiogeography (Prieto-Marquez 2010b). Beringia is also recognised as the location of at least two east-to-west dispersal events within the Hadrosaurinae, which stands in contrast to the predominantly west-to-east direction observed in other dinosaurian groups (Russell 1993, Prieto-Marquez 2010b and references therein). The Late Cretaceous terrains of Alaska and Russia, therefore, should be regarded important sites for understanding and identifying potential intermediaries between 'typical' North American hadrosaurines (*Edmontosaurus*, *Saurolophus osborni*) and their Asian counterparts (*Kerberosaurus, Saurolophus angustirostris*). To date, only a single genus (*Edmontosaurus*) has been identified from the late Campanian-early Maastrichtian of Alaska (Gangloff and Fiorillo 2010) during a time when the aforementioned dispersal events are hypothesised to have occurred. The poor hadrosaurid record in Alaska highlights the current lack of understanding of how this region influenced dispersal patterns and what (if any) evolutionary changes took place during such

dispersal events. While a picture of Late Cretaceous hadrosaurid diversity is beginning to emerge from far eastern Russia and China (Bolotsky and Godefroit 2004, Godefroit et al. 2001, 2008), the mechanisms, timing of dispersal events, and indeed the actual routes taken are poorly resolved.

Palaeobiogeographically important reports of *Saurolophus* from the Moreno Formation of California could not be confirmed. The description in Chapter 4 of the best of two skulls (LACM/CIT 2852) assigned to cf. *Saurolophus* by Morris (1973) failed to identify diagnostic characters that would permit unambiguous assignment to *Saurolophus* or any other hadrosaurine. Critical diagnostic elements (such as the frontals and nasals) are missing and plastic deformation of the remaining material further hampers interpretations. A phylogenetic analysis places this specimen as either the sister taxon of *Saurolophus* or as the sister taxon to a clade comprising *Edmontosaurus* and *Anatotitan.* Given its geographic setting and morphological uncertainties, it is possible that the Moreno specimen represents a separate taxon; but in the absence of better material, LACM/CIT 2852 is regarded as Hadrosaurinae indet.

In addition to extensive skin impressions previously mentioned, the Dragon's Tomb bonebed has helped elucidate aspects of ontogeny, biology, and behaviour of *Saurolophus angustirostris*. The excellent ontogenetic series of skulls from this site (complemented by specimens from additional nearby localities) demonstrates for the first time the development features including the fusion sequence of the cranial vault and the development of a postorbital boss on the largest individuals. Using histology, it may be possible in the future to associate these ontogenetic changes with the actual age of the individual, thereby providing a proxy for relative age assessment of other specimens.

Evaluation of the caudal skeleton in Chapter 7 demonstrates elongation (both absolute and relative) of the neural spines throughout ontogeny. In addition, mediolateral and anteroposterior expansion of the distal ends of the neural spines is reminiscent of the 'club-like' (Maryańska and Osmólska 1981a, p.246) spines in *Barsboldia sicinskii*. Comparison with the skeleton of *Barsboldia* failed to rule out the possibility that *Barsboldia* and *Saurolophus* are in fact conspecific. Due to the lack of diagnostic characters (Prieto-Marquez 2010a) and in the absence of more complete specimens, it is probably prudent to regard *Barsboldia* as a junior synonym of *Saurolophus angustirostris.* As *Barsboldia* is the only other putative hadrosaurid from the Nemegt Formation, the reassignment of that taxon to *Saurolophus* reduces the number of hadrosaurid taxa from the Nemegt to one. From a phenetic palaeobiogeographic standpoint, the Nemegt Formation is virtually identical to the Dinosaur Park Formation in Canada (Holtz et al. 2004); however, hadrosaurid diversity differs dramatically between the two formations. Whereas *Saurolophus angustirostris* is the only hadrosaurid taxon from the Nemegt, the Dinosaur Park Formation represents the highest hadrosaurid diversity of any Late Cretaceous Formation comprising at least eight taxa (Ryan and Evans 2005). Moreover, other penecontemporaneous Asian and North American faunas (exclusive of the Nemegt Formation) are tend to be dominated by lambeosaurines (Ryan and Evans 2005, Godefroit et al. 2008). It is notable, however, that the Horseshoe Canyon Formation, from which *Saurolophus osborni* originates, is dominated by the hadrosaurine *Edmontosaurus* in the lower part and by the lambeosaurine *Hypacrosaurus* above the Drumheller Marine Tongue (Russell and Chamney 1967). whereas, theropod assemblages from the Dinosaur Park and Nemegt formations are largely the same

(Weishampel et al. 2004). Such glaring differences (and similarities) have yet to be explained although it is probable that dispersal histories and/or environmental controls were important limiting factors. Given the trend towards climatic/environmental provincialism within the Hadrosauridae (Russell and Chamney 1967, Lehman 2001, Ryan and Evans 2005), it may be speculated that hadrosaurines (and certainly *Saurolophus* itself) were better adapted to 'inland' environments than lambeosaurines in general; however, there are undoubtedly exceptions to this statement.

Bonebeds are crucial in the understanding of intraspecific variation, ontogenetic change, relative growth rates, aggregation behaviour, palaeoecology, and even predator-prey relationships (Brinkman et al. 2007). Monodominant bonebeds such as the Dragon's Tomb (Mongolia) and the Danek Bonebed (Alberta, Canada) are typically the result of intrinsic biogenic accumulations (i.e. gregariousness; Eberth et al. 2007). Gregarious behaviour—as inferred from bonebed data—among hadrosaurids is widespread but not ubiquitous. The Dragon's Tomb preserves at least six *Saurolophus angustirostris* ranging from juveniles to full-grown adults and provides the first evidence of gregariousness in that taxon. More significantly, the Dragon's Tomb is unique among all other bonebeds in that it is the only one that preserves multiple hadrosaurid 'mummies'. All other examples of soft tissue preservation in dinosaurs are limited to isolated specimens within a given stratigraphic interval rather than a single event horizon.

The Horseshoe Canyon Formation in southern Alberta preserves a number of hadrosaurid-dominated bonebeds. Aside from the taphonomic assessment of an *Albertosaurus* bonebed from the upper part of that formation

(Eberth and Currie 2010), no detailed investigations of bonebed genesis have been carried out in the Horseshoe Canyon Formation. The Danek Bonebed is an *Edmontosaurus*-dominated bonebed from the lower Horseshoe Canyon Formation. Based on field activities spanning approximately five summers, at least eight *Edmontosaurus*, from juveniles to adults, and one adult *Albertosaurus* were identified within the assemblage. A thorough taphonomic treatment presented in Chapter 8 found skeletons at the Danek Bonebed to be entirely disarticulated. Carcasses were heavily scavenged prior to entombment, which probably contributed to the intense post-mortem fracturing and dismemberment, and to the overrepresentation of large (Voohries group III) specimens. Remains were deposited on a periodically inundated floodplain and entombed within an organic-rich shale interpreted as an overbank flood deposit. Although the cause of death is unknown, a sudden, catastrophic death could explain the demographic spread, faunal diversity, rare greenstick fractures, and homogeneous weathering/abrasion categories of the assemblage. The frequency of bite-marked bones (30%) within the Danek Bonebed is the highest recorded for any known hadrosaurid or ceratopsid bonebed. Evidence for scavenging (shed teeth, bite-marked bone) is nearly ubiquitous for monodominant ornithischian bonebeds, yet it comprises a relatively minor taphonomic component of such assemblages (Eberth and Getty 2005, Currie et al. 2008, Gangloff and Fiorillo 2010). At many of these sites, the minimum number of individuals exceeds several tens or even hundreds of animals. The cumulative effect of so many carcasses presumably 'diluted' the impact of scavenging compared to relatively small assemblages, such as the Danek Bonebed, where bite-marked bones are common. These results suggest scavenging plays in important role the

biostratinomy of bonebeds (and isolated skeletons), and whose effects may be dampened or amplified depending on the size (number of individuals and areal extent) of the assemblage. This study also highlights the importance of collecting and properly examining otherwise unidentifiable bone fragments within a bonebed. As illustrated in Fig. 7.16, the highest incidence of bite mark trauma was identified on ribs (many of which were fragmentary), ossified tendons and unidentified bone shards. Often small and of limited anatomical value, these remains are of critical taphonomic importance. In many cases, only select quadrats are systematically excavated to include all fragments of bone (Ryan et al. 2001, Gangloff and Fiorillo 2010) and are otherwise discarded; however, failure to include such fragments may simplify and skew taphonomic results.

Gregariousness, while not universal, is revealing itself as an increasingly common phenomenon among hadrosaurids. Although this picture is by no means complete, there is no evidence to support a gregarious trend among either hadrosaurines or lambeosaurines. Instead, this behaviour appears to have evolved multiple times within the Hadrosauridae. In modern ungulates, the evolution of gregariousnes is frequently attributed to minimising risk of predation while obtaining food or other finite resources (Hirth 1977, Molvar and Bowyer 1994) and an increase in foraging efficiency due to increased vigilance of the herd (Beauchamp 2003). The latter may be an adaptation aquired following a shift to social behaviour rather than an a priori selective advantage that led to gregariousness. Although speculative, it is not unreasonable to suppose that similar constraints drove the evolution of social behaviour in hadrosaurids also and that their success may, in part, be related to such behaviour.

Future Directions

Despite an exceptionally rich hadrosaurine fossil record, phylogenetic relationships within this group are far from resolved. Phylogenetic analyses consistently recover Hadrosaurinae as a monophletic clade, yet there is little concensus regarding the relationships of taxa that form this subfamily (Godefroit et al. 2001, 2008, Bolotsky and Godefroit 2004, Horner et al. 2004, Prieto-Marquez 2005, 2010a, Gates and Sampson 2007, Bell 2010,). Retention indices and decay values, where given, are unfailingly low, reflecting the poor resolution of phylogenetic relationships within this group. The most thorough review of the Hadrosauridae (Prieto-Marquez 2010a), which included a comprehensive list of taxa and 286 characters (196 cranial and 90 postcranial, including 136 newly-defined characters) failed to recover a robustly supported cladogram. Among hadrosaurines, relationships within multispecific genera (*Edmontosaurus, Saurolophus, Gryposaurus*) and the *Brachylophosaurus-Maiasaura* clade are best resolved (Godefroit et al. 2001, 2008, Prieto-Marquez 2005, 2010a, Bell 2010). Phylogenetic relationships also have an important bearing on palaeobiogeographical reconstructions and dispersal histories. Given the current non-consensus regarding hadrosaurine interrelationships, both the number and timing of dispersal events must be read with caution (Godefroit et al. 2001, 2008, Bolotsky and Godefroit 2004, Prieto-Marquez 2010b). A revision of Hadrosaurinae is therefore recommended with special attention paid to relative ages of compared taxa (i.e. immature versus mature individuals), character selection (especially ontogenetically variable and convergent characters), and phylogenetic techniques.

Due to the poor understanding of hadrosaurine interrelationships, the origin of the Hadrosaurinae is equivocal. *Wulagasaurus,* from northwestern China, was posited as the most basal hadrosaurine by Godefroit et al. (2008) thus providing the best evidence for an Asian origin for both Hadrosaurinae and Hadrosauridae in general. Recent work by Prieto-Marquez (2010a), however, recovered *Wulagasaurus* as a considerably more derived hadrosaurine with several North American forms occupying the basal-most positions on the hadrosaurine family tree. As stated previously, phylogenetic relationships are weakly supported and palaeobiogeographical information taken from these cladograms are similarly equivocal. It is remarkable that despite the fact hadrosaurs were the most common and best-represented group of Late Cretaceous dinosaurs, such fundamental questions as, 'from which continent did the Hadrosaurinae (or Hadrosauridae) originate?' remain unanswered.

Chapter 5 identifies for the first time integumentary patterns that permit differentiation of species within a single hadrosaurid genus (*Saurolophus*). While promising, the picture of scale architecture in both species is far from complete and lacs resolution in ontogenetic and individual variation. The Dragon's Tomb locality in the Nemegt Basin will no doubt be an important source of additional skin impressions and, in all probability, complete dinosaur 'mummies' that will help fill these gaps. The discussion of scale variation within Hadrosauridae, also presented in Chapter 5, is by no means comprehensive and deserving of a more thorough synthesis. The findings presented in that chapter and hinted at by other authors (Brown 1916, Lull and Wright 1942, Negro 2001) suggest a hitherto overlooked suite of phylogenetic information. Indeed, a preliminary phylogenetic assessment of scale morphology supports this notion (Negro 2001).

Other important specimens, representing taxa unknown from skin impressions have received only cursory attention (e.g. *Brachylophosaurus*, Murphy et al. 2007) or await description entirely (*Prosaurolophus*, TMP 1998.50.01; *Maiasaura,* ROM 44770). Emphasis must also be placed on the exact location of skin impressions when they are found. Frequently, they are removed from around the skeleton and curated without reference to their anatomical position; however, regionalisation of scale morphs and patterns are critical to understanding not only the physical appearance of the animal but also the taxonomic bearing of such impressions.

The absence of neonate and hatchling-sized individuals in both the Dragon's Tomb and the Danek Bonebed poses an interesting biological question. Monodominant hadrosaurid bonebeds (and cerapodans in general; Ryan et al. 2001, Eberth and Getty 2005, Currie et al. 2008, Godefroit et al. 2008, Gangloff and Fiorillo 2010) almost invariably represent assemblages of late juveniles (*sensu* Horner et al. 2000) and older individuals in varying proportions, whereas neonates and hatchlings (for the sake of brevity, neonates and hatchlings are herein referred to as 'nestlings') are conspicuously absent. More commonly, the bones of nestlings are found within mixed-faunal micro- and macro-fossil bonebeds (Ryan et al. 1998, Tanke and Brett-Surman 2001, Fanti and Miyashita 2010), which have decidedly different biological origins and taphonomic histories (Eberth et al. 2007). A notable exception is a *Maiasaura* nesting ground from the Two Medicine Formation that preserves nestling-sized bones in association with adult material (Horner and Makela 1979, Horner 1982). Although a case of negative evidence could be cited, the question becomes inevitable: where are the nestlings within monodominant hadrosaurid bonebeds?

The skeletons of such diminutive animals are without question subject to taphonomic parameters that differ considerably from more mature individuals. Nevertheless, taphonomic equivalency would be expected between the small elements of large animals (e.g. teeth, carpals, phalanges) and the more robust bones of nestlings (e.g. femora, tibiae; Eberth et al. 2007). Moreover, 'background' microfossil assemblages are common within macrovertebrate bonebeds (Ryan et al. 2001, Lauters et al. 2008, Larson et al. 2010) that remain despite their often-destructive taphonomic histories involving hydrologic winnowing, scavenging, and trampling. Such lines of evidence suggest the absence of nestlings in virtually all known hadrosaurid bonebeds is a real phenomenon, which begs new unanswered questions. Did such arguably gregarious animals abandon their eggs leaving the young to form crèches as suggested by juvenile-dominated bonebeds (Varricchio and Horner 1993, Gangloff and Fiorillo 2010)? Alternatively, given the evidence for parental care (Horner and Makela 1979, Horner 1982, Horner et al. 2004), did herds rear their young to a given age/size at relatively 'safe' nesting grounds before relocating to more volatile environments where chances of mass-mortality events were greater? Although generalisations may be made regarding select taxa (most obviously, *Maiasaura*), future answers may come from a thorough review of hadrosaurid bonebeds and alledged nesting grounds, their palaeoenvironmental settings and taphonomic histories. Additional discoveries of new nesting areas and bonebeds may also provide some statistical grounds on which to base future comments on the biology of these animals.

References

Beauchamp, G. 2003. Group-size effect on vigilance: a search for mechanisms. Behaviour Proceedings 46: 227–265.

Bell, P.R. 2010. Redescription of the skull of *Saurolophus osborni* Brown 1912 (Ornithischia: Hadrosauridae) Cretaceous Research Doi:10,1016/j.cretres.2010.10.002

Bolotsky, Y.L. and Godefroit, P. 2004. A new hadrosaurine dinosaur from the Late Cretaceous of far eastern Russia. Journal of Vertebrate Paleontology 24: 351–365.

Brown, B. 1916. *Corythosaurus casuarius*: skeleton, musculature and epidermis. Bulletin of the American Museum of Natural History 35:709–723.

Currie, P. J., Langston Jr., W., and Tanke, D. H. 2008. A new species of *Pachyrhinosaurus* (Dinosauria, Ceratopsidae) from the Upper Cretaceous of Alberta, Canada, *in* Currie, P.J., Langston Jr., W., and Tanke, D.H., eds., A new horned dinosaur from an Upper Cretaceous bone bed in Alberta: NRC Research Press, Ottawa, Ontario, p. 1–108.

Dodson P. 1975. Taxonomic implications of relative growth in lambeosaurine hadrosaurs. Systematic Zoology 24:37–54.

Eberth, D.A. and Currie, P.J. 2010. Stratigraphy, sedimentology, and taphonomy of an *Albertosaurus* bonebed (upper Horseshoe Canyon Formation; Maastrichtian), southern Alberta, Canada. Canadian Journal of Earth Sciences 47:1119–1143.

Eberth, D.A., and Getty, M.A. 2005, Ceratopsian bonebeds: occurrence, origin and significance. In: Currie, P.J., and Koppelhus, E.B. (eds.), Dinosaur

Provincial Park; a Spectacular Ancient Ecosystem Revealed: Indiana University Press, Indianapolis, p. 501–536.

Eberth, D.A., Shannon, M., and Noland, B.G. 2007. A bonebed database: classification, biases, and patterns of occurrence. In: R.R. Rogers, D.A. Eberth, and A.R. Fiorillo (eds.) Bonebeds: Genesis, Analysis, and Paleobiological Significance. University of Chicago Press, Chicago, Illinois, pp.103–220.

Evans, D.C. 2010. Cranial anatomy and systematics of *Hypacrosaurus altispinus*, and a comparative analysis of skull growth in lambeosaurine hadrosaurids. Zoological Journal of the Linnean Society 159:398–434.

Evans, D.C., Reisz, R.R., and Dupuis, K. 2007. A juvenile *Parasaurolophus* (Ornithischia: Hadrosauridae) braincase from Dinosaur Provincial Park, Alberta, with comments on crest ontogeny in the genus. Journal of Vertebrate Paleontology 27: 642–650.

Fanti, F. and Miyashita, T. 2009. A high-latitude vertebrate fossil assemblage from the Late Cretaceous of west-central Alberta, Canada: evidence for dinosaur nesting and vertebrate latitudinal gradient. Palaeogeography, Palaeoclimatology, Palaeoecology 275: 37–53.

Gangloff, R.A., and Fiorillo, A.R. 2010, Taphonomy and paleoecology of a bonebed from the Prince Creek Formation, North Slope, Alaska: PALAIOS, v. 25, p. 299–317.

Gates, T.A. and Sampson, S.D. 2007. A new species of *Gryposaurus* (Dinosauria: Hadrosauridae) from the late Campanian Kaiparowits Formation, southern Utah, USA. Zoological Journal of the Linnean Society 151, 351–376.

Godefroit, P., Zan, S., and Jin, L. 2001. The Maastrichtian (Late Cretaceous) lambeosaurine dinosaur *Charonosaurus jiayinensis* from north-eastern China. Bulletin de l'Institut royal des Sciences naturelles de Belgique, Sciences de la Terre 71, 119–168.

Godefroit, P., Hai, S., Yu, T., and Lauters, P. 2008. New hadrosaurid dinosaurs from the uppermost Cretaceous of northeastern China. Acta Palaeontologica Polonica 53, 47–74.

Hirth, D.H. 1977. Social behavior of white-tailed deer in relation to habitat. Wildlife Monographs 53: 1–55.

Holtz Jr., T.R., Chapman, R.E., and Lamanna, M.C. 2004. Mesozoic biogeography of Dinosauria. In D.B. Weishampel, P. Dodson, and H. Osmólska (eds.), The Dinosauria, second edition. University of California Press, Berkeley, California, pp. 627–642.

Horner, J.R. 1982. Evidence of colonial nesting and 'site fidelity' among ornithischian dinosaurs. Nature 297: 675–676.

Horner, J.R. and Makela, R. 1979. Nest of juveniles provides evidence of family structure among dinosaurs. Nature 282: 296–298.

Horner, J.R., De Ricqles, A.J., and Padian, K. 2000. Long bone histology of the hadrosaurid dinosaur *Maiasaura peeblesorum*: growth dynamics and physiology based on an ontogenetic series of skeletal elements. Journal of Vertebrate Paleontology 20: 115–129.

Horner, J.R., Weishampel, D.B., and Forster, C.A. 2004. Hadrosauridae. In: D.B. Weishampel, P. Dodson, H. Osmólska (Eds.), The Dinosauria, (Second Edition). University of California Press, Berkeley, California, pp. 438-463.

Larson, D.W, Brinkman, D.B., and Bell, P.R. 2010. Faunal assemblages from the upper Horseshoe Canyon Formation, an early Maastrichtian cool-climate assemblage from Alberta, with special reference to the *Albertosaurus sarcophagus* bonebed. Canadian Journal of Earth Sciences 47:1159–1181.

Lauters, P., Bolotsky, Y.L., Van Itterbeeck, J., and Godefroit, P. 2008. Taphonomy and age profile of a latest Cretaceous dinosaur bonebed in far eastern Russia. Palaios 23: 153–162.

Lehman, T.M. 2001. Late Cretaceous dinosaur provinciality. In: D.H. Tanke and K. Carpenter (eds.) Mesozoic Vertebrate Life. Indiana University Press, Bloomington, IN, pp. 310–328.

Lull, R.S. and Wright, N.E. 1942. Hadrosaurian dinosaurs of North America. Geological Society of America, Special Paper 40, 242 pp.

Maryańska, T. and Osmólska, H. 1979. Aspects of hadrosaurian cranial anatomy. Lethaia 12: 265–273.

Maryańska, T. and Osmólska, H. 1981a. First lambeosaurine dinosaur from the Nemegt Formation, Upper Cretaceous, Mongolia. Acta Palaeontologica Polonica 26: 243–255.

Maryańska, T. and Osmólska, H. 1981b. Cranial anatomy of *Saurolophus angustirostris* with comments on the Asian Hadrosauridae (Dinosauria). Palaeontologia Polonica 42: 5–24.

Maryańska, T. and Osmólska, H. 1984. Post-cranial anatomy of *Saurolophus angustirostris* with comments on other hadrosaurs. Palaeontologia Polonica 46: 119–141.

Molvar, E.M. and Bowyer, R.T. 1994. Costs and benefits of group living in a recently social ungulate: the Alaskan moose. Journal of Mammalogy 75: 621–630

Morris, W.J. 1973. A review of Pacific coast hadrosaurs. Journal of Paleontology, 47: 551–561.

Murphy, N.L., Trexler, D., and Thompson, M. 2006. "Leonardo", a mummified *Brachylophosaurus* from the Judith River Formation. In K. Carpenter (ed.) Horns and Beaks: Ceratopsian and Ornithopods Dinosaurs. Indiana University Press, Bloomington, Indiana, pp. 117–133.

Negro, G. 2001. Phylogenetic interpretation of hadrosaurian dinosaur skin. Journal of Vertebrate Paleontology 21: 83A.

Norman, D. and Sues, H.-D. 2000. Ornithopods from Kazakhstan, Mongolia and Siberia. In M.J. Benton, M.A. Shishkin, D.M. Unwin, and E.N. Korochin (eds.), The Age of Dinosaurs in Russia and Mongolia. Cambridge University press, Cambridge, UK, pp. 462-479.

Prieto-Marquez, A. 2005. New information on the cranium of *Brachylophosaurus canadensis* (Dinosauria, Hadrosauridae), with a revision of its phylogenetic position. *Journal of Vertebrate Paleontology* 25: 144–156.

Prieto-Marquez, A. 2010a. Global phylogeny of Hadrosauridae (Dinosauria: Ornithopoda) using parsimony and Bayesian methods. Zoological Journal of the Linnean Society 159: 435–502.

Prieto-Marquez, A. 2010b. Global historical biogeography of hadrosaurid dinosaurs. Zoological Journal of the Linnean Society 159: 503–525.

Rozhdestvenskii, A.K. 1952. A new representative of duckbilled dinosaurs from the Upper Cretaceous deposits of Mongolia (in Russian). Doklody Akademic SSSR 86, 405–408.

Rozhdestvensky, A.K. 1957. The Duck-billed dinosaur *Saurolophus* from the Upper Cretaceous of Mongolia [in Russian]. Vertebrata Palasiatica 1: 129–149.

Rozhdestvensky, A.K. 1965. Growth changes in Asian dinosaurs and some problems of their taxonomy [in Russian]. Paleontologicheskii Zhurnal 3: 95–109.

Russell, D.A. 1993. The role of Central Asia in dinosaurian biogeography. Canadian Journal of Earth Science 30: 2002–2012.

Russell, D.A. and Chamney, T.P. 1967. Notes on the biostratigraphy of dinosaurian and microfossil faunas in the Edmonton Formation (Cretaceous), Alberta. National Museum of Canada Natural History Papers 35, 22 p.

Ryan, M.J. and Evans, D.A. 2005. Ornithischian dinosaurs. In Currie, P.J., and Koppelhus, E.B. (eds.) Dinosaur Provincial Park; a spectacular ancient ecosystem revealed. Indiana University Press, Indianapolis, p. 312–348.

Ryan, M.J., Currie, P.J., Gardner, J.D., Vickaryous, M.K., and Lavigne, J.M. 1998. Baby hadrosaurid material associated with an unusually high abundance of *Troodon* teeth from the Horseshoe Canyon Formation, Upper Cretaceous, Alberta, Canada. Gaia 15: 123–133.

Ryan, M.J., Russell, A.P., Eberth, D.A., and Currie, P.J. 2001. The taphonomy of a *Centrosaurus* (Ornithischia: Ceratopsidae) bonebed from the Dinosaur

Park Formation (upper Campanian), Alberta, Canada, with comments on cranial ontogeny: PALAIOS 16: 482–506.

Tanke, D.H., and Brett-Surman, M.K. 2001. Evidence on hatchling and nestling-size hadrosaurs (Reptilia: Ornithischia) from Dinosaur Provincial Park (Dinosaur Park Formation: Campanian), Alberta. In Tanke, D.H. and Carpenter, K. (eds.) Mesozoic Vertebrate Life. Indiana University Press, Bloomington, p. 206–218

Weishampel, D.B., Barrett, P.M., Coria, R.A., le Loeuff, J., Zhao, X., Sahni, A., Gomani, E.M.P., and Noto, C.R. 2004. Dinosaur distribution. In D. Weishampel, P. Dodson, and H. Osmólska (eds.) The Dinosauria, second edition. University of California Press, Berkeley, pp. 517–606.